Theoretical Nuclear Physics

Chong Qi
chongq@kth.se
Department of Physics, Royal Institute of Technology (KTH)

April 14, 2015

Contents

List of Figures

List of Tables

Introduction

The atomic nucleus is a quantum man-body object composed of A nucleons (mass number): Z protons (atomic number) and N neutrons. An atomic species with the specified numbers A and Z is also often called a nuclide [1]. One denotes by ${}^{A}_{Z}X_{N}$ the nucleus X with the total number of nucleons $A = N + Z$ (although the simpler notation ${}^{A}X$ is often used). Such a system is stable only for certain combinations of numbers Z and N. Presently, around 300 stable nuclides are known. Systems different from stable configurations undergo spontaneous radioactive decays until the stability is reached. A nucleus of such an unstable nuclide is considered as a well defined object if its half-life is much longer than 10^{-21} s which is a characteristic timescale for processes governed by strong interaction. These nuclides are bound by the nuclear force and/or by Coulomb and centrifugal barriers. The number of unstable nuclides synthesized in laboratories is constantly growing, and up to now more than 3000 were identified.

Nomenclature

- Nuclide: A specific nuclear species, with a given proton number Z and neutron number N
- Nucleon: Neutron or proton
- Isotopes: Nuclides of same Z and different N
- Isotones: Nuclides of same N and different Z
- Isobars: Nuclides of same mass number A (A = Z + N)
- Isomer: Nuclide in an excited state with a measurable half-life
- Mesons: Unstable particles composed of one quark and one antiquark. Some light mesons are the associated quantum-field particles that transmit the nuclear force.

A brief history of nuclear (structure) physics:

- 1896: Discovery of radioactivity (Becquerel)
- 1911: Discovery of the nucleus (Rutherford)
- 1932: Discovery of the neutron (Chadwick)
- 1935: Bethe-Weiszaker mass formula
- 1939: Discovery of (neutron-induced) fission
- 1949: Shell model (Goeppert-Mayer, Jensen)
- 1951: Collective model (Bohr, Mottelson, Rainwater)
- 1957: Nuclear superfluidity (Bohr, Mottelson)
- Since then: Nuclear forces, many-body methods (HF, HFB, RPA, GCM, Green function, etc).

It is very difficult to treat the nuclear many-body system. On the one hand, the nucleon-nucleon interaction provided by fundamental theories, as Quantum Chromo Dynamics (QCD), is extremely difficult to apply. On the other hand the many-body problem itself is very difficult since the number of particles is large, but not large enough to be able to be treated in statistical terms, as it happens with other many-body systems like e. g. condensed matter. Therefore the main tasks in nuclear structure studies is first to find effective forces that explain the available experimental data and then to be able to perform this task within a manageable theoretical framework. In this course we will present the most important solutions that have been found to perform those tasks.

Effective forces are introduced to explain in a treatable fashion nuclear properties. Thus, it is known that all nuclei with N even and Z even (even-even nuclei) have in the ground state spin and parity 0^{+}. This indicates that nucleons of the same kind are arranged in pairs. The nucleons in each pair are coupled with the corresponding spins pointing in opposite directions, such that the pair is coupled to zero angular momentum. The force inducing this pairing of nucleons is called "pairing force".

The nucleus is an isolated system with a well defined total angular momentum. It is common practice to represent this total angular momentum of a nucleus by the symbol I (or J) and to call it nuclear spin. Associated with each nuclear spin is a nuclear magnetic moment which produces magnetic interactions with its environment. It should be noted that for electrons in atoms we make a clear distinction between electron spin and electron orbital angular momentum and then combine them to give the total angular momentum.

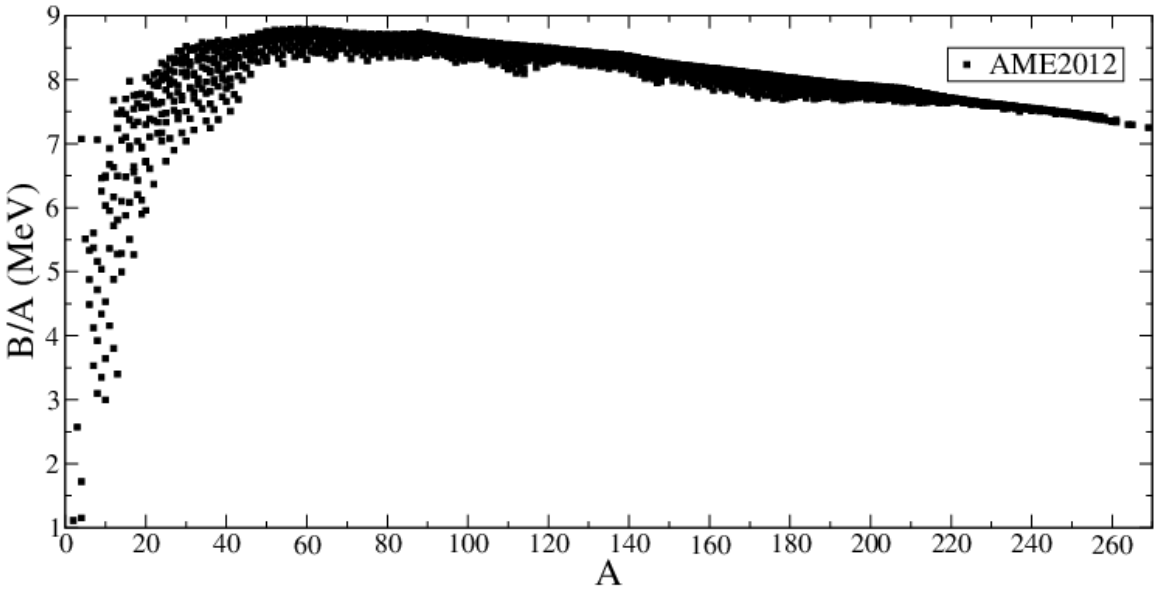

Figure 1: Experimental values of nuclear binding energies per nucleon (in MeV) for all known nuclei from Ref. [2]. The three cases with binding energies per nucleon less than 2 MeV correspond to ^{4}H (1.720 MeV), ^{4}Li (1.154 MeV) and ^{2}H (1.112MeV). In comparison, ^{4}He is bound by as much as 7.074 MeV.

The atomic mass M_{at}, the nuclear mass M_{nu} and the electron mass Mel are related by

$$M_{at} = M_{nu} + ZM_{el} - B_{el}/c^2 \tag{1}$$

where Z is the number of electrons (and therefore of protons in a non-ionized atom) and B_{el} is the binding energies of the electrons (notice that B_{el} is subtracted). It is therefore straightforward, by using the above relation, to obtain the nuclear mass from the atomic mass. Usually what is given not the measured atomic masses but what is called the "mass excess", which is defined by

$$\Delta M = M_{at} - A \cdot amu \tag{2}$$

where $A = N + Z$ is the atomic number and M_u is the atomic mass unit, which is defined as one-twelfth of the mass of a neutral ^{12}C atom.

The convenient unit for measuring the nuclear mass is called the atomic mass unit or for short amu. The mass of a ^{12}C atom (including all six electrons) is defined as 12 amu. We have

$$1amu = 1.6605402(10) \times 10^{-27} kg = 931.49432(28) MeV/c^2. \tag{3}$$

The total binding energy $B(N, Z)$ is defined as the total minimum work that an external agent must do to disintegrate the whole nucleus completely. By doing so the nucleus would no longer be existent but disintegrated into separated nucleons. This can also be considered as the total amount of energy released when nucleons, with zero kinetic energy initially, come close enough together to form a stable nucleus. The $B(N, Z)$ is the binding energy of the nuclide related to its mass $M(N, Z)$ as

$$M(N, Z) = Z\, M_H + N\, m_n - B(N, Z), \tag{4}$$

where M_H and m_n are masses of the hydrogen atom and the neutron, respectively.

Another important nuclear quantity is the binding energy per nucleon, which for some nucleon numbers N and Z is larger than the average. These numbers are called "magic numbers". They include

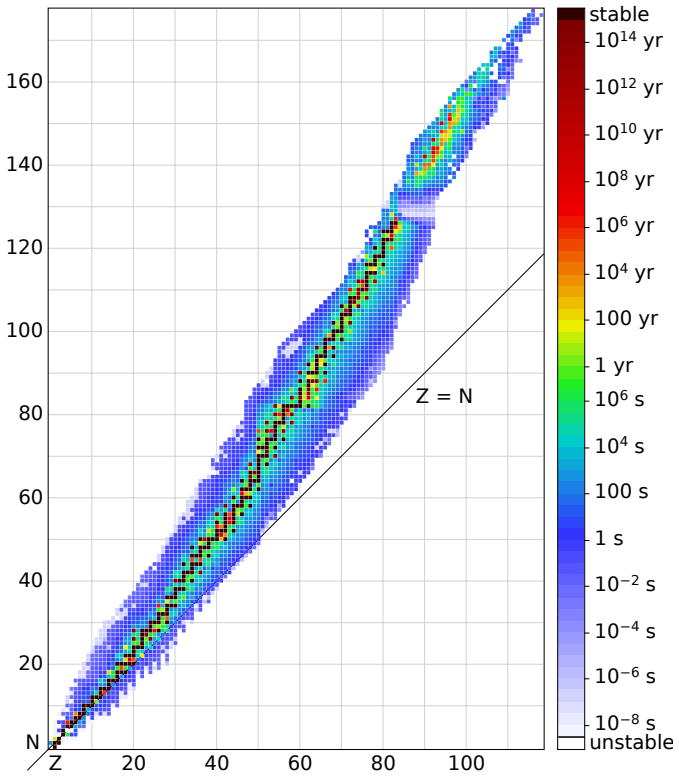

Figure 2: Stability of nuclides as a function of N and Z from Ref. [1].

the numbers 2, 8, 20, 28, 50, 82 and 126. A nucleus having magic N and Z, like e. g. ${}^{16}_{8}O_8$ (Oxygen 16), ${}^{48}_{20}Ca_{28}$ (Calcium 48) and ${}^{208}_{82}Pb_{126}$ (Lead 208) are very bound. It was found that a nucleon moving outside the nuclear field induced by a double magic nucleus does not influence appreciably the motion of the nucleons inside the nucleus. The double magic nucleus is as a "frozen core". The field induced by the core acts as a whole upon the odd nucleon moving outside the even-even core. In other words, the low-lying excitations of even-odd or odd-even nuclei outside a magic core can be considered as single-particle excitations.

The proton- and the neutron separation energy of a nuclide with numbers N and Z are given by

$$S_p(N,Z) = B(N,Z) - B(N,Z-1) \tag{5}$$
$$S_n(N,Z) = B(N,Z) - B(N-1,Z). \tag{6}$$

When we move along the line of isotopes with the given atomic number Z, starting from stability towards neutron-deficient nuclides, the proton separation energy S_p decreases and at certain location it becomes negative. The proton drip-line is defined as the border between the last proton-bound isotope and the first one with the negative value of the S_p. In the fully analogous way, the neutron drip-line for a given neutron number N is defined as a border between the last neutron bound isotone, when counting from stability, and the first one for which the neutron separation energy S_n is negative. The drip lines as defined above are very useful in identifying and discussing limits of stability. The two-nucleon separation energies are given as

$$S_{2p}(N,Z) = B(N,Z) - B(N,Z-2) \tag{7}$$
$$S_{2n}(N,Z) = B(N,Z) - B(N-2,Z). \tag{8}$$

The separation energy of an α particle is given as

$$S_\alpha(N,Z) = B(N,Z) - B(N-2,Z-2) - B(2,2). \tag{9}$$

Most heavy nuclei with masses $A > 150$ are unstable against α emission with negative S_α (or positive Q_α). The Q_α for α decay is given as

$$Q_\alpha(N,Z) = B(N-2,Z-2) + B(2,2) - B(N,Z). \tag{10}$$

Bibliography

[1] http://en.wikipedia.org/wiki/Nuclide

[2] G. Audi, M. Wang, A.H.Wapstra, F.G.Kondev, M.MacCormick, X.Xu, and B. Pfeiffer, Chinese Phys. C 36, 1157 (2012); M. Wang, G. Audi, A. Wapstra, F. Kondev, M. MacCormick, X. Xu, and B. Pfeiffer, Chinese Phys. C 36, 1603 (2012). http://amdc.impcas.ac.cn/evaluation/data2012/data/mass.mas12

Chapter 1

Basic Quantum Mechanics concepts

Hermitian operators. Physical meaning of the eigenvectors and eigenvalues of Hermitian operators. Representations and their use. Unitary Operator: symmetries and conservation laws. Sum of angular momenta. 3j, 6j and 9j symbols.

1.1 The Hilbert space

In Quantum Mechanics the states are represented by vectors in an abstract space called Hilbert space. Thus, a state α is a vector which, in Dirac notation, is written as $|\alpha\rangle$. As we will see below, this vector can be associated either to a function $\Psi_\alpha(\vec{r})$, which is regular and square integrable, or to a one-dimensional matrix (spinor). In the first case the metric of the space is defined by the scalar product in the region V of the three-dimensional (physical) space where the functions are square integrable. Usually V includes the whole space. Thus, the scalar product between the vectors $|\alpha\rangle$ and $|\beta\rangle$ is defined by

$$\langle\beta|\alpha\rangle = \int_V d\vec{r}\ \Psi^*_\beta(\vec{r})\Psi_\alpha(\vec{r}) \tag{1.1}$$

For the case of an N-dimensional spinor the vector α is associated to the one-dimensional matrix given by

$$\begin{pmatrix} \alpha_1 \\ \alpha_2 \\ . \\ . \\ . \\ \alpha_N \end{pmatrix} \tag{1.2}$$

and the scalar product between the vectors α and β is given by

$$\langle\beta|\alpha\rangle = \begin{pmatrix} \beta_1^*, & \beta_2^*, & ., & ., & ., & \beta_N^* \end{pmatrix} \begin{pmatrix} \alpha_1 \\ \alpha_2 \\ . \\ . \\ . \\ \alpha_N \end{pmatrix} = \sum_{i=1}^{N} \beta_i^* \alpha_i \tag{1.3}$$

The vector $\langle\alpha|$ is called "bra" and $|\alpha\rangle$ is called "ket". The scalar product $\langle\alpha|\beta\rangle$ is called "bracket".

One sees from the definition of the scalar product that it is $\langle\alpha|\beta\rangle = \langle\beta|\alpha\rangle^*$. Therefore the norm N_α of a vector $|\alpha\rangle$, i. e. $N_\alpha = \sqrt{\langle\alpha|\alpha\rangle}$ is a real number. In Quantum Mechanics N_α^2 is the probability of measuring the system in the state α. Since the system exists, this probability should be $N_\alpha^2 = 1$. Notice that we assume that the system is stationary, that is all processes are time-independent. Therefore if the system is in the state α, it will remain there for ever. Below we will describe this system in terms of a set of vectors $|n\rangle$. The probability of measuring the system in the state $|n\rangle$ is $|\langle\alpha|n\rangle|^2$.

1.2 Eigenvalues and eigenvectors of matrices

The word "eigenvector" almost always means a "'right column" vector that must be placed to the "right" of the matrix A. The eigenvalue equation for a matrix A is

$$Av - \lambda v = 0 \tag{1.4}$$

which is equivalent to

$$(A - \lambda I)v = 0. \tag{1.5}$$

There may be also single-"row" vectors that are unchanged when they occur on the "left" side of a product with a square matrix A,

$$uA = \lambda u. \tag{1.6}$$

The left eigenvectors of A, are transposes of the right eigenvectors of the transposed matrix A^T,

$$A^T u^T = \lambda u^T. \tag{1.7}$$

In matrix form we can write,

$$\begin{pmatrix} A_{1,1} & A_{1,2} & \dots & A_{1,n} \\ A_{2,1} & A_{2,2} & \dots & A_{2,n} \\ \vdots & \vdots & \ddots & \vdots \\ A_{n,1} & A_{n,2} & \dots & A_{n,n} \end{pmatrix} \begin{pmatrix} v_1 \\ v_2 \\ \vdots \\ v_n \end{pmatrix} = \lambda \begin{pmatrix} v_1 \\ v_2 \\ \vdots \\ v_n \end{pmatrix} \tag{1.8}$$

where for each element we have,

$$w_i = A_{i1}v_1 + A_{i2}v_2 + \cdots + A_{in}v_n = \sum_{j=1}^{n} A_{ij}v_j = \lambda v_i. \tag{1.9}$$

The inverse of a matrix is given as

$$AA^{-1} = A^{-1}A = I, \tag{1.10}$$

where I is the identity matrix. For a simple 2×2 matrix we have

$$A^{-1} = \frac{1}{A_{11}A_{2,2} - A_{1,2}A_{2,1}} \begin{pmatrix} A_{2,2} & -A_{1,2} \\ -A_{2,1} & A_{1,1} \end{pmatrix}. \tag{1.11}$$

The determinant of a 2×2 matrix A is given as

$$det(A) = A_{11}A_{2,2} - A_{1,2}A_{2,1}. \tag{1.12}$$

The trace pf a $n \times n$ matix is given as

$$tr(A) = \sum_{i=1}^{n} A_{ii}. \tag{1.13}$$

For a 2×2 matrix the eigenvalues are found to be

$$\lambda = \frac{\mathrm{tr}(A) \pm \sqrt{\mathrm{tr}^2(A) - 4\mathrm{det}(A)}}{2}. \tag{1.14}$$

For the eigen vectors we have

$$\frac{v_1}{v_2} = \frac{A_{12}}{\lambda - A_{11}} = \frac{\lambda - A_{22}}{A_{21}}. \tag{1.15}$$

1.3 Hermitian operators

An operator A acting upon a vector $|\alpha\rangle$ in the Hilbert space converts this vector into another one $|\beta\rangle$. It is important to point out that the Hilbert space we consider is closed, that is all vectors belong to the space. In the applications that we will encounter in the course of these lectures only small subspaces of the total Hilbert space (which usually has infinite dimension) will be chosen. In such a case the operator $\hat{A}$ may bring $|\alpha\rangle$ to a vector $|\beta\rangle$ lying outside the subspace. But we will not treat such situations here. In other words, the systems we will treat are always closed.

The operator $\hat{A}$ is called Hermitian if

$$\hat{A}^\dagger = \hat{A} \qquad \text{Hermitian} \tag{1.16}$$

The eigenvalues a and eigenvectors $|\alpha\rangle$ of the operator $\hat{A}$ satisfy the equation

$$\hat{A}|\alpha\rangle = a|\alpha\rangle \tag{1.17}$$

and for the adjoint operator $A^\dagger$ it is,

$$\langle\alpha|\hat{A}^\dagger = a^*\langle\alpha| \tag{1.18}$$

If the operator $\hat{A}$ is Hermitian one has

$$\langle\beta|\hat{A}|\alpha\rangle = \langle\beta|\hat{A}^\dagger|\alpha\rangle \tag{1.19}$$

If, in addition, $|\alpha\rangle$ and $|\beta\rangle$ are eigenvectors of $\hat{A}$, then one gets

$$a\langle\beta|\alpha\rangle = b^*\langle\beta|\alpha\rangle \tag{1.20}$$

Which implies that

$$\begin{cases} |\alpha\rangle \neq |\beta\rangle; & \langle\beta|\alpha\rangle = 0 \\ |\alpha\rangle = |\beta\rangle; & a \text{ real} \end{cases} \tag{1.21}$$

That is, the eigenvectors of a Hermitian operator form an orthogonal set and the corresponding eigenvalues are real. These two properties play a fundamental role in Quantum Mechanics, as we repeatedly will see in the course of these lectures. In quantum mechanics, the expectati on value of any physical quantity must be be real and therefore an operator that corresponds to a physical observable must also be Hermitian.

Physical meaning of the eigenvectors and eigenvalues of Hermitian operators

The most important property of Hermitian operators in Quantum Mechanics is that their eigenvalues are real. This property has allowed one to interpret these operators as the devices used to measure physical quantities. One postulates that the Hermitian operator represents the apparatus used to measure a physical quantity and the corresponding eigenvalues are all the possible values that one can obtain from the measurement. In other words, only those values are allowed and nothing else. This is a radical departure from Classical Mechanics, where one can give any value one wishes to all physical quantities (for instance the energy).

The eigenvectors of Hermitian operators are the corresponding wave functions that allow one to evaluate all probabilities, in particular transition probabilities. Besides, they play a fundamental role in Quantum Mechanics. Thus, normalizing the eigenvectors in Eq. (1.20) as $\langle\alpha|\alpha\rangle = 1$ and from Eq. (1.21) one finds that they satisfy

$$\langle\alpha|\beta\rangle = \delta_{\alpha\beta} \tag{1.22}$$

which means that they form an orthonormal set of vectors in the Hilbert space. They can be used as a basis to describe any vector belonging to the space. In a more rigorous statement one can say that the eigenvectors of an Hermitian operator span the Hilbert space on which the operator acts. To see the great importance of this property, assume a Hilbert space of dimension N and a Hermitian operator $\hat{A}$ acting on this space such that,

$$\hat{A}|\alpha_i\rangle = a_i|\alpha_i\rangle, \qquad i = 1, 2, \cdots, N \tag{1.23}$$

Any vector $|v\rangle$ in the space spanned by the basis $\{|\alpha\rangle\}$ can be written as

$$|v\rangle = \sum_{i=1}^{N} c_i|\alpha_i\rangle \tag{1.24}$$

From Eq. (1.22) one obtains

$$c_i = \langle\alpha_i|v\rangle \tag{1.25}$$

The numbers $\langle\alpha_i|v\rangle$ are called "amplitudes". If the vector $|v\rangle$ represents a physical (quantum) state, then the amplitudes have to obey the normality relation given by,

$$\langle v|v\rangle = \sum_{i=1}^{N} c_i\langle v|\alpha_i\rangle = \sum_{i=1}^{N}\langle v|\alpha_i\rangle^*\langle v|\alpha_i\rangle = \sum_{i=1}^{N}|\langle v|\alpha_i\rangle|^2 = 1 \tag{1.26}$$

From Eq. (1.25) the vector $|v\rangle$ can be written as,

$$|v\rangle = \sum_{i=1}^{N} \langle \alpha_i | v \rangle |\alpha_i\rangle = \sum_{i=1}^{N} |\alpha_i\rangle\langle\alpha_i|v\rangle \tag{1.27}$$

which shows that

$$\sum_{i=1}^{N} |\alpha_i\rangle\langle\alpha_i| = \hat{I} \tag{1.28}$$

This is the projector into the space spanned by the set $\{|\alpha\rangle\}$. We will use the projector often in these lectures.

Representations and their use

One of the most important problems in theoretical nuclear physics is to evaluate the eigenvectors and eigenvalues of a given operator $\hat{B}$. That is, to find the vectors β and numbers b defined by

$$\hat{B}|\beta\rangle = b|\beta\rangle \tag{1.29}$$

This is called the "Eigenvalue problem". To evaluate the eigenvectors and eigenvalues one first chooses a basis, that is a set of orthonormal vectors $\{|\alpha\rangle\}$ which are usually provided by the diagonalization of a Hermitian operator. This basis is also called "Representation", for reason which will become clear below. If the number of vectors forming the orthonormal set $\{|\alpha\rangle\}$, i. e. the dimension of the basis, is N one has, applying Eq. (1.28)

$$\hat{B}|\beta\rangle = b|\beta\rangle = \hat{B}\sum_{i=1}^{N} |\alpha_i\rangle\langle\alpha_i|\beta\rangle \Longrightarrow \sum_{i=1}^{N} \left(\langle\alpha_j|\hat{B}|\alpha_i\rangle - b\delta_{ij}\right)\langle\alpha_i|\beta\rangle = 0 \tag{1.30}$$

which provides the equation to evaluate the amplitudes as,

$$\sum_{i=1}^{N} \left(\langle\alpha_j|\hat{B}|\alpha_i\rangle - b\delta_{ij}\right)\langle\alpha_i|\beta\rangle = 0 \tag{1.31}$$

This is a set of $N \times N$ homogeneous linear equations in the N unknowns amplitudes $\langle\alpha_i|\beta\rangle$. Besides the trivial solution $\langle\alpha_i|\beta\rangle$=0 for all i, one finds the physical solutions by requiring that the equations (1.31) are linearly dependent upon each other. This occurs if the corresponding determinant vanishes. That is

$$\left|\left|\langle\alpha_j|\hat{B}|\alpha_i\rangle - b\delta_{ij}\right|\right| = 0 \tag{1.32}$$

which allows one to calculate N values of b. To calculate the amplitudes one disregard one of the Eqs. (1.31) and the remaining $N-1$ equations plus the normalization condition given by

$$\sum_{i=1}^{N} |\langle\alpha_i|\beta\rangle|^2 = 1 \tag{1.33}$$

give a non-linear $N \times N$ set of equations from which the amplitudes $\langle\alpha_i|\beta\rangle$ are extracted.

The set $\{|\alpha\rangle\}$ can be a continuum set. An example of this is the eigenvectors corresponding to the distance operator, i. e.

$$\hat{r}|\boldsymbol{r}\rangle = r|\boldsymbol{r}\rangle \tag{1.34}$$

The operator $\hat{r}$ represents the device used to measure the distance (a rule for instance), $|\boldsymbol{r}\rangle$ is the corresponding vector in the Hilbert space and r the length one measures. Since

$$\hat{r} = \hat{r}^{\dagger} \tag{1.35}$$

one gets the projector as

$$\int \mathrm{d}\boldsymbol{r}|\boldsymbol{r}\rangle\langle\boldsymbol{r}| = \hat{I} \tag{1.36}$$

where, in spherical coordinates, it is $\boldsymbol{r} = (r, \theta, \varphi)$ and $\mathrm{d}\boldsymbol{r} = r^2 \mathrm{d}r \sin\theta \mathrm{d}\theta \mathrm{d}\varphi$. One cannot speak of a number of dimensions of this continuous basis, since it comprises all real numbers (which cannot be labeled by integers). Therefore one uses the name "representation" for the projector (1.36). In $\boldsymbol{r}$-representation the eigenvalue problem is

$$\hat{B}|\beta\rangle = b|\beta\rangle = \hat{B} \int \mathrm{d}\boldsymbol{r}'|\boldsymbol{r}'\rangle\langle\boldsymbol{r}'|\beta\rangle \tag{1.37}$$

$$\hat{B} \int \mathrm{d}\boldsymbol{r}'\langle\boldsymbol{r}|\boldsymbol{r}'\rangle\langle\boldsymbol{r}'|\beta\rangle = b\langle\boldsymbol{r}|\beta\rangle \tag{1.38}$$

With $\langle\boldsymbol{r}|\boldsymbol{r}'\rangle = \delta(\boldsymbol{r} - \boldsymbol{r}')$ and $\Psi_\beta(\boldsymbol{r}) = \langle\boldsymbol{r}|\beta\rangle$, one gets

$$\hat{B}\Psi_\beta(\boldsymbol{r}) = b\Psi_\beta(\boldsymbol{r}) \tag{1.39}$$

and the matrix elements can readily be evaluated as,

$$\langle\alpha_j|\hat{B}|\alpha_i\rangle = \int \mathrm{d}\boldsymbol{r} \int \mathrm{d}\boldsymbol{r}'\langle\alpha_j|\boldsymbol{r}\rangle\langle\boldsymbol{r}|\hat{B}|\boldsymbol{r}'\rangle\langle\boldsymbol{r}'|\alpha_i\rangle = \int \mathrm{d}\boldsymbol{r}\Psi_j^*(\boldsymbol{r})\hat{B}\Psi_i(\boldsymbol{r}) \tag{1.40}$$

1.4 Unitary Operator: symmetries and conservation laws

An operator is Unitary if its inverse equal to its adjoints

$$U^{-1} = U^\dagger, \tag{1.41}$$

or

$$UU^\dagger = U^\dagger U = 1. \tag{1.42}$$

Unitary operators are of a fundamental importance to describe transformations of the system (basis). We will analyze in this Lecture the cases of translations, rotations and parity.

Translation symmetry

The translation operator $\hat{T}$ is defined by,

$$\hat{T}(\Delta\boldsymbol{r})|\boldsymbol{r}\rangle = |\boldsymbol{r} + \Delta\boldsymbol{r}\rangle \tag{1.43}$$

which applied to the vector $|\Psi\rangle$ gives,

$$\hat{T}(\Delta\boldsymbol{r})|\Psi\rangle = \int \mathrm{d}\boldsymbol{r}'\hat{T}(\Delta\boldsymbol{r})|\boldsymbol{r}'\rangle\langle\boldsymbol{r}'|\Psi\rangle = \int \mathrm{d}\boldsymbol{r}'|\boldsymbol{r}' + \Delta\boldsymbol{r}\rangle\langle\boldsymbol{r}'|\Psi\rangle \tag{1.44}$$

and, in r-representation, the translated function is

$$\Psi_t(\boldsymbol{r}) = \langle\boldsymbol{r}|\hat{T}(\Delta\boldsymbol{r})|\Psi\rangle = \int \mathrm{d}\boldsymbol{r}'\delta(\boldsymbol{r} - \boldsymbol{r}' - \Delta\boldsymbol{r})\langle\boldsymbol{r}'|\Psi\rangle = \Psi(\boldsymbol{r} - \Delta\boldsymbol{r}) \tag{1.45}$$

Since

$$\langle\boldsymbol{r}|\hat{T}^\dagger(\Delta\boldsymbol{r})\hat{T}(\Delta\boldsymbol{r})|\boldsymbol{r}\rangle = \langle\boldsymbol{r} + \Delta\boldsymbol{r}|\boldsymbol{r} + \Delta\boldsymbol{r}\rangle = 1 \tag{1.46}$$

one obtains

$$\hat{T}^\dagger\hat{T} = 1 \tag{1.47}$$

which defines the operator $\hat{T}$ as unitary.

The invariance of a wave function with respect to translations implies the conservation of the linear momentum, This can be seen by noticing that the time dependence of an operator $\hat{A}$ is given by

$$\frac{\mathrm{d}\hat{A}}{\mathrm{d}t} = \frac{\partial\hat{A}}{\partial t} + \frac{\mathrm{i}}{\hbar}[H, \hat{A}] \tag{1.48}$$

Assume a system for which

$$H\Psi_n(x) = E_n\Psi_n(x) \tag{1.49}$$

If there is translation invariance, then

$$H\Psi_n(x+\Delta x) = E_n\Psi_n(x+\Delta x) \tag{1.50}$$

Making a Taylor expansion of Ψ_n one gets,

$$\Psi_n(x+\Delta x) = \sum_{k=1}^{\infty}\frac{(\Delta x)^k}{k\,!}\frac{\mathrm{d}^k\Psi_n(x)}{\mathrm{d}x^k} = \sum_{k=1}^{\infty}\frac{1}{k\,!}\left(\Delta x\frac{\mathrm{d}}{\mathrm{d}x}\right)^k\Psi_n(x) = \mathrm{e}^{\Delta x\frac{\mathrm{d}}{\mathrm{d}x}}\Psi_n(x) \tag{1.51}$$

and defining the linear momentum operator in the usual fashion as,

$$p_x = \frac{\hbar}{\mathrm{i}}\frac{\mathrm{d}}{\mathrm{d}x} \tag{1.52}$$

one obtains,

$$\Psi_n(x+\Delta x) = \mathrm{e}^{\frac{\mathrm{i}}{\hbar}\Delta x p_x}\Psi_n(x) \tag{1.53}$$

Therefore the translation operator is

$$\hat{T}(\Delta x) = \mathrm{e}^{\frac{\mathrm{i}}{\hbar}\Delta x p_x} \tag{1.54}$$

and one has

$$\begin{aligned} H\hat{T}(\Delta x)\Psi_n(x) &= H\Psi_n(x+\Delta x) \\ &= E_n\Psi_n(x+\Delta x) \\ &= E_n\hat{T}(\Delta x)\Psi_n(x) = \hat{T}(\Delta x)H\Psi_n(x) \end{aligned} \tag{1.55}$$

which implies,

$$[H,\hat{T}] = 0 \tag{1.56}$$

i. e.

$$[H,p_x] = 0 \tag{1.57}$$

Since p_x is time independent it is $\partial\hat{p_x}/\partial dt$ =0 and from Eq. (1.48) one gets $\mathrm{d}\hat{p_x}/\mathrm{d}t$=0, which means that the linear momentum is conserved.

Rotational symmetry

Performing a rotation of the system by an angle $\delta\boldsymbol{\varphi}$, as shown in Fig. 1.1, a function $\Psi(\boldsymbol{r})$ is transformed to $\Psi(\boldsymbol{r}+\boldsymbol{a})$. As seen in the Figure, it is $a = \delta\varphi\, r sin\theta$ and the relation among the vectors $\boldsymbol{a}$, $\delta\boldsymbol{\varphi}$ and $\boldsymbol{r}$ is

$$\boldsymbol{a} = \delta\boldsymbol{\varphi}\times\boldsymbol{r} \tag{1.58}$$

Calling

$$F(\boldsymbol{r}) = \Psi(\boldsymbol{r}+\boldsymbol{a}) \tag{1.59}$$

one gets

$$\Psi(\boldsymbol{r}) = F(\boldsymbol{r}-\boldsymbol{a}) = F(\boldsymbol{r}) - \boldsymbol{a}\cdot\boldsymbol{\nabla}F(\boldsymbol{r}) + \cdots \tag{1.60}$$

Performing a Taylor expansion as,

$$\begin{aligned} &F(x+\Delta x, y+\Delta y, z+\Delta z) = \\ &\qquad F(x,y,z) + \frac{\partial F(x,y,z)}{\partial x}\Delta x + \frac{\partial F(x,y,z)}{\partial y}\Delta y + \frac{\partial F(x,y,z)}{\partial z}\Delta z + \cdots \end{aligned} \tag{1.61}$$

one gets,

$$F(\boldsymbol{r}+\Delta\boldsymbol{r}) = F(\boldsymbol{r}) + \Delta\boldsymbol{r}\cdot\boldsymbol{\nabla}F(\boldsymbol{r}) + \cdots \tag{1.62}$$

With $\delta\boldsymbol{\varphi}$ infinitesimal it is,

$$\Psi(\boldsymbol{r}) - F(\boldsymbol{r}) = -(\delta\boldsymbol{\varphi}\times\boldsymbol{r})\cdot\boldsymbol{\nabla}F(\boldsymbol{r}) = -\delta\boldsymbol{\varphi}\cdot(\boldsymbol{r}\times\boldsymbol{\nabla}F(\boldsymbol{r})) \tag{1.63}$$

and replacing momenta by the corresponding operators one gets,

$$\boldsymbol{p} = \frac{\hbar}{\mathrm{i}}\boldsymbol{\nabla} \Longrightarrow \boldsymbol{r}\times\boldsymbol{\nabla} = \frac{\mathrm{i}}{\hbar}\boldsymbol{r}\times\boldsymbol{p} = \frac{\mathrm{i}}{\hbar}\boldsymbol{L} \tag{1.64}$$

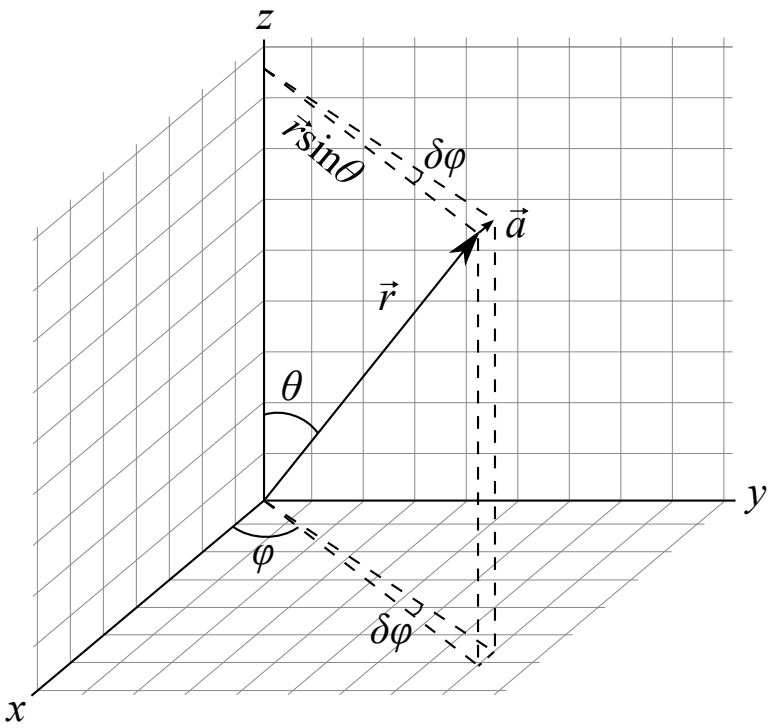

Figure 1.1: Angle $\delta\varphi$ corresponding to the rotation of the system and the relation among the radius $\vec{r}$, the radius increment $\vec{a}$ and the angle increment $\delta\varphi$.

Finally one obtains,

$$\Psi(\boldsymbol{r}) = F(\boldsymbol{r}) - \frac{\mathrm{i}}{\hbar}\delta\boldsymbol{\varphi}\cdot\boldsymbol{L}F(\boldsymbol{r}) = \left(1 - \frac{\mathrm{i}}{\hbar}\delta\boldsymbol{\varphi}\cdot\boldsymbol{L}\right)F(\boldsymbol{r}) \tag{1.65}$$

For a finite angle $\boldsymbol{\varphi}$ one defines a small angle by using $\delta\boldsymbol{\varphi} = \boldsymbol{\varphi}/n$, where n is a large number. Rotating n times, i. e. applying the rotation operator n times, and in the limit of $n = \infty$, one gets,

$$\Psi(\boldsymbol{r}) = \lim_{n\to\infty}\left(1 - \frac{\mathrm{i}}{\hbar}\frac{\boldsymbol{\varphi}\cdot\boldsymbol{L}}{n}\right)^n F(\boldsymbol{r}) \tag{1.66}$$

Since the Euler's number e is

$$\mathrm{e} = \lim_{n\to\infty}(1 + 1/n)^n \tag{1.67}$$

one can write

$$\Psi(\boldsymbol{r}) = \mathrm{e}^{-\frac{\mathrm{i}}{\hbar}\boldsymbol{\varphi}\cdot\boldsymbol{L}}F(\boldsymbol{r}) = \mathrm{e}^{-\frac{\mathrm{i}}{\hbar}\boldsymbol{\varphi}\cdot\boldsymbol{L}}\Psi(\boldsymbol{r}+\boldsymbol{a}) \tag{1.68}$$

Therefore the rotation operator is

$$U_R = \mathrm{e}^{-\frac{\mathrm{i}}{\hbar}\boldsymbol{\varphi}\cdot\boldsymbol{L}} \tag{1.69}$$

and one gets

$$\Psi(\boldsymbol{r}+\boldsymbol{a}) = U_R^{-1}\Psi(\boldsymbol{r}) \tag{1.70}$$

If the Hamiltonian is rotational invariant

$$H\Psi_n(\boldsymbol{r}+\boldsymbol{a}) = E_n\Psi(\boldsymbol{r}+\boldsymbol{a}) = E_nU_R^{-1}\Psi(\boldsymbol{r}) = U_R^{-1}H\Psi(\boldsymbol{r}) \tag{1.71}$$

$$U_RH\Psi_n(\boldsymbol{r}+\boldsymbol{a}) = U_RHU_R^{-1}\Psi(\boldsymbol{r}) = H\Psi(\boldsymbol{r}) \tag{1.72}$$

$$[H, U_R] = 0 \Longrightarrow [H, \boldsymbol{L}] = 0 \tag{1.73}$$

That is, if there is rotational invariance, then the angular momentum is conserved.

Parity symmetry

The parity operator $\hat{\pi}$ is defined as,

$$\hat{\pi}|x\rangle = |-x\rangle \tag{1.74}$$

it is $\hat{\pi}^\dagger = \hat{\pi}$ (exercise) The eigenvalues of the parity operator are obtained as,

$$\hat{\pi}|\Psi_\lambda\rangle = \lambda|\Psi_\lambda\rangle \Longrightarrow \hat{\pi}^2|\Psi_\lambda\rangle = \lambda^2|\Psi_\lambda\rangle \tag{1.75}$$

since

$$\hat{\pi}^2|x\rangle = |x\rangle \tag{1.76}$$

one gets

$$\lambda^2|\Psi_\lambda\rangle = |\Psi_\lambda\rangle \Longrightarrow \lambda = \pm 1 \tag{1.77}$$

in x-space it is

$$\langle x|\hat{\pi}|\Psi_\lambda\rangle = \langle -x|\Psi_\lambda\rangle = \Psi_\lambda(-x) = \lambda\Psi_\lambda(x) \tag{1.78}$$

$$\Psi_\lambda(x) = \begin{cases} \text{even}, & \lambda = 1 \\ \text{odd}, & \lambda = -1 \end{cases} \tag{1.79}$$

If $[H, \hat{\pi}]$=0, as it happens with potentials with reflection symmetry, parity is conserved and λ is a good quantum number.

1.5 Sum of angular momenta

We will first analyze the possible angular momentum values of a two-particle system. The angular momenta of the particles are $\boldsymbol{l}_1$ and $\boldsymbol{l}_2$ and the total angular momentum is $\boldsymbol{L} = \boldsymbol{l}_1 + \boldsymbol{l}_2$. The components $\hat{L}_x, \hat{L}_y, \hat{L}_z$ of $\boldsymbol{L}$ satisfy the commutation relations

$$[\hat{\boldsymbol{L}}^2, \hat{L}_i] = 0 \quad (i = x, y, z) \tag{1.80}$$

$$[\hat{L}_x, \hat{L}_y] = \mathrm{i}\hbar\hat{L}_z, \quad [\hat{L}_y, \hat{L}_z] = \mathrm{i}\hbar\hat{L}_x, \quad [\hat{L}_z, \hat{L}_x] = \mathrm{i}\hbar\hat{L}_y \tag{1.81}$$

and the same for $\boldsymbol{l}_1$ and $\boldsymbol{l}_2$.

Besides, since the degrees of freedom of the particles are independent of each other one also has

$$[\hat{\boldsymbol{l}}_1, \hat{\boldsymbol{l}}_2] = 0, \quad [\hat{\boldsymbol{l}_2}^2, \hat{\boldsymbol{l}}_1] = [\hat{\boldsymbol{l}_1}^2, \hat{\boldsymbol{l}}_2] = 0. \tag{1.82}$$

The eigenvectors corresponding to these operators are given by

$$\begin{array}{rclcrcl} \hat{\boldsymbol{L}}_1^2|l_1m_1\rangle & = & \hbar^2 l_1(l_1+1)|l_1m_1\rangle & ; & \hat{L}_{1z}|l_1m_1\rangle & = & \hbar m_1|l_1m_1\rangle \\ \hat{\boldsymbol{L}}_2^2|l_2m_2\rangle & = & \hbar^2 l_2(l_2+1)|l_2m_2\rangle & ; & \hat{L}_{2z}|l_2m_2\rangle & = & \hbar m_2|l_2m_2\rangle \\ \hat{\boldsymbol{L}}^2|lm\rangle & = & \hbar^2 l(l+1)|lm\rangle & ; & \hat{L}_z|lm\rangle & = & \hbar m|lm\rangle \end{array} \tag{1.83}$$

$$|l_1 - l_2| \leqslant l \leqslant l_1 + l_2, \quad m = m_1 + m_2. \tag{1.84}$$

We have

$$-l_i \leqslant m_i \leqslant l_i, \quad -l \leqslant m \leqslant l \tag{1.85}$$

Not all the quantum numbers related to these operators can be used to label the states. In other words, not all of them can be taken as good quantum numbers. To see the reason for this we will analyze the behavior of commuting operators.

Given two operators and their eigenstates as

$$\hat{A}|\alpha\rangle = a|\alpha\rangle \quad \text{and} \quad \hat{B}|\beta\rangle = b|\beta\rangle \tag{1.86}$$

and assuming that they commute, i. e. $[\hat{A}, \hat{B}] = 0$, then they have common eigenvalues (see Homework-problems 1), i. e.,

$$\hat{A}|\alpha\beta\rangle = a|\alpha\beta\rangle, \quad \hat{B}|\alpha\beta\rangle = b|\alpha\beta\rangle \tag{1.87}$$

Therefore one cannot choose as quantum numbers to label simultaneously the states the eigenvalues of, e. g., $\hat{\boldsymbol{L}}_1^2$, $\hat{L}_{1z}$, $\hat{L}_{2x}$ and $\hat{L}_{2z}$, since these two last operators do not commute with each other. But

there are many combinations one can choose. For instance, one can choose the eigenvalues of $\hat{\boldsymbol{L}}_1^2$, $\hat{L}_{1x}$, $\hat{\boldsymbol{L}}_2^2$, $\hat{L}_{2x}$. However, it is standard in Quantum Mechanics to choose as quantum numbers the eigenvalues of the z-component of all angular momenta. Therefore the standard choose (which corresponds to all existing Tables of angular momentum coefficients) is $\hat{\boldsymbol{L}}_1^2$, $\hat{L}_{1z}$, $\hat{\boldsymbol{L}}_2^2$, $\hat{L}_{2z}$ or $\hat{\boldsymbol{L}}_1^2$, $\hat{\boldsymbol{L}}_2^2$, $\hat{\boldsymbol{L}}^2$, $\hat{L}_z$, i.e. the standard eigenvectors used to label the angular momenta are

$$|l_1 m_1 l_2 m_2\rangle \quad \text{or} \quad |l_1 l_2 l m\rangle \tag{1.88}$$

and, therefore, the standard projectors are

$$\sum_{l_1 m_1 l_2 m_2} |l_1 m_1 l_2 m_2\rangle\langle l_1 m_1 l_2 m_2| = \hat{I} \quad \text{or} \quad \sum_{l_1 l_2 l m} |l_1 l_2 l m\rangle\langle l_1 l_2 l m| = \hat{I} \tag{1.89}$$

One can write the vector in one representation in terms of the other representation, for instance

$$|l_1 m_1 l_2 m_2\rangle = \sum_{lm} |l_1 l_2 l m\rangle\langle l_1 l_2 l m|l_1 m_1 l_2 m_2\rangle, \tag{1.90}$$

and

$$|l_1 m_1 l_2 m_2\rangle = \sum_{lm} \langle l_1 m_1 l_2 m_2|l m\rangle|l_1 l_2 l m\rangle \tag{1.91}$$

The number $\langle l_1 m_1 l_2 m_2|lm\rangle = \langle l_1 l_2 lm|l_1 m_1 l_2 m_2\rangle$ is real and is called Clebsch-Gordan coefficient. Due to the orthonormality of the basis elements

$$|l_1 l_2 l m\rangle = \sum_{m_1 m_2} \langle l_1 m_1 l_2 m_2|l m\rangle|l_1 m_1 l_2 m_2\rangle \tag{1.92}$$

If the Hamiltonian corresponding to the two-particle system is spherically symmetric then the eigenstates of the Hamiltonian can be labeled by the eigenvalues of the angular momenta shown above.

Symmetry properties of the Clebsch-Gordan coefficient

The Clebsch-Gordan coefficient can best be written in terms of the 3-j symbol defined as

$$\begin{pmatrix} l_1 & l_2 & l \\ m_1 & m_2 & -m \end{pmatrix} = \frac{(-1)^{l_1 - l_2 + m}}{\sqrt{2l+1}} \langle l_1 m_1 l_2 m_2|lm\rangle \tag{1.93}$$

with the properties that

1. $\begin{pmatrix} l_1 & l_2 & l \\ m_1 & m_2 & m \end{pmatrix} = \begin{pmatrix} l_2 & l & l_1 \\ m_2 & m & m_1 \end{pmatrix} = \begin{pmatrix} l & l_1 & l_2 \\ m & m_1 & m_2 \end{pmatrix}$
2. $\begin{pmatrix} l_1 & l_2 & l \\ m_1 & m_2 & m \end{pmatrix} = (-1)^{l_1+l_2+l} \begin{pmatrix} l_2 & l_1 & l \\ m_2 & m_1 & m \end{pmatrix}$
3. $\begin{pmatrix} l_1 & l_2 & l \\ -m_1 & -m_2 & -m \end{pmatrix} = (-1)^{l_1+l_2+l} \begin{pmatrix} l_1 & l_2 & l \\ m_1 & m_2 & m \end{pmatrix}$
4. $m_1 + m_2 - m = 0$

Short Algebraic Table of the 3-j Symbols

$$\begin{aligned} \begin{pmatrix} j_1 & j_2 & j_3 \\ 0 & 0 & 0 \end{pmatrix} &= (-1)^{J/2} \left[\frac{(J-2j_1)!(J-2j_2)!(J-2j_3)!}{(J+1)!}\right]^{1/2} \\ &\quad \times \frac{(\frac{1}{2}J)!}{(\frac{1}{2}J - j_1)!(\frac{1}{2}J - j_2)!(\frac{1}{2}J - j_3)!} \end{aligned} \tag{1.94}$$

where $J = j_1 + j_2 + j_3$ is even.

$$\begin{pmatrix} j & j & 0 \\ m & -m & 0 \end{pmatrix} = (-1)^{j-m}\left[\frac{1}{2j+1}\right]^{1/2} \tag{1.95}$$

$$\begin{pmatrix} j+\frac{1}{2} & j & \frac{1}{2} \\ m & -m-\frac{1}{2} & \frac{1}{2} \end{pmatrix} = (-1)^{j-m-\frac{1}{2}}\left[\frac{j-m+\frac{1}{2}}{(2j+2)(2j+1)}\right]^{1/2} \tag{1.96}$$

$$\begin{pmatrix} j+1 & j & 1 \\ m & -m-1 & 1 \end{pmatrix} = (-1)^{j-m-1}\left[\frac{(j-m)(j-m+1)}{(2j+3)(2j+2)(2j+1)}\right]^{1/2} \tag{1.97}$$

$$\begin{pmatrix} j+1 & j & 1 \\ m & -m & 0 \end{pmatrix} = (-1)^{j-m-1}\left[\frac{2(j+m+1)(j-m+1)}{(2j+3)(2j+2)(2j+1)}\right]^{1/2} \tag{1.98}$$

$$\begin{pmatrix} j & j & 1 \\ m & -m-1 & 1 \end{pmatrix} = (-1)^{j-m}\left[\frac{2(j-m)(j+m+1)}{(2j+2)(2j+1)(2j)}\right]^{1/2} \tag{1.99}$$

$$\begin{pmatrix} j & j & 1 \\ m & -m & 0 \end{pmatrix} = (-1)^{j-m}\frac{2m}{[(2j+2)(2j+1)(2j)]^{1/2}} \tag{1.100}$$

The orthogonality relations,

$$(2j+1)\sum_{m_1 m_2}\begin{pmatrix} j_1 & j_2 & j \\ m_1 & m_2 & m \end{pmatrix}\begin{pmatrix} j_1 & j_2 & j' \\ m_1 & m_2 & m' \end{pmatrix} = \delta_{jj'}\delta_{mm'}. \tag{1.101}$$

$$\sum_{jm}(2j+1)\begin{pmatrix} j_1 & j_2 & j \\ m_1 & m_2 & m \end{pmatrix}\begin{pmatrix} j_1 & j_2 & j \\ m_1' & m_2' & m \end{pmatrix} = \delta_{m_1 m_1'}\delta_{m_2 m_2'}. \tag{1.102}$$

6-j symbols

In the sum of three angular momenta one can choose the partition

$$\boldsymbol{J} = \boldsymbol{j}_1 + \boldsymbol{j}_2 + \boldsymbol{j}_3 = \boldsymbol{J}_{12} + \boldsymbol{j}_3 = \boldsymbol{j}_1 + \boldsymbol{J}_{23} \tag{1.103}$$

where

$$\boldsymbol{J}_{12} = \boldsymbol{j}_1 + \boldsymbol{j}_2, \quad \boldsymbol{J}_{23} = \boldsymbol{j}_2 + \boldsymbol{j}_3 \tag{1.104}$$

One can write the basis vector in one representation in terms of the other representation as

$$|(j_1 j_2)J_{12} j_3; JM\rangle = \sum_{J_{23}}\langle j_1(j_2 j_3)J_{23}; J|(j_1 j_2)J_{12} j_3; J\rangle |j_1(j_2 j_3)J_{23}; JM\rangle \tag{1.105}$$

The symmetry properties of the expansion coefficient can best be seen by introducing the 6-j symbol as

$$\langle j_1(j_2 j_3)J_{23}; J|(j_1 j_2)J_{12} j_3; J\rangle = (-1)^{j_1+j_2+j_3+J}\sqrt{(2J_{12}+1)(2J_{23}+1)}\begin{Bmatrix} j_1 & j_2 & J_{12} \\ j_3 & J & J_{23} \end{Bmatrix} \tag{1.106}$$

which is a real number (therefore it is the same for $\langle (j_1 j_2)J_{12} j_3; J|j_1(j_2 j_3)J_{23}; J\rangle$). The 6-j symbol does not change if two columns are inter changed, for instance

$$\begin{Bmatrix} j_1 & j_2 & J_{12} \\ j_3 & J & J_{23} \end{Bmatrix} = \begin{Bmatrix} j_1 & J_{12} & j_2 \\ j_3 & J_{23} & J \end{Bmatrix}. \tag{1.107}$$

The 6-j symbol is also invariant if upper and lower arguments are interchanged in any two columns,

$$\begin{Bmatrix} j_1 & j_2 & j_3 \\ j_4 & j_5 & j_6 \end{Bmatrix} = \begin{Bmatrix} j_4 & j_5 & j_3 \\ j_1 & j_2 & j_6 \end{Bmatrix} = \begin{Bmatrix} j_1 & j_5 & j_6 \\ j_4 & j_2 & j_3 \end{Bmatrix} = \begin{Bmatrix} j_4 & j_2 & j_6 \\ j_1 & j_5 & j_3 \end{Bmatrix} \tag{1.108}$$

.

The angular momentum triangular relation must be satisfied for (j_1, j_2, J_{12}), (j_1, J, J_{23}), (j_3, j_2, J_{23}) and (j_3, J, J_{12}). Thus, e.g.,

$$\begin{Bmatrix} 1/2 & 1/2 & 0 \\ 1/2 & 1/2 & 2 \end{Bmatrix} = 0 \tag{1.109}$$

since $1/2 + 1/2 < 2$.

In general, When $j_6 = 0$ the expression for the 6-j symbol can be written as

$$\begin{Bmatrix} j_1 & j_2 & j_3 \\ j_4 & j_5 & 0 \end{Bmatrix} = \frac{\delta_{j_2,j_4}\delta_{j_1,j_5}}{\sqrt{(2j_1+1)(2j_2+1)}}(-1)^{j_1+j_2+j_3}\{j_1, j_2, j_3\}. \tag{1.110}$$

The function $\{\}$ is equal to 1 when the triad satisfies the triangle conditions, and zero otherwise.

The 6-j symbols satisfy the orthogonality relation,

$$\sum_{j_3}(2j_3+1)\begin{Bmatrix} j_1 & j_2 & j_3 \\ j_4 & j_5 & j_6 \end{Bmatrix}\begin{Bmatrix} j_1 & j_2 & j_3 \\ j_4 & j_5 & j_6' \end{Bmatrix} = \frac{\delta_{j_6 j_6'}}{2j_6+1}\{j_1, j_5, j_6\}\{j_4, j_2, j_6\}. \tag{1.111}$$

9-j symbols

In the case of 4 angular momenta

$$\boldsymbol{J} = \boldsymbol{j}_1 + \boldsymbol{j}_2 + \boldsymbol{j}_3 + \boldsymbol{j}_4 \tag{1.112}$$

one can write, e.g.,

$$\boldsymbol{J} = \boldsymbol{J}_{12} + \boldsymbol{J}_{34} = \boldsymbol{J}_{13} + \boldsymbol{J}_{24} \tag{1.113}$$

where $\boldsymbol{J}_{12} = \boldsymbol{j}_1 + \boldsymbol{j}_2$, $\boldsymbol{J}_{34} = \boldsymbol{j}_3 + \boldsymbol{j}_4$, $\boldsymbol{J}_{13} = \boldsymbol{j}_1 + \boldsymbol{j}_3$ and $\boldsymbol{J}_{24} = \boldsymbol{j}_2 + \boldsymbol{j}_4$.

One can thus write

$$\begin{aligned} |(j_1 j_3)J_{13}(j_2 j_4)J_{24}; JM\rangle \quad = \quad & \sum_{J_{12}J_{34}} \langle (j_1 j_2)J_{12}(j_3 j_4)J_{34}; J|(j_1 j_3)J_{13}(j_2 j_4)J_{24}; JM\rangle \\ & \times |(j_1 j_2)J_{12}(j_3 j_4)J_{34}; J\rangle \end{aligned} \tag{1.114}$$

and the 9-j symbol is defined by,

$$\begin{aligned} &\langle (j_1 j_2)J_{12}(j_3 j_4)J_{34}; J|(j_1 j_3)J_{13}(j_2 j_4)J_{24}; J\rangle \\ &\qquad = \sqrt{(2J_{12}+1)(2J_{34}+1)(2J_{13}+1)(2J_{24}+1)}\begin{Bmatrix} j_1 & j_2 & J_{12} \\ j_3 & j_4 & J_{34} \\ J_{13} & J_{24} & J \end{Bmatrix} \end{aligned} \tag{1.115}$$

which is also a real number.

The symmetry properties of the 9-j symbols are

1. Any permutation of rows and columns does not change the 9-j symbol except the sign, which is plus if the permutation is even and $(-1)^S$, where S is the sum of all angular momenta, if the permutation is odd.

   For example, we have,

   $$\begin{Bmatrix} j_1 & j_2 & j_3 \\ j_4 & j_5 & j_6 \\ j_7 & j_8 & j_9 \end{Bmatrix} = (-1)^S \begin{Bmatrix} j_4 & j_5 & j_6 \\ j_1 & j_2 & j_3 \\ j_7 & j_8 & j_9 \end{Bmatrix} = (-1)^S \begin{Bmatrix} j_2 & j_1 & j_3 \\ j_5 & j_4 & j_6 \\ j_8 & j_7 & j_9 \end{Bmatrix}, \tag{1.116}$$

   where

   $$S = \sum_{i=1}^{9} j_i. \tag{1.117}$$

2. The 9-j symbol does not change under a reflection about either diagonal.

   $$\begin{Bmatrix} j_1 & j_2 & j_3 \\ j_4 & j_5 & j_6 \\ j_7 & j_8 & j_9 \end{Bmatrix} = \begin{Bmatrix} j_1 & j_4 & j_7 \\ j_2 & j_5 & j_8 \\ j_3 & j_6 & j_9 \end{Bmatrix} = \begin{Bmatrix} j_9 & j_6 & j_3 \\ j_8 & j_5 & j_2 \\ j_7 & j_4 & j_1 \end{Bmatrix} \tag{1.118}$$

The 9-j symbols can be calculated as sums over triple-products of 6-j symbols where the summation extends over all "x" admitted by the triangle condition,

$$\begin{Bmatrix} j_1 & j_2 & j_3 \\ j_4 & j_5 & j_6 \\ j_7 & j_8 & j_9 \end{Bmatrix} = \sum_x (-1)^{2x}(2x+1)\begin{Bmatrix} j_1 & j_4 & j_7 \\ j_8 & j_9 & x \end{Bmatrix}\begin{Bmatrix} j_2 & j_5 & j_8 \\ j_4 & x & j_6 \end{Bmatrix}\begin{Bmatrix} j_3 & j_6 & j_9 \\ x & j_1 & j_2 \end{Bmatrix}. \tag{1.119}$$

When $j_9 = 0$ the 9-j symbol is proportional to a 6-j symbol as

$$\left\{ \begin{array}{ccc} j_1 & j_2 & j_3 \\ j_4 & j_5 & j_6 \\ j_7 & j_8 & 0 \end{array} \right\} = \frac{\delta_{j_3,j_6}\delta_{j_7,j_8}}{\sqrt{(2j_3+1)(2j_7+1)}}(-1)^{j_2+j_3+j_4+j_7} \left\{ \begin{array}{ccc} j_1 & j_2 & j_3 \\ j_5 & j_4 & j_7 \end{array} \right\}. \tag{1.120}$$

The 9-j symbols satisfy this orthogonality relation,

$$\sum_{j_7 j_8}(2j_7+1)(2j_8+1) \left\{ \begin{array}{ccc} j_1 & j_2 & j_3 \\ j_4 & j_5 & j_6 \\ j_7 & j_8 & j_9 \end{array} \right\} \left\{ \begin{array}{ccc} j_1 & j_2 & j_3' \\ j_4 & j_5 & j_6' \\ j_7 & j_8 & j_9 \end{array} \right\} = \frac{\delta_{j_3 j_3'}\delta_{j_6 j_6'}\{j_1 j_2 j_3\}\{j_4 j_5 j_6\}\{j_3 j_6 j_9\}}{(2j_3+1)(2j_6+1)}. \tag{1.121}$$

1.6 Homework problems

Exercise 1:

Using the eigenvectors and eigenvalues of the Pauli matrix σ_z as a basis evaluate the eigenvalues and eigenvectors of σ_x and σ_y, where $\sigma_x = \begin{pmatrix} 0 & 1 \\ 1 & 0 \end{pmatrix}$, $\sigma_y = \begin{pmatrix} 0 & -i \\ i & 0 \end{pmatrix}$ and $\sigma_z = \begin{pmatrix} 1 & 0 \\ 0 & -1 \end{pmatrix}$.

Exercise 2:

a) Why translating the system of coordinates by an amount $+\Delta\mathbf{r}$ the function $\Psi(\mathbf{r})$ becomes $\Psi(\mathbf{r} - \mathbf{\Delta r})$? (Eq. (1.45) of Chapter 1).

b) Show that the parity operator is Hermitian.

Exercise 3:

Show that if the operators A and B commute, then they have common eigenvectors.

Exercise 4:

a) Show that $|j_1 j_2 JM\rangle = (-1)^{j_1+j_2-J}|j_2 j_1 JM\rangle$

b) Evaluate the following Clebsh-Gordan coefficients:

i) $\langle j+1/2\ j-1/2\ 1/2\ 1/2|j\ j\rangle$,

ii) $\langle j+1/2\ j+1/2\ 1/2\ -1/2|j\ j\rangle$,

iii) $\langle j-1/2\ j-1/2\ 1/2\ 1/2|j\ j\rangle$ and

iv) $\langle j-1/2\ j+1/2\ 1/2\ \ -1/2|j\ j\rangle$.

Exercise 5:

a) Which is the relation between m_1, m_2 and m, and between j_1, j_2 and j in the Clebsh-Gordon coefficient $CG = \langle j_1 m_1 j_2 m_2|jm\rangle$.

b) Show that $CG = \langle jmjm|JM\rangle$=0 if $2j - J$ is odd. Which is the value of J if $j = 1/2$?

c) Show that $\left\{ \begin{array}{ccc} \frac{9}{2} & 1 & \frac{7}{2} \\ \frac{5}{2} & 2 & \frac{3}{2} \end{array} \right\} = 0$ and $\left\{ \begin{array}{ccc} 2 & 1 & 1 \\ 2 & 1 & 1 \\ 3 & 2 & 2 \end{array} \right\} = 0.$

Chapter 2

Gamow states and the Berggren representation

One of the main difficulties when studying processes occurring in the continuum is that the relevant physical processes are time-dependent. The system is sensitive to the initial conditions and can easily fall into chaos. The Gamow model presents a way to study the continuum by time-independent formalisms in the complex energy plane. The physical reason behind is that, when the system is trapped by a high enough barrier, it can remain in a localized region of space for a considerable long time. In this case the system can be treated as quasistationary. In the following we will present these time-independent formalisms for the evolution of the system in the complex energy plane.

2.1 One-particle Hamiltonian in one dimension

The one-dimension Hamiltonian is.

$$\left[-\frac{\hbar^2}{2\mu}\frac{\mathrm{d}^2}{\mathrm{d}x^2}+V(x)\right]\Phi_n(x)=E_n\Phi_n(x) \tag{2.1}$$

and we will consider the square well potential shown in Fig. 2.1. There can be discrete and continuum states in this case, as seen in Fig. 2.1. To solve the eigenvalue problem given by Eq. (2.1) we notice that there are two regions:

Region (1): $0<x<a$; $V(x)=-V_0$
Region (2): $x\geqslant a$; $V(x)=0$

There are also two possibilities for the energy: Continue ($E=E_c>0$) and Bound ($E=-E_b<0$)

$$\begin{aligned}
\text{Region (1):} \quad & \left[-\frac{\hbar^2}{2\mu}\frac{\mathrm{d}^2}{\mathrm{d}x^2}-V_0\right]\Phi_n^{(1)}(x) &=& E_n\Phi_n^{(1)}(x)\\
\text{Region (2):} \quad & \left[-\frac{\hbar^2}{2\mu}\frac{\mathrm{d}^2}{\mathrm{d}x^2}\right]\Phi_n^{(2)}(x) &=& E_n\Phi_n^{(2)}(x)
\end{aligned}$$

with

$$q^2=\frac{2\mu}{\hbar^2}(E_n+V_0);\quad k^2=\frac{2\mu}{\hbar^2}E_n$$

the eigenvectors solution of the eigenvalue problem are

$$\begin{cases}\Phi_n^{(1)}(x)=A_n\mathrm{e}^{\mathrm{i}qx}+B_n\mathrm{e}^{-\mathrm{i}qx}\\ \Phi_n^{(2)}(x)=C_n\mathrm{e}^{\mathrm{i}kx}+D_n\mathrm{e}^{-\mathrm{i}kx}\end{cases}$$

To determine the constant A_n, B_n, C_n and D_n, the boundary conditions of continuity of density and current have to be applied. In addition, since $V(x)=\infty$ for $x\leqslant 0$, one has

$$\Phi_n^{(1)}(x=0)=0\Longrightarrow A_n+B_n=0$$

I) Bound states

$$q^2=\frac{2\mu}{\hbar^2}(V_0-E_b)>0;\quad k^2=-\frac{2\mu}{\hbar^2}E_b<0$$

Notice that we assume $E_b>0$ and, therefore, the energy of the bound state is $-E_b$.

$$k=\pm\mathrm{i}\chi;\quad \chi=\sqrt{\frac{2\mu E_b}{\hbar^2}}$$

$$\begin{cases}\Phi_n^{(1)}(a)=\Phi_n^{(2)}(a)\\ \dfrac{\mathrm{d}}{\mathrm{d}x}\Phi_n^{(1)}(x)\Big|_{x=a}=\dfrac{\mathrm{d}}{\mathrm{d}x}\Phi_n^{(2)}(x)\Big|_{x=a}\end{cases}$$

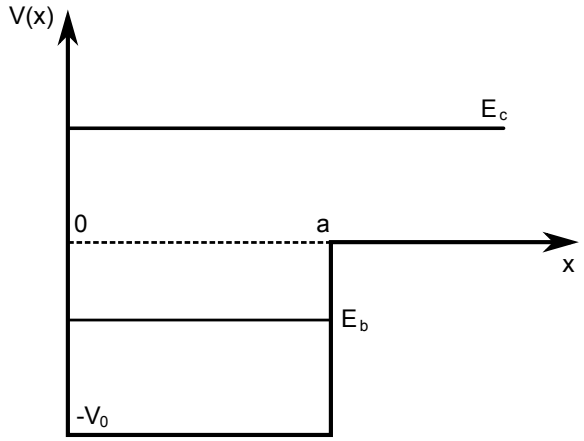

Figure 2.1: Square well potential in one-dimension. The range of the potential is a and the depth is $-V_0$. For $x < 0$ the potential is infinite and, therefore, the wave function vanishes at $x = 0$. E_b (E_c) is the energy of a bound (continuum) state.

An additional condition in $\Phi_n^{(2)}(x) = C_n \mathrm{e}^{-\chi x} + D_n \mathrm{e}^{\chi x}$ is that since $\mathrm{e}^{\chi x}$ diverges as $x \to \infty$ one has to impose $D_n = 0$. Besides there is the normalization condition. With the constants thus evaluated one obtains the possible energies as those for which the continuity relations are satisfied.

II) Continuum

$$q^2 = \frac{2\mu}{\hbar^2}(V_0 + E_c) > 0; \quad k^2 = \frac{2\mu}{\hbar^2} E_c > 0$$

assuming that the system is confined in the region

$$0 < x < L \Longrightarrow \int_0^L |\Phi_n(x)|^2 \, \mathrm{d}x = 1$$

Notice that all energies $E_c > 0$ are allowed in the continuum, but only a discrete number of energies $-E_b < 0$ are allowed as bound states.

In these cases the projector becomes,

$$\hat{I} = \sum_{n=1}^{N} |n\rangle\langle n| + \int \mathrm{d}\alpha |\alpha\rangle\langle\alpha| \tag{2.2}$$

where $|n\rangle$ ($|\alpha\rangle$) is a discrete (continuum) state.

The orthonormalization condition now reads,

$$\delta(\boldsymbol{r} - \boldsymbol{r}') = \sum_{n=1}^{N} \Psi_n^*(\boldsymbol{r}) \Psi_n(\boldsymbol{r}') + \int \mathrm{d}\alpha \Psi_\alpha^*(\boldsymbol{r}) \Psi_\alpha(\boldsymbol{r}') \tag{2.3}$$

2.2 Square barrier

This potential is defined as

$V(x < 0) = \infty; V(0 < x < a) = 0; V(a < x < b) = V_0 > 0; V(x > b) = 0$

There are three regions.

Region **I**, $0 < x < a; V_I(x) = 0$

Schrödinger equation

$$H\varphi_I(k, x) = -\frac{\hbar^2}{2m} \frac{d^2}{dx} \varphi_I(k, x) = E\varphi_I(k, x)$$

i. e., $(d^2/dx^2 + k^2)\varphi_I(k,x) = 0$, where $k = \pm\sqrt{2mE}/\hbar$.

$\varphi_I(k,0) = 0 \Longrightarrow \varphi_I(k,x) = A\sin(kx)$

Region **II**, $a < x < b; V_{II}(x) = V_0$

$$H\varphi_{II}(k,x) = (-\frac{\hbar^2}{2m}\frac{d^2}{dx} + V_0)\varphi_{II}(k,x) = E\varphi_{II}(k,x)$$

i. e., $(d^2/dx^2 - \kappa^2)\varphi_{II}(\kappa,x) = 0$, where $\kappa^2 = 2m(V_0 - E)/\hbar^2 > 0$.

$$\varphi_{II}(\kappa,x) = A_1 e^{\kappa x} + A_2 e^{-\kappa x} \tag{2.4}$$

Region **III**, $x > b; V_{III}(x) = 0$

$\varphi_{III}(k,x) = B_o e^{ikx} + B_i e^{-ikx}$

Boundary conditions

1) At x=a

$$A\sin(ka) = A_1 e^{\kappa a} + A_2 e^{-\kappa a}$$
$$Ak\cos(ka) = \kappa(A_1 e^{\kappa a} - A_2 e^{-\kappa a})$$

Which gives,

$A_1 = A\Delta_1/\Delta$, $A_2 = A\Delta_2/\Delta$, where

$$\Delta_1 = \begin{vmatrix} \sin(ka) & e^{-\kappa a} \\ k\cos(ka) & -\kappa e^{-\kappa a} \end{vmatrix} = -e^{-\kappa a}(\kappa\sin(ka) + k\cos(ka))$$

$$\Delta_2 = \begin{vmatrix} e^{\kappa a} & \sin(ka) \\ \kappa e^{\kappa a} & k\cos(ka) \end{vmatrix} = e^{\kappa a}(k\cos(ka) - \kappa\sin(ka))$$

$$\Delta = \begin{vmatrix} e^{\kappa a} & e^{-\kappa a} \\ \kappa e^{\kappa a} & -\kappa e^{-\kappa a} \end{vmatrix} = -2\kappa$$

2) At x=b

$$A_1 e^{\kappa b} + A_2 e^{-\kappa b} = B_o e^{ikb} + B_i e^{-ikb}$$
$$\kappa A_1 e^{\kappa b} - \kappa A_2 e^{-\kappa b} = ikB_o e^{ikb} - ikB_i e^{-ikb}$$

i. e.

$B_o = \Delta_3/\Delta_0$, $B_i = \Delta_4/\Delta_0$, where

$$\Delta_3 = \begin{vmatrix} A_1 e^{\kappa b} + A_2 e^{-\kappa b} & e^{-ikb} \\ \kappa A_1 e^{\kappa b} - \kappa A_2 e^{-\kappa b} & -ike^{-ikb} \end{vmatrix}$$

$$\Delta_4 = \begin{vmatrix} e^{ikb} & A_1 e^{\kappa b} + A_2 e^{-\kappa b} \\ ike^{ikb} & \kappa A_1 e^{\kappa b} - \kappa A_2 e^{-\kappa b} \end{vmatrix}$$

$$\Delta_0 = \begin{vmatrix} e^{ikb} & e^{-ikb} \\ ike^{ikb} & -ike^{-ikb} \end{vmatrix} = -2ik$$

The ratio between the incoming and outgoing wave function amplitudes is

$$\frac{B_i}{B_o} = \frac{\Delta_4}{\Delta_3}$$

Outgoing boundary conditions

This corresponds to $B_i = 0$, i. e. $\Delta_4 = 0$

Phase shift

The wave function in region III can be written as,

$$\varphi_{III}(k,x) = (B_o + B_i)cos(kx) + i(B_o - B_i)sin(kx)$$

calling $B_1 = B_o + B_i$, $B_2 = i(B_o - B_i)$, one gets

$$\varphi_{III}(k,x) = B_2(sin(kx) + \frac{B_1}{B_2}cos(kx))$$

and one defines the phase shift δ as

$$tan\delta = \frac{B_1}{B_2}$$

from where one gets,

$$\varphi_{III}(k,x) = Csin(kx+\delta) \tag{2.5}$$

where C is a constant.

Notice that the difference between regions I and III is a phase shift in the wave function. This is the reason of the name of the angle δ.

At the point $x = b$ the continuity of the density and current can be expressed as the logarithmic derivative of the wave function. This quantity, usually called β, is given by,

$$\beta = \varphi'_{II}(x,b)/\varphi_{II}(x,b)$$

which is evaluated by using the expression (2.4). Continuity implies that it is also,

$$\beta = \varphi'_{III}(x,b)/\varphi_{III}(x,b) = \frac{kcos(kx+\delta)}{sin(kx+\delta)}|_{x=b}$$

By writting $sin(kx+\delta)$ and $cos(kx+\delta)$ in terms of $exp(i(kx+\delta))$ and $exp(-i(kx+\delta))$ one gets,

$$e^{2i\delta} = e^{-2ikb}\frac{\beta+ik}{\beta-ik}$$

The quantity

$$S = e^{2i\delta}$$

is called $S-matrix$. If β is real then it is $S^* = S^{-1}$, that is the S-matrix is unitary.

The value of $\delta(E)$ when E cross the energy of a resonance changes by an angle π.

2.3 Gamow states

The wave function of a resonance with a peak at energy E_0 and a width Γ can be factorized as

$$\Phi(E,\mathbf{r}) = \sqrt{\frac{\Gamma/2}{\pi\left[(E-E_0)^2 + (\Gamma/2)^2\right]}}\,\Psi(\mathbf{r}), \tag{2.6}$$

where $\Psi(\mathbf{r}) = \sqrt{\pi\Gamma/2}\,\Phi(E_0,\mathbf{r})$. Through the Fourier transform, we obtain the time evolution of the resonance

$$\Phi(t,\mathbf{r}) = \int_{-\infty}^{\infty}\Phi(E,\mathbf{r})e^{-iEt/\hbar}dE = \Psi(\mathbf{r})e^{-i\tilde{E}t/\hbar}, \tag{2.7}$$

which gives us the resonance in the form of a stationary state, but with a complex energy

$$\tilde{E} = E_0 - i\frac{\Gamma}{2}. \tag{2.8}$$

The probability of measuring the system at t is given by

$$|\Phi(t,\mathbf{r})|^2 = |\Psi(\mathbf{r})|^2 e^{-\Gamma t/\hbar}. \tag{2.9}$$

The half-life of the resonance can be obtained from

$$T_{1/2} = \frac{\hbar\ln 2}{\Gamma}. \tag{2.10}$$

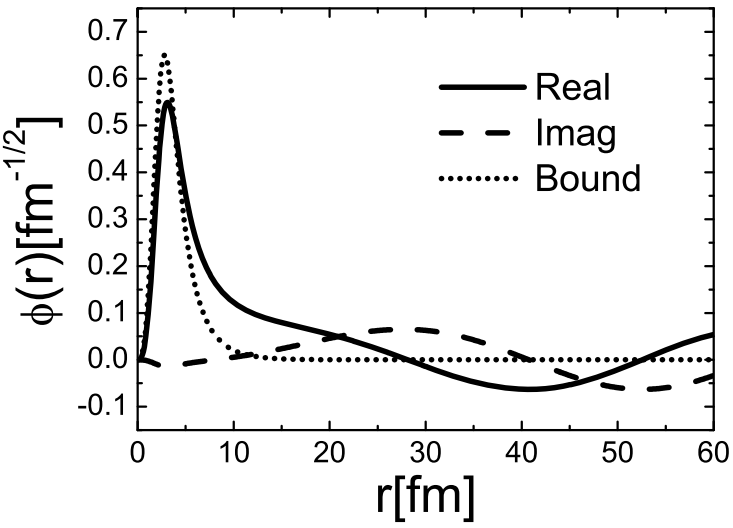

Figure 2.2: Radial function of a narrow resonance and a bound state. The solid and the dashed line denote the real and imaginary part of the wave function of a narrow resonance respectively, while the dotted line denotes the wave function of a bound state.

Therefore a time-dependent process has now been transformed into a stationary problem by going to the complex energy plane. The complex solutions to the corresponding stationary Schrödinger equation are called Gamow states. The wave numbers k_n are a discrete set of complex values, which satisfy

$$\tilde{E}_n = \frac{\hbar^2}{2\mu} k_n^2. \tag{2.11}$$

They can be written as

$$k_n = \kappa_n + i\gamma_n. \tag{2.12}$$

The states can be classified into four classes, namely:

1. bound states, for which $\kappa_n = 0$ and $\gamma_n > 0$;
2. antibound states with $\kappa_n = 0$ and $\gamma_n < 0$;
3. decay resonant states with $\kappa_n > 0$ and $\gamma_n < 0$;
4. capture resonant states with $\kappa_n < 0$ and $\gamma_n < 0$.

Since the radial wave function has the form of $w(E_n, r) \sim e^{ik_n r}$, one can see that the wave function of the resonant states will diverge at infinity. However a narrow resonance can still be treated stationary since the wave function does not diverge at small distance. As shown in Fig. 2.2, the narrow resonance has the same wave function as a bound state inside of the nucleus, but at a large radius far out from the nuclear surface it starts to oscillate and diverge. Since we are interested in the processes occurring at the scale of nuclear distances, we can eventually consider the narrow resonance as a bound state and solve the time-independent Schrödinger equation approximately.

The antibound state has a pure negative imaginary wave number $k_n = -i|\gamma_n|$, which gives the corresponding energy real and negative, as the bound state. However unlike the bound state, whose wave function diminishes exponentially at large distances, the antibound state diverges exponentially. As a result, the antibound state can be physically meaningful only if it is sufficiently close to the threshold. Therefore it may have a great influence on low-energy cross sections and nuclear spectroscopy.

We plotted in Fig. 2.4 the $1s_{1/2}$ antibound state. One sees that it extends in an increasing rate far out from the nuclear surface, as expected in this halo nucleus (the standard value of the radius is here $1.2 \times 11^{1/3}$=2.7 fm).

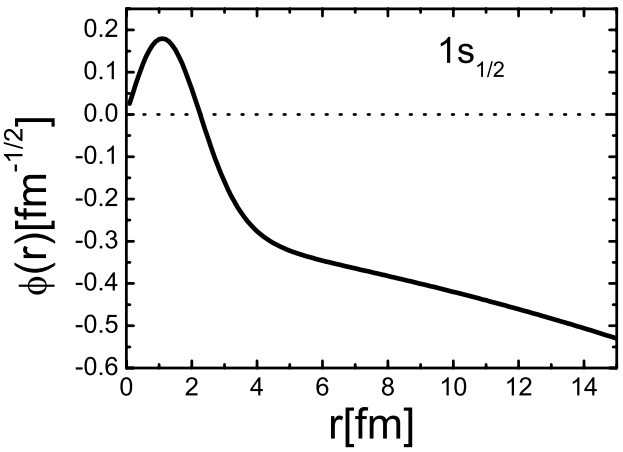

Figure 2.3: Radial function $\phi(r)$ corresponding to the single-particle neutron antibound state $0s_{1/2}$ at an energy of -0.050 MeV. Taken from Ref. [1].

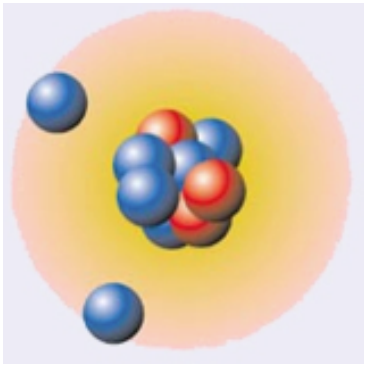

Figure 2.4: A schematic picture of the halo nucleus ^{11}Li.

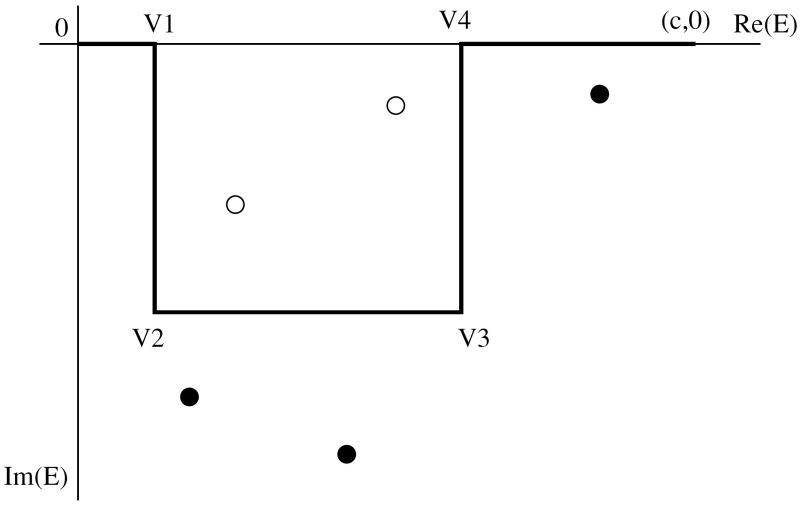

Figure 2.5: Integration contour L^+ in the complex energy plane. The open circles denote the resonances included in the sum of Eq. (2.14), while the solid circles are those excluded. The vertex $(c, 0)$ corresponds to the energy cutoff point c.

2.4 Berggren completeness relation

The eigenvectors of a Hamiltonian provide a representation projector which allows one to write

$$\delta(r - r') = \sum_n w_n(r) w_n(r') + \int_0^\infty dE u(r, E) u(r', E), \tag{2.13}$$

where $w_n(r)$ are the wave functions of the bound states and $u(r, E)$ are the scattering states. The integration contour is along the real energy axis, and all the energies and radial wave functions are real, or more precisely, can be chosen to be real. Notice that only bound states and scattering states enter in Eq. (2.13).

In order to include other Gamow states, Berggren extended the integration contour to the complex energy plane. By using Cauchy theorem, one gets

$$\delta(r - r') = \sum_n \tilde{w}_n^*(r) w_n(r') + \int_{L^+} dE \tilde{u}^*(r, E) u(r', E), \tag{2.14}$$

where $w_n(r)$ are now the wave functions for all the bound and antibound states plus the resonances lying between the real energy axis and the integration contour L^+, as shown in Fig. 2.5. In principle the contour should start at the origin $(0, 0)$, and end at infinity $(\infty, 0)$. However, one usually cuts the basis at a certain maximum energy as in any shell model, within which only a limited number of shells are included.

The tilde over the wave function $w_n(r)$ denotes the mirror state of $w_n(r)$, namely $\tilde{k}_n = -k_n^*$. With this one can prove that $\tilde{w}_n^*(r) = w_n(r)$, and the same for the scattering state $u(r, E)$. Therefore the internal product in Eq. (2.14) is the wave function times itself, and not its complex conjugate. This internal product is called the Berggren metric.

To make the representation useful in real calculations, one has to discretize the contour integral, i.e.

$$\int_{L^+} dE u(r, E) u(r', E) = \sum_p h_p u(r, E_p) u(r', E_p), \tag{2.15}$$

where the quantities E_p are usually selected by the Gaussian method on the contour and h_p are the corresponding weights. Therefore the complete set of orthonormal vectors $|\varphi_j\rangle$ now includes all the bound states, antibound states and resonances inside the contour, i.e., $\langle r|\varphi_n\rangle = w_n(r, E_n)$, and also the discretized scattering states on the contour, i.e., $\langle r|\varphi_p\rangle = \sqrt{h_p} u_p(r, E_p)$. This is the Berggren representation used in the complex shell model calculations.

2.5 Homework problems

Exercise 1: a) Find the eigenvalues and eigenvectors of the impulse operator in one dimension, i. e. $p_x\varphi(x) = k\varphi(x)$, where $p_x = \frac{\hbar}{i}\frac{d}{dx}$, within the range $0 \leq x \leq L$ and the boundary condition $\varphi(0) = \varphi(L)$.
b) The same for p_x^2 with $\varphi(0) = \varphi(L) = 0$.

Exercise 2: Write the unit operator (projector) corresponding to the Hilbert space spanned by the representation given by the eigenfunctions $\varphi(x)$ of the one-particle Hamiltonian

$$H = -\frac{\hbar^2}{2m}\frac{d^2}{dx^2} + V(x),$$

where $V(x) = \infty$ for $x = 0$, $V(x) = -V_0$ for $0 < x \leq a$ and $V(x) = 0$ for $x > a$. Assume that the wave function in the continuum is normalized to unity within the region $0 < x \leq L$.

Bibliography

[1] Z.X. Xu, R.J. Liotta, C. Qi, T. Roger, P. Roussel-Chomaz, H. Savajols, R. Wyss, Nucl. Phys. A 850, 53-68 (2011).

Chapter 3

Nuclear Shell Model

Introduction to the shell model. Shell model representation. Shell model central potential. Shell closures and the magic numbers. Particle excitations. Hole excitations.

3.1 Introduction to the shell model

The general Hamiltonian corresponding to the motion of the A=N+Z nucleons in a nucleus is

$$H = \sum_{i=1}^{A} \frac{\boldsymbol{p_i^2}}{2m_i} + \sum_{i<j=1}^{A} V_{ij} \tag{3.1}$$

where m_i is the mass of the ith nucleon ($m_i c^2 \approx 940$ (938) MeV for neutrons (protons)) and V_{ij} is the nucleon-nucleon interaction. To find the eigenvectors and eigenvalues of this Hamiltonian exactly is beyond of what is possible at present and even in the foreseeable future. The main reason why the nuclear Hamiltonian cannot be treated is that one does not know how to evaluate the nucleon-nucleon interaction starting from the underlying theory (QCD). It is not only this what is the problem. Even if the interaction were known the task of treating the Hamiltonian (3.1) for medium and heavy nuclei would be overwhelming. At a difference with other fields, like condensed matter, the number of nucleons in a nucleus is never so large as to be possible to apply statistical concepts. However, there have been rather successful attempts to perform just this task during the last couple of decades. In this calculations the interaction is not the one provided by QCD, since this is unknown, but rather it is an effective interaction that fulfills the symmetries required by QCD and also reproduces nucleon-nucleon data. Even with this limitation one has not been able to treat nucleons with $A > 16$ so far. This procedure to solve the nuclear many-body problem is called "ab initio shell model" or "no core shell model" because one starts just from the nucleon-nucleon system ("ab initio") and from there one adds nucleons up the A-particle system. No core is present in this approach and therefore its name.

Another approach to obtain approximate solutions of the eigenvectors and eigenvalues of the nuclear Hamiltonian (3.1) is based in the property that we have already discussed in the previous Chapter, i. e. that double magic nuclei (i. e. nuclei with both N and Z magic numbers) are very stable. Some of the points mentioned in that Chapter are very relevant here also and, therefore, we will insist on them. As we have seen there, nuclear magnetic moments indicate that a nucleon moving outside a double-magic core feels the interactions from the nucleons in the core as a whole. But this is not the only property supporting the existence of magic numbers in nuclei. Other experimental evidences include:
1. The binding energies of magic-number nuclei is much larger than in the neighboring nuclei. Thus larger energy is required to separate a single nucleon from magic nuclei.
2. The number of stable nuclei with magic values of Z or N is much larger than the corresponding number in neighboring nuclei.
3. Naturally occurring isotopes with magic Z or N have greater relative abundances.
4. The first excited states in nuclei with magic numbers of neutrons or protons lie at higher energies than the same states in neighboring nuclei.
5. Electric quadrupole moments of magic-number nuclei is zero as expected in closed shell nuclei, since they should be spherically symmetric.
6. The energy of alpha or beta particles emitted by magic-number radioactive nuclei is larger than that from other nuclei.

All this suggests that a double-magic nucleus is so stable that a particle moving outside this "frozen core" does not affect appreciably its internal structure. It is therefore reasonable to assume that the frozen core induces a central field which only depends upon the distance r between the particle outside

the core and the center of the core (notice that it does not depend on the direction of $\mathbf{r}$, i. e. it is spherically symmetric). This interaction, which we will call $U(r)$, will be studied in detail below. Here we will analyze its general features and its consequences on the nuclear many-body problem.

The nuclear Hamiltonian (3.1) can be written as

$$H = \sum_{i=1}^{A}(\frac{\boldsymbol{p_i}^2}{2m_i} + U(r_i)) + \sum_{i<j=1}^{A} V_{ij} - \sum_{i=1}^{A} U(r_i) \tag{3.2}$$

Calling

$$H_0 = \sum_{i=1}^{A}(\frac{\boldsymbol{p_i}^2}{2m_i} + U(r_i)) \tag{3.3}$$

and

$$V = \sum_{i<j=1}^{A} V_{ij} - \sum_{i=1}^{A} U(r_i) \tag{3.4}$$

one gets,

$$H = H_0 + V \tag{3.5}$$

This is the shell model Hamiltonian.

We are assuming that for cases where there is only a particle outside a double-magic core the interaction $U(r)$ describes the spectrum well and, therefore, in this situation it should be $V = 0$. When more than one particle move outside the core, then V represents the interaction among these outside particles, which are usually called "valence particles". It would be an impossible task to determine V from Eq. (3.4). Instead one uses effective forms which reproduce as many experimental data as possible. One of these effective forces is the pairing interaction mentioned in the previous Chapter but there are many others, as we will see.

The formalism presented so far is based on the assumption that the bulk of the nuclear forces acting upon the nucleons in a double-magic nucleus induces a frozen core. This is by far the major component of the outcome of the nucleon-nucleon interaction and its consequence is reflected in the eigenvectors of the central potential U. Therefore it is very suitable to use the eigenvectors of the Hamiltonian (3.3) to describe the Hamiltonian (3.5), even when many valence particles are present, since its diagonalization within such representation (as we did in Eq. (6) of Chapter 1) would need only a few of the infinite members of the representation. This is an important point which is worthwhile to clarify farther. In principle one can use as representation to diagonalize the shell model Hamiltonian the eigenvectors of any other Hamiltonian, for instance the plane waves corresponding to free particles. But this would require to include a huge number of vectors in the representation. Instead, very few eigenvectors of the Hamiltonian (3.3) would be needed to describe accurately enough the nuclear properties. The dimensions of the shell model Hamiltonian matrix is relatively small by using the shell model representation. Yet the main advantage of this representation is not that the matrix dimensions are small but rather that it provides a clear physical picture of the property that is analyzed. For instance, to describe a bound state in terms of plane waves would require a huge number of basis states, all of them with approximately the same value (and therefore very small, since the wave function should be normalized to one). Such wave function contains no clue about the characteristics of the state under study. Instead, within the shell model representation perhaps only one state may be enough, and the single-particle components in this state depict clearly the nature of the state. This is the essence and reason of the success of the Shell Model, which we will analyze in detail throughout this Course.

3.2 Shell model representation

The shell model representation consists of the eigenvectors of the Hamiltonian (3.3) where each of the A nucleons move under the influence of the central potential U. Calling $H_0(i)$ the Hamiltonian corresponding to the ith particle, one has

$$H_0 = \sum_{i=1}^{A} H_0(i) \tag{3.6}$$

the eigenvectors $|\varphi_{n_i}>$ and eigenvalues ϵ_{n_i} of $H_0(i)$ satisfy

$$H_0(i) < \mathbf{r_i}|\varphi_{\mathbf{n}}> = (\frac{\mathbf{p_i^2}}{\mathbf{2m_i}} + \mathbf{U(r_i)}) < \mathbf{r_i}|\varphi_{\mathbf{n_i}}> = \epsilon_{\mathbf{n_i}} < \mathbf{r_i}|\varphi_{\mathbf{n}}> \tag{3.7}$$

Since the Hamiltonian H_0, with eigenvalues given by

$$H_0|\Psi_\alpha> = E_\alpha|\Psi_\alpha> \ , \tag{3.8}$$

is a sum of the Hamiltonians $H_0(i)$ and the degrees of freedom of different particles are independent of each other, the states $|\Psi_\alpha>$ can be written as,

$$< n_1\mathbf{r}_1, n_2\mathbf{r}_2....n_A\mathbf{r}_A|\Psi_\alpha> = \Psi_\alpha(n_1\mathbf{r}_1, n_2\mathbf{r}_2, ...n_A\mathbf{r}_A) = \varphi_{n_1}(\mathbf{r}_1)\varphi_{n_2}(\mathbf{r}_2)...\varphi_{n_A}(\mathbf{r}_A) \tag{3.9}$$

and the eigenvalues are

$$E_\alpha = \epsilon_{n_1} + \epsilon_{n_2} + ... + \epsilon_{n_A} \tag{3.10}$$

From $<\varphi_i|\varphi_j> = \delta_{ij}$, it follows that $<\Psi_\alpha|\Psi_\beta> = \delta_{\alpha\beta}$.

Assuming that one chooses N of the infinite number of single-particle states, the representation to be formed with the functions (3.9) consists of all possible combinations of the A particles in the different states $|n_{i=1,2,...,N}>$. However one has still to consider the Pauli principle, which requires that when two particles change position the wave function changes sign. This is called antisymmetric wave function. Such a function can be built as a linear combination of the functions (3.9). For instance, assuming A = 2 a particular antisymmetric wave function would be

$$\Psi_\alpha^{(a)}(n_1\mathbf{r}_1, n_2\mathbf{r}_2) = N_\alpha(\varphi_{n_1}(\mathbf{r}_1)\varphi_{n_2}(\mathbf{r}_2) - \varphi_{n_1}(\mathbf{r}_2)\varphi_{n_2}(\mathbf{r}_1)) \tag{3.11}$$

which has the property that $\Psi_\alpha^{(a)}(n_1\mathbf{r}_1, n_2\mathbf{r}_2) = -\Psi_\alpha^{(a)}(n_1\mathbf{r}_2, n_2\mathbf{r}_1)$. The constant N_α has to be included due to the normalization of the wave function, which requires that $N_\alpha = 1/\sqrt{2}$. Since $\varphi_{n_1}(\mathbf{r}_2)\varphi_{n_2}(\mathbf{r}_1) = \varphi_{n_2}(\mathbf{r}_1)\varphi_{n_1}(\mathbf{r}_2)$ one sees that two particles cannot occupy the same state since, in that case, $\Psi_\alpha^{(a)}(n_1\mathbf{r}_1, n_1\mathbf{r}_2) = 0$. In general the antisymmetric wave function satisfies,

$$\Psi_\alpha^{(a)}(n_1\mathbf{r}_1, n_2\mathbf{r}_2, ..., n_p\mathbf{r}_p, ..., n_q\mathbf{r}_q, ..., n_A\mathbf{r}_A) = -\Psi_\alpha^{(a)}(n_1\mathbf{r}_1, n_2\mathbf{r}_2, ..., n_p\mathbf{r}_q, ..., n_q\mathbf{r}_p, ..., n_A\mathbf{r}_A) \tag{3.12}$$

We will analyze this general case later, but here it is important to stress that the many-body representation is the set of states $\{\Psi_\alpha^{(a)}(n_1\mathbf{r}_1, n_2\mathbf{r}_2, ..., n_p\mathbf{r}_p, ..., n_q\mathbf{r}_q, ..., n_A\mathbf{r}_A)\}$ that can be formed through the combination of the A particles placed in the different states $n_{i=1,2,...,N}$.

The property that two particles cannot be in the same single-particle state implies that the lowest state of the non-interacting A-particle system consists of a particle occupying the lowest single-particle state, the second particle occupying the second lowest state and so on. Such a system of non-interacting particles fulfilling the Pauli principle is called "a Fermi gas".

The important conclusion of this discussion is that the potential U should provide a set of single-particle states which, placing the particles in the order required by the Fermi gas, explains the appearance of magic numbers. To find such a potential is the task that we will confront now.

3.3 Shell model central potential

We have solved the Schrödinger equation corresponding to a one-dimension square well potential in the previous Chapter. We will now proceed to the more realistic case of three dimensions following the historical developments in this subject. In the beginning the spin of the nucleon was neglected and therefore we will start in spherical coordinates with a Hamiltonian corresponding to a spinless particle moving in the central field $U(r)$, i. e.

$$H = \frac{\boldsymbol{p}^2}{2m} + U(r) = \frac{\hat{\boldsymbol{l}}^2}{2mr^2} - \frac{\hbar^2}{2mr^2}\frac{\partial}{\partial r}\left(r^2\frac{\partial}{\partial r}\right) + U(r) \tag{3.13}$$

One sees that the angular coordinates $(\theta\varphi)$ are included in the orbital angular momentum operator $\hat{\boldsymbol{l}}^2$ only while the radial coordinate r is in the rest of the Hamiltonian. Since there is no term which mixes

them, the eigenfunction of this Hamiltonian is a product of radial and angular coordinates. As we have already seen, with

$$\hat{\boldsymbol{l}}^2 Y_{lm}(\theta\varphi) = \hbar^2 l(l+1) Y_{lm}(\theta\varphi) \tag{3.14}$$

one can write the total eigenfunction as

$$\Psi_{nlm}(\boldsymbol{r}) = R_{nl}(r) Y_{lm}(\theta\varphi), \tag{3.15}$$

It is convenient to replace the radial eigenfunction $R_{nl}(r)$ by the function $u_{nl}(r)$ defined as

$$R_{nl}(r) = u_{nl}(r)/r \tag{3.16}$$

and the eigenvalue problem acquires the simpler, one dimensional, form,

$$-\frac{\hbar^2}{2\mu}\frac{\mathrm{d}^2}{\mathrm{d}r^2}u_{nl}(r) + \left[\frac{l(l+1)\hbar^2}{2\mu r^2} + U(r)\right] u_{nl}(r) = E_{nl} u_{nl}(r) \tag{3.17}$$

The first problem that had to be confronted by the pioneers in the study of the structure of nuclei was to determine the form of the central potential. For this purpose it was taken into account that the nuclear force is very strong and of a very short range. Besides, the binding energy of the particle bound to the core is strong, of the order of several MeV. Therefore the mean field itself should be deep and of a short range. A convenient potential to describe such states which, as seen in Fig. 3.1, lie far from the continuum threshold, is an harmonic oscillator potential. A more realistic one is the Woods-Saxon potential U_{WS} given by,

$$U_{WS}(r) = -\frac{U_0}{1 + e^{(r-R_0)/a}} \tag{3.18}$$

where U_0 is a positive constant such that $U_{WS}(r)$ is attractive, R_0 is the radius of the nucleus, which is taken to be $R_0 \approx 1.2A^{1/3}$ fm and a is the diffuseness, which usually has a value around 0.5-0.6 fm.

In the next Chapter we will introduce the Hartree-Fock potential which is a nuclear mean field derived microscopically i. e. from the degrees of freedom of the nucleons that constitute the nucleus and their interactions.

The use of the harmonic oscillator potential has the advantage of providing eigenvectors, i. e. a representation, which is very convenient in many-body studies. One thus describes bound states lying far from the continuum threshold by using a Harmonic oscillator potential of the form $U(r) = m\omega^2 r^2/2$

$$-\frac{\hbar^2}{2m}\frac{\mathrm{d}^2}{\mathrm{d}r^2}u_{nl}(r) + \left[\frac{l(l+1)\hbar^2}{2mr^2} + \frac{1}{2}m\omega^2 r^2\right] u_{nl}(r) = E_{nl} u_{nl}(r) \tag{3.19}$$

The eigenvalues corresponding to this potential are

$$E_{nl} = (2n + l + \frac{3}{2})\hbar\omega \tag{3.20}$$

where $n \geq 0$ is and integer. One sees that the energy depends only upon the number N, which is called "principal quantum number", given by

$$N = 2n + l \tag{3.21}$$

which, like n, is also integer and $N \geq 0$. The energy becomes

$$E_N = (N + \frac{3}{2})\hbar\omega \tag{3.22}$$

Since $\hbar\omega$ is a free parameter that defines the Harmonic oscillator potential, it can be chosen large enough so that there are in the spectrum a series of bands, each band labelled by the number N. The gap between bands was found to be related to the mass number A by the relation,

$$\hbar\omega = 45A^{-1/3} - 25A^{-2/3}, \tag{3.23}$$

thus allowing to determine the frequency ω in different regions of the nuclear chart.

It is important to notice that the lowest (ground) state, i. e. the one corresponding to $N = 0$, is not at zero energy but rather at $E_{N=0} = (3/2)\hbar\omega$. This is a Quantum Mechanics effect. It is as if there is a motion due to the uncertainties inherent to Quantum Mechanics that produces an energy even if, classically, there is no real motion. This energy is therefore called "zero-point energy". It shows that in

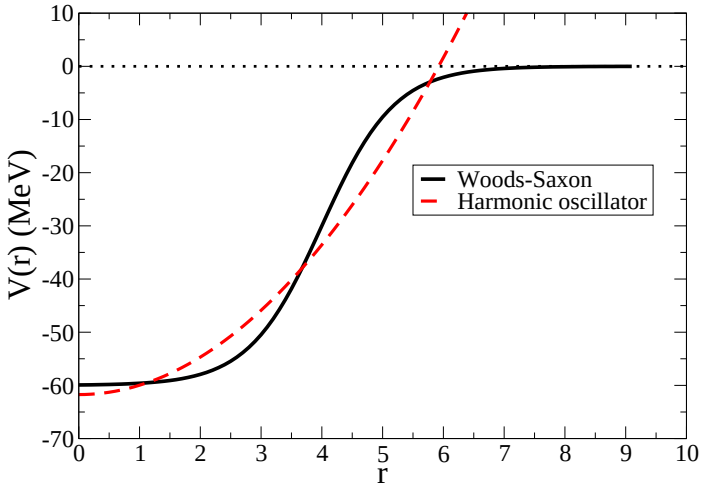

Figure 3.1: Potential describing bound single-particle states. The nuclear central field is well approximated by the Woods-Saxon potential (3.18). In the region where the single-particle states lie the nuclear (Woods-Saxon) potential can be approximated by an Harmonic oscillator potential. Close to the continuum threshold the nuclear potential vanishes and the centrifugal plus Coulomb potentials become dominant.

Quantum Mechanics (particularly in Field Theories) the vacuum is not a real vacuum. Everywhere there is the zero-point energy associated to the ground states of all fields.

The spectrum of the Harmonic oscillator is given by Eq. (3.22). Each value of N implies several values of (n,l), following Eq. (3.21). The corresponding level sequence is as shown in Table 3.1. One sees in this Table that between one value of N and the next there is an energy gap $\hbar\omega$. Therefore the set of (n,l) values corresponding to a particular value of N would be clustered together in bands separated by an energy $\hbar\omega$. In the Table the levels are labelled by (n,l), where the states $l = 0,1,2,3,4,..$ are traditionally called $s,p,d,f,g....$

Table 3.1: Energy levels corresponding to an Harmonic oscillator potential of frequency ω. The states are labelled by $N = 2n+l$. The energies E_{nl} are in units of $\hbar\omega$. D_l is the degeneracy of the state (n,l).

N	n	l	E_{nl}	$\|nl\rangle$	parity	$D_l = 2(2l+1)$	$\sum D_l$
0	0	0	3/2	0s	+	2	2
1	0	1	1+3/2	0p	-	6	8
2	0	2	2+3/2	0d	+	10	20
	1	0	2+3/2	1s	+	2	
3	0	3	3+3/2	0f	-	14	40
	1	1	3+3/2	1p	-	6	
4	0	4	4+3/2	0g	+	18	70
	1	2	4+3/2	1d	+	10	
	2	0	4+3/2	2s	+	2	

Since there is no term in the Hamiltonian that mixes the **l** and **s** angular momenta, the levels for the same N are degenerate, as seen in the level scheme labelled by $(N+3/2)\hbar\omega$ in Fig. 3.2. It is important to notice that the notation in this Figure is different than the one in the Table. In the Table we have used the Harmonic oscillator quantum values for the labels. Therefore the lowest state correspond to $n = 0$. Besides providing the energy, the number n is the number of nodes of the function $u_{nl}(r)$ in Eq. (3.16) (the number of nodes is the number of times that $u_{nl}(r)$ vanishes). This function has always a node since $u_{nl}(r = 0) = 0$ for all l. Therefore some shell model practitioners label the lowest state with

the value $n = 1$, as in the Figure. We will use throughout this course the convention that the lowest state corresponds to $n = 0$.

As with the magnetic moments discussed in the previous Chapter, this different conventions for the value of n is unfortunate, but it should not produce any confusion.

3.4 Shell closures and the magic numbers

We are now in a position to give an explanation to the shell closures that give rise to the magic numbers, i. e. the numbers 2, 8, 20, 28, 50, 82 and 126. As we have discussed above, experimental data show that nuclei with a magic number of neutrons or protons have properties that are very different than other nuclei. In particular, if N and Z are both magic the nucleus is very stable and can be considered a frozen core.

One has to consider the spherical symmetry of the potential in order to count the number of particles that can be placed in each state satisfying the Pauli principle. That symmetry implies that the energy do not depend upon the projection l_z of the angular momentum, i. e. upon the quantum number m. Therefore in a given state (nl) one can place $2l+1$ particles, each in one of the 2l+1 values of m (remember that $-l \leqslant m \leqslant l$). In addition each particle has its own intrinsic spin $s = 1/2$, which gives an additional degeneracy $2s + 1 = 2$. Therefore the total degeneracy of the state $N_l = 2n + l$ is $D_l = 2(2l + 1)$. As seen in Table (3.1) this procedure reproduces the lowest magic numbers, i. e. 2, 8 and 20, but not the others. Besides, it was found that experimentally different values of l have different energies. In an attempt to explain this feature an attractive term proportional to $D\mathbf{l^2}$, with D a negative number, was included. This contributes to the energy with the value $Dl(l + 1)$, as seen in the corresponding level scheme of Fig. 3.2. But still the sequence of the levels was not well explained.

In 1949 Goeppert-Mayer and, independently, Haxel, Jensen and Suess proposed the existence of an strong spin-orbit potential that could account for the observed magic numbers. For this Goeppert-Mayer and Jensen got the 1963 Physics Nobel Prize (it was the last time so far that a lady, Maria Goeppert-Mayer, was awarded the Nobel Prize in Physics. Incidentally, the other lady who is a physics Nobel laureate, Marie Curie, was also a nuclear physicist).

The spin-orbit potential proposed by Goepper-Mayer and Jensen et. al. has the form, $V_{so}(r)\boldsymbol{l} \cdot \boldsymbol{s}$, where $\boldsymbol{l}$ is the orbital angular momentum and $\boldsymbol{s}$ is the intrinsic spin of the nucleon. The shell model Hamiltonian acquires the form,

$$H = \frac{\boldsymbol{p}^2}{2m} + \frac{1}{2}m\omega^2 r^2 + V_{so}(r)\, \boldsymbol{l} \cdot \boldsymbol{s} \tag{3.24}$$

The orbital and spin angular momenta must be coupled to a total angular momentum $\boldsymbol{j} = \boldsymbol{l} + \boldsymbol{s}$. As we have seen in Chapter 1 the eigenstates of the spin-orbit term are determined by the quantum number $j = |l \pm 1/2|$ and by the quantum number m associated with the third component of $\boldsymbol{j}$. Therefore the corresponding eigenvectors are $\{|nlsjm\rangle\}$ and with

$$\boldsymbol{j}^2 = \boldsymbol{l}^2 + \boldsymbol{s}^2 + 2\,\boldsymbol{l} \cdot \boldsymbol{s} \tag{3.25}$$

$$\boldsymbol{l} \cdot \boldsymbol{s} = (\boldsymbol{j}^2 - \boldsymbol{l}^2 - \boldsymbol{s}^2)/2 \tag{3.26}$$

one gets,

$$\boldsymbol{l} \cdot \boldsymbol{s}|nlsjm\rangle = \frac{\hbar^2}{2}\big[j(j+1) - l(l+1) - s(s+1)\big]|nlsjm\rangle \tag{3.27}$$

In r-representation it is,

$$\langle \boldsymbol{r}|nlsjm\rangle = R_{nlj}(r)\left[Y_l(\theta\varphi)\chi_{1/2}\right]_{jm}, \quad R_{nlj}(r) = u_{nlj}(r)/r \tag{3.28}$$

and the Schrödinger equation becomes

$$-\frac{\hbar^2}{2m}\frac{\mathrm{d}^2}{\mathrm{d}r^2}u_{nl}(r) + \left\{\frac{l(l+1)\hbar^2}{2mr^2} + \frac{1}{2}m\omega^2 r^2 + \right.$$
$$\left. + \frac{\hbar^2}{2}\big[j(j+1) - l(l+1) - 3/4\big]V_{so}(r)\right\}u_{nl}(r) = E_{nl}u_{nl}(r). \tag{3.29}$$

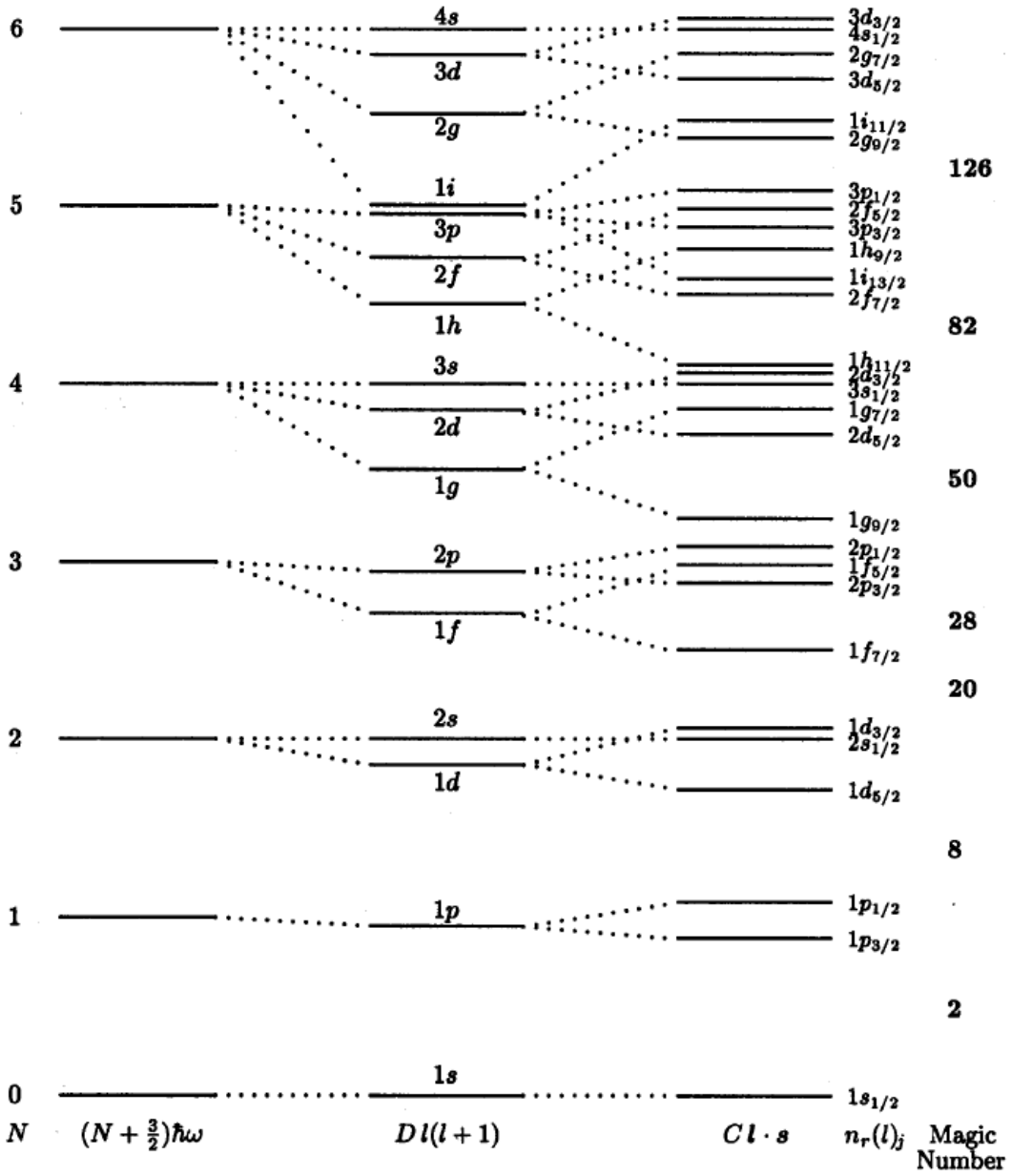

Figure 3.2: In the left is the energy spectrum corresponding to a Harmonic oscillator potential of frequency ω. In the middle is the same plus a term $D\mathbf{l}^2$, with D negative. The spectrum to the rigth corresponds to the shell model Hamiltonian (3.5), which follows very well the tendencies of the experimental data.

Since $|l-1/2| \leqslant j \leqslant l+1/2$ and $j = l \pm 1/2$ one gets

$$\big[j(j+1) - l(l+1) - 3/4\big] V_{so}(r) = V_{so}(r) \begin{cases} l; & j = l+1/2 \\ -l-1; & j = l-1/2 \end{cases} \tag{3.30}$$

and one understands the experimental level scheme by assuming an attractive spin-orbit interaction, for instance a constant term $V_{so}(r) = -V_0$. With this term one gets the level scheme labeled by $C\mathbf{l}.\mathbf{s}$ in Fig. 3.2.

One sees from Eq. (3.30) that the spin-orbit interaction is strongest for the state with the larger value of the spin j and, due to the attractive character of the interaction, the total energy of this state lies below the corresponding energy for the lower spin. This has as a consequence that the state in a band with highest spin is so strongly affected by the spin-orbit interaction that they become mixed with states of the band below. This can be observed in Fig. 3.2, where for $l > 2$ the states with highest spin, for instance $1f_{7/2}$, $1g_{9/2}$, etc, crosses the number N below, mixing with the states $N-1$. These are called "intruder" states, and there appearance is due to the spin-orbit interaction. The parity of the intruder state is $(-1)^N$, i. e. it has different parity than the ones belonging to the band $N-1$.

The states in the shell model level schemes, i. e. the one at the right in Figure 3.2, carry as quantum number the total spin j and therefore, again due to spherical symmetry, each level has a degeneracy of $2j+1$. As seen in the Figure, one can then explain very well all magic numbers. One also sees that the intruder states play a fundamental role. In particular, the intruder state $1f_{7/2}$ contains the eight nucleons necessary to explain the magic number 28.

The spin orbit potential can be shown to have the form

$$V_{so}(r) = -v_{so} \frac{1}{r} \frac{dU_{WS}(r)}{dr}. \tag{3.31}$$

where v_{so} is a positive number and $U_{WS}(r)$ is the Woods-Saxon potential (3.18). Due to the form of this potential the spin orbit potential above is peaked in the surface of the nucleus and, therefore, its influence is mainly felt just in that surface.

The presence of the spin-orbit potential was found to be a result of relativistic effects.

Parity

Since we assume that the nucleon-core potential is spherically symmetric the quantum numbers $l.j, m$ are conserved (as discussed in the previous Chapter). This potential will also be assumed to be invariant under reflections, and therefore the parity π of the state $|nljm>$ will also be conserved. To find the value of the parity one has to analyze the Spherical Harmonics $Y_{lm_l}(\theta\varphi)$ which, for $m_l \geqslant 0$, is given by

$$Y_{lm_l}(\theta\varphi) = \sqrt{\frac{2l+1}{4\pi}} \sqrt{\frac{(l-m_l)!}{(l+m_l)!}} (-1)^{m_l} \mathrm{e}^{\mathrm{i}m_l\varphi} P_l^{m_l}(\cos\theta) \tag{3.32}$$

where

$$P_l^{m_l}(\xi) = \frac{(-1)^{m_l}}{2^l l!} \frac{(l+m_l)!}{(l-m_l)!} (1-\xi^2) \frac{\mathrm{d}^{l-m_l}}{\mathrm{d}\xi^{l-m_l}} (\xi^2-1)^l \tag{3.33}$$

For $m_l < 0$ it is,

$$Y_{lm_l}(\theta\varphi) = (-1)^{m_l} Y^*_{l-m_l}(\theta\varphi) \tag{3.34}$$

The parity transformation corresponds to $\boldsymbol{r} \longrightarrow -\boldsymbol{r}$, that is $(r, \theta, \varphi) \longrightarrow (r, \pi-\theta, \varphi+\pi)$, and since for spherically symmetric potentials the value of r is the same for all values of the angles, only the transformation of the Spherical Harmonics has to be considered. Therefore one finds,

$$\Psi_{nljm}(-\boldsymbol{r}) \quad \longrightarrow \quad (-1)^l \Psi_{nljm}(\boldsymbol{r}) \tag{3.35}$$

The spin-orbit part of the wave function is as above independently of the spherically invariant potential, but the radial part has to be studied separately for each potential one has to deal with.

We have seen that the parity associated to this wave function is $(-1)^l$ and since $N = 2n+l$ the parity also is $(-1)^N$. That is, all the states in a band corresponding to the quantum number N has the same parity.

Analytic expressions for the first few orthonormalized spherical harmonics in the Condon-Shortley phase convention,

$$Y_0^0(\theta,\varphi) = \frac{1}{2}\sqrt{\frac{1}{\pi}} \tag{3.36}$$

$$Y_1^{-1}(\theta,\varphi) = \frac{1}{2}\sqrt{\frac{3}{2\pi}}\,\sin\theta\, e^{-i\varphi} \tag{3.37}$$

$$Y_1^0(\theta,\varphi) = \frac{1}{2}\sqrt{\frac{3}{\pi}}\,\cos\theta \tag{3.38}$$

$$Y_1^1(\theta,\varphi) = \frac{-1}{2}\sqrt{\frac{3}{2\pi}}\,\sin\theta\, e^{i\varphi} \tag{3.39}$$

$$Y_2^{-2}(\theta,\varphi) = \frac{1}{4}\sqrt{\frac{15}{2\pi}}\,\sin^2\theta\, e^{-2i\varphi} \tag{3.40}$$

$$2^{-1}(\theta,\varphi) = \frac{1}{2}\sqrt{\frac{15}{2\pi}}\,\sin\theta\,\cos\theta\, e^{-i\varphi} \tag{3.41}$$

$$Y_2^0(\theta,\varphi) = \frac{1}{4}\sqrt{\frac{5}{\pi}}\,(3\cos^2\theta - 1) \tag{3.42}$$

$$Y_2^1(\theta,\varphi) = \frac{-1}{2}\sqrt{\frac{15}{2\pi}}\,\sin\theta\,\cos\theta\, e^{i\varphi} \tag{3.43}$$

$$Y_2^2(\theta,\varphi) = \frac{1}{4}\sqrt{\frac{15}{2\pi}}\,\sin^2\theta\, e^{2i\varphi} \tag{3.44}$$

Particle excitations

We have seen that a nucleus ${}^{A}_{Z_m}X_{N_m}$, where N_m and Z_m are magic numbers, acts as a frozen core. The total angular momentum of this core is zero and a nucleon moving outside it feels the interaction of the nucleons inside the core as a whole. The core induces a central field which generates the shell model set of single-particle states, that is the shell model representation of Fig. 3.2. The nucleons in the core form a Fermi gas such that each one of these nucleons occupy a level of the shell model representation. Since the core is in the lowest excitation the nucleons occupy the lowest states. For instance, the nucleus ${}^{40}_{20}Ca_{20}$ (Calcium 40) is a core, since 20 is a magic number. In terms of the shell model the 20 neutrons as well as the 20 protons occupy the states $1s_{1/2}$, $1p_{3/2}$, $1p_{1/2}$, $1d_{5/2}$, $2s_{1/2}$ and $1d_{3/2}$. In the same fashion, adding a nucleon, for instance a neutron, one would get the spectrum of ${}^{41}_{20}Ca_{21}$. The lowest (ground) state of this Ca isotope is, according to the shell model (Fig. 3.2), $f_{7/2}$, that is $7/2^-$, as indeed it is experimentally. The ground state of ${}^{57}_{28}Ni_{29}$ (Nickel 57) should be $3/2^-$, the first excited state should be $5/2^-$ and the second excited state $1/2^-$, as also it is experimentally.

The nuclear experimental spectra are found in many publications, but a convenient way of getting them is through Internet. In the site

http : *//www.nndc.bnl.gov/nudat*2*/*

one finds all the available nuclear experimental spectra.

It is important to stress that the analysis we have carried out so far is based on the assumption that the nucleus consists of freely moving nucleons in the shell model potential fulfilling the Pauli principle. Considering that the nucleus is a bunch of strongly interacting nucleons packed in an extremely dense environment it may seem nearly as a wonder that the independent particle shell model works so well. There are arguments which allow one to justify this feature, but the importance of the single-particle shell model lies not so much in its predicting power but rather in that it provides an excellent representation to describe many-nucleon states, as we will see.

In order to complete the representation one has to know the energies of the single-particle states. These can be taken from experiment, or from calculations that fit the experimental data as closely as possible.

The single-particle energies ϵ_{n_i} are the eigenvalues of the Hamiltonian $H_0(i)$, Eq. (3.7). They are depicted in Fig. 3.3, where the origin of energies is the continuum threshold. That implies that all values of ϵ in the Figure are negative, as it should be for bound states. At positive energy there is the continuum, which does not have any quantized state and, therefore, all energies are allowed. These are all the possible kinetic energies of the particle at infinite, where the nuclear potential vanishes. One sees

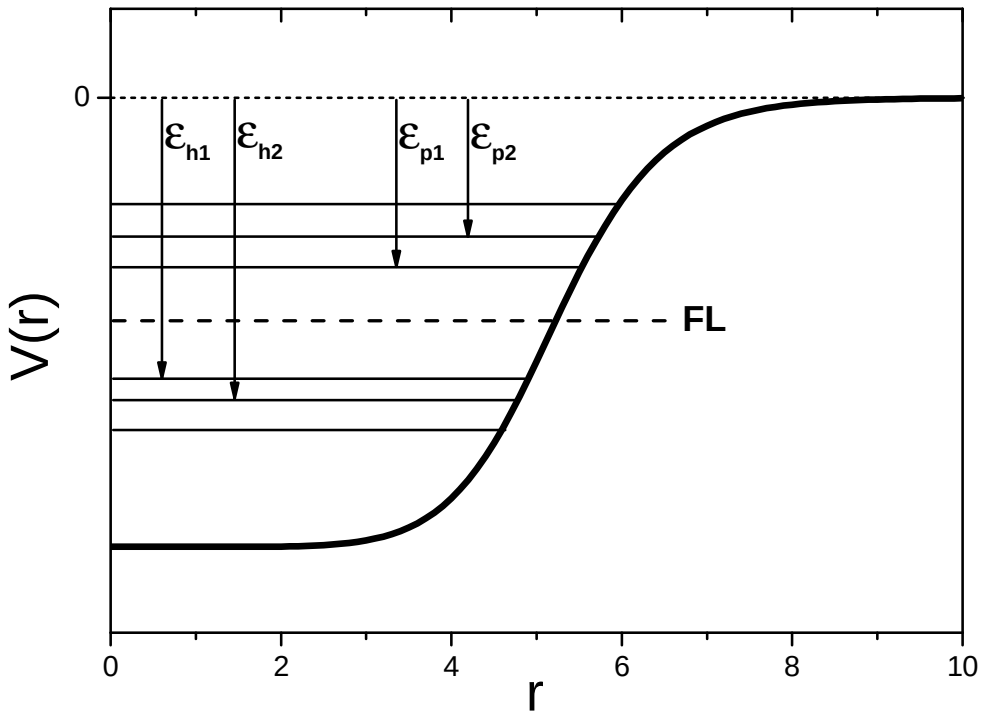

Figure 3.3: Single particle states in the shell model potential. The energies ϵ are measured from the continuum threshold. The Fermi level is indicated as FL.

from the Figure that ϵ_{n_i} is the energy necessary to bring a particle in the bound state n_i to a rest state (zero kinetic energy) at infinity. This is called "separation energy", which thus is the same as $-\epsilon_{n_i}$.

We have seen that the A nucleons in a double magic core occupy the lowest shell model single-particle states. In Fig. 3.3 these states are labeled by h_i, where $i = 1, 2..., A$, and the highest one is called "Fermi level". From the Fermi level and below all states are occupied. Above the Fermi level all states are empty, i. e. unoccupied. They are labeled p_k in the Figure, where $k = 1, 2, ..., N$ and N is the number of unoccupied states. Therefore, and since we assume that the core is frozen and neutral, the nucleus with $A + 1$ nucleons has to be in one of the states p_k.

According to Eq. (3.10) the energy of the core is

$$E_{core} = \sum_{i=1}^{A} \epsilon_{h_i} \tag{3.45}$$

and the energy of $A + 1$ nucleus in the state p_k is

$$E_{A+1}(p_k) = E_{core} + \epsilon_{p_k} \tag{3.46}$$

from where one gets,

$$\epsilon_{p_k} = E_{A+1}(p_k) - E_{core} \tag{3.47}$$

Since all single-particle energies are negative one finds that

$$E_{A+1}(p_k) < E_{core} \tag{3.48}$$

The experimental values of E_A are tabulated in many publications. A convenient way of getting them is also through Internet. In the site

http://ie.lbl.gov/toi2003/MassSearch.asp

one finds the available binding energies $B(A)$ of all nuclei in the ground state. The binding energy is defined as $B(A) = -E_A$, i. e. $B(A)$ is a positive quantity such that $B_{A+1}(p_k) > B_{core}$, according to Eq. (3.48).

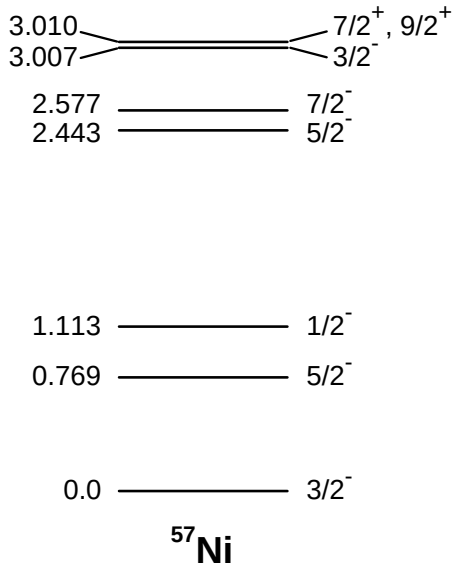

Figure 3.4: Experimental spectrum of the nucleus $^{57}Ni_{29}$ taken from the Internet site mentioned in the text. Energies are in MeV. The level at 3.010 MeV has not been completely determined yet. It can be $7/2^+$ as well as $9/2^+$.

To obtain the single-particle energies from experiment one uses Eq. (3.47). We will show this, as well as the limitations of the independent single-particle model, in an illuminating example.

As we have seen above, the neutron single-particle states between 28 and 50 can be extracted from the spectrum of $^{57}Ni_{29}$. The experimental spectrum in Fig. 3.4 shows that the ground state is $3/2^-$, i. e. the state $1p_{3/2}$ (remember that we use the convention that for the lowest state it is $n = 0$). The first excited state lies at 0.769 MeV and is $5/2^-$, i. e. $0f_{5/2}$. The second excited state lies at 1.113 MeV and is $1/2^-$, i. e. $1p_{1/2}$. After this there are a number of states which do not correspond to the ones in Fig. 3.2. Only at the rather high energy of 3.010 MeV appears a state that may be $9/2^+$. This indicates that after the state $1p_{1/2}$ the energy is high enough to disturb the core, probably by exciting single-particle states from below to above the Fermi level. But one can still assume that the states $9/2^+$ at 3.010 MeV is the $0g_{9/2}$ level of Fig. 3.2.

The experimental energies in the spectrum are given relative to the ground state of the nucleus, as seen in Fig. 3.4. To obtain the corresponding values of ϵ one has to evaluate the binding energies $B(Z, N)$. In the Internet site mentioned above are given the values of $B(Z, N)/A$. For our case we need the binding energies of ^{56}Ni (the core) and of ^{57}Ni (see Eq. (3.47)), It is $B(28, 28)/56 = 8.643$ MeV and $B(28, 29)/57 = 8.671$ MeV, i. e. $\epsilon_{1p_{3/2}} =$ - 10.239 MeV. This is the lowest state. It corresponds to the state labelled p_1 in Fig. 8.7. The state $0f_{5/2}$, at 0.769 MeV, corresponds to p_2 (is less negative). Therefore one gets $\epsilon_{0f_{5/2}} =$ (- 10.239 + 0.769) MeV = - 9.470 MeV. In the same fashion it is $\epsilon_{1p_{1/2}} =$ -9.126 MeV and $\epsilon_{0g_{9/2}} =$ - 7.229 MeV.

The evaluation of the single-particle energies follows this procedure in all cases.

Hole excitations

We will now analyze the spectrum of a nucleus with a particle *less* than a magic number. According to the shell model, the structure of such a nucleus is determined by filling the single-particle states as if the system were a Fermi gas. This we did above with the core and with the core plus one-particle nucleus. In the present case all the A-1 particles will occupy the levels below the Fermi level, i. e. the levels called h_i in Fig. 3.1. As seen in Fig. 3.5, the resulting spectrum is that of the core (all levels below the Fermi level are occupied) except the level, called h_1 in the Figure, where the last particle was not placed. Therefore this excitation is called "hole" since it is like a hole in the spectrum of the core. The energy of

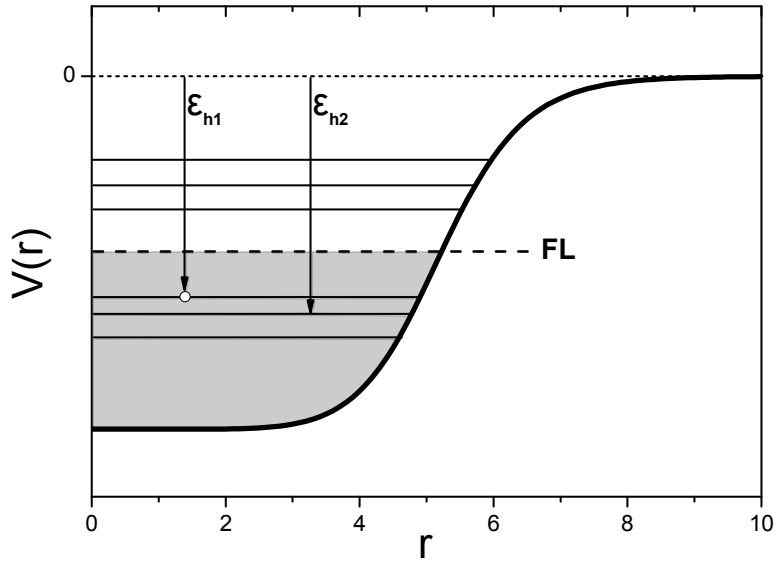

Figure 3.5: Excitations h_i in the (A-1)-particle nucleus. It looks like at the level h_1 there is a hole in the completely filled states of the core. Therefore the states below the Fermi level are called "hole excitations". A hole at the more deeply bound level h_2 induces a higher excitation than the one at h_1.

the nucleus referred to the core is now (see Eq. (3.47))

$$E_{A-1}(h_1) - E_{core} = -\epsilon_{h_1} \tag{3.49}$$

which is a *positive* number. This implies that a state which is more bound than h_1, for instance the one labeled h_2 in Fig. 3.5, lies at higher energy than h_1 since $|\epsilon_{h_2}| > |\epsilon_{h_1}|$.

We will again clarify this point with an example, which is the spectrum of the nucleus ^{131}Sn, with Z=50 and N=81. That is, the single-particle excitations of this nucleus are holes in the neutron core below N=82. Therefore the ground state should be the first hole state, the first excited state the second hole state and so on. And indeed we see that the level sequence of the experimental spectrum of Fig. 3.6 is the one predicted by the independent-particle shell model in Fig. 3.2. That is, the shell model (experimental) levels are $1d_{3/2}$ (ground state), $0h_{11/2}$ (0+x MeV), i. e. experimentally has not been possible yet to disentangle this from the ground state. Notice also that this is an intruder state. After these states follow the levels $2s_{1/2}$ (0.332 MeV), $1d_{5/2}$ (1.655 MeV) and $0g_{7/2}$ (2.434 MeV). In this case there is a good agreement between the experimental and the shell model sequence of levels, since only the last two states are in a reverse sequence (the first two states are nearly degenerate). But in general one expects that the levels predicted by the shell model should be there, but not with the exact sequence.

The ground state single-particle energy is, according to Eq. (3.49), $\epsilon_{h_1} = E_{core} - E_{A-1}(h_1)$, where h_1 is the hole state $1d_{3/2}$ and the core is ^{132}Sn(gs) (*gs* means ground state). The binding energies of interest are $B(50,81)/131$ = 8.363 MeV and $B(50,82)/132$ = 8.355 MeV. Therefore it is E_{core} = -$B(50,82)$ = -1102.860 Mev and $E_{A-1}(h_1)$ = -$B(50,81)$ = -1095.553 MeV, from where one gets $\epsilon_{1d_{3/2}}$ = -7.307 MeV. For the other states it is $\epsilon_{0h_{11/2}}$ = -7.307 MeV also, $\epsilon_{2s_{1/2}}$ = (-7.307 - 0.332) MeV = -7.639 MeV, $\epsilon_{1d_{5/2}}$ = -8.962 MeV and $\epsilon_{0g_{7/2}}$ = -9.741 MeV.

3.5 Parameterization of the Woods-Saxon Potential

arXiv:0709.3525

A number of parameterizations of the Woods-Saxon potential have been published, created with different objectives and relevant to different nuclear mass regions. Most commonly used is the so-called "Universal" parameterization [3] , which was adjusted to reproduce the single-particle binding energies

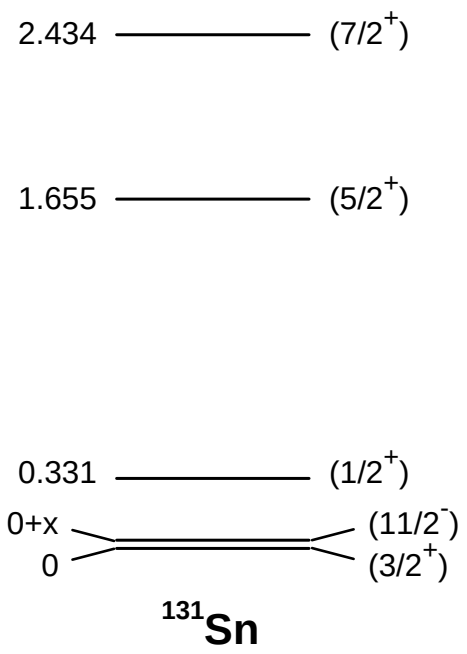

Figure 3.6: Experimental spectrum of the nucleus $^{131}_{50}Sn_{81}$. The levels are in parenthesis, meaning that they are not completely determined yet. The level $11/2^-$ is at 0.0+x MeV, implying that it is only slightly above the $3/2^+$ ground state.

of proton and neutron orbitals around the doubly-magic nucleus ^{208}Pb and correct ground state spins for nuclei of masses around A=180, but claimed to be applicable to lighter mass regions as well. Characteristic for the "Universal" parameterization is the choice of different radii for the proton- and neutron potentials. It has been pointed out, that this parameterization has shortcomings with respect to lighter nuclei and that it predicts charge radii inconsistent with experiment. [4].

Basis for this investigation are the experimental single particle spectra around the doubly magic nuclei ^{16}O, ^{40}Ca, ^{48}Ca, ^{56}Ni, ^{132}Sn and ^{208}Pb. These systems were chosen, because they are expected to show the most pure experimental manifestation of single-particle excitations.

Woods and Saxon [2] suggested to model the nuclear mean field i.e. the nucleon-core interaction with a spherically symmetric potential that has a Fermi-function form

$$f(r, R, a) = \left[1 + \exp\left(\frac{r - R}{a}\right)\right]^{-1}, \tag{3.50}$$

where the size R and diffuseness of the surface a are fixed parameters of the same units of length as r.

The total nuclear potential is defined as

$$V(r) = -V f(r, R, a), \tag{3.51}$$

where V represents total strength and the minus sign is introduced to represent the attractive nature of the interaction.

The electromagnetic force is a second part contributing to the proton-core interaction. This repulsive potential is fully determined with the assumption of a given nuclear charge distribution $\rho(r)$. The solution of the corresponding electrostatics problem gives

$$V_c(r) = 4\pi e \left(\frac{1}{r}\int_0^r r'^2 \rho(r')dr' + \int_r^\infty r'\rho(r')dr'\right). \tag{3.52}$$

In the spirit of the Woods-Saxon parameterization it is often assumed that the nuclear charge distribution is proportional in shape to the same function (3.50) $\rho(r) \sim f(r, R_c, a_c)$, where the coefficient of proportionality must be determined from the normalization of density to the total nuclear charge. The

integration in Eq. (3.52) along with a normalization of density must be done numerically, which is often too time consuming. The influence of surface terms on the strength of the Coulomb interaction is, however, weak. We have numerically tested, that the diffuseness of the charge distribution can be set to zero within the precision of the fit discussed below. Furthermore, for the same reason we have assumed $R_c = R$ which removes an extra unnecessary parameter that has little influence on the outcome. Except for special cases [**?**] these assumptions are typical in other Woods-Saxon parameterizations. Through this paper we adopt the following form of the Coulomb potential

$$V_c(r) = Z' e^2 \begin{cases} (3R^2 - r^2)/(2R^3), & r \le R, \\ 1/r, & r > R, \end{cases} \tag{3.53}$$

which as a result of the above assumptions corresponds to a uniformly charged sphere of radius R, which can be treated analytically.

Thus, the total effective Hamiltonian becomes

$$H = \frac{\mathbf{p}^2}{2\mu} + V(r) + V_c(r) + \frac{1}{2\mu^2 r}\left(\frac{\partial}{\partial r}\tilde{V}(r)\right)\ \mathbf{l}\cdot\mathbf{s}, \tag{3.54}$$

where – unlike for the Coulomb field – the potential $\tilde{V}(r)$ is not equal to the original potential $V(r)$ and may have a different form factor [**?**]. Therefore, the form factor of $\tilde{V}(r)$ is another assumption that goes into construction of the Woods-Saxon Hamiltonian

$$\tilde{V}(r) = \tilde{V} f(r, R_{SO}, a_{SO}). \tag{3.55}$$

Here, R_{SO} and a_{SO} stand for the radius and the diffuseness of the spin-orbit term.

The parameters of the potential change as one goes over the nuclear chart. The dependence of the above 7 parameters on the number of protons and neutrons in the core-nucleon problem defines the *structure of parameterization*. In the following, we will describe our choice of structure parameterization, which we call the "Seminole" parameterization.

In the conventional parameterization of the Woods-Saxon potential, as well as in our work, the size of nuclear potential is calculated as

$$R = R_C = R_0 A^{1/3}, \quad R_{SO} = R_{0,SO} A^{1/3}, \tag{3.56}$$

in terms of the parameters R_0 and $R_{0,SO}$, which are constant over the nuclear chart.

The surface diffuseness for both the central and spin-orbit potential is assumed to be constant and size independent

$$a = a_{SO} = const. \tag{3.57}$$

While the isospin dependence of the Coulomb force is obvious, the behavior of the effective nuclear potential on the isospin of the nucleon $\mathbf{t}$ and the core $\mathbf{T}'$ has to be introduced phenomenologically. We adopted the suggestion by Lane [6] to introduce an isospin dependence to the potential by the lowest order isospin invariant term

$$V = V_0\left(1 - \frac{4\kappa}{A}\langle \mathbf{t}\cdot\mathbf{T}'\rangle\right). \tag{3.58}$$

We chose the "minus" sign so that the parameter κ will be consistent with conventions. For the ground-state of a nucleus, the isospin quantum number is $T = |T_z| = |N - Z|/2$, which together with the relation $\mathbf{t} + \mathbf{T}' = \mathbf{T}$ leads to

$$-4\langle \mathbf{t}\cdot\mathbf{T}'\rangle = \begin{cases} 3 & N = Z \\ \pm(N - Z + 1) + 2 & N > Z \\ \pm(N - Z - 1) + 2 & N < Z \end{cases}, \tag{3.59}$$

where here and below we use upper sign for the proton and the lower sign for the neutron. Traditionally, the isospin-dependence of the Woods-Saxon potential had been parameterized by the expression.

$$V = V_0\left(1 \pm \kappa\frac{(N - Z)}{A}\right) \tag{3.60}$$

For heavy nuclei with large neutron excess, the difference between the two definitions is small. However, the definition of Eq. 3.59 leads to significantly different predictions in lighter nuclides around N=Z.

Table 3.2: Commonly used Woods-Saxon parameter sets in the literature.

Parameterization		$V_0[MeV]$	κ	R_0 [fm]	a [fm]	λ	R_{0SO}[fm]
'Rost'[7]	n	49.6	0.86	1.347	0.7	31.5	1.28
	p			1.275		17.8	0.932
'Optimized'[8]	n	49.6	0.86	1.347	0.7	36	1.30
	p			1.275		36	1.30
'Universal'[3]	n	49.6	0.86	1.347	0.7	35	1.31
	p			1.275		36	1.32
'Chepurnov'[9]		53.3	0.63	1.24	0.63	23.8 *	1.24
'Wahlborn'[10]		51	0.67	1.27	0.67	32	1.27

Existing parameterizations

A number of parameterizations and parameter sets are available in the literature. We list the most commonly used ones in Table 3.2. All of these parameterizations use Eq. (3.60) for the isospin dependence of the nuclear potential. In contrast to the "Seminole" parameterization, the same isospin dependence enters into spin-orbit term via $\tilde{V} = \lambda V$.

The "Rost" parameters [7] were determined from the orbital energies of ^{208}Pb. The "Optimized" [8] parameter set took the central potential parameters from "Rost", but changed the spin-orbit interaction in order to improve predictions for high-spin spectra in the lead region. A further refinement of these parameters was introduced as the "Universal" parameter set, which improved the description of high spin states in ^{146}Gd [3]. The "Chepurnov" parameterization introduced an additional isospin-dependence for the spin-orbit interaction in deviation from the commonly used proportionality to the central potential.

3.6 Homework problems

Exercise 1:

Show that $\boldsymbol{J}^2$, $\boldsymbol{l}^2$, $\boldsymbol{s}^2$ and J_z, where $\boldsymbol{J} = \boldsymbol{l} + \boldsymbol{s}$, commute with the Hamiltonian

$$H = \frac{p^2}{2\mu} + V(r) + V_{ls}(r)\boldsymbol{l} \cdot \boldsymbol{s}$$

What does this implies?

Show that under a parity transformation a particle with angular momentum l and total spin j carries a parity $\pi = (-1)^l$.

Hint: $[j\ (or\ j_z), H] = 0$, $[l\ (or\ l_z), H] \neq 0$.

Exercise 2:

Draw the first 7 levels corresponding to the Hamiltonian

$$H = \frac{p^2}{2\mu} + \frac{1}{2}\mu\omega r^2 + V_{ls}\boldsymbol{l} \cdot \boldsymbol{s}$$

where $\hbar\omega = 5$ MeV and V_{ls} = -0.5MeV.

Comment on the structure of the spectrum.

Exercise 3:

a) Determine the single-particle levels (including energy, l and j) for neutrons above the magic numbers Z=50, N=82.

b) Do the same for protons.

Hint: You may just extract the excitation energies (relative the ground state) or the total energies of the single-particle states from experimental data.

Exercise 4:

a) Determine the hole levels ((including energy, l and j)) in nuclei with protons below the magic numbers Z=82, N=126.

b) Repeat for neutrons.

The nuclear experimental spectra are found in the site

http : *//www.nndc.bnl.gov/nudat2/*

Bibliography

[1] M. Goeppert-Mayer, Phys. Rev. **75**, 1969 (1949).

[2] R.D. Woods and D.S. Saxon, Phys. Rev. **95**, 577 (1954).

[3] J. Dudek, Z. Szymanski, T. Werner, A. Faessler and C. Lima: Phys. Rev. **C26** 1712 (1982)

[4] Z. Lojewski, B. Nerlo-Pomorska, K. Pomorski, J. Dudek, Phys. Rev. **C 51**, 601 (1995)

[5] H. Koura and M. Yamada, Nucl. Phys. **A671**, 96 (2000).

[6] A. M. Lane, Phys. Rev. Lett. **8**, 171 (1962); Nucl. Phys. **35**, 676 (1962).

[7] E. Rost, Phys. Lett. **B 26** 184 (1968)

[8] J. Dudek, A. Majhofer, J. Skalski, T. Werner, S. Cwiok and W. Nazarewicz: J. Phys. **G 5,10** 1359 (1979)

[9] V.A. Chepurnov, Yad.Fiz 955 (1967)

[10] J. Blomqvist and S. Wahlborn, Ark. Fys. 16 (1960) 543

Chapter 4

Magnetic resonances in nuclei

Charge particles in a magnetic field. Time dependent magnetic fields. Time-dependent perturbation treatment. Rabi formula. Magnetic Resonance Imaging (MRI). Dipole magnetic moments in nuclei. Schmidt values.

4.1 Charge particles in a magnetic field

Assume a nucleon in the presence of a magnetic field carrying only its intrinsic angular momentum, i. e. its 1/2-spin. This would happen is the nucleon is trapped within the region where the experiment is performed. For instance, a proton in some molecules forming a crystal, or a proton in a molecule of human tissue, which is largely composed of water with two hydrogen atoms (where the nucleus is the proton itself) in each H_2O (water) molecule.

Assuming also that the magnetic field applied externally has the form

$$\boldsymbol{B} = B_0 \boldsymbol{k} \tag{4.1}$$

where B_0 is constant and $\boldsymbol{k}$ is the unit vector in the z-direction, the Hamiltonian is

$$H = -\boldsymbol{\mu} \cdot \boldsymbol{B} = -\mu_z B_0 \tag{4.2}$$

where the magnetic moment is defined by,

$$\boldsymbol{\mu} = \frac{gq}{2mc} \boldsymbol{s} \tag{4.3}$$

In contrast to what we presented above, the magnetic moment is now defined with dimensions. This is an unfortunate change of notation. We keep the notation used in each field. In Nuclear Physics the Hamiltonian is as in Eq. (4.3), while in the applications of magnetic resonances to be analyzed here we will use the Hamiltonian (4.2).

Since only the intrinsic spin of the particle is considered, the g-factor in Eq. (4.3) is as the g_s factor above, but for clarity of presentation we give them again here. In the cases of interest in the applications the g-factors are

$$g = \begin{cases} 2.00 & \text{electron} \\ 5.58 & \text{proton} \\ -3.82 & \text{neutron} \end{cases} \tag{4.4}$$

As before, q is the charge of the particle ($q = -e$ for electron) and $\boldsymbol{s} = (s_x, s_y, s_z)$ are the Pauli matrices given by,

$$s_x = \frac{\hbar}{2} \begin{pmatrix} 0 & 1 \\ 1 & 0 \end{pmatrix}; \quad s_y = \frac{\hbar}{2} \begin{pmatrix} 0 & -\mathrm{i} \\ \mathrm{i} & 0 \end{pmatrix}; \quad s_z = \frac{\hbar}{2} \begin{pmatrix} 1 & 0 \\ 0 & -1 \end{pmatrix} \tag{4.5}$$

The Hamiltonian becomes,

$$H = -\boldsymbol{\mu} \cdot \boldsymbol{B} = -\frac{gq}{2mc} B_0 \boldsymbol{s} \cdot \boldsymbol{k} = \omega_0 s_z = \frac{\omega_0 \hbar}{2} \begin{pmatrix} 1 & 0 \\ 0 & -1 \end{pmatrix} \tag{4.6}$$

where

$$\omega_0 = -\frac{gq}{2mc} B_0 \tag{4.7}$$

and the eigenvalues are,

$$H \begin{pmatrix} 1 \\ 0 \end{pmatrix} = \frac{\omega_0 \hbar}{2} \begin{pmatrix} 1 \\ 0 \end{pmatrix}; \quad H \begin{pmatrix} 0 \\ 1 \end{pmatrix} = -\frac{\omega_0 \hbar}{2} \begin{pmatrix} 0 \\ 1 \end{pmatrix} \tag{4.8}$$

There are two stationary (i.e. time independent) states with energies

$$E_{\pm} = \pm\frac{\omega_0\hbar}{2} \tag{4.9}$$

If the particle is in the state +, it will not decay unless a perturbation disturbs it. When it decays a photon with energy $E_+ - E_- = \hbar\omega_0$ will be emitted which can be measured with great precision, thus allowing one to determine precisely quantities like the g-factor.

4.2 Time dependent magnetic fields

A convenient way to perturb the system is by applying a weak and time-dependent magnetic field in the x-direction. Rabi chose for this purpose the form $B_1 \cos\omega t\, \boldsymbol{i}_x$. The perturbation will then vary from $-B_1$ to $+B_1$ as the time increases. The hope is that at a certain value of ω the transition will take place. Notice that B_1 has to be very small in comparison to B_0 in order not to destroy the spectrum determined by B_0 (i.e. the levels $E_{\pm}$). The problem is then to solve the Hamiltonian

$$H = \omega_0 s_z - \frac{gqB_1}{2mc}\cos\omega t s_x \tag{4.10}$$

with $\omega_1 = -\dfrac{gqB_1}{2mc}$, one gets

$$H = \frac{\omega_0\hbar}{2}\begin{pmatrix} 1 & 0 \\ 0 & -1 \end{pmatrix} + \frac{\omega_1\hbar}{2}\cos\omega t\begin{pmatrix} 0 & 1 \\ 1 & 0 \end{pmatrix} = \frac{\hbar}{2}\begin{pmatrix} \omega_0 & \omega_1\cos\omega t \\ \omega_1\cos\omega t & -\omega_0 \end{pmatrix} \tag{4.11}$$

where $|\omega_1| \ll |\omega_0|$. One has to use the time-dependent Schrödinger equation, i.e.

$$H\Psi(t) = \mathrm{i}\hbar\frac{\mathrm{d}\Psi(t)}{\mathrm{d}t} \tag{4.12}$$

Time-dependent perturbation treatment

Since B_1 is very small the solution $\Psi(t)$ should not be very different from the solution corresponding to $B_1 = 0$. We will therefore solve first the case $B_1 = 0$, i. e.

$$\frac{\hbar}{2}\begin{pmatrix} \omega_0 & 0 \\ 0 & -\omega_0 \end{pmatrix}\begin{pmatrix} a(t) \\ b(t) \end{pmatrix} = \mathrm{i}\hbar\begin{pmatrix} \dot{a}(t) \\ \dot{b}(t) \end{pmatrix} \tag{4.13}$$

where $\dot{a}(t) = \dfrac{\mathrm{d}a(t)}{\mathrm{d}t}$. One thus has

$$\begin{cases} \dfrac{\hbar}{2}\omega_0 a(t) &= \mathrm{i}\hbar\dfrac{\mathrm{d}a(t)}{\mathrm{d}t} \\ -\dfrac{\hbar}{2}\omega_0 b(t) &= \mathrm{i}\hbar\dfrac{\mathrm{d}b(t)}{\mathrm{d}t} \end{cases} \quad\Longrightarrow\quad \begin{cases} a(t) &= a(0)\,\mathrm{e}^{-\mathrm{i}\omega_0 t/2} \\ b(t) &= b(0)\,\mathrm{e}^{\mathrm{i}\omega_0 t/2} \end{cases} \tag{4.14}$$

The general case is

$$\frac{\hbar}{2}\begin{pmatrix} \omega_0 & \omega_1\cos\omega t \\ \omega_1\cos\omega t & -\omega_0 \end{pmatrix}\begin{pmatrix} a(t) \\ b(t) \end{pmatrix} = \mathrm{i}\hbar\begin{pmatrix} \dot{a}(t) \\ \dot{b}(t) \end{pmatrix} \tag{4.15}$$

since $|\omega_1| \ll |\omega_0|$, one proposes as solution

$$\begin{pmatrix} a(t) \\ b(t) \end{pmatrix} = \begin{pmatrix} \mathrm{e}^{-\mathrm{i}\omega_0 t/2}\, c(t) \\ \mathrm{e}^{\mathrm{i}\omega_0 t/2}\, d(t) \end{pmatrix} \tag{4.16}$$

which contains the main term explicitly.

The Schrödinger equation becomes

$$\frac{\hbar}{2}\begin{pmatrix} \omega_0 & \omega_1\cos\omega t \\ \omega_1\cos\omega t & -\omega_0 \end{pmatrix}\begin{pmatrix} \mathrm{e}^{-\mathrm{i}\omega_0 t/2}\,c(t) \\ \mathrm{e}^{\mathrm{i}\omega_0 t/2}\,d(t) \end{pmatrix} = \mathrm{i}\hbar\begin{pmatrix} -\mathrm{i}\frac{\omega_0}{2}\mathrm{e}^{-\mathrm{i}\omega_0 t/2}c(t) + \mathrm{e}^{-\mathrm{i}\omega_0 t/2}\dot{c}(t) \\ \mathrm{i}\frac{\omega_0}{2}\mathrm{e}^{\mathrm{i}\omega_0 t/2}d(t) + \mathrm{e}^{\mathrm{i}\omega_0 t/2}\dot{d}(t) \end{pmatrix} \tag{4.17}$$

with $\cos\omega t = \left(\mathrm{e}^{\mathrm{i}\omega t/2} + \mathrm{e}^{-\mathrm{i}\omega t/2}\right)/2$,

$$\mathrm{i}\begin{pmatrix} \dot{c}(t) \\ \dot{d}(t) \end{pmatrix} = \frac{\omega_1}{4}\begin{pmatrix} \left[\mathrm{e}^{\mathrm{i}(\omega_0+\omega)t} + \mathrm{e}^{\mathrm{i}(\omega_0-\omega)t}\right]d(t) \\ \left[\mathrm{e}^{-\mathrm{i}(\omega_0-\omega)t} + \mathrm{e}^{-\mathrm{i}(\omega_0+\omega)t}\right]c(t) \end{pmatrix} \tag{4.18}$$

The idea is to change ω in the perturbation term $B_1\cos\omega t$ such that $\hbar\omega_0 \approx \hbar\omega$. Since ω_0 is large, the highly oscillating functions $\mathrm{e}^{\pm\mathrm{i}(\omega_0+\omega)t}$ can be neglected. One thus gets

$$\begin{cases} \mathrm{i}\dot{c}(t) = \dfrac{\omega_1}{4}\,\mathrm{e}^{\mathrm{i}(\omega_0-\omega)t}d(t) \\ \mathrm{i}\dot{d}(t) = \dfrac{\omega_1}{4}\,\mathrm{e}^{-\mathrm{i}(\omega_0-\omega)t}c(t) \end{cases} \tag{4.19}$$

which is a coupled set of two first order differential equations. To solve it one transforms it in a second order differential equation as follows.

$$\begin{cases} \mathrm{i}\ddot{c}(t) = \dfrac{\omega_1}{4}\,\mathrm{e}^{\mathrm{i}(\omega_0-\omega)t}\Big[\mathrm{i}(\omega_0-\omega)d(t) + \dot{d}(t)\Big] \\ \mathrm{i}\ddot{d}(t) = \dfrac{\omega_1}{4}\,\mathrm{e}^{-\mathrm{i}(\omega_0-\omega)t}\Big[-\mathrm{i}(\omega_0-\omega)c(t) + \dot{c}(t)\Big] \end{cases} \tag{4.20}$$

and replacing $c(t)$ and $\dot{c}(t)$ from Eq. (4.19)

$$\begin{aligned} \mathrm{i}\ddot{d}(t) &= \frac{\omega_1}{4}\,\mathrm{e}^{-\mathrm{i}(\omega_0-\omega)t}\Big[-\mathrm{i}(\omega_0-\omega)\,\frac{4\mathrm{i}}{\omega_1}\,\mathrm{e}^{\mathrm{i}(\omega_0-\omega)t}\dot{d}(t) + \frac{\omega_1}{4\mathrm{i}}\,\mathrm{e}^{\mathrm{i}(\omega_0-\omega)t}d(t)\Big] \\ &= (\omega_0-\omega)\dot{d}(t) - \mathrm{i}\left(\frac{\omega_1}{4}\right)^2 d(t) \end{aligned}$$

$$\ddot{d}(t) + \mathrm{i}(\omega_0-\omega)\dot{d}(t) + \left(\frac{\omega_1}{4}\right)^2 d(t) = 0 \tag{4.21}$$

which has the solution

$$d(t) = A\mathrm{e}^{-\mathrm{i}(\omega_0-\omega)t/2}\sin\Omega t, \quad \Omega = \frac{1}{2}\sqrt{(\omega_0-\omega)^2 + (\omega_1/2)^2} \tag{4.22}$$

where A is a constant which is determined by the normalization condition, i.e.,

$$\big(c^*(t), d^*(t)\big)\begin{pmatrix} c(t) \\ d(t) \end{pmatrix} = \big|c(t)\big|^2 + \big|d(t)\big|^2 = 1 \tag{4.23}$$

One proceeds in the same fashion with $c(t)$ to obtain

$$c(t) = 2A\,\frac{\omega_0-\omega_1}{\omega_1}\,\mathrm{e}^{\mathrm{i}(\omega_0-\omega)t/2}\left(-\sin\Omega t - \mathrm{i}\sqrt{1 + \frac{\omega_1^2}{4(\omega_0-\omega)^2}}\cos\Omega t\right) \tag{4.24}$$

Rabi formula

We have assumed that before the perturbation the system is in the state (+), i.e.

$$c(0) = 1; \quad d(0) = 0 \tag{4.25}$$

$$\big|c(0)\big|^2 + \big|d(0)\big|^2 = \big|c(0)\big|^2 = 1 \tag{4.26}$$

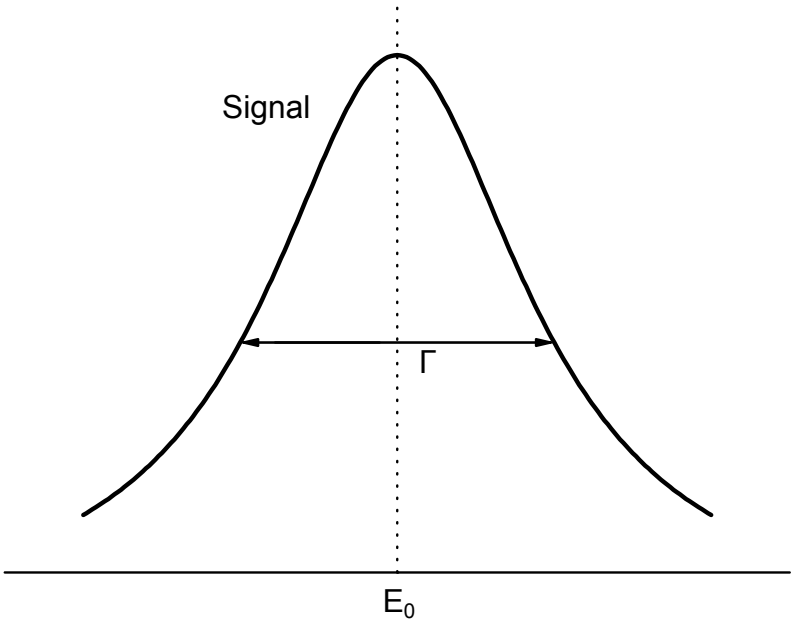

Figure 4.1: The resonant form of the signal as the energy E, corresponding to the weak magnetic field $\mathbf{B}_1$, approaches the energy E_0 induced by $\mathbf{B}_0$. The width of the resonance is Γ.

From $\left|c(0)\right|^2 = 1$, and after some algebra, one gets,

$$\left|A\right|^2 = \frac{(\omega_1/2)^2}{(\omega_0-\omega)^2+(\omega_1/2)^2} \tag{4.27}$$

and the probability that the transition takes place, i.e. that the system is in the state $(-)$ is

$$\left|d(t)\right|^2 = \frac{(\omega_1/2)^2}{(\omega_0-\omega)^2+(\omega_1/2)^2}\,\sin^2\Omega t \tag{4.28}$$

and a resonance occurs when $\omega = \omega_0$. Eq. (4.28) is the Rabi's formula.

Nuclear magnetic resonance was first described and measured in molecular beams by Isidor Isaac Rabi in 1938. In 1944, Rabi was awarded the Nobel Prize in physics for this work.

`http://www.nobelprize.org/nobel_prizes/physics/laureates/1944/`

4.3 Nuclear magnetic resonance (NMR)

Nuclear magnetic resonance (NMR) is a physical phenomenon in which magnetic nuclei in a magnetic field absorb and re-emit electromagnetic radiation. This energy is at a specific resonance frequency which depends on the strength of the magnetic field and the magnetic properties of the isotope of the atoms.

One sees that A shows a form similar to that of the Breit-Wigner formula

$$\frac{(\omega_1/2)^2}{(\omega_0-\omega)^2+(\omega_1/2)^2}\,\frac{\hbar^2}{\hbar^2} = \frac{(\Gamma_1/2)^2}{(E_0-E)^2+(\Gamma_1/2)^2} \tag{4.29}$$

from which one can define $E = \hbar\omega_0$ as the magnetic resonance energy and $\Gamma_1 = \hbar\omega_1$ as the the width.

In Fig. 4.1 the form of the signal resulting from this expression is shown. The signal-energy plot shown in Fig. 4.1 has been used to investigate the inner structure of materials. Many scientific techniques exploit NMR phenomena to study molecular physics, crystals, and non-crystalline materials through NMR spectroscopy. NMR allows the observation of specific quantum mechanical magnetic properties

Table 4.1: the gyromagnetic ratio γ of typical nuclei.

Nucleus	Spin	γ(MHz/T)	Natural Abundance
^{1}H	1/2	42.576	99.985
^{2}H	1	6.536	0.015
^{13}C	1/2	10.705	1.11
^{14}N	1	3.077	99.63

of the atomic nucleus. In particular, it is used in Medicine to image nuclei of atoms inside the body (magnetic resonance imaging (MRI)).

In all applications of MRI one uses SI units and introduces the Bohr magneton

$$\mu_B = \frac{q\hbar}{2mc} \tag{4.30}$$

In these units the frequency becomes

$$\omega_0 = \frac{gqB_0}{2mc} = \frac{g\mu_B B_0}{\hbar} = \gamma B_0 \tag{4.31}$$

This is known as the Larmor Equation. As already mentioned, for electrons it is $g = 2.00$ and $\mu_B = 5.79\times10^{-5}$eV/T, where the unit Tesla is $1\text{T} = 10^4$gauss. Remember $\hbar c \approx 200$MeVfm. The precise value of $\hbar$ is $\hbar = 6.58\times10^{-22}$MeVsec. For protons $g = 5.58$ (as also already mentioned) and $\mu_N = 3.15\times10^{-8}$eV/T. In practical applications, the frequency is similar to VHF and UHF television broadcasts (60−1000 MHz).

Magnetic Resonance Imaging (MRI)

An MRI machine uses a powerful magnetic field to align the magnetization of some atoms in the body, and radio frequency fields to systematically alter the alignment of this magnetization. This causes the nuclei to produce a rotating magnetic field detectable by the scanner and this information is recorded to construct an image of the scanned area of the body. Strong magnetic field gradients cause nuclei at different locations to rotate at different speeds. 3-D spatial information can be obtained by providing gradients in each direction.

MRI provides good contrast between the different soft tissues of the body, which make it especially useful in imaging the brain, muscles, the heart, and cancers compared with other medical imaging techniques such as computed tomography (CT) or X-rays. Unlike CT scans or traditional X-rays, MRI uses no ionizing radiation.

This last is a very important point, since it implies that no damage of the human tissue is associated with MRI.

All isotopes that contain an odd number of protons and/or of neutrons have an intrinsic magnetic moment. The most commonly studied nuclei are ^{1}H and ^{13}C (both with spin 1/2). Hydrogen is highly abundant, especially in biological systems in water (H_2O) and lipid (CH_2) molecules. It is the nucleus most sensitive to NMR signal (apart from ^{3}H which is not commonly used due to its instability and radioactivity). Proton NMR produces narrow chemical shift with sharp signals. Fast acquisition of quantitative results (peak integrals in stoichiometric ratio) is possible due to short relaxation time. The ^{1}H signal has been the sole diagnostic nucleus used for clinical MRI. Nuclei from isotopes of many other elements (e.g., ^{2}H, ^{6}Li, ^{10}B, ^{11}B, ^{14}N, ^{15}N, ^{17}O, ^{19}F, ^{23}Na, ^{29}Si, ^{31}P, ^{35}Cl, ^{113}Cd, ^{129}Xe, ^{195}Pt) have been studied by high-field NMR spectroscopy as well. Most even-even nuclei have zero nuclear magnetic moments, and they also have zero magnetic dipole and quadrupole moments. Hence, such nuclides do not exhibit any NMR absorption spectra.

The biological abundance describes the fraction of certain atom in the human body. The biological abundances of H, O, C and N in the body are 0.63, 0.26, 0.094, 0.015, respectively.

`http://www.cis.rit.edu/htbooks/mri/`

Electron spin resonance

The magnetic moment of an electron amounts to 658 times the magnetic moment of a proton. The electron does not contribute to the signal in MRI, though it can undergo a similar process as the nucleus,

called electron spin resonance (ESR). ESR is a related technique in which transitions between electronic spin levels are detected rather than nuclear ones. The basic principles are similar but the instrumentation, data analysis, and detailed theory are significantly different.

The electron gyromagnetic ratio is given by 28024.95266(62) MHz/T. The magnetic field produced by an electron is much stronger than that produced by a proton. However, in most substances the electrons are paired, resulting in a weak net magnetic field. There is a much smaller number of molecules and materials with unpaired electron spins that exhibit ESR (or electron paramagnetic resonance (EPR)) absorption than those that have NMR absorption spectra.

Nuclear magnetic resonance quantum computer

NMR quantum computing uses the spin states of molecules as qubits. Operations are performed on the ensemble through radio frequency pulses applied perpendicular to a strong, static field, created by a very large magnet. Some early success was obtained in performing quantum algorithms in NMR systems due to the relative maturity of NMR technology. For instance, in 2001 researchers at IBM reported the successful implementation of Shor's algorithm in a 7-qubit NMR quantum computer
(http://www.nature.com/nature/journal/v414/n6866/full/414883a.html).

4.4 Magnetic fields and magnetic moments

A nucleon moving in a single-particle state outside a central potential, as discussed above, will be affected by the presence of an external magnetic field. The corresponding Hamiltonian is,

$$H = -\frac{q}{2mc}\boldsymbol{\mu}\cdot\boldsymbol{B} \tag{4.32}$$

where q is the effective charge of the nucleon, $\boldsymbol{B}$ is the magnetic field and $\boldsymbol{\mu}$ is the dimensionless nuclear dipole moment defined as,

$$\boldsymbol{\mu} = g_l\hat{l} + g_s\hat{s} \tag{4.33}$$

The effective charge should be $q = 1.0\ e$ (e is the absolute value of the electron charge) for protons and 0 for neutrons. However, its value is taken to be about 1.5 e for protons and about 1.0 e for neutrons (these are illustrative values that can vary in different nuclear regions, i. e. for different values of N and Z). The reason why the effective charge was introduced is that the odd nucleon affects the core and it has been shown that its influence can be taken into account by the effective charge.

The magnetic moments can be measured with great precision, thus providing precise value for the g-factors also. These are given by,

$$g_l = \begin{cases} 1 & \text{proton} \\ 0 & \text{neutron} \end{cases} \qquad g_s = \begin{cases} 5.58 & \text{proton} \\ -3.82 & \text{neutron} \end{cases} \tag{4.34}$$

Dipole magnetic moments in nuclei

When the magnetic field is applied the energies observed experimentally are quantized according to the allowed angular momenta in Eq. (4.33). To measure the dipole magnetic moment μ one chooses the maximum splitting of the levels. One sees from Eq. (4.32) that the maximum effect of the magnetic field would be induced by the maximum alignment of $\boldsymbol{\mu}$ and $\boldsymbol{B}$. This is what one chooses experimentally. Classically this occurs when $j_z = j$ (since $\boldsymbol{B}$ is in the z-direction). In Quantum Mechanics one has to choose the projection m of the total angular momentum such that $m = j$. Therefore one defines the dipole magnetic moment as

$$\mu = \langle jm = j|g_l\hat{l}_z + g_s\hat{s}_z|jj\rangle \tag{4.35}$$

notice that μ is just a number without dimensions.

Since $\boldsymbol{l} = \boldsymbol{j} - \boldsymbol{s}$ one can write

$$\mu = \langle jj|g_l\hat{j}_z + (g_s - g_l)\hat{s}_z|jj\rangle \tag{4.36}$$

To calculate the values obtained by the application of the operator $\hat{s}_z$ upon the state $|jj\rangle$, we expand this state in terms of the eigenvectors of $\hat{s}_z$, i. e.

$$|jm\rangle = \sum_{m_l m_s} \langle lm_l 1/2m_s|jm\rangle|lm_l 1/2m_s\rangle \tag{4.37}$$

and one obtains

$$\begin{aligned}\mu &= \langle jj| \sum_{m_l m_s} \langle l m_l 1/2 m_s|jj\rangle \left[\, g_l j + (g_s - g_l) m_s \right] |l m_l 1/2 m_s\rangle \\ &= \sum_{m_l m_s} \langle l m_l 1/2 m_s|jj\rangle^2 \left[\, g_l j + (g_s - g_l) m_s \right]\end{aligned}$$

It is $m_l = j - m_s$ and $m_s = \pm 1/2$, $m_l = j \mp 1/2$. Therefore

$$\begin{aligned}\mu &= \left\langle l, j - \frac{1}{2}, \frac{1}{2}, \frac{1}{2} \middle| jj \right\rangle^2 \left[g_l j + \frac{g_s - g_l}{2} \right] \\ &\quad + \left\langle l, j + \frac{1}{2}, \frac{1}{2}, -\frac{1}{2} \middle| jj \right\rangle^2 \left[g_l j - \frac{g_s - g_l}{2} \right]\end{aligned} \tag{4.38}$$

Schmidt values of single-particle states

The general expression for the magnetic moments corresponding to a nucleon moving outside a central field is given by Eq. (4.38). There are two different possibilities, namely a) $l = j + 1/2$; b) $l = j - 1/2$.

a) $j = l - 1/2$

$$\begin{aligned}\left\langle j + \frac{1}{2}, j - \frac{1}{2}, \frac{1}{2}, \frac{1}{2} \middle| jj \right\rangle^2 &= \frac{1}{2(j+1)} \\ \left\langle j + \frac{1}{2}, j + \frac{1}{2}, \frac{1}{2}, -\frac{1}{2} \middle| jj \right\rangle^2 &= \frac{2j+1}{2(j+1)}\end{aligned}$$

$$\mu = g_l j - (g_s - g_l) \frac{j}{2(j+1)} \tag{4.39}$$

b) $j = l + 1/2$

$$\begin{aligned}\left\langle j - \frac{1}{2}, j - \frac{1}{2}, \frac{1}{2}, \frac{1}{2} \middle| jj \right\rangle^2 &= 1 \\ \left\langle j - \frac{1}{2}, j + \frac{1}{2}, \frac{1}{2}, -\frac{1}{2} \middle| jj \right\rangle^2 &= 0\end{aligned}$$

$$\mu = g_l j + (g_s - g_l)/2 \tag{4.40}$$

Our assumption that the nucleon moves around the core without farther disturbances (for instance without exciting other nucleons in the core) is equivalent to assume that the nucleon moves in a single-particle state. If this is valid, then one can estimate probable values of the angular momenta l and j (we will perform this task in this Course). Since also the Schmidt values for the magnetic moment should be valid, then one can compare these magnetic moments with experiment to probe the models used to infere the angular momenta as well as the single-particle assumption that this implies. We will attest the success of this in the exercises.

4.5 Homework problems

Exercise 1:

a) Calculate the spectrum corresponding to a spin 1/2 particle with magnetic moment $\vec{\mu} = gq/(2mc)\vec{s}$ situated in a magnetic field $\vec{B} = B_x\vec{i} + B_y\vec{j}$ where B_x and B_y are constants.

b) Which is the probability that in the lowest state thus calculated the spin projection of the particle is measured to be s_z=-1/2.

Exercise 2:

a) In the Rabi formula one has to assume $|B_1/B_0| \ll 1$. Why?.

b) Show that $d(t)$ (Eq. (4.22) in Chapter 3) is solution of Eq. (4.21).

Exercise 3 (not mandatory):

Consider medical applications of Magnetic Resonance Imaging (MRI). In these applications,

a) Only protons are considered, while other heavier isotopes, like ^{16}O, are neglected. Why?.

b) Why are the interferences of electrons also neglected?.

c) The intrinsic spin of the proton is considered to be $\mathbf{j} = \mathbf{s}$. Why?.

Exercise 4:

Which is the width of a MRI resonance if the variable field perpendicular to B_0=1 T is B_1=10 gauss?. How much changes this width if B_0=2 T?.

Exercise 5:

Evaluate ω_0 for a proton in a magnetic field B_0=1.0 T (which is the most common value used in medical applications of MRI). Compare this frequency with the one corresponding to the x-rays in computed tomography (CT), with an energy of 10 keV, and the γ-rays of radiation therapy, with an energy of 1 MeV.

Exercise 6:

Evaluate the magnetic dipole moment (Schmidt value) corresponding to

a) A proton moving in an orbital $l = 2, j = 5/2$.

b) A neutron moving in an orbital $l = 1, j = 1/2$.

Exercise 7:

a) The magnetic dipole moments corresponding to the ground states of the nuclei $^{17}F_8$ and $^{41}Sc_{20}$ are observed to be 4.72 and 5.53, respectively. Which are the corresponding values of l and j?.

b) Which values of l and j would have the ground states of $^{17}O_9$ and $^{41}Ca_{21}$, for which the magnetic dipole moments are measured to be -1.83 and -1.59, respectively?.

Chapter 5

Rotational model

Rotational model

5.1 Rotational model

So far we have considered the nucleus as a Fermi gas consisting of neutrons and protons moving freely under the influence of the shell model central potential. We have indicated that the success of the shell model was in the beginning considered a wonder since the very short range of the nuclear force acting upon the tightly packed nucleons make it difficult to understand their free motion. There are arguments to justify this, but still one would rather think that those characteristics are more suitable to generate a collective behavior where all nucleons move together as a whole preserving the nuclear volume. These considerations gave rise to the so-called liquid drop model in which the individual nucleons do not play any role. It is the nucleus as a whole that determines its dynamics. Like a liquid drop, the surface of the nucleus vibrates and rotates generating bands of quantized states. An even more limited collective model considers the nucleus as a rigid body with fixed center of mass. The only possible motions of such an object are rotations. This is the rotational model, where the conglomerate of individual nucleons form a compact entity, like a top or a rugby ball.

From classical mechanics it is known that three angles are needed to define the position of a rigid body with fixed center of mass. These are called Euler angles. One chooses an intrinsic axis system, called (x',y',z') in Fig. 5.1, and determines the direction of one of the axis, say z', with respect to the laboratory system (x,y,z). This operation requires two of the Euler angles. The third one is used to obtain the orientation of the body along the intrinsic axis z'. The Euler angles are denoted by (θ, ϕ, φ). The energy of the rotating rigid body, with the center of mass fixed at the center of coordinates, is

$$E = \frac{J_{x'}^2}{2\mathfrak{I}_{x'}} + \frac{J_{y'}^2}{2\mathfrak{I}_{y'}} + \frac{J_{z'}^2}{2\mathfrak{I}_{z'}} \tag{5.1}$$

where $\mathfrak{I}_{x'}$ is the x' component of the moment of inertia and $J_{x'}$ is the corresponding angular momentum component.

We will assume that the rigid body has cylindrical symmetry along the z' axis. Therefore the component $J_{z'}$ of the angular momentum, which is usually denoted by the letter K, is conserved. This symmetry also implies that $\mathfrak{I}_{x'} = \mathfrak{I}_{y'}$. We will use the symbol $\mathfrak{I}$ to denote this moment of inertia.

In the intrinsic system the rigid body is at rest and here the symmetry is only cylindrical. But in the laboratory system the symmetry is spherical because the rigid body rotates in all directions and there is no way to distinguish one of these directions from another. Therefore the angular momentum **J** is conserved in the laboratory system and that implies, as we have seen in Chapter 1, that J^2 and J_z are good quantum numbers which can be used to label the rotational state. The quantum number associated with J_z is usually called M. The state thus carries J, M, K as quantum numbers, i. e. it can be written as $|JMK\rangle$ or,

$$D^J_{MK}(\theta, \phi, \varphi) = \langle \theta\phi\varphi | JMK \rangle \tag{5.2}$$

which are called "d-functions". They satisfy the eigenvalue equations,

$$\begin{aligned} \boldsymbol{J}^2 D^J_{MK}(\theta, \phi, \varphi) &= \hbar^2 J(J+1) D^J_{MK}(\theta, \phi, \varphi), \\ J_z D^J_{MK}(\theta, \phi, \varphi) &= \hbar M D^J_{MK}(\theta, \phi, \varphi), \\ J_{z'} D^J_{MK}(\theta, \phi, \varphi) &= \hbar K D^J_{MK}(\theta, \phi, \varphi) \end{aligned} \tag{5.3}$$

In classical mechanics one can distinguish whether an spherically symmetric body rotates or not, but in quantum mechanics all directions are the same and the body appears to be at rest. Therefore there is

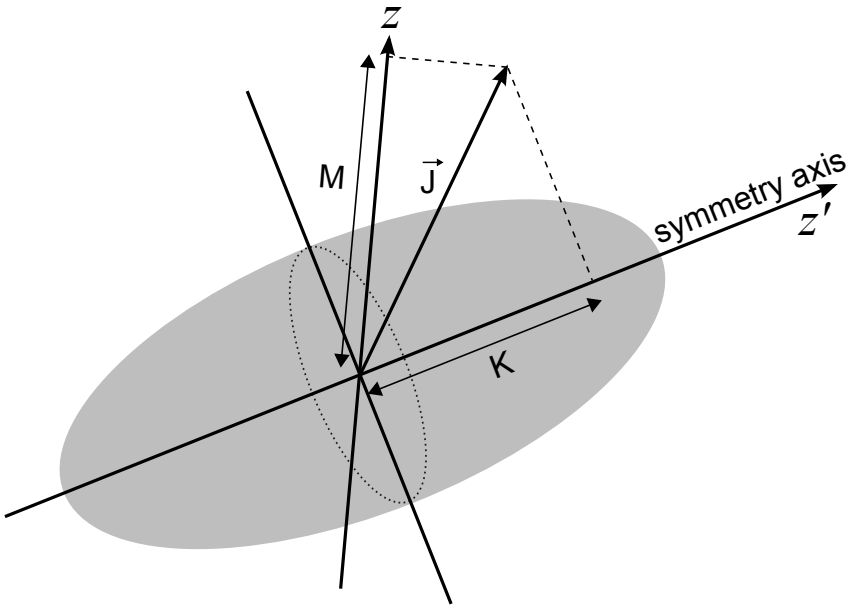

Figure 5.1: A cylindrically symmetric rotator. The symmetry axis is z'. The projection of the angular momentum upon this axis is K, and upon the z-axis in the laboratory frame is M.

no rotational energy associated to such a system or, in general, to degrees of freedom corresponding to a cylindrical symmetry. The Hamiltonian (5.1) thus becomes,

$$H = \frac{J_{x'}^2 + J_{y'}^2}{2\mathfrak{I}} = \frac{J^2 - J_{z'}^2}{2\mathfrak{I}} \tag{5.4}$$

The eigenfunctions of this Hamiltonian satisfying all the symmetries of the system, including the cylindrical symmetry, the reflection symmetry with respect to the (x',y') plane and the parity symmetry (notice that the Hamiltonian is invariant under the parity operation of changing $\mathbf{r}$ by $-\mathbf{r}$) is,

$$\langle \theta\phi\varphi | JMK \rangle = c\left(D^J_{MK} + (-1)^J D^J_{M-K}\right) \tag{5.5}$$

where c is a normalization constant. The corresponding eigenenergies are, from Eq. (5.4),

$$E(J,K) = \hbar^2 \frac{J(J+1) - K^2}{2\mathfrak{I}} \tag{5.6}$$

Since $J \geq K$ and positive for a given $K \geq 0$ there is a band of states with energies proportional to $J(J+1)$. This is call "rotational band". The lowest lying of these bands is the one corresponding to $K = 0$, and its lowest state, i. e. $E(0,0) = 0$, is the ground state of the rotational nucleus. Therefore this band is called ground state band. From Eq. (5.5) one sees that for the ground state band $\langle \theta\phi\varphi | JMK \rangle$ vanishes if J is odd. Therefore the members of the ground state band have even J and parity $(-1)^J = +1$ (since parity is conserved) and the energy is

$$E(J,0) = \hbar^2 \frac{J(J+1)}{2\mathfrak{I}} \tag{5.7}$$

This is a very characteristic spectrum and many nuclei follows it. An example is the nucleus ^{238}Pu which spectrum is shown in Fig. 5.2.

An important sign that a spectrum corresponds to a ground state band is that the relation between the energies of the first 4^+ and 2^+ states should be 10/3, as shown by Eq. (5.7). In general, the levels of a rotational ground band are related to the energy of the first excited state 2^+ by the relation $E(J,0) = E(2,0)\ J(J+1)/6$. The agreement between theory and experiment can be excellent, as is seen in Fig. 5.2. The moment of inertia of a rotational nucleus can be extracted from the experimental energy $E(2,0)$, since

$$\mathfrak{I} = \hbar^2 \frac{J(J+1)}{2E(2,0)}. \tag{5.8}$$

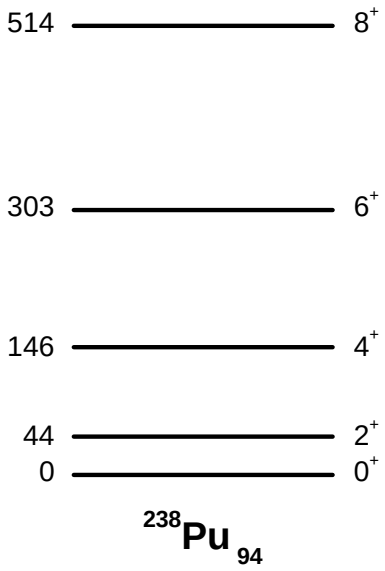

Figure 5.2: Ground rotational band (i. e. K=0) of ^{238}Pu. Energies are in keV. The rotational energies $E(J,0) = E(2,0)\ J(J+1)/6$, where $E(2,0) = 44keV$ in this case, are $E(4,0)$=147 keV, $E(6,0)$=308 keV and $E(8,0)$=528 keV.

For the $K > 0$ bands one can show that K must be even and J=K, K+1, K+2,... The lowest of the states of a band is called bandhead, and it corresponds to J=K. Therefore the bandhead energy E_{bh} is given by,

$$E_{bh}(K) = \hbar^2 \frac{K}{2\mathfrak{J}} \tag{5.9}$$

The rotational model has been very successful to explain the spectra of a large number of nuclei. It was formulated by A. Bohr and B. Mottelson in the beginning of the 1950's and it was corroborated experimentally by J. Rainwater. They were awarded the 1975 Nobel Prize in Physics for this work.

This model complements the shell model since it works very well in the middle of the major shells of Fig. 3.2, i. e. with values of the number of neutrons and protons which are far from magic numbers. However the shell model is, more than a model, a procedure to obtain a very good representation to solve the nuclear many-body problem. Therefore there have been many attempts to explain rotational spectra by using the shell model. This, which is even been pursued at present, has had a great importance in the understanding of nuclear correlations.

One can separate out the deformed nuclei from the others by making use of the ratio excitation energies

$$R_{42} = \frac{E_4}{E_2}. \tag{5.10}$$

It is a good indicator of the character of the nucleus and has the value $R_{42} = 10/3$ for an axial rotor. A histogram of R_{42} for all the nuclei for which the energies are known is shown in Fig. 5.3. There is a sharp peak around the rotor value.

5.2 Deformed shell model (Nilsson model)

The spherical shell model can explain many features of spherical nu- clei, but needs modifying to describe nuclei with many nucleons outside a closed shell. The residual interaction between these many valence nucleons may be more simply described by a deformed potential. For nuclear rotation to be observable, the nuclei have to be non-spherical, so that they have a preferred axis.

Quadrupole ($\lambda = 2$) deformations can give rise to asymmetric shapes. These triaxial distortions are governed by the γ shape degree of freedom, and this describes a stretching/squashing effect at right angles

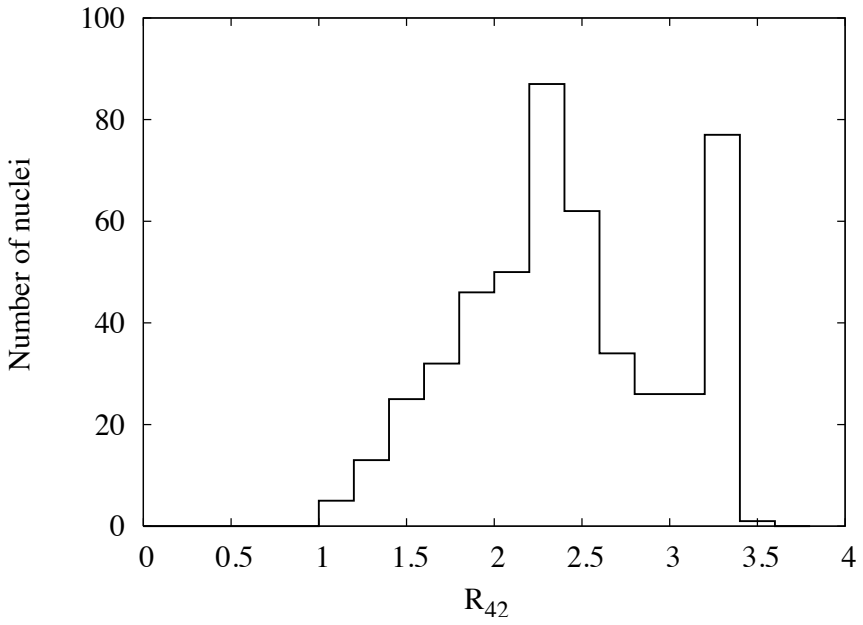

Figure 5.3: Distribution of nuclei with respect to deformation indicator R_{42}. Taken from GF Bertsch, arXiv:1203.5529.

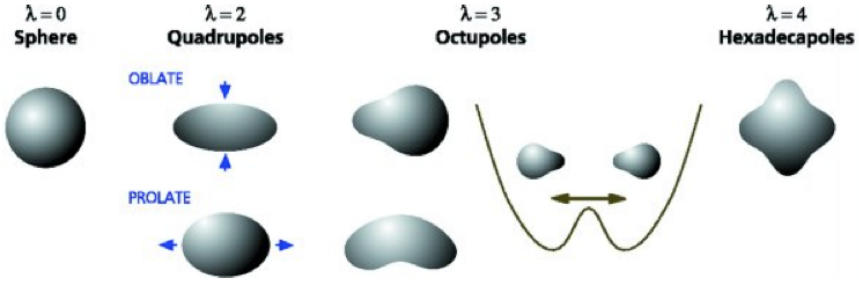

Figure 5.4: The different nuclear shapes that can be parametrised by spherical harmonic functions, where λ characterises the different orders of the corresponding distributions.

to the major nuclear axis. Gamma is measured in degrees, where $\gamma = 0°$ and $\gamma = 60°$ correspond to prolate and oblate shapes respectively. Completely triaxial shapes have $\gamma = 30°$.

The model that describes axially symmetric nuclei is called the Deformed Shell Model. In this model the Schrödinger equation is solved using the potential that describes the shape of the nucleus. An result of the deformation is that the orbital angular momentum, l, and the intrinsic spin, s, are no longer good quantum numbers and thus, states with different l-values but the same parity can mix. The energy of the states now depends on the component of the single-particle angular momentum (j) along the symmetry axis, which is denoted by Ω. For each orbital with angular momentum j, there are 2j+1 values of Ω ($= m_j$ in the absence of other couplings). However, levels with $+\Omega$ and Ω have the same energy due to the reflection symmetry of axially symmetric nuclei, so that each state is now doubly degenerate, i.e. two particles can be placed in each state. For example the f7/2 orbital can have $|\Omega|$ equal to 7/2, 5/2, 3/2 and 1/2. The ordering of these Ω levels depends on the particular shape of the nucleus since the lowest in energy is the orbital which interacts (overlaps) the most with the nuclear core. For prolate shaped nuclei the states with the lowest Ω values are the most tightly bound, whereas for oblate shaped nuclei, the states with the highest Ω occur lowest in energy. Such deformed shell model calculations were first performed in 1955 by Nilsson with an anisotropic harmonic oscillator potential and the calculated states (called Nilsson orbitals) are labelled by $\Omega[Nn_z\Lambda]$ where N is the total oscillator shell quantum number and determines the parity, given by $(-1)^N$. Lambda is the projection of the particle orbital angular momentum, l, on the nuclear symmetry axis, and n_z is the number of oscillator shell quanta along the direction of the symmetry axis.

5.3 Homework problems

Exercise 1:

Determine the moment of inertia from the experimental spectrum corresponding to the rotational ground state band in

(a) ^{238}Pu.

(b) ^{168}Yb.

Hint: Experimental data could be found in
http://www.nndc.bnl.gov/nudat2/

Chapter 6

Two-particle states

Two-particle states. Parity of n-particle states. Isospin. Sum of isospins. Consequences of antisymmetry.

In order to evaluate the two-particle matrix elements we have to extend the formalism to r-space. To this end we will assume that the particles move in the shells $|p\rangle = |n_p l_p j_p m_p\rangle$ and $|q\rangle = |n_q l_q j_q m_q\rangle$ of the chosen single-particle representation. Since $\mathbf{j} = \mathbf{l} + \mathbf{s}$ the corresponding single-particle wave function is (Chapter 1),

$$\langle \boldsymbol{r}|p\rangle = R_{n_p l_p j_p}(r)\left[Y_{l_p}(\hat{r})\chi_{1/2}\right]_{j_p m_p} \tag{6.1}$$

The two-particle representation consists of the product of the one-particle states, i. e.

$$\langle 12|pq\rangle = \langle \boldsymbol{r}_1|p\rangle\langle \boldsymbol{r}_2|q\rangle \tag{6.2}$$

and the corresponding antisymmetric wave function is.

$$\langle 12|pq\rangle_a = N(\langle 12|pq\rangle - \langle 21|pq\rangle) \tag{6.3}$$

where N is a normalization constant, which in this case is $N = 1/\sqrt{2}$. Writing explicitly the brackets in terms of the radial and spin coordinates one gets,

$$\Psi_a(pq;\boldsymbol{r}_1\boldsymbol{r}_2) = \frac{1}{\sqrt{2}}\Big[R_p(r_1)\left[Y_{l_p}(\hat{r}_1)\chi_{1/2}\right]_p R_q(r_2)\left[Y_{l_q}(\hat{r}_2)\chi_{1/2}\right]_q - R_p(r_2)\left[Y_{l_p}(\hat{r}_2)\chi_{1/2}\right]_p R_q(r_1)\left[Y_{l_q}(\hat{r}_1)\chi_{1/2}\right]_q\Big] \tag{6.4}$$

In this equation each index carries all the quantum numbers, e. g. $\{p \equiv n_p l_p j_p m_p\}$ although in the angular momentum function Y_{l_p} the orbital angular momentum is shown explicitly. The quantum numbers associated to Eq. (6.4) are $\{n_p l_p j_p m_p n_q l_q j_q m_q\}$. This is called the m-scheme. In this scheme the Pauli principle forbids all quantum numbers to be the same since if $q = p$, then $\Psi_a(pq;\boldsymbol{r}_1\boldsymbol{r}_2) = 0$. .

We have also seen that one can choose another coupling scheme, in which the two particles carry total angular momentum $\boldsymbol{J} = \boldsymbol{j}_p + \boldsymbol{j}_q$ with projection $M = m_p + m_q$, such that $|j_p - j_q| \leqslant J \leqslant j_p + j_q$ and $-J \leqslant M \leqslant J$. This is called *coupled*-scheme. In this scheme the two-particle wave function reads,

$$\Psi_a(pq,JM;\boldsymbol{r}_1\boldsymbol{r}_2) = \mathcal{N}\Big[R_p(r_1)R_q(r_2)\left[\left[Y_{l_p}(\hat{r}_1)\chi_{1/2}\right]_{j_p}\left[Y_{l_q}(\hat{r}_2)\chi_{1/2}\right]_{j_q}\right]_{JM} - R_p(r_2)R_q(r_1)\left[\left[Y_{l_p}(\hat{r}_2)\chi_{1/2}\right]_{j_p}\left[Y_{l_q}(\hat{r}_1)\chi_{1/2}\right]_{j_q}\right]_{JM}\Big] \tag{6.5}$$

The quantum numbers associated to this wave function are $\{n_p n_q l_p l_q j_p j_q JM\}$. There are eight quantum numbers in both schemes, as it should be since the quantum numbers express symmetries of the system that do not depend upon the chosen scheme.

In the *coupled*-scheme the quantum numbers m_p and m_q do not appear (remember that the radial wave functions $R_p(r)$ do not depend on m_p). Yet in the shells j_p and j_q one can place $2j_p + 1$ and $2j_q + 1$ particles, respectively. Therefore in the *coupled*-scheme all quantum numbers can be the same. This can be seen from Eq. (6.5) since it is not apparent that the wave function vanishes when $p = q$. To see how the Pauli principle works in this case it is convenient to exchange the angular momentum coupling of the second term in Eq. (6.5), from $(j_p j_q; JM)$ to $(j_q j_p; JM)$. One gets (see Exercise 4a of Homeworkproblems 1),

$$\Psi_a(pq,JM;\boldsymbol{r}_1\boldsymbol{r}_2) = \mathcal{N}\Big[R_p(r_1)R_q(r_2)\left[\left[Y_{l_p}(\hat{r}_1)\chi_{1/2}\right]_{j_p}\left[Y_{l_q}(\hat{r}_2)\chi_{1/2}\right]_{j_q}\right]_{JM} - R_p(r_2)R_q(r_1)(-1)^{j_p+j_q-J}\left[\left[Y_{l_q}(\hat{r}_1)\chi_{1/2}\right]_{j_q}\left[Y_{l_p}(\hat{r}_2)\chi_{1/2}\right]_{j_p}\right]_{JM}\Big] \tag{6.6}$$

For $p = q$ it is,

$$\Psi_a(pp, JM; \boldsymbol{r}_1\boldsymbol{r}_2) = \mathcal{N} R_p(r_1)R_p(r_2)\left[\left[Y_{l_p}(\hat{r}_1)\chi_{1/2}\right]_{j_p}\left[Y_{l_p}(\hat{r}_2)\chi_{1/2}\right]_{j_p}\right]_{JM}(1-(-1)^{2j_p-J}) \tag{6.7}$$

Since j_p is a semi integer one gets $(-1)^{2j_p}$ = -1. Therefore the Pauli principle requires that if $p = q$ the total angular momentum J should be even. One sees in the equation above that in this case the normalization constant is $\mathcal{N}$=1/2, and the antisymmetrized wave function becomes,

$$\Psi_a(pp, JM; \boldsymbol{r}_1\boldsymbol{r}_2) = R_p(r_1)R_p(r_2)\left[\left[Y_{l_p}(\hat{r}_1)\chi_{1/2}\right]_{j_p}\left[Y_{l_p}(\hat{r}_2)\chi_{1/2}\right]_{j_p}\right]_{JM} \tag{6.8}$$

Parity of n-particle states

We have seen in the previous Chapter that within the shell model the correlated two-particle states (that is the eigenvectors of the total Hamiltonian) are expanded in terms of the basis states (6.4) in m-scheme or (6.5) in *coupled*-scheme. In both cases the angular part of the wave function is a product of the single-particle Harmonic functions, e. g. in Eq. (6.4) this product appears as $\left[Y_{l_p}(\hat{r}_1)\chi_{1/2}\right]_{j_p m_p}\left[Y_{l_q}(\hat{r}_2)\chi_{1/2}\right]_{j_q m_q}$. The parity operation consists of making the transformation $(\mathbf{r_1}, \mathbf{r_2}) \rightarrow (-\mathbf{r_1}, -\mathbf{r_2})$ and, as we have seen in Chapter 1, this transformation adds a phase $(-1)^l$ in the Harmonic function Y_{lm}. Therefore the term above becomes $(-1)^{l_p+l_q}\left[Y_{l_p}(\hat{r}_1)\chi_{1/2}\right]_{j_p m_p}\left[Y_{l_q}(\hat{r}_2)\chi_{1/2}\right]_{j_q m_q}$ and the parity of the state is $(-1)^{l_p+l_q}$. For instance, if a particle is in a state with $j_p = s_{1/2}$ and the other in a state $j_q = p_{3/2}$ the parity of the possible states is -1. The possible total angular momenta are $|1/2 - 3/2| \leq J \leq 1/2 + 3/2$, that is the possible states are 1^- and 2^-. In the same fashion, if $p = q$ and $l_p = l_q = 3$, $j_p = j_q = 5/2$ the possible states are 0^+, 2^+ and 4^+.

In the n-nucleon case the basis consists of the product of n single-particle states (since they are eigenvectors of the free Hamiltonian H_0), The Harmonic functions in this product is given by $\left[Y_{l_{p_1}}(\hat{r}_1)\chi_{1/2}\right]_{j_{p_1} m_{p_1}}$ $\left[Y_{l_{p_2}}(\hat{r}_2)\chi_{1/2}\right]_{j_{p_2} m_{p_2}}$ ... $\left[Y_{l_{p_n}}(\hat{r}_n)\chi_{1/2}\right]_{j_{p_n} m_{p_n}}$ and, as before, the parity is $(-1)^{l_1+l_2+\ldots+l_n}$.

6.1 Isospin

Except the electric charge, protons and neutrons are very similar to each other. Not only they possess almost the same mass ($M_n/M_p = 1.0014$), but they also show a far reaching symmetry with regard to the nuclear interaction. Thus, experimental results extracted from proton-proton and proton-neutron scattering show that the nuclear forces are virtually the same for the proton-proton and neutron-proton systems. The properties of mirror nuclei, i. e. nuclei in which the number of protons and neutrons are exchanged retaining the same nuclear number A, are also very similar to each other. In particular the energy spectra of these nuclei are very much alike if effects induced by the Coulomb force are subtracted, as we will see.

One can consider neutrons and protons to be two states of the same particle, the nucleon. The nucleon is determined by the strong nuclear force. The Coulomb interaction is much weaker and has a very long range. At difference with the nuclear case, the Coulomb interaction is very well known and it is relatively easy to include its influence independently of the nuclear force.

The two states of the nucleon suggest a similarity with the spin and its two projections. This similarity prompted Heisenberg in 1932 (soon after the neutron was discovered) to introduce a new quantum number, the isospin $\hat{\mathbf{t}}$, with value 1/2 and two projections in an abstract space, the isospin space. The projection up of the isospin, $|\nu\rangle$, is a neutron and the isospin down, $|\pi\rangle$, a proton, i. e. for neutrons $\hat{t}_z|\nu\rangle = \frac{1}{2}|\nu\rangle$ and for protons $\hat{t}_z|\pi\rangle = -\frac{1}{2}|\pi\rangle$. The reason why one has taken the convention of given the value $+1/2$ to the neutron eigenvalue of $\hat{t}_z$ and $-1/2$ to proton, is that for the vast majority of nuclei it is $N \geq Z$. This implies that the total isospin projection of the nucleus (N, Z) is $(N - Z)/2 \geq 0$.

One defines the isospin projection in terms of the Pauli matrices following the spin relations, i. e.

$$\hat{t}_z = \frac{1}{2}\hat{\tau}_z = \frac{1}{2}\begin{pmatrix} 1 & 0 \\ 0 & -1 \end{pmatrix}; \quad |\nu\rangle = \begin{pmatrix} 1 \\ 0 \end{pmatrix}, \quad |\pi\rangle = \begin{pmatrix} 0 \\ 1 \end{pmatrix} \tag{6.9}$$

and the isospin is defined also following the spin algebra, i. e. $\hat{\boldsymbol{t}}^2 = \hat{t}_x^2 + \hat{t}_y^2 + \hat{t}_z^2$. The components (t_x, t_y, t_z) satisfy the same conmutation relations as the spin and, therefore, one can choose the eigenvalues $(t, t_z) = (1/2, t_z)$ to label the isospin states.

For the operator $\hat{\boldsymbol{t}}^2$ it is,

$$\hat{\boldsymbol{t}}^2|1/2\, t_z\rangle = t(t+1)|1/2\, t_z\rangle = \frac{3}{4}|1/2\, t_z\rangle \tag{6.10}$$

and for $\hat{\boldsymbol{t_z}}$,

$$\hat{\boldsymbol{t_z}}|1/2\, t_z\rangle = t_z|1/2\, t_z\rangle \tag{6.11}$$

One can define a charge operator in terms of the z-component of the isospin as,

$$\hat{Q} = \frac{1}{2}(1 - \hat{\tau}_z) = \frac{1}{2}\left[\begin{pmatrix} 1 & 0 \\ 0 & 1 \end{pmatrix} - \begin{pmatrix} 1 & 0 \\ 0 & -1 \end{pmatrix}\right] = \begin{pmatrix} 0 & 0 \\ 0 & 1 \end{pmatrix} \tag{6.12}$$

One finds that $\hat{Q}$ is indeed the charge operator since its eigenvalues are the same as those of $\hat{t}_z$, that is

$$\hat{Q}|\nu\rangle = \hat{Q}\begin{pmatrix} 1 \\ 0 \end{pmatrix} = e_\nu \begin{pmatrix} 1 \\ 0 \end{pmatrix}; \quad \hat{Q}|\pi\rangle = \hat{Q}\begin{pmatrix} 0 \\ 1 \end{pmatrix} = e_\pi \begin{pmatrix} 0 \\ 1 \end{pmatrix} \tag{6.13}$$

and the eigenvalues are the charges, with the values e_ν=0 and e_π=1, as it should be.

Since the Hamiltonian conserves charge one has

$$[H, \hat{Q}] = 0 \Longrightarrow [H, \hat{t}_z] = 0 \tag{6.14}$$

i.e. t_z is a constant of the motion and, therefore, a quantum number.

The single-particle wave function can then be labeled by the spatial-spin quantum numbers $|nlsjm\rangle$ (where $s = 1/2$) and the isospin quantum numbers $|tt_z\rangle$ ($t = 1/2$). The corresponding wave function is,

$$\langle \mathbf{r}|nlsjmtt_z\rangle = R_{nlj}(r)\,[Y_l(\hat{r})\chi_s]_{jm}\,\tau_{tt_z} \tag{6.15}$$

where τ_{tt_z} is the isospin state. It should be stressed that the isospin bears no relation to ordinary space.

Before finishing this Section it has to be emphasized that since the masses of the neutron and proton are not exactly the same, isospin is not an exact symmetry, although for all practical purposes one can consider isospin a good quantum number. The reason of this broken of symmetry is explained by the theory behind strong interactions, Quantum Chromo Dynamics (QCD). This theory describes the nucleon as been composed of three quarks, called up and down quarks, with different masses which are not possible to measure directly because the theory predicts that free quarks cannot be observed. The neutron contains 1 quark up and 2 down, while the proton contains 2 up and 1 down.

Ladder operators

In analogy with angular momentum one can define raising and lowering operators as

$$t_+ = \frac{1}{2}(\tau_x + i\tau_y) = \begin{pmatrix} 0 & 1 \\ 0 & 0 \end{pmatrix}, \tag{6.16}$$

and

$$t_- = \frac{1}{2}(\tau_x - i\tau_y) = \begin{pmatrix} 0 & 0 \\ 1 & 0 \end{pmatrix}. \tag{6.17}$$

The commutation relations between the ladder operators and t_z can easily be obtained as

$$\begin{aligned} [t_z, t_\pm] &= \pm\, t_\pm, \\ [t_+, t_z] &= 2t_z. \end{aligned} \tag{6.18}$$

Direct application of the explicit matrix representations to the isospinors yields the relations (i.e., beta decay process)

$$\begin{aligned} t_+|p\rangle &= |n\rangle, \\ t_+|n\rangle &= 0, \\ t_-|n\rangle &= |p\rangle, \\ t_-|p\rangle &= 0. \end{aligned} \tag{6.19}$$

or

$$t_\pm|tt_z\rangle = \sqrt{(t \mp t_z)(t \pm t_z + 1)}|tt_z \pm 1\rangle. \tag{6.20}$$

Sum of isospins

Since the isospin operators obey the angular momentum algebra (that is, the same commutation relations as the angular momentum operators) all the studies done for the case of sum of angular momenta is valid also here. Thus, given the isospins $\mathbf{t_1}$ and $\mathbf{t_2}$, the two-nucleon state can be labeled by using the m-scheme, i. e. $(t_1 t_{1z} t_2 t_{2z})$, with $t_1 = t_2 = 1/2$. One can also use the *coupled*-scheme by introducing the total isosspin $\boldsymbol{T} = \boldsymbol{t}_1 + \boldsymbol{t}_2$ with z-projection $T_z = t_{1z} + t_{2z}$ and the state can be labelled by $(t_1 t_2 T T_z)$. Both schemes can be used to describe any state in the space of isospin. In particular one can write a state in the m-scheme in in term of the states in *coupled*-scheme, as done in Eq. (1.91) of Chapter 1, by

$$|t_1 t_{1z} t_2 t_{2z}\rangle = \sum_{TT_z} \langle t_1 t_{1z} t_2 t_{2z} | TT_z\rangle |t_1 t_2 T T_z\rangle \tag{6.21}$$

or the other way around, as done in Eq. (1.92) of Chapter 1,

$$|t_1 t_2 T T_z\rangle = \sum_{t_{1z} t_{2z}} \langle t_1 t_{1z} t_2 t_{2z} | TT_z\rangle |t_1 t_{1z} t_2 t_{2z}\rangle \tag{6.22}$$

where $\langle t_1 t_{1z} t_2 t_{2z} | TT_z\rangle$ is the Clebsh-Gordan coefficient.

The triangular relation in this isospin case is, as usual, $|t_1 - t_2| \leqslant T \leqslant t_1 + t_2$ and $-T \leqslant T_z \leqslant T$. Since $t_1 = t_2 = 1/2$ one has $T = 0, 1$. The $T = 0$ ($T = 1$) excitation is called "isoscalar" ("isovector").

In general, with A nucleons with isospin $\mathbf{t_i}$ ($i = 1, 2...A$), one has

$$\mathbf{T} = \sum_{i=1}^{A} \mathbf{t}_i \Longrightarrow T_z = \sum_{i=1}^{A} t_{iz} \tag{6.23}$$

and with $A = N + Z$ one gets

$$\hat{T}_z |A\rangle = \frac{N - Z}{2} |A\rangle \tag{6.24}$$

i.e. the isospin projection is $(N - Z)/2$.

We define

$$T_\pm = \sum_i t_{i\pm}. \tag{6.25}$$

It can be shown that one has

$$T_\pm |TT_z\rangle = \sqrt{(T \mp T_z)(T \pm T_z + 1)} |TT_z \pm 1\rangle. \tag{6.26}$$

Since T_z is bounded by the value of $-T \leq T_z \leq T$ we have

$$T_\pm |T \pm T\rangle = 0. \tag{6.27}$$

Consequences of antisymmetry

The isospin symmetry that we are assuming implies that an A-body state defined by the space-spin quantum numbers bears also the isospin quantum numbers and therefore the wave function of such an state carries the quantum numbers

$$\{(n_1 l_1 s_1 j_1 m_1 t_1 t_{z1}, n_2 l_2 s_2 j_2 m_2 t_1 t_{z1}, ..., n_A l_A s_A j_A m_A t_A t_{zA})\}. \tag{6.28}$$

The meaning of the isospin symmetry is that an A-nucleon state with isospin T will be present in all nuclei with A nucleons satisfying $A = N + Z$. But this requires that all the other quantum numbers, i. e. those corresponding to the space-spin degrees of freedom, are the same. Therefore generally the isospin is a useful quantity only when the nucleons move all in the same orbits. This means that the core should have $N \approx Z$, but preferably it should be self conjugate, i. e. $N = Z$.

The antisymmetric wave function of two nucleons moving outside a frozen core is like in Eq. (6.6) but including also the isospin component of the wave function. If the two nucleons move in the same shell, as it was the case in Eq. (6.7), the wave function including isospin satisfies,

$$\langle 12 | (nlj)^2_{JM} (1/2\, 1/2)_{TT_z}\rangle_a = \mathcal{N}\big(1 - (-1)^{J+T}\big) \langle 12 | (nlj)^2_{JM} (1/2\, 1/2)_{TT_z}\rangle \tag{6.29}$$

which shows that the wave function vanishes unless $J+T$ is odd.

Since the space-spin part of the wave function is decoupled from the isospin part one can write,

$$\langle 12|(nlj)^2_{JM}(t_1,t_2)_{TT_z}\rangle_a = \big(\langle 12|(nlj)^2_{JM}\rangle\langle 12|(1/2\,1/2)_{TT_z}\rangle\big)_a \tag{6.30}$$

That is, either the spatial-spin part is symmetric and the isospin part antisymmetric, or the other way around. This is determined by the value of T, as can be seen by expanding the isospin part of the wave function,

$$\langle 12|(t_1t_2)_{TT_z}\rangle = \sum_{t_{1z}t_{2z}} \langle t_1t_{1z}t_2t_{2z}|TT_z\rangle\langle 12|t_1t_{1z}t_2t_{2z}\rangle \tag{6.31}$$

With $T=0$ and $t_1=t_2=t=1/2$, it is

$$\begin{aligned}\langle 12|(tt)_{00}\rangle &= \sum_{m=-1/2}^{1/2} \langle tmt-m|00\rangle\langle 1|tm\rangle\langle 2|t-m\rangle \\ &= \sum_{m=-1/2}^{1/2} \frac{(-1)^{1/2-m}}{\sqrt{2}}\langle 1|tm\rangle\langle 2|t-m\rangle \\ &= \frac{1}{\sqrt{2}}\big(\langle 12|\nu\pi\rangle - \langle 12|\pi\nu\rangle\big) = \frac{1}{\sqrt{2}}\langle 12|\nu\pi\rangle_a\end{aligned} \tag{6.32}$$

the isospin part is antisymmetric and therefore the spatial-spin part has to be symmetric which, in turn, requires J odd.

If $T=1$ the isospin part is symmetric and the spatial-spin part is antisymmetric.

6.2 Homework problems

Exercise 1: Derive Eqs. (6.7) and (6.8).
Exercise 2: Derive Eq. (6.29). What does it imply?

Chapter 7

Second Quantization

Creation and annihilation operators. Occupation number. Anticommutation relations. Normal product. Wick's theorem. One-body operator in second quantization. Hartree-Fock potential. Two-particle Random Phase Approximation (RPA). Two-particle Tamm-Dankoff Approximation (TDA).

7.1 Creation and annihilation operators

In Fig. 3 of the previous Chapter it is shown the single-particle levels generated by a double-magic core containing A nucleons. Below the Fermi level (FL) all states h_i are occupied and one can not place a particle there. In other words, the A-particle state $|0\rangle$, with all levels h_i occupied, is the ground state of the inert (frozen) double magic core.

Above the FL all states are empty and, therefore, a particle can be created in one of the levels denoted by p_i in the Figure. In Second Quantization one introduces the creation operator $c^\dagger_{p_i}$ such that the state $|p_i\rangle$ in the nucleus containing A+1 nucleons can be written as,

$$|p_i\rangle = c^\dagger_{p_i}|0\rangle \tag{7.1}$$

this state has to be normalized, that is,

$$\langle p_i|p_i\rangle = \langle 0|c_{p_i}c^\dagger_{p_i}|0\rangle = \langle 0|c_{p_i}|p_i\rangle = 1 \tag{7.2}$$

from where it follows that

$$|0\rangle = c_{p_i}|p_i\rangle \tag{7.3}$$

and the operator c_{p_i} can be interpreted as the annihilation operator of a particle in the state $|p_i\rangle$. This implies that the hole state h_i in the (A-1)-nucleon system is

$$|h_i\rangle = c_{h_i}|0\rangle \tag{7.4}$$

Occupation number and anticommutation relations

One notices that the number

$$n_j = \langle 0|c^\dagger_j c_j|0\rangle \tag{7.5}$$

is $n_j = 1$ is j is a hole state and $n_j = 0$ if j is a particle state. In the same fashion it is $\langle 0|c_j c^\dagger_j|0\rangle = 1$ (0) if j is a particle (hole) state, that is $\langle 0|c_j c^\dagger_j|0\rangle = 1$ - n_j. Therefore n_j is called occupation number of the state j.

In general it is

$$\langle 0|c^\dagger_j c_k|0\rangle = n_j\delta_{jk}, \tag{7.6}$$

and

$$\langle 0|c_k c^\dagger_j|0\rangle = (1-n_j)\delta_{jk}. \tag{7.7}$$

Summing these two equations one gets,

$$\langle 0|c_k c^\dagger_j + c^\dagger_j c_k|0\rangle = \delta_{jk} \tag{7.8}$$

which is valid independently of whether $|j\rangle$ and $|k\rangle$ are particle or hole states. It is a general equation and, therefore, the creation-annihilation operators satisfy

$$\{c_j, c^\dagger_k\} = \delta_{jk}. \tag{7.9}$$

The operation

$$\{A, B\} = AB + BA \tag{7.10}$$

is called the anticommutator of A and B, and these operators anticommute if

$$\{A, B\} = 0 \tag{7.11}$$

In second quantization the antisymmetrized two-particle state is $|ij\rangle_a = c_i^\dagger c_j^\dagger |0\rangle$, since it implies

$$c_i^\dagger c_j^\dagger = -c_j^\dagger c_i^\dagger \Longrightarrow c_i^\dagger c_i^\dagger = 0 \tag{7.12}$$

as required by the Pauli principle. In the same fashion

$$c_i c_j = -c_j c_i \tag{7.13}$$

Therefore

$$\{c_i, c_j\} = \{c_i^\dagger, c_j^\dagger\} = 0 \tag{7.14}$$

Since the state $|0\rangle$ corresponds to a nucleus with $A = N + Z$ nucleons, the state $c_i^\dagger c_j^\dagger |0\rangle$ corresponds to $A + 2$ nucleons. Therefore

$$\langle 0|c_i^\dagger c_j^\dagger|0\rangle = 0, \quad \langle 0|c_i c_j|0\rangle = 0 \tag{7.15}$$

for all i and j.

7.2 Normal product

Since $\langle 0|c_i c_j^\dagger|0\rangle = (1 - n_i)\delta_{ij}$, one can write

$$c_i c_j^\dagger = (1 - n_i)\delta_{ij} + : c_i c_j^\dagger : \tag{7.16}$$

where $: c_i c_j^\dagger :$ is defined by the relation,

$$\langle 0| : c_i c_j^\dagger : |0\rangle = 0 \tag{7.17}$$

The operator $: AB :$ is called normal product between A and B. In the same fashion

$$c_i^\dagger c_j = n_i \delta_{ij} + : c_i^\dagger c_j : \tag{7.18}$$

From these equations one gets (using $\{c_i, c_j^\dagger\} = \delta_{ij}$)

$$c_j c_i^\dagger = \delta_{ij} - c_i^\dagger c_j = (1 - n_i)\delta_{ij} - : c_i^\dagger c_j : \tag{7.19}$$

but

$$c_j c_i^\dagger = (1 - n_i)\delta_{ij} + : c_j c_i^\dagger : \tag{7.20}$$

$$: c_j c_i^\dagger := - : c_i^\dagger c_j : \tag{7.21}$$

One uses the notation

$$\overbrace{c_i c_j^\dagger} = (1 - n_i)\delta_{ij}; \quad \overbrace{c_i^\dagger c_j} = n_i \delta_{ij} \tag{7.22}$$

The operation $\overbrace{AB}$ is called contraction of the operators A and B. The contraction is a number. It is defined as the difference between the ordinary and the normal product of the operators A and B.

Therefore,

$$\overbrace{c_i^\dagger c_j^\dagger} = \overbrace{c_i c_j} = 0 \tag{7.23}$$

from where one gets,

$$c_i^\dagger c_j^\dagger =: c_i^\dagger c_j^\dagger :, \quad c_i c_j =: c_i c_j : \tag{7.24}$$

Wick's theorem

One can write any product of creation and annihilation operators in normal form by using the Wick's Theorem. It says that the product of operators,

$$A_1 A_2 A_3 \cdots A_{n-1} A_n \tag{7.25}$$

where A_i is $c_i^\dagger$ or c_i, can be written as

$$\begin{aligned} A_1 A_2 A_3 \cdots A_{n-1} A_n = &: A_1 A_2 A_3 \cdots A_{n-1} A_n : \\ &+ \overbrace{A_1 A_2} : A_3 \cdots A_{n-1} A_n : \\ &- \overbrace{A_1 A_3} : A_2 \cdots A_{n-1} A_n : \\ &+ \cdots \text{ (all single-contractions)} \\ &+ \overbrace{A_1 A_2}\,\overbrace{A_3 A_4} : A_5 \cdots A_{n-1} A_n : \\ &- \overbrace{A_1 A_3}\,\overbrace{A_2 A_4} : A_5 \cdots A_{n-1} A_n : \\ &+ \cdots \text{ (all double-contractions)} \\ &+ \cdots \text{ (upto } n/2\text{-contractions)} \end{aligned} \tag{7.26}$$

The plus or minus sign in each term is determined by the number of permutations one must do in order to arrive to the final form of the term. An odd (even) number of permutation gives a minus (plus) sign.

The great property of this theorem is that it allows one to get in a straightforward fashion the mean value of the product of operators, which is what one usually needs. This number is just the term without normal products, i. e. the last term in the equation above.

We have

$$\begin{aligned} \langle 0| : A_1 A_2 A_3 \cdots A_{n-1} A_n : |0\rangle = &\langle 0| A_1 A_2 A_3 \cdots A_{n-1} A_n |0\rangle \\ &- \langle 0| A_1 A_2 A_3 \cdots A_{n-1} A_n |0\rangle \langle 0|0\rangle \\ = &0 \end{aligned} \tag{7.27}$$

The "normal product" of a normal product

$$:: AB ::= \overbrace{: AB :} + :: AB ::=: AB : \tag{7.28}$$

The best way of understanding how this theorem works is by applying it to simple cases, We start by the product

$$c_i^\dagger c_j = \overbrace{c_i^\dagger c_j} + : c_i^\dagger c_j : \tag{7.29}$$

where only one contraction is possible and no permutation is needed to reach the final value, that is the sign is plus. As expected, one gets, $\langle 0| c_i^\dagger c_j |0\rangle = \overbrace{c_i^\dagger c_j}$

The next degree of complication is when two contractions are possible, for instance

$$\begin{aligned} c_i^\dagger c_j c_k c_l^\dagger = &: c_i^\dagger c_j c_k c_l^\dagger : \\ &+ \overbrace{c_i^\dagger c_j} : c_k c_l^\dagger : - \overbrace{c_i^\dagger c_k} : c_j c_l^\dagger : - \overbrace{c_j c_l^\dagger} : c_i^\dagger c_k : + \overbrace{c_k c_l^\dagger} : c_i^\dagger c_j : \\ &+ \overbrace{c_i^\dagger c_j}\,\overbrace{c_k c_l^\dagger} - \overbrace{c_i^\dagger c_k}\,\overbrace{c_j c_l^\dagger} \end{aligned} \tag{7.30}$$

one needs one permutation to get the term $\overbrace{c_i^\dagger c_k} : c_j c_l^\dagger$ and therefore a minus sign is added. The same is done to get the signs of all other terms. The mean value of this operator is,

$$\langle 0| c_i^\dagger c_j c_k c_l^\dagger |0\rangle = \overbrace{c_i^\dagger c_j}\,\overbrace{c_k c_l^\dagger} - \overbrace{c_i^\dagger c_k}\,\overbrace{c_j c_l^\dagger} = n_i \delta_{ij} (1 - n_k) \delta_{kl} - n_i \delta_{ik} (1 - n_j) \delta_{jl} \tag{7.31}$$

Further examples

We have

$$\begin{aligned} : c_i^\dagger c_i : c_\alpha^\dagger c_\beta^\dagger = &+ \overbrace{c_i c_\alpha^\dagger} : c_i^\dagger c_\beta^\dagger : - \overbrace{c_i c_\beta^\dagger} : c_i^\dagger c_\alpha^\dagger : \\ &+ : c_i^\dagger c_i c_\alpha^\dagger c_\beta^\dagger :, \end{aligned} \tag{7.32}$$

and

$$\begin{aligned} c_\alpha^\dagger c_\beta^\dagger : c_i^\dagger c_i := &- \overbrace{c_\alpha^\dagger c_i} : c_i^\dagger c_\beta^\dagger : + \overbrace{c_\beta^\dagger c_i} : c_i^\dagger c_\alpha^\dagger : \\ &+ : c_\alpha^\dagger c_\beta^\dagger c_i^\dagger c_i :, \end{aligned} \tag{7.33}$$

from which we get

$$[: c_i^\dagger c_i :, c_\alpha^\dagger c_\beta^\dagger] = \delta_{i\alpha} : c_i^\dagger c_\beta^\dagger : - \delta_{i\beta} : c_i^\dagger c_\alpha^\dagger : . \tag{7.34}$$

We also have

$$\begin{aligned} : c_\alpha^\dagger c_\beta^\dagger c_\gamma c_\delta : c_i^\dagger c_j^\dagger = &: c_\alpha^\dagger c_\beta^\dagger c_\gamma c_\delta c_i^\dagger c_j^\dagger : \\ &- \overbrace{c_\gamma c_i^\dagger} : c_\alpha^\dagger c_\beta^\dagger c_\delta c_j^\dagger : + \cdots \text{ (other three single contractions)} \\ &- \overbrace{c_\gamma c_i^\dagger}\, \overbrace{c_\delta c_j^\dagger} : c_\alpha^\dagger c_\beta^\dagger : + \overbrace{c_\gamma c_j^\dagger}\, \overbrace{c_\delta c_i^\dagger} : c_\alpha^\dagger c_\beta^\dagger : \end{aligned} \tag{7.35}$$

and one finds, after some algebra

$$\begin{aligned} [: c_\alpha^\dagger c_\beta^\dagger c_\gamma c_\delta :, c_i^\dagger c_j^\dagger] = &- \delta_{\gamma i} : c_\alpha^\dagger c_\beta^\dagger c_\delta c_j^\dagger : + \cdots \text{ (other three single contractions)} \\ &+ (1 - n_i - n_j)(-\delta_{\gamma i}\delta_{\delta j} + \delta_{\gamma i}\delta_{\delta j}) : c_\alpha^\dagger c_\beta^\dagger : \end{aligned} \tag{7.36}$$

7.3 One-body operator in second quantization

One-body operators depend upon one radial coordinate $\mathbf{r}$ only. In second quantization a one-body operator $\hat{M}$ can be written as,

$$\hat{M} = \sum_{pq} \langle p|\hat{M}|q\rangle c_p^\dagger c_q = \sum_{pq} \langle p|\hat{M}|q\rangle [: c_p^\dagger c_q : + \overbrace{c_p^\dagger c_q}] \tag{7.37}$$

where p and q run over all single-particle states (particle- as well as hole-states). To proof that this is correct we will evaluate the matrix element of $\hat{M}$ between two single-particle states, i. e. (A+1)-states of the form $|i\rangle = c_i^\dagger|0\rangle$ for which $n_i = 0$. The final result of this calculation should be that we get the matrix element itself again.

We then evaluate

$$\begin{aligned} \langle i|\hat{M}|j\rangle =& \langle 0|c_i \hat{M} c_j^\dagger|0\rangle = \sum_{pq} \langle p|\hat{M}|q\rangle \langle 0|c_i c_p^\dagger c_q c_j^\dagger|0\rangle \\ =& \sum_{pq} \langle p|\hat{M}|q\rangle \langle 0| \overbrace{c_i c_p^\dagger}\, \overbrace{c_q c_j^\dagger} + \overbrace{c_i c_j^\dagger}\, \overbrace{c_p^\dagger c_q} |0\rangle \\ =& \sum_{pq} \langle p|\hat{M}|q\rangle \Big[(1 - n_i)\delta_{ip}(1 - n_j)\delta_{qj} + (1 - n_i)\delta_{ij} n_p \delta_{pq}\Big] \\ =& (1 - n_i)(1 - n_j)\langle i|\hat{M}|j\rangle + (1 - n_i)\delta_{ij} \sum_p n_p \langle p|\hat{M}|p\rangle \end{aligned} \tag{7.38}$$

and we see that with $n_i = n_j = 0$ we get the matrix element we needed, i. e. $\langle i|\hat{M}|j\rangle$, but that there is also another contribution which appears only when $i = j$. This corresponds to the sum of the mean values of $\hat{M}$ over all hole states. It is the interaction of the particles in the A-nucleon core among themselves, leaving the particle in the (A+1)-nucleus untouched. This term is called "core polarization".

To avoid polarization effects one defines

$$\hat{M} = \sum_{pq} \langle p|\hat{M}|q\rangle : c_p^\dagger c_q : \tag{7.39}$$

that is, one assumes that $\hat{M}$ itself includes polarization. One sees that this avoids the core polarization term, since one cannot contract the indexes p and q (i. e. the term δ_{pq} in Eq. (7.38)). Therefore

the core polarization effects were assumed to be contained in the operator itself. This procedure is called "renormalization". It is done by introducing some parameters that takes proper account of the polarization. We will see that in electromagnetic transitions this is done by defining an effective charge for protons and also for neutrons which, without polarization, has no charge at all.

7.4 Two-body operator in second quantization

To avoid effects related to the interaction of the particles in the core, as it was the core polarization effect in the one-particle case above, one defines the two-body operator in second quantization in normal form, i. e. as,

$$\hat{M} = \sum_{\alpha\beta\gamma\delta} \langle \alpha\beta|\hat{M}|\gamma\delta\rangle : c_\alpha^\dagger c_\beta^\dagger c_\delta c_\gamma : \tag{7.40}$$

and evaluate the matrix element of this operator between antisymmetrized two-particle states, i. e. states in the (A+2)-nucleus. Our aim is to show that this procedure will indeed provide the antisymmetrized matrix element. In this context it is worthwhile to point out that a great advantage of second quantization is that in the many-particle case the Pauli principle is automatically taken into account.

The antisymmetrized two-particle states are,

$$|ij\rangle_a = c_i^\dagger c_j^\dagger|0\rangle \Longrightarrow {}_a\langle ij| = \langle 0|(c_i^\dagger c_j^\dagger)^\dagger = \langle 0|c_j c_i \tag{7.41}$$

and the matrix element is,

$${}_a\langle ij|\hat{M}|kl\rangle_a = \sum_{\alpha\beta\gamma\delta} \langle \alpha\beta|\hat{M}|\gamma\delta\rangle\langle 0|c_j c_i : c_\alpha^\dagger c_\beta^\dagger c_\delta c_\gamma : c_k^\dagger c_l^\dagger|0\rangle \tag{7.42}$$

Since the mean value of operators in normal form vanishes, the terms that survive contain only contractions. They are,

$$c_j c_i : c_\alpha^\dagger c_\beta^\dagger c_\delta c_\gamma : c_k^\dagger c_l^\dagger = \Big[\overbrace{c_i c_\alpha^\dagger}\,\overbrace{c_j c_\beta^\dagger} - \overbrace{c_i c_\beta^\dagger}\,\overbrace{c_j c_\alpha^\dagger}\Big]\Big[\overbrace{c_\gamma c_k^\dagger}\,\overbrace{c_\delta c_l^\dagger} - \overbrace{c_\gamma c_l^\dagger}\,\overbrace{c_\delta c_k^\dagger}\Big] \tag{7.43}$$

which give,

$$\begin{aligned} {}_a\langle ij|\hat{M}|kl\rangle_a = &\sum_{\alpha\beta\gamma\delta} \langle \alpha\beta|\hat{M}|\gamma\delta\rangle\Big[(1-n_i)\delta_{i\alpha}(1-n_j)\delta_{j\beta} - (1-n_i)\delta_{i\beta}(1-n_j)\delta_{j\alpha}\Big] \\ &\times \Big[(1-n_k)\delta_{k\gamma}(1-n_l)\delta_{l\delta} - (1-n_k)\delta_{k\delta}(1-n_l)\delta_{l\gamma}\Big] \\ =&(1-n_i)(1-n_j)(1-n_k)(1-n_l)\Big[\langle ij|\hat{M}|kl\rangle_a - \langle ji|\hat{M}|kl\rangle_a\Big] \\ &-(1-n_i)(1-n_j)(1-n_k)(1-n_l)\Big[\langle ij|\hat{M}|lk\rangle_a - \langle ji|\hat{M}|lk\rangle_a\Big] \end{aligned} \tag{7.44}$$

In r-representation the matrix element is

$$\langle ij|\hat{M}|kl\rangle = \int \mathrm{d}\boldsymbol{r}_1\mathrm{d}\boldsymbol{r}_2\big(\Psi_i(\boldsymbol{r}_1)\Psi_j(\boldsymbol{r}_2)\big)^*\hat{M}(\boldsymbol{r}_1,\boldsymbol{r}_2)\Psi_k(\boldsymbol{r}_1)\Psi_l(\boldsymbol{r}_2) \tag{7.45}$$

and due to the principle of action and reaction it is, $\hat{M}(\boldsymbol{r}_1,\boldsymbol{r}_2) = \hat{M}(\boldsymbol{r}_2,\boldsymbol{r}_1)$ which, according to Eq. (7.45), implies $\langle ij|\hat{M}|kl\rangle = \langle ji|\hat{M}|lk\rangle$.

The matrix element antisymmetrized to the right only becomes,

$$\langle ji|\hat{M}|kl\rangle_a = \langle ji|\hat{M}\big[|kl\rangle - |lk\rangle\big] = \langle ij|\hat{M}\big[|lk\rangle - |kl\rangle\big] = -\langle ij|\hat{M}|kl\rangle_a \tag{7.46}$$

and Eq. (7.44) becomes,

$${}_a\langle ij|\hat{M}|kl\rangle_a = (1-n_i)(1-n_j)(1-n_k)(1-n_l)\,{}_a\langle ij|\hat{M}|kl\rangle_a \tag{7.47}$$

which is just what we wanted to show. However, one does not need to take the matrix element with antisymmetric wave functions in bra as well as in ket positions since ${}_a\langle ij|\hat{M}|kl\rangle_a = 2\langle ij|\hat{M}|kl\rangle_a$. Therefore to obtain the matrix element $\langle ij|\hat{M}|kl\rangle_a$ one has to add a factor 1/4 to the expression (7.40), i. e.

$$\hat{M} = \frac{1}{4}\sum_{\alpha\beta\gamma\delta} \langle \alpha\beta|\hat{M}|\gamma\delta\rangle : c_\alpha^\dagger c_\beta^\dagger c_\delta c_\gamma : \tag{7.48}$$

This is the expression that is used in general. We will use it here also.

7.5 Hartree-Fock potential

We found that to avoid core excitations the one-body operator should be defined in terms of normal products. That is to use $:c_\alpha^\dagger c_\beta:$ instead of $c_\alpha^\dagger c_\beta$. It was due to this that we wrote the two-body operator in normal form also. But in doing so we bypassed what maybe an important physics. And indeed there is an important physics behind the core excitations in the case of two-body operators, particularly in the Hamiltonian. This is what we will explore now.

To this end we write the Hamiltonian $H = T + V$ in a representation consisting of the eigenvectors of another Hamiltonian. This is often chosen to be an Harmonic oscillator representation because it is mathematically easy to deal with and also because the nuclear bound states are well described by Harmonic oscillator potentials, as we have seen in the previous Chapter. Within the chosen representation (labeled by Greek letters below) the Hamiltonian becomes,

$$H = \sum_{\alpha\beta}\langle\alpha|T|\beta\rangle c_\alpha^\dagger c_\beta + \frac{1}{4}\sum_{\alpha\beta\gamma\delta}\langle\alpha\beta|V|\gamma\delta\rangle c_\alpha^\dagger c_\beta^\dagger c_\delta c_\gamma. \tag{7.49}$$

Converting to normal form one gets,

$$\begin{aligned} H = &\sum_{\alpha\beta}\langle\alpha|T|\beta\rangle(:c_\alpha^\dagger c_\beta: + \overbrace{c_\alpha^\dagger c_\beta}) + \frac{1}{4}\sum_{\alpha\beta\gamma\delta}\langle\alpha\beta|V|\gamma\delta\rangle[:c_\alpha^\dagger c_\beta^\dagger c_\delta c_\gamma: \\ &+ :c_\alpha^\dagger c_\gamma:\overbrace{c_\beta^\dagger c_\delta} - :c_\alpha^\dagger c_\delta:\overbrace{c_\beta^\dagger c_\gamma} - :c_\beta^\dagger c_\gamma:\overbrace{c_\alpha^\dagger c_\delta} + :c_\beta^\dagger c_\delta:\overbrace{c_\alpha^\dagger c_\gamma} \\ &+ \overbrace{c_\alpha^\dagger c_\gamma}\,\overbrace{c_\beta^\dagger c_\delta} - \overbrace{c_\alpha^\dagger c_\delta}\,\overbrace{c_\beta^\dagger c_\gamma}], \end{aligned} \tag{7.50}$$

where, as was shown before, we have $\overbrace{c_i c_j^\dagger} = (1-n_i)\delta_{ij}$ and $\overbrace{c_i^\dagger c_j} = n_i\delta_{ij}$. After some algebra to be performed,

$$H = E_0 + H_{HF} + \frac{1}{4}\sum_{\alpha\beta\gamma\delta}\langle\alpha\beta|V|\gamma\delta\rangle :c_\alpha^\dagger c_\beta^\dagger c_\delta c_\gamma: \tag{7.51}$$

where

$$E_0 = \sum_\alpha n_\alpha\langle\alpha|T|\alpha\rangle + \frac{1}{2}\sum_{\alpha\beta} n_\alpha n_\beta\langle\alpha\beta|V|\alpha\beta\rangle_a \tag{7.52}$$

This is the kinetic energy of particles in the occupied states plus the interaction between particles placed in any pair of levels of the representation. It is the energy carried by the core, as can also be seen by noticing that $E_0 = \langle 0|H|0\rangle$.

The one-body Hamiltonian is

$$H_{HF} = \sum_{\alpha\beta}\left(\langle\alpha|T|\beta\rangle + \sum_\gamma n_\gamma\langle\alpha\gamma|V|\beta\gamma\rangle_a\right):c_\alpha^\dagger c_\beta: \tag{7.53}$$

In this Hamiltonian the levels α and β include all states of the representation. These are the levels that we will occupied by particles which eventually will be added to the core. One thus sees that H_{HF} contains the core excitations through the interaction of particles in all occupied states (called $|\gamma\rangle$ in H_{HF}) with the rest of the particles (including those in the core). The Hamiltonian H_{HF}, which is called the Hartree-Fock Hamiltonian, thus corresponds to the core excitation which in the one-body case were assumed to be contained in the renormalized operators.

The diagonalization of H_{HF} provides the Hartree-Fock representation. This is not a very easy task because it is not a linear problem. To see this we write H_{HF} in Dirac notation, i.e.

$$H_{HF} = \sum_{\alpha\beta}|\alpha\rangle\left(\langle\alpha|T|\beta\rangle + \sum_\gamma n_\gamma\langle\alpha\gamma|V|\beta\gamma\rangle_a\right)\langle\beta| \tag{7.54}$$

and the Hartree-Fock representation will be defined by the eigenvectors $\{|i\rangle\}$ given by,

$$H_{HF}|i\rangle = \varepsilon_i|i\rangle \tag{7.55}$$

To solve this eigenvalue problem we multiply by $\langle\alpha|$ from the left to get,

$$\sum_\beta \left(\langle\alpha|T|\beta\rangle + \sum_\gamma n_\gamma \langle\alpha\gamma|V|\beta\gamma\rangle_a \right) \langle\beta|i\rangle = \varepsilon_i \langle\alpha|i\rangle \tag{7.56}$$

and the eigenvectors are obtained by imposing the normalization condition,

$$|i\rangle = \sum_\alpha \langle\alpha|i\rangle|\alpha\rangle, \quad \langle i|i\rangle = 1 \tag{7.57}$$

Within the representation $\{|i\rangle\}$ it should be

$$\langle j|H_{HF}|i\rangle = \varepsilon_i \delta_{ij} \tag{7.58}$$

If it is not then one uses as representation these vectors $\{|i\rangle\}$ (instead of the one labeled by Greek letters) to obtained new eigenvectors, which we call $\{|i'\rangle\}$, satisfying

$$H_{HF}|i'\rangle = \varepsilon_{i'}|i'\rangle, \quad |i'\rangle = \sum_i \langle i|i'\rangle|i\rangle \tag{7.59}$$

If the condition $\langle j'|H_{HF}|i'\rangle = \varepsilon'_i \delta_{i'j'}$ is still not fulfilled, then one proceeds as before and chooses $\{|i'\rangle\}$ as representation. One repeats this procedure until one arrives after n attempts, to

$$\langle j^{(n)}|H_{HF}|i^{(n)}\rangle = \varepsilon_{i^{(n)}} \delta_{i^{(n)} j^{(n)}} \tag{7.60}$$

and the states $\{|i^{(n)}\rangle\}$ form the Hartree-Fock representation.

This representation is used very often in shell model studies. It has the advantage of being based in a fully microscopical formalism. This can be contrasted with the one obtained as diagonalization of the shell model potential discussed in the previous Chapter.

7.6 Two-particle Random Phase Approximation (RPA)

In this Section we will study the dynamics of the (A+2)- and (A-2)-nuclei, that is of two nucleons added or subtracted from the core. For this we will write the Hamiltonian in the Hartre-Fock representation which we will label with Greek as well as Latin letters. It is,

$$H = \sum_\alpha \varepsilon_\alpha : c^\dagger_\alpha c_\alpha : + \frac{1}{4} \sum_{\alpha\beta\gamma\delta} \langle\alpha\beta|V|\gamma\delta\rangle : c^\dagger_\alpha c^\dagger_\beta c_\delta c_\gamma : \tag{7.61}$$

where ε_α is the Hartrre-Fock single-particle energy. The constant energy E_0, Eq. (7.52), is not included because all eigenvalues of the Hamiltonian (7.61) will be referred to the core and, therefore, E_0 plays no role.

To obtain the two-particle energies we evaluate the commutator,

$$\begin{aligned} \left[H, c^\dagger_\alpha c^\dagger_\beta\right] =& \sum_i \varepsilon_i \left[: c^\dagger_i c_i :, c^\dagger_\alpha c^\dagger_\beta \right] + \frac{1}{4} \sum_{ijkl} \langle ij|V|kl\rangle \left[: c^\dagger_i c^\dagger_j c_l c_k :, c^\dagger_\alpha c^\dagger_\beta \right] \\ =& (\varepsilon_\alpha + \varepsilon_\beta) c^\dagger_\alpha c^\dagger_\beta + \frac{1}{2}(1 - n_\alpha - n_\beta) \sum_{ij} \langle ij|V|\alpha\beta\rangle_a c^\dagger_i c^\dagger_j \\ & - \frac{1}{2} \sum_{ijl} \langle ij|V|\beta l\rangle_a : c^\dagger_i c^\dagger_j c_l c^\dagger_\alpha : + \frac{1}{2} \sum_{ijl} \langle ij|V|\alpha l\rangle_a : c^\dagger_i c^\dagger_j c_l c^\dagger_\beta : \end{aligned} \tag{7.62}$$

One sees in this equation that the two-particle creation operators are mixed with three-particle one-hole excitations, that is with core excitation components. In the Random Phase Approximation (RPA) one

neglects the core excitations, that is terms of the form $\langle n_2| : c_i^\dagger c_j^\dagger c_\alpha^\dagger c_l : |0\rangle$, because they are supposed to generate states which lie high in the spectrum, thus having little influence over the low-lying two-particle states. With this and noticing that,

$$H|n_2\rangle = E_{n_2}|n_2\rangle, \quad H|0\rangle = E_0|0\rangle \tag{7.63}$$

one gets,

$$\begin{aligned}\langle n_2| \left[H, c_\alpha^\dagger c_\beta^\dagger\right] |0\rangle =&(E_{n_2} - E_0)\langle n_2|c_\alpha^\dagger c_\beta^\dagger|0\rangle \\ =&(\varepsilon_\alpha + \varepsilon_\beta)\langle n_2|c_\alpha^\dagger c_\beta^\dagger|0\rangle + (1 - n_\alpha - n_\beta)\sum_{i<j}\langle ij|V|\alpha\beta\rangle_a \langle n_2|c_i^\dagger c_j^\dagger|0\rangle\end{aligned} \tag{7.64}$$

which is the RPA equation. The term $1 - n_\alpha - n_\beta$ in the RPA equations shows that one can place two particles above the Fermi level, in which case it is $1 - n_\alpha - n_\beta = 1$, or below it ($1 - n_\alpha - n_\beta$ = -1). These two forms of excitations are mixed to each other, given rise to the so-called RPA correlations. This also implies that within the RPA one evaluates simultaneously the (A+2)- and (A-2)-systems and, therefore, there is an influence of one system upon the other.

With $\omega_{n_2} = E_{n_2} - E_0$ the RPA equation can be written in matrix form as

$$\omega_{n_2}\begin{pmatrix} X_{n_2} \\ Y_{n_2}\end{pmatrix} = \begin{pmatrix} A & B \\ -C & -D\end{pmatrix}\begin{pmatrix} X_{n_2} \\ Y_{n_2}\end{pmatrix} \tag{7.65}$$

where $X_{n_2}(\alpha\beta) = \langle n_2|c_\alpha^\dagger c_\beta^\dagger|0\rangle$ with α and β particle states and $Y_{n_2}(\alpha\beta) = \langle n_2|c_\alpha^\dagger c_\beta^\dagger|0\rangle$ but with α and β hole states. In the same fashion the indices of A are all particle states and the indices of D are all hole states. Instead in the matrices B and C the indices are mixed. For instance $C(\alpha\beta\gamma\delta) = \langle\gamma\delta|V|\alpha\beta\rangle_a$, where α and β are hole states while γ and δ are particle states. Notice that the minus sign in front of the matrices C and D comes from the factor $1 - n_\alpha - n_\beta$ in Eq. (7.64). Due to this, the RPA matrix (7.74) is not Hermitian and, therefore, the energies ω_{n_2} can become complex quantities.

Eq. (7.74) can also be written as,

$$\omega_{n_2}\begin{pmatrix} X_{n_2} \\ Y_{n_2}\end{pmatrix} = \begin{pmatrix} A & B \\ C & D\end{pmatrix}\begin{pmatrix} X_{n_2} \\ -Y_{n_2}\end{pmatrix} \tag{7.66}$$

and taking the adjoint of this equation one gets,

$$\omega_{n_2}^*(X_{n_2}^*, Y_{n_2}^*) = (X_{n_2}^*, -Y_{n_2}^*)\begin{pmatrix} A & B \\ C & D\end{pmatrix} \tag{7.67}$$

where the properties $A^\dagger = A$, $D^\dagger = D$, $C^\dagger = B$ (and, therefore, $C = B^\dagger$) were used.

Multiplying Eq. (7.67) to the right by $\begin{pmatrix} X_{m_2} \\ -Y_{m_2}\end{pmatrix}$ and using Eq. 7.66 one gets,

$$(\omega_{n_2}^* - \omega_{m_2})(X_{n_2}^*, Y_{n_2}^*)\begin{pmatrix} X_{m_2} \\ -Y_{m_2}\end{pmatrix} = 0 \tag{7.68}$$

If $n_2 \neq m_2$ this Equation implies that

$$(X_{n_2}^*, Y_{n_2}^*)\begin{pmatrix} X_{m_2} \\ -Y_{m_2}\end{pmatrix} = 0 \tag{7.69}$$

and normalizing it to unity one gets,

$$\sum_{\alpha\leq\beta}(1 - n_\alpha - n_\beta)\langle n_2|c_\alpha^\dagger c_\beta^\dagger|0\rangle^*\langle m_2|c_\alpha^\dagger c_\beta^\dagger|0\rangle = \delta_{n_2 m_2} \tag{7.70}$$

which defines the RPA scalar product, or metric. In functional analysis it is also called indefinite inner product.

The two-particle state can be written as,

$$|n_2\rangle = \sum_{\alpha\leq\beta} X(\alpha\beta, n_2)c_\alpha^\dagger c_\beta^\dagger|0\rangle \tag{7.71}$$

and multiplying by $\langle m_2|$ one gets

$$\delta_{n_2 m_2} = \sum_{\alpha\leq\beta} X(\alpha\beta, n_2)\langle m_2|c^\dagger_\alpha c^\dagger_\beta|0\rangle \tag{7.72}$$

since the basis elements form an independent set one finds, comparing with Eq. (7.70),

$$X(\alpha\beta, n_2) = (1 - n_\alpha - n_\beta)\langle n_2|c^\dagger_\alpha c^\dagger_\beta|0\rangle^* \tag{7.73}$$

which is the RPA wave function amplitude.

As an example, we evaluate the energy of the a system with one particle orbital (α) and one hole orbital (β). The RPA equation can be written in a 2×2 matrix form as

$$\omega_{n_2} \begin{pmatrix} x \\ y \end{pmatrix} = \begin{pmatrix} A & B \\ -C & -D \end{pmatrix} \begin{pmatrix} x \\ y \end{pmatrix}. \tag{7.74}$$

We have $A = 2\varepsilon_\alpha + \langle\alpha\alpha|V|\alpha\alpha\rangle^{JT}$ where JT denote the spin and isospin of the two particle state. $D = -2\varepsilon_\beta + \langle\beta\beta|V|\beta\beta\rangle^{JT}$. $B = C = \langle\alpha\alpha|V|\beta\beta\rangle^{JT}$. In such a case we get two solutions for the eigen values, $\omega_{n_2} = \frac{A-D}{2} \pm \sqrt{\left(\frac{A-D}{2}\right)^2 + AD - C^2}$, corresponding to the particle-particle and hole-hole excitations respectively. For a system with no particle-hole correlation, we get $\omega_{n_2} = A$ for the two-particle state and $\omega_{n_2} = -D$ for the two-hole state.

7.7 Tamm-Dankoff Approximation (TDA)

We will concentrate in the shell model in this course, and here one has either two-particle or two-hole excitations, and the (A+2) and (A-2) systems are independent of each other. The shell model cases are actually particular cases of the RPA since one gets them by imposing the condition that only particles can occupied particle states and only holes can occupied hole states. This is called Tamm-Dankoff approximation (TDA).

This approximation implies that the matrices B and C vanish in Eq. (7.74). The particle- and hole-states decoupled and the RPA equation transforms in two TDA equations, one for particle states, i. e.

$$\omega_{n_2} X_{n_2} = A X_{n_2} \tag{7.75}$$

and the other one for hole states,

$$-\omega_{n_2} Y_{n_2} = D Y_{n_2} \tag{7.76}$$

Since the matrices A and D are Hermitian the energies are real, as they should be.

We will study these two cases separately starting from Eq. (7.64). For the two-particle case the TDA thus means $n_\alpha = n_\beta = 0$. That is

$$\begin{aligned} \langle n_2|\left[H, c^\dagger_\alpha c^\dagger_\beta\right]|0\rangle =& (E_{n_2} - E_0)\langle n_2|c^\dagger_\alpha c^\dagger_\beta|0\rangle \\ =& (\varepsilon_\alpha + \varepsilon_\beta)\langle n_2|c^\dagger_\alpha c^\dagger_\beta|0\rangle + \sum_{i<j}\langle ij|V|\alpha\beta\rangle_a \langle n_2|c^\dagger_i c^\dagger_j|0\rangle \end{aligned} \tag{7.77}$$

which is the TDA equation. It is also the shell model equation, which we will apply in the next Chapter.

The equation for the two-hole states is better obtained starting from the transverse of the RPA operator form, i. e. by performing the operation $\left[H, c^\dagger_\alpha c^\dagger_\beta\right]^\dagger = (Hc^\dagger_\alpha c^\dagger_\beta)^\dagger - (c^\dagger_\alpha c^\dagger_\beta H)^\dagger = c_\beta c_\alpha H - H c_\beta c_\alpha$ $= [H, c_\alpha c_\beta]$ in Eq. (7.62). One thus obtains,

$$[H, c_\alpha c_\beta] = -(\varepsilon_\alpha + \varepsilon_\beta)c_\alpha c_\beta - (1 - n_\alpha - n_\beta)\sum_{i<j}\langle ij|V|\alpha\beta\rangle_a c_i c_j \tag{7.78}$$

where the contribution from three-particle one-hole operators have been neglected. Since the single-particle levels are hole states, one has $(1 - n_\alpha - n_\beta)$ = -1 and the TDA equation for the states $|n_2\rangle$ in the (A-2) nucleus is

$$\begin{aligned} \langle n_2|\left[H, c_\alpha c_\beta\right]|0\rangle =& (E_{n_2} - E_0)\langle n_2|c_\alpha c_\beta|0\rangle \\ =& -(\varepsilon_\alpha + \varepsilon_\beta)\langle n_2|c^\dagger_\alpha c^\dagger_\beta|0\rangle + \sum_{i<j}\langle ij|V|\alpha\beta\rangle_a \langle n_2|c_i c_j|0\rangle \end{aligned} \tag{7.79}$$

This TDA equation is also the shell model equation for two-hole states. It is usually written as,

$$\begin{aligned}&\omega(n_2)\langle n_2|c_\alpha c_\beta|0\rangle\\ =&(\varepsilon_\alpha+\varepsilon_\beta)\langle n_2|c_\alpha^\dagger c_\beta^\dagger|0\rangle-\sum_{i<j}\langle ij|V|\alpha\beta\rangle_a\langle n_2|c_ic_j|0\rangle\end{aligned}\tag{7.80}$$

and the eigenvalues $\omega(n_2) = -(E_{n_2} - E_0)$ are minus the energies of the (A-2)-nucleus referred to the ground state of the A-nucleus, i. e. to the core. Remember that for convention these energies are minus the binding energies (with this convention the binding energies are all positive). The binding energy of a nucleus increases with the nuclear number A. Therefore $E_{n_2} - E_0 > 0$ and $\omega(n_2) < 0$. The eigenvalues of the TDA equation for the (A+2) nucleons, Eq. (7.77), are also negative, as it should be for bound states. The difference between particles and holes is that for holes the interaction contributes with a minus sign, as seen in Eq. (7.80).

The TDA wave function can be written in the two-particle basis $\{c_\alpha^\dagger c_\beta^\dagger|0\rangle\}$, where it should be $\alpha < \beta$ because the states $\alpha\beta$ and $\beta\alpha$ are related by $\{c_\alpha^\dagger c_\beta^\dagger|0\rangle\}$ = -$\{c_\beta^\dagger c_\alpha^\dagger|0\rangle\}$. One thus gets,

$$|n_2\rangle=\sum_{\alpha<\beta}X(\alpha\beta;n_2)c_\alpha^\dagger c_\beta^\dagger|0\rangle\tag{7.81}$$

The TDA eigenvectors $\langle n_2|c_\alpha^\dagger c_\beta^\dagger|0\rangle$ and the wave function amplitudes X are related by,

$$\langle m_2|n_2\rangle=\delta_{m_2n_2}=\sum_{\alpha<\beta}X(\alpha\beta;n_2)\langle m_2|c_\alpha^\dagger c_\beta^\dagger|0\rangle\tag{7.82}$$

since the basis states $c_\alpha^\dagger c_\beta^\dagger|0\rangle$ form an independent set of unit vectors, it should be $X(\alpha\beta;n_2) = \langle n_2|c_\alpha^\dagger c_\beta^\dagger|0\rangle^*$.

For a system with two particles in one orbital α, we simply have $\omega_{n_2} = 2\varepsilon_\alpha + \langle\alpha\alpha|V|\alpha\alpha\rangle^{JT}$ where JT denote the spin and isospin of the two particle state.

7.8 Homework problems

Exercise 1:

a) Write the operator $c_p^+ c_q$ in normal form.

b) Write the operator $c_p^+ c_q^+ c_r c_s$ in normal form.

Exercise 2:

a) Write the Hamiltonian $H = \sum_{\alpha\beta} < \alpha|T|\beta > c_\alpha^+ c_\beta + \frac{1}{4}\sum_{\alpha\beta\gamma\delta} < \alpha\beta|V|\gamma\delta > c_\alpha^+ c_\beta^+ c_\delta c_\gamma$ in normal form and extract the Hartree-Fock potential.

b) Evaluate $< 0|H|0 >$.

Exercise 3:

Write the operator $: c_p^+ c_q^+ c_r c_s :: c_i^+ c_j^+ :$ in normal form.

Exercise 4:

a) With the Hamiltonian H written in the Hartree-Fock representation, i. e. $H = \sum_\alpha \epsilon_\alpha : c_\alpha^+ c_\alpha : +(1/2)\sum_{\alpha\beta\gamma\delta} < \alpha\beta|V|\gamma\delta >: c_\alpha^+ c_\beta^+ c_\delta c_\gamma :$ evaluate the commutator $[H, c_\alpha^+ c_\beta^+]$ in normal form and extract the two-particle RPA equation.

b) Starting from the RPA metric deduce the metric of the TDA space.

Chapter 8

Shell model excitations

Two-particle energies and wave functions. Interaction matrix elements. The separable matrix element. Pairing force.

8.1 Two-particle energies and wave functions

We have seen that the second quantization formalism is very appropriate to treat a many-nucleon system because it takes into account the Pauli principle in a straightforward fashion. Within this formalism we have derived the two-particle shell model (TDA) equations, which we will apply in this Chapter. As discussed in the previous Chapter, the first step in the solution of a many-body problem in nuclei is to choose a representation. Within the shell model the vectors $\{|\alpha\rangle\}$ in the representation are the eigenvectors of the free shell model Hamiltonian H_0, i. e. $H_0|\alpha\rangle = \varepsilon_\alpha|\alpha\rangle$. The core consists of a double magic nucleus with A nucleons in its ground state with energy $E_0(A)$. The single-particle energy ε_α is the energy of the $A+1$ nucleus referred to the core, i. e. $\varepsilon_\alpha = E_\alpha(A+1) - E_0(A)$. The energies of the $A+2$ nucleus are $E_{n_2}(A+2)$. All energies, i. e. $E_0(A)$, $E_\alpha(A+1)$ and $E_{n_2}(A+2)$ are *minus* the binding energies of the nuclei in their respective states. Notice that if $|n_2\rangle$ is an excited state of the (A+2)-nucleus, then the binding energy is the binding energy of the ground state minus the energy of the excited state $|n_2\rangle$ (since the excited state is less bound than the ground state).

The TDA equation provides the energies of the $A+2$ nucleus relative to the core in terms of the interaction matrix elements as,

$$(E_{n_2} - E_0)\langle n_2|c^\dagger_\alpha c^\dagger_\beta|0\rangle = (\varepsilon_\alpha + \varepsilon_\beta)\langle n_2|c^\dagger_\alpha c^\dagger_\beta|0\rangle + \sum_{\gamma<\delta}\langle\gamma\delta|V|\alpha\beta\rangle_a\langle n_2|c^\dagger_\gamma c^\dagger_\delta|0\rangle \tag{8.1}$$

The two-particle wave functions is

$$|n_2\rangle = \sum_{\gamma\leq\delta} X(\gamma\delta;n_2)c^\dagger_\gamma c^\dagger_\delta|0\rangle \tag{8.2}$$

where the indices are all *particle* states.

With $\omega_{n_2} = E_{n_2} - E_0$ the shel model systems of equations becomes,

$$\sum_{\gamma<\delta}\left[(-\omega_{n_2} + \varepsilon_\alpha + \varepsilon_\beta)\delta_{\alpha\gamma}\delta_{\beta\delta} + \langle\gamma\delta|V|\alpha\beta\rangle_a\right]X(\gamma\delta;n_2) = 0 \tag{8.3}$$

where we have replaced $X(\gamma\delta;n_2) = \langle n_2|c^\dagger_\gamma c^\dagger_\delta|0\rangle$, and not its complex conjugate, because we will take the interaction matrix elements as real.

The system of equations (8.3) has no trivial solution only if the determinant vanishes, i. e.

$$||(\varepsilon_\alpha + \varepsilon_\beta)\delta_{\alpha\gamma}\delta_{\beta\delta} + \langle\gamma\delta|V|\alpha\beta\rangle_a|| = 0 \tag{8.4}$$

If there are M elements in the representation, then one gets M energies ω_{n_2} from this condition, and one of the equations in Eq. (8.3) becomes a linear combination of the others. One thus disregards one of the equations and, instead, uses the normalization condition

$$\sum_{\gamma\leq\delta} X^2(\gamma\delta;n_2) = 1 \tag{8.5}$$

We will apply the two-particle shell model equations in an illustrative example. For this purpose we consider the case of two protons outside the core $^{88}_{38}Sr_{50}$. The number $Z = 38$ can be considered a semi-magic number, since for the low lying states the effects of the shells below $Z = 38$ are not important.

The neutrons and protons fills different shells and the isospin formalism is not well suited in this case. We will consider neutrons and protons as different particles. The neutrons, filling the shell $N = 50$, are frozen and do not contribute to the two-proton spectrum. The single-particle states are then those proton shells between $Z = 38$ and $Z = 50$, which are $p_{1/2}$ and $g_{9/2}$. We will designate the corresponding single-particle energies as $\varepsilon_1 = \varepsilon_{p_{1/2}}$ and $\varepsilon_2 = \varepsilon_{g_{9/2}}$.

The possible two-proton states are

$$\begin{array}{rcl} (p_{1/2})^2 & \longrightarrow & 0^+ \\ (p_{1/2}g_{9/2}) & \longrightarrow & 4^-, 5^- \\ (g_{9/2})^2 & \longrightarrow & 0^+, 2^+, 4^+, 6^+, 8^+ \end{array} \tag{8.6}$$

Which shows that in this case there is only one basis state, except for 0^+ for which there are two. We will start analyzing these 0^+ states.

With $|\alpha\rangle = |(p_{1/2})^2; 0^+\rangle$ and $|\beta\rangle = |(g_{9/2})^2; 0^+\rangle$ the shell model equations read,

$$\begin{array}{l} (2\varepsilon_1 + \langle\alpha|V|\alpha\rangle - \omega_n)X(\alpha; n) + \langle\alpha|V|\beta\rangle X(\beta; n) = 0 \\ \langle\beta|V|\alpha\rangle X(\alpha; n) + (2\varepsilon_2 + \langle\beta|V|\beta\rangle - \omega_n)X(\beta; n) = 0 \end{array} \tag{8.7}$$

which provides the determinant,

$$\left| \begin{array}{cc} 2\varepsilon_1 + \langle\alpha|V|\alpha\rangle - \omega_n & \langle\alpha|V|\beta\rangle \\ \langle\beta|V|\alpha\rangle & 2\varepsilon_2 + \langle\beta|V|\beta\rangle - \omega_n \end{array} \right| = 0 \tag{8.8}$$

from where the energies are obtained, i. e.

$$\omega_n = \varepsilon_1 + \varepsilon_2 + \frac{V_{\alpha\alpha} + V_{\beta\beta}}{2} \pm \left[\left(\varepsilon_1 - \varepsilon_2 + \frac{V_{\alpha\alpha} - V_{\beta\beta}}{2} \right)^2 + V_{\alpha\beta}^2 \right]^{1/2} \tag{8.9}$$

where the notation $V_{\gamma\delta} = \langle\gamma|V|\delta\rangle$ was used.

With these values of the energies the two shell model Eqs. (8.7) are linearly dependent upon each other. One obtains the wave function amplitudes from one of them as,

$$X(\beta; n) = -\frac{2\varepsilon_1 + \langle\alpha|V|\alpha\rangle - \omega_n}{\langle\alpha|V|\beta\rangle} X(\alpha; n) \tag{8.10}$$

and the other is the normalization condition which gives,

$$X^2(\alpha; n) + X^2(\beta; n) = X^2(\alpha; n)\big(1 + (\frac{2\varepsilon_1 + \langle\alpha|V|\alpha\rangle - \omega_n}{\langle\alpha|V|\beta\rangle})^2\big) = 1 \tag{8.11}$$

which provides $X(\alpha; n)$ and from Eq. (8.10) one obtains $X(\beta; n)$.

For the other states there is only one configuration which we will call $|\alpha\rangle$. Therefore the wave function amplitude is $X(\alpha; n) = 1$ and the energy of the state is, $\omega_n = 2\varepsilon + V_{\alpha\alpha}$

In the next Section we will outline procedures to evaluate the interaction matrix elements.

8.2 Interaction matrix elements

One important assumption of the shell model is that it exists a frozen core and that the nucleons moving outside the core feels the interaction of the core as a mean field. This is the shell model potential that we have described in Chapter 4. The dynamics of the nucleus is then determined by the particles moving outside the core. These are called *valence* particles.

An accurate knowledge of the interaction among the valence particles is of a fundamental importance for a proper description of the nuclear spectra. This is not an easy task since the interaction among nucleons inside the nucleus is very different than the one corresponding to free nucleons. The core induces the central field that generates the shell model representation. But the interaction among valence particles is also affected by the core. Due to this one uses effective forces which somehow take into account the influence of the nucleons in the core upon the valence particles. A sensible way to include the influence of the core upon the interacting particles is to determine the interaction matrix elements

from the experimental data of the two-nucleon system. That is, the two-nucleon shell model equations (8.3) can be written as

$$[\omega_{n_2} - (\varepsilon_\alpha + \varepsilon_\beta)]X(\alpha\beta; n_2) = \sum_{\gamma<\delta} \langle\gamma\delta|V|\alpha\beta\rangle_a X(\gamma\delta; n_2) \tag{8.12}$$

and since $\sum_{n_2} |n_2\rangle\langle n_2| = 1$ one gets,

$$\langle\gamma\delta|V|\alpha\beta\rangle_a = \sum_{n_2} X(\alpha\beta; n_2)[\omega_{n_2} - (\varepsilon_\alpha + \varepsilon_\beta)]X(\gamma\delta; n_2) \tag{8.13}$$

where we have assumed that the matrix elements, and therefore the amplitudes X, are real numbers. This expression shows that one can extract the interaction matrix elements from experiment if the amplitudes as well as the single-particle and the two-particle energies are measured. This happens in some cases, specially when the dimension of the shell model space is small. The ^{88}Sr example given above is one of those cases. But in general what one does is to extract as many matrix elements from experiment as possible and to determine the others by variations around reasonable values. One gets the final matrix elements when the spectra of the nuclei under study are fairly reproduced. This is a procedure been used at present. With the relatively few parameters that includes such fitting process (all corresponding to the two-nucleon system) one can study the dynamics of a nucleus with many valence particles. The dimensions of the corresponding shell model matrices can reach huge values, like 10^{10} and even more.

The "reasonable" values of the interaction matrix elements mentioned above are often taken to be those provided by well probed two-nucleon potentials. Some of the simplest of those potentials, namely the separable potential and the pairing potential, are described below.

The separable matrix element

One of the interaction matrix element which is often used in nuclear physics is taken to be separable. This is defined, for states of spin J, as

$$\langle pq; J|V|rs; J\rangle = -Gf(pq; J)f(rs; J) \tag{8.14}$$

where G is a constant called "strength" and $f(pq; J)$ is a function of the states p and q. One uses various expressions for this function, although an important criterion to judge its quality is how well it fits experimental data.

With the separable matrix element the shell model equations become,

$$\sum_{r\leqslant s} \Big[(\varepsilon_p + \varepsilon_q - \omega_n)\delta_{pr}\delta_{qs} - Gf(pq; J)f(rs; J)\Big]X(rs; n) = 0 \tag{8.15}$$

which can be written as,

$$X(pq; n) = G\frac{f(pq; J)}{\varepsilon_p + \varepsilon_q - \omega_n} \sum_{r\leqslant s} f(rs; J)X(rs; n) \tag{8.16}$$

multiplying this equation by $\sum_{p\leqslant q} f(pq; J)$ one gets

$$\sum_{p\leqslant q} f(pq; J)X(pq; n) = G\sum_{p\leqslant q} \frac{f^2(pq; J)}{\varepsilon_p + \varepsilon_q - \omega_n} \sum_{r\leqslant s} f(rs; J)X(rs; n) \tag{8.17}$$

that is,

$$G\sum_{p\leqslant q} \frac{f^2(pq; J)}{\varepsilon_p + \varepsilon_q - \omega_n} = 1 \tag{8.18}$$

This equation is called "Dispersion Relation". To get the energies from the dispersion relation one has first to determine the strength G. This is extracted from the dispersion relation by using for ω_n the experimental value of the energy of the lowest state with spin J (this is called "yrast" state), which for

the spin 0^+ is the ground state. The energies of the other states with spin J are those that satisfies the dispersion relation.

The wave function amplitudes are, according to Eq. (8.16), given by

$$X(pq;n) = N_n \frac{f(pq;J)}{\varepsilon_p + \varepsilon_q - \omega_n} \tag{8.19}$$

where N_n is the normalization constant, i. e.

$$N_n = \Big[\sum_{p\leqslant q} \frac{f^2(pq;J)}{\varepsilon_p + \varepsilon_q - \omega_n}\Big]^{-1/2} \tag{8.20}$$

Pairing force

In nuclear physics the pairing force is a particular case of the separable force. It is generally applied to study the states 0^+. It is assumed that the orbitals p and q are time reversal states of each other. This implies that in a coupled-scheme the two states are exactly the same. The corresponding value of the function f is,

$$f(pp;0^+) = \sqrt{2j_p + 1} \tag{8.21}$$

To illustrate how the separable force in general, and the pairing force in particular, is applied we will briefly present the states in ^{90}Zr studied above. In this case the functions f acquire the values,

$$f(\alpha;0^+) = f(p^2_{1/2};0^+) = \sqrt{2}; \quad f(\beta;0^+) = f(g^2_{9/2};0^+) = \sqrt{10} \tag{8.22}$$

from where one evaluates the strength as,

$$G = \left(\frac{2}{2\varepsilon_1 - E_{0^+_1}} + \frac{10}{2\varepsilon_2 - E_{0^+_1}}\right)^{-1} \tag{8.23}$$

and the wave function amplitudes are,

$$X(\alpha;n) = N_n \frac{\sqrt{2}}{2\varepsilon_1 - \omega_n}, \quad X(\beta;n) = N_n \frac{\sqrt{10}}{2\varepsilon_2 - \omega_n} \tag{8.24}$$

The numerical values of the energies are obtained by solving Eq. (8.18). With these energies one evaluates the wave function amplitudes with the normalization calculated as in Eq. (8.20).

8.3 Isospin symmetry in nuclei

As an illustrative example we will analyze the case of two nucleons outside the core $^{16}_{8}O_8$ (Oxygen 16). The total isospin of the two-nucleon systems can be T=0 or T=1. For the nuclei with $T_z = \pm 1$ it must be $T \geq 1$. This is the case in $^{18}_{10}Ne_8$ (Neon 18) and $^{18}_{8}O_{10}$. In $^{18}_{8}F_9$ (Fluor 18) it is $T \geq 0$.

The single-particle states above the magic number 8 are $0d_{5/2}$, $1s_{1/2}$ and $0d_{3/2}$. However the lowest two-nucleon states should be mostly due to the lowest shell, i. e. $0d_{5/2}$. Therefore the lowest two nucleons states have to be 0^+, 2^+ and 4^+ if $T = 1$ and 1^+, 3^+ and 5^+ if $T = 0$.

As seen in Fig. 8.1 one indeed finds that the three lowest levels are 0^+, 2^+ and 4^+ for the two-proton $^{18}_{10}Ne_8$ and the two-neutron $^{18}_{8}O_{10}$ nuclei, for which it has to be $T = 1$. But even the $T = 1$, $T_z = 0$ state 0^+ is seen in ^{18}F, although here the corresponding 2^+ and 4^+ states have not been detected yet. Instead in this $T = 0$ nucleus the odd states 1^+, 3^+ and 5^+ appear.

We notice that the relative energies of the $T = 1$ states, i. e. the states in ^{18}Ne and ^{18}O, should not be influenced by the Coulomb energy since this affects equally to all levels of a given nucleus, and the energy difference cancels those effects. This explains why the excitation energy of the states 2^+ are very similar in both nuclei, although this is not the case for the state 4^+. These differences between theory and experiment in the isoscalar as well as in the isovector excitations are due to the shells $1s_{1/2}$ and $0d_{3/2}$ which we neglected. Their influence is more important as the energy of the excited level increases.

A detailed calculation of these levels requires the inclusion of many shells as well as a proper knowledge of the interaction matrix elements. We will do this within the shell model (TDA) formalism that we developed in the previous Chapter.

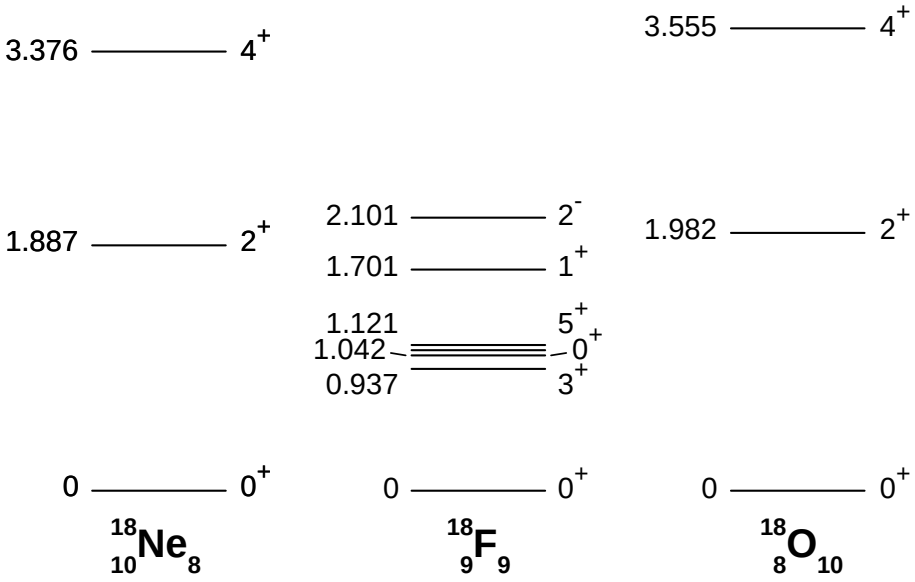

Figure 8.1: Nuclear spectra of the nuclei ${}^{18}_{10}O_8$, ${}^{18}_{9}F_9$ and ${}^{18}_{8}O_{10}$.

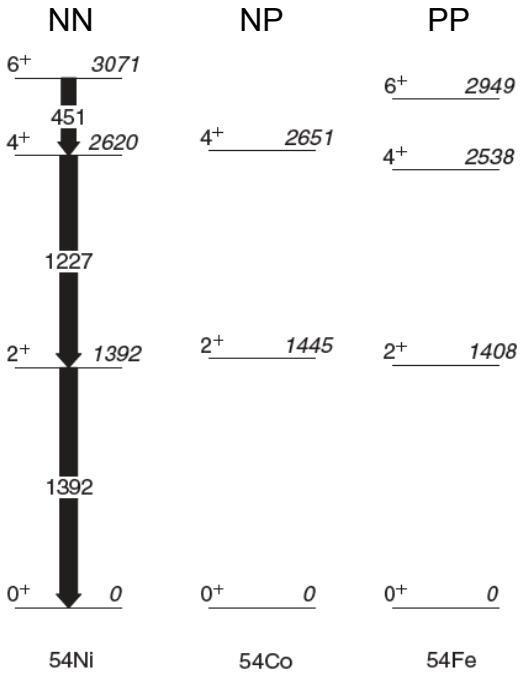

Figure 8.2: The spectra of mirror nuclei ^{54}Ni, ^{54}Co and ^{54}Fe (with $T = 1$). From PRL 97, 152501 (2006).

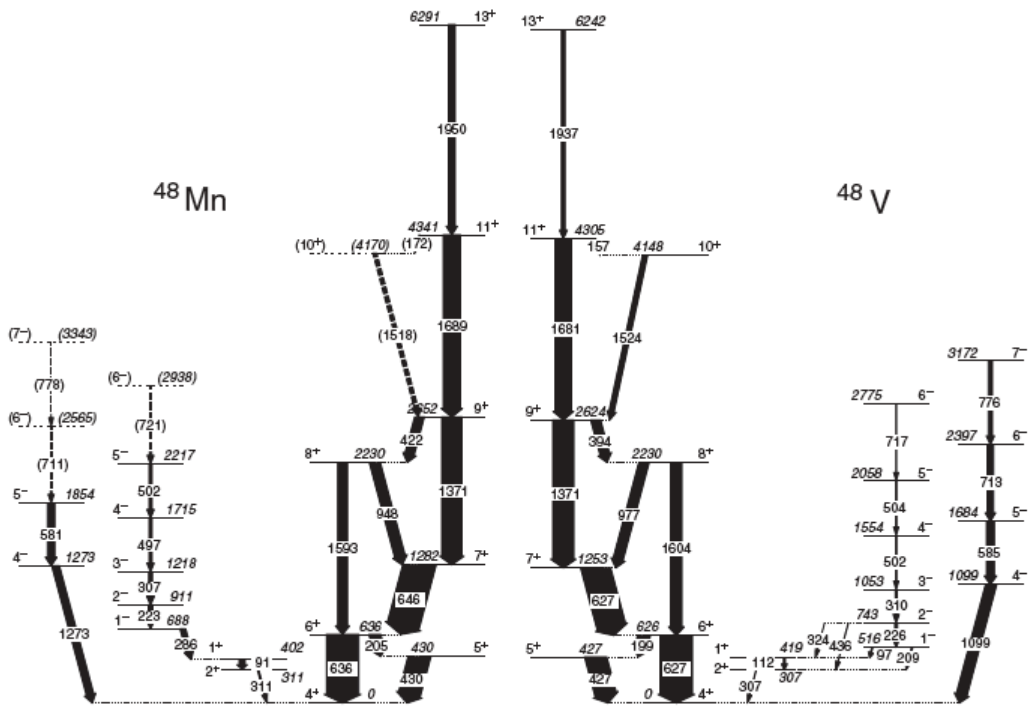

Figure 8.3: The spectra of mirror nuclei ^{48}Mn and ^{48}V (with $T = 3/2$). From PRL 97, 132501 (2006).

8.4 Nucleon-Nucleon Interaction and LS coupling

If one is interested in the low-energy region where the nucleons hardly get excited internally, we can treat the nucleons as inert, structureless elementary particles, and we can understand many of the properties of the multi-nucleon systems by the nucleon-nucleon interactions. If the nucleons are non-relativistic, the interaction can be described by a potential. Since the fundamental theory governing the nucleon-nucleon interactions is QCD, the interactions shall be calculable from the physics of quarks and gluons. Nonetheless, the problem is quite complicated and only limited progress has been made from the first principles so far. Therefore, the approach we are going take is a phenomenological one: One first tries to extract the nucleon- nucleon interaction from the nucleon-nucleon scattering data or few nucleon properties, and then one tries to use these interactions to make predictions for the nuclear many-body system.

General Aspects of the Nucleon-Nucleon interaction

For the two-nucleon system, the experimental information consists of two particle scattering phase shifts in various partial waves, and the bound state properties of the deuteron. From data, one learns that the nuclear force has the following the main features:

- Attractive: to form nuclear bound states
- Short Range: of order 1 fm
- Spin-Dependent
- Noncentral: there is a tensor component
- Isospin Symmetric
- Hard Core: so that the nuclear matter does not collapse
- Spin-Orbit Force
- Parity Conservation

In phenomenology, one tries to come up with the forms of the forces which will satisfy the above properties. In particular, one parametrize the short distance potentials consistent with fundamental symmetries and fit the parameters to experimental data.

If we consider the nucleons as elementary particles, their strong interactions are known have a short range from α particle scattering experiments of Rutherford. In fact, the range of the interaction is roughly the size of the atomic nuclei, namely on the order of a few fermis (fm) (1fm $= 10^{-15}$m). The first theory of the nucleon force was put forward by H. Yukawa, who suggested that the interaction between two nucleons is effected by the exchange of a particle, just like the interaction between the electric charges by the exchange of a photon. However, because the nucleon interactions appear to be short-ranged, the particle must have a finite mass. In fact, one can correlate the range and mass roughly by the quantum uncertainty principle

$$r \sim 1/m \tag{8.25}$$

therefore, the mass of the quanta exchanged is about 1/fm which is about 200 MeV. The particle was discovered almost 20 years later and was identified as π meson (140 MeV). The most significant aspect of the Yukawa theory is generalizing the relation between particles and forces – the existence of strong interactions implies the existence of a new particle! This was considered a novel and radical idea at that time.

The modern theory of interactions through particle exchanges is made possible by the development of quantum field theory. However, at low-energy, one can assume the interactions is instantaneous and therefore the concept of interaction potential becomes useful.

Yukawa theory and One-Pion Exchange potential

To illustrate the derivation of a potential through particle exchange, consider the interaction of a scalar particle with the nucleons. Introducing a quantum field ϕ to represent the particle, the Yukawa interaction has the form,

$$V(r) = -\frac{g^2}{4\pi}\frac{\mathrm{e}^{-mr}}{r} \tag{8.26}$$

which is an attractive interaction, independent of the spin of the nucleon. When $m = 0$, the interaction is Coulomb-like and is long range. For a finite m, the interaction is negligible beyond the distance $r \sim 1/m$.

Pi-meson is the lightest meson because of the spontaneous chiral symmetry breaking. It is responsible to the longest range nucleon-nucleon force. One of the important new features here is isospin symmetry. Pi-meson has iso-spin 1, and can be represented by a vector $\boldsymbol{\pi} = (\pi_1, \pi_2, \pi_3)$ in isospin space. Combinations of $\pi_{1,2}$ generate positive and negative charged pions $\pi^{\pm}$, and π_3 corresponds to a neutral pion π^0.

Because the pion is a pseudo-scalar particle, parity conservation requires that it be emitted or absorbed in the p-wave. Therefore there is a factor of $\boldsymbol{p}$ associated with the interaction vertex in the momentum space. This factor is multiplied by the spin operator $\boldsymbol{\sigma}$ forms a pseudo-scalar. Putting together all the factors, one finds that the nucleon-nucleon potential from one pion exchange as,

$$V(\boldsymbol{r}) = \frac{g^2}{4M_N^2}(\boldsymbol{\tau}_1 \cdot \boldsymbol{\tau}_2)(\boldsymbol{\sigma}_1 \cdot \boldsymbol{\nabla})(\boldsymbol{\sigma}_2 \cdot \boldsymbol{\nabla})\frac{\mathrm{e}^{-m_\pi r}}{r} \tag{8.27}$$

where the isospin factor $\boldsymbol{\tau}_1 \cdot \boldsymbol{\tau}_2$ depends on the isospin states of the two nucleons. This potential matches the phenomenological forms extracted from experimental data at large N-N separations ($\sim 2 - 3$ fm). It is therefore advantageous to form states of good isospin to describe a system of 2 nucleons. Note the combination $\boldsymbol{\tau}_1 \cdot \boldsymbol{\tau}_2$ is given by

$$\boldsymbol{\tau}_1 \cdot \boldsymbol{\tau}_2 = 2\left[T(T+1) - \frac{3}{2}\right] = \begin{cases} -3, & T = 0 \\ 1, & T = 1 \end{cases} \tag{8.28}$$

At smaller distance, there is also exchanges from scalar meson (isospin 0) of about 500 MeV. The interaction is attractive as we seen above, corresponding to a medium range attraction. Finally there are also exchanges from vector mesons, ω (isospin-0) meson and ρ meson (spin-1). The interactions from the ρ and ω meson are short-range repulsive. One can build a phenomenological nucleon-nucleon interaction based on the meson exchanges. The so-called Nijmegen potential and Bonn potential are generated through this approach. The short range interactions are model dependent by nature, there is no unique picture for them. This is so because only in the low-energy processes, potentials are useful concept, however, the short range interactions are not so sensitive to the low-energy observables. Therefore, either

one can adopt a more phenomenological approach or use the so-called effective field theory approach to parameterize the unknowns systematically. During the 1990s several groups have constructed socalled high-precision, charge-dependent NN potentials (CD-Bonn, AV18, etc).

A brief history of NN interactions

- 1935 Yukawa (meson theory or Meson Hypothesis)
- 1950s Full One-Pion-Exchange potential (OPEP): Hamada-Jonston
- 1960s non-relativistic One-Boson-Exchange potential (OBEP) (pions, Many pions, scalar mesons, 782(ω), 770(ρ), 600(σ; not observed yet))
- 1970s fully relativistic OBEPs
  – 2-pion exchange
  – Paris, Bonn potential
- 1990s High-precision Nijmegen, Argonne V18, Reid93, Bonn potentials
- 1990-2000s Chiral or Effective Field Theory potentials (2 and 3 body), Lattice QCD

Comonly used simple NN potentials

- Square well $V = -V_0(0)$ for $r \leq R(r > R)$ where $R \sim 2$fm.
- Gaussian: $V = -V_0 e^{-(\mu r)^2} = -V_0 e^{-(r/R)^2}$ where $R \sim 1.5$fm.
- Exponential: $V = -V_0 e^{-\mu r} = -V_0 e^{-r/R}$ where $R \sim 0.75$fm.
- Yukawa: $V = -V_0 e^{-\mu r}/\mu r = -V_0 e^{-r/R}/(r/R)$ where $R \sim 2.5$fm.
- One-boson-exchange potentials: $V = -V_0(1+1/\mu r)e^{-\mu r}/\mu r$, $V = -V_0(1+3/\mu r+3/(\mu r)^2)e^{-\mu r}/\mu r$

LS coupling

For the system of two nucleons, use $\boldsymbol{r} = \boldsymbol{r}_1 - \boldsymbol{r}_2$ to represent relative position and $\boldsymbol{p} = (\boldsymbol{p}_1 - \boldsymbol{p}_2)/2$ relative momentum, $\boldsymbol{s}_1$ and $\boldsymbol{s}_2$ their respective spins. The relative orbital angular momentum is $\boldsymbol{L} = \boldsymbol{r} \times \boldsymbol{p}$ and the total spin is $\boldsymbol{S} = \boldsymbol{s}_1 + \boldsymbol{s}_2$. When the spins are coupled, the total spin can either be 0 or 1. For the case of $S = 0$, we have a single spin state which is called singlet. For the case of $S = 1$, we have three spin states which are called triplet. The total angular momentum is the sum of orbital angular momentum and total spin: $\boldsymbol{J} = \boldsymbol{L} + \boldsymbol{S}$. In the singlet spin case, we have $J = L$ because $S = 0$. For the triplet states, $J = L - 1, L, L + 1$ if $L \neq 0$, and $J = 0$ if $L = 0$. A state with (S, L, J) is usually labeled as $^{2S+1}L_J$, where $L = 0, 1, 2, 3$, are usually called $S, P, D, F, G...$ states. We choose the basis states with good J, $|n(LS)JM\rangle$ where,

$$|n(LS)JM\rangle = \sum_{m_L} |Y_{Lm_L}\rangle|(s_1, s_2)Sm_S\rangle\langle LmSm_S|JM\rangle \tag{8.29}$$

where $\langle LmSm_S|JM\rangle$ is the Clebsch-Gordon coefficient. In the coordinate representation, we use $\mathcal{Y}^M_{LSJ}$ to label the above total angular momentum eigenstates. Therefore, the eigenfunction can be written as

$$\psi_{nLSJM} = R_{n(SL)J}(r)\mathcal{Y}^M_{LSJ} \tag{8.30}$$

where $R_{n(SL)J}(r)$ is the corresponding radial wave function.

For the two nucleon system, the spin S and isospin T can either be 1 or 0. Isospin symmetry requires that the wave function reverse its-sign upon an odd permutation of alI coordinates (i.e. space, spin and isospin) of any two nucleons. Since the total wave function has to be antisymmetric, let us consider what are the possible value of T, S, and L to make that happen. If we use $+1$ to represent symmetric wave function and -1 to represent antisymmetric, then the spin wave function is $(-1)^{S+1}$ and the isospin wave function has symmetry factor $(-1)^{T+1}$. The orbital wave function is $(-1)^L$ (i.e., $\boldsymbol{r} \to -\boldsymbol{r}$). The total symmetry factor is $(-1)^{L+S+T}$ which has to be -1. Therefore $L + S + T$ has to be odd. We have

$$\langle 12|\psi_{nLSJMTT_z}\rangle_a = R_{n(SL)J}(r)(\langle 12|Y_{Lm_L}(\boldsymbol{r})\rangle\langle 12|(1/21/2)_{SS_z}\rangle\langle 12|(1/21/2)_{TT_z}\rangle)_a \tag{8.31}$$

and

$$\langle 12|\psi_{nLSJM}\rangle_a = \mathcal{N}(1 - (-1)^{L+S+T})R_{n(SL)J}(r)\langle 12|Y_{Lm_L}(\boldsymbol{r})\rangle\langle 12|(1/21/2)_{SS_z}\rangle\langle 12|(1/21/2)_{TT_z}\rangle \tag{8.32}$$

Table 8.1: The four LST combinations that are compatible with the Pauli principle.

$\phi(L)$	$\chi(S)$	ζ(T)
even+	singlet(S=0)−	triplet(even,T=1)+
even+	triplet(S=1)+	singlet(odd,T=0)−
odd−	singlet(S=0)−	singlet(odd,T=0)−
odd−	triplet(S=1)+	triplet(even,T=1)+

LS coupling in laboratory frame

One may also rewritten the wave functions of Eqs. (6.6) & (6.7) in term of LS coupling. In the case of two nucleon in l_p we have

$$\begin{aligned}\langle 12|\psi_{(l_p,l_p)LSJM}\rangle_a =&\mathcal{N}(1-(-1)^{L+S+T})R_p(r_1)R_p(r_2)\\ &\times\langle 12|(l_pl_p)_{LM}\rangle\langle 12|(1/21/2)_{SS_z}\rangle\langle 12|(1/21/2)_{TT_z}\rangle.\end{aligned}\tag{8.33}$$

In general we have

$$\begin{aligned}\langle 12|\psi_{(l_p,l_q)LSJM}\rangle_a =&\mathcal{N}\,[R_p(r_1)R_q(r_2)\langle 12|(l_pl_q)_{LM}\rangle\langle 12|(1/21/2)_{SS_z}\rangle\langle 12|(1/21/2)_{TT_z}\rangle\\ &-(-1)^{l_p+l_p+L+S+T})R_q(r_1)R_p(r_2)\\ &\times\langle 12|(l_ql_p)_{LM}\rangle\langle 12|(1/21/2)_{SS_z}\rangle\langle 12|(1/21/2)_{TT_z}\rangle]\end{aligned}\tag{8.34}$$

The parity of the system is determined by $-1^{l_p+l_q}$. In the relative frame it is -1^L.

Tensor force

I. Central force

What are the possible forms of the nuclear force? The simplest is a pure **central force** which just dependent on the relative distance $V_C(r)$. In this case, different L states have different energies. The eigen-functions of the system can chosen to be $|nLm_LSm_S\rangle \sim R_{nL}(r)Y_{Lm_L}\chi_{Sm_S}$.

There could be also a pure **spin-dependence force**. The most general form is $V_S(r)\boldsymbol{\sigma}_1\cdot\boldsymbol{\sigma}_2$. In fact, we can write

$$\boldsymbol{\sigma}_1\cdot\boldsymbol{\sigma}_2 = 2\boldsymbol{S}^2-3\tag{8.35}$$

Therefore the matrix element of the spin operator depends on the total spin of the two particles. In the singlet state, we have $\boldsymbol{\sigma}_1\cdot\boldsymbol{\sigma}_2=-3$, the potential is V_C-3V_S; in the triplet state ($S=1$), we have $\boldsymbol{\sigma}_1\cdot\boldsymbol{\sigma}_2=1$, and the potential is V_C+V_S. Now, the energy not only depends on the quantum number L but also on S. However, the eigen-function of the system can still be chosen as $|nLm_LSm_S\rangle$; the radial wave function depends on S, $R_{nLS}(r)$, because the potential does.

There can be also a pure iso-spin-dependence force. The most general form is $V_I(r)\boldsymbol{\tau}_1\cdot\boldsymbol{\tau}_2$; There can be a spin-isospin dependent force. The most general form is $V_{SI}(r)\boldsymbol{\sigma}_1\cdot\boldsymbol{\sigma}_2\boldsymbol{\tau}_1\cdot\boldsymbol{\tau}_2$.

II. Spin-orbit force

The spin-orbit force can be written as $V_{LS}(r)\boldsymbol{L}\cdot\boldsymbol{S}=\frac{1}{2}V_{LS}(r)\boldsymbol{L}\cdot(\boldsymbol{\sigma_1}+\boldsymbol{\sigma_2})$. We may also have a spin-orbit-isospin dependent force $V_{LSI}(r)\boldsymbol{L}\cdot\boldsymbol{S}=\frac{1}{2}V_{LSI}(r)\boldsymbol{L}\cdot(\boldsymbol{\sigma_1}+\boldsymbol{\sigma_2})(\boldsymbol{\tau}_1\cdot\boldsymbol{\tau}_2)$.

The matrix element of the operator would be simple in the basis which is formed by the common eigenstates of $\boldsymbol{J}^2$, J_3, $\boldsymbol{L}^2$, $\boldsymbol{S}^2$ and T^2. The potential used for solving the radial Schroedinger equation is

$$\begin{aligned}V_{LSJT}(r) =&V_C(r)+[2S(S+1)-3]V_S(r)+[2T(T+1)-3]V_I(r)\\ &+[2S(S+1)-3][2T(T+1)-3]V_{SI}(r)\\ &+\frac{1}{2}[J(J+1)-L(L+1)-S(S+1)]V_{LS}(r)\\ &+\frac{1}{2}[J(J+1)-L(L+1)-S(S+1)][2T(T+1)-3]V_{LS}(r)\end{aligned}\tag{8.36}$$

Another useful way is to write the potential in the singlet($S=0$)-triplet($S=1$)-odd($T=0$)-even($T=1$) representation. For the central force we have four components

$$\begin{aligned}
V_C^{SO}(r) =& U_C^{SO}(r)\frac{1}{4}(1-\boldsymbol{\sigma}_1\cdot\boldsymbol{\sigma}_2)\frac{1}{4}(1-\boldsymbol{\tau}_1\cdot\boldsymbol{\tau}_2) = V_C(r) - 3V_S(r) - 3V_I(r) + 9V_{SI}(r)\\
V_C^{SE}(r) =& U_C^{SE}(r)\frac{1}{4}(1-\boldsymbol{\sigma}_1\cdot\boldsymbol{\sigma}_2)\frac{1}{4}(3+\boldsymbol{\tau}_1\cdot\boldsymbol{\tau}_2) = V_C(r) - 3V_S(r) + V_I(r) - 3V_{SI}(r)\\
V_C^{TE}(r) =& U_C^{TE}(r)\frac{1}{4}(3+\boldsymbol{\sigma}_1\cdot\boldsymbol{\sigma}_2)\frac{1}{4}(1-\boldsymbol{\tau}_1\cdot\boldsymbol{\tau}_2) = V_C(r) + V_S(r) - 3V_I(r) - 3V_{SI}(r)\\
V_C^{TO}(r) =& U_C^{TO}(r)\frac{1}{4}(3+\boldsymbol{\sigma}_1\cdot\boldsymbol{\sigma}_2)\frac{1}{4}(3+\boldsymbol{\tau}_1\cdot\boldsymbol{\tau}_2) = V_C(r) + 3V_S(r) + V_I(r) + V_{SI}(r)
\end{aligned} \tag{8.37}$$

The spin-orbit force has two components for the isovector (even) and isoscalar (odd) channels

$$\begin{aligned}
V_{LSE}(r) =& U_{LSE}(r)\frac{1}{2}\boldsymbol{L}\cdot(\boldsymbol{\sigma_1}+\boldsymbol{\sigma_2})\frac{1}{4}(1-\boldsymbol{\tau}_1\cdot\boldsymbol{\tau}_2)\\
V_{LSO}(r) =& U_{LSO}(r)\frac{1}{2}\boldsymbol{L}\cdot(\boldsymbol{\sigma_1}+\boldsymbol{\sigma_2})\frac{1}{4}(3+\boldsymbol{\tau}_1\cdot\boldsymbol{\tau}_2)
\end{aligned} \tag{8.38}$$

They only work on the $S=1$ channel.

II. Tensor force

Finally, there is an interaction of the type

$$V_T(r)\left[3\frac{(\boldsymbol{\sigma}_1\cdot\boldsymbol{r})(\boldsymbol{\sigma}_2\cdot\boldsymbol{r})}{r^2} - \boldsymbol{\sigma}_1\cdot\boldsymbol{\sigma}_2\right] \tag{8.39}$$

which is called the **tensor interaction** and the associated structure is often denoted as S_{12}. As before, one may also have a tensor-isospin dependent force V_{TI}. Tn the singlet-triplet-odd-even representation, the tensor force also has two components for the isovector (even) and isoscalar (odd) channels

$$\begin{aligned}
V_{TNE}(r) =& U_{TNE}(r)\left[3\frac{(\boldsymbol{\sigma}_1\cdot\boldsymbol{r})(\boldsymbol{\sigma}_2\cdot\boldsymbol{r})}{r^2} - \boldsymbol{\sigma}_1\cdot\boldsymbol{\sigma}_2\right]\frac{1}{4}(1-\boldsymbol{\tau}_1\cdot\boldsymbol{\tau}_2)\\
V_{TNO}(r) =& U_{TNO}(r)\left[3\frac{(\boldsymbol{\sigma}_1\cdot\boldsymbol{r})(\boldsymbol{\sigma}_2\cdot\boldsymbol{r})}{r^2} - \boldsymbol{\sigma}_1\cdot\boldsymbol{\sigma}_2\right]\frac{1}{4}(3+\boldsymbol{\tau}_1\cdot\boldsymbol{\tau}_2)
\end{aligned} \tag{8.40}$$

The following property of the Pauli matrics is useful

$$(\boldsymbol{\sigma}\cdot\boldsymbol{A})(\boldsymbol{\sigma}\cdot\boldsymbol{B}) = (\boldsymbol{A}\cdot\boldsymbol{B}) + i\boldsymbol{\sigma}\cdot(\boldsymbol{A}\times\boldsymbol{B}), \tag{8.41}$$

from which we have

$$(\boldsymbol{\sigma}\cdot\boldsymbol{r})^2 = (\boldsymbol{r}\cdot\boldsymbol{r}) + i\boldsymbol{\sigma}\cdot(\boldsymbol{r}\times\boldsymbol{r}) = r^2. \tag{8.42}$$

Thus one has

$$\begin{aligned}
2(\boldsymbol{\sigma}_1\cdot\boldsymbol{r})(\boldsymbol{\sigma}_2\cdot\boldsymbol{r}) =& (\boldsymbol{\sigma}_1\cdot\boldsymbol{r}+\boldsymbol{\sigma}_2\cdot\boldsymbol{r})^2 - (\boldsymbol{\sigma}_1\cdot\boldsymbol{r})^2 - (\boldsymbol{\sigma}_2\cdot\boldsymbol{r})^2\\
=& (\boldsymbol{\sigma}_1\cdot\boldsymbol{r}+\boldsymbol{\sigma}_2\cdot\boldsymbol{r})^2 - 2r^2.
\end{aligned} \tag{8.43}$$

Using the total spin operator, we can write

$$(\boldsymbol{\sigma}_1\cdot\boldsymbol{r})(\boldsymbol{\sigma}_2\cdot\boldsymbol{r}) = 2(\boldsymbol{S}\cdot\boldsymbol{r})^2 - r^2, \tag{8.44}$$

Then the tensor structure becomes

$$S_{12} = 2\left[3\frac{(\boldsymbol{S}\cdot\boldsymbol{r})^2}{r^2} - \boldsymbol{S}^2\right]. \tag{8.45}$$

It can be easily show that for $Q = \frac{(\boldsymbol{S}\cdot\boldsymbol{r})^2}{r^2} = \frac{1}{2}\left[1 + \frac{(\boldsymbol{\sigma}_1\cdot\boldsymbol{r})(\boldsymbol{\sigma}_2\cdot\boldsymbol{r})}{r^2}\right]$ we have

$$Q^2 \quad = \quad Q. \tag{8.46}$$

The action of $\hat{Q}$ on the total angular momentum eigenstates are then

$$\begin{aligned} Q\mathcal{Y}^M_{J0J} &= 0 \\ Q\mathcal{Y}^M_{J1J} &= \mathcal{Y}^M_{J1J} \\ (2J+1)Q\mathcal{Y}^M_{J+11J} &= J\mathcal{Y}^M_{J+11J} + \sqrt{J(J+1)}\mathcal{Y}^M_{J-11J} \\ (2J+1)Q\mathcal{Y}^M_{J-11J} &= \sqrt{J(J+1)}\mathcal{Y}^M_{J+11J} + (J+1)\mathcal{Y}^M_{J-11J}. \end{aligned} \tag{8.47}$$

In the presence of the tensor interaction, $\boldsymbol{L}^2$ and $\boldsymbol{S}^2$ no longer commute with the Hamiltonian. The states with the same J but different L can mix under the interaction. The states can mix only when their orbital angular momenta differ by 2 unit.

Going back to the one-pion exchange potential, it can be shown that

$$(\boldsymbol{\sigma}_1 \cdot \boldsymbol{\nabla})(\boldsymbol{\sigma}_2 \cdot \boldsymbol{\nabla})\frac{\mathrm{e}^{-m_\pi r}}{r} = \frac{1}{3}m_\pi^2 \left[\boldsymbol{\sigma}_1 \cdot \boldsymbol{\sigma}_2 + S_{12}\left(1 + \frac{3}{m_\pi r} + \frac{3}{m_\pi^2 r^2}\right)\right]\frac{\mathrm{e}^{-m_\pi r}}{r}. \tag{8.48}$$

8.5 Homework problems

Exercise 1:

Taking the nucleus ^{40}Ca as a core,

a) Determine the energy of the neutron state $0f_{7/2}$

b) Determine the values of the matrix elements $< f^2_{7/2}; \lambda|V|f^2_{7/2}; \lambda >$, with $0 \leq \lambda \leq 6$, that adjust the experimental spectrum in ^{42}Ca.

Hint: Assume that the last neutrons only occupy the neutron orbital $0f_{7/2}$ for low-lying states in ^{42}Ca.

Exercise 2 (see Section 8.1):

a) Assume ^{88}Sr as the core and the pairing interaction $\langle j^2; J = 0|V|j'^2; J = 0\rangle = -G\sqrt{(2j+1)(2j'+1)}$, evaluate the strength G of the pairing force for the states 0^+ in the nucleus ^{90}Zr.

b) Applying the pairing interaction with the strength thus evaluated calculate the energies and wave functions of the states 0^+.

c) Extract from the experimental spectrum of ^{90}Zr the following interaction matrix elements:
$< 1p_{1/2}0g_{9/2}; 4^-|V|1p_{1/2}0g_{9/2}; 4^- >$,
$< 1p_{1/2}0g_{9/2}; 5^-|V|1p_{1/2}0g_{9/2}; 5^- >$,
$< 0g^2_{9/2}; 2^+|V|0g^2_{9/2}; 2^+ >$,
$< 0g^2_{9/2}; 4^+|V|0g^2_{9/2}; 4^+ >$,
$< 0g^2_{9/2}; 6^+|V|0g^2_{9/2}; 6^+ >$ and
$< 0g^2_{9/2}; 8^+|V|0g^2_{9/2}; 8^+ >$.

Hint: Extract the single-particle energies in ^{89}Y from experimental data
http://www.nndc.bnl.gov/nudat2/
You do not need to deduct the influence of the Coulomb field.

Exercise 3:

a) Show that the isospin of two-particle states in a single shell determines whether the space-spin part of the wave function is symmetric or antisymmetric.

b) Derive Eq. (6.29): Write the state $< 12|(nlj)^2_{JM}(1/2\ 1/2)_{TT_z} >_a$ in terms of the corresponding non-antisymmetrized states. Transform the wave functions back to the neutron-proton scheme for $T_z = 0$.

Exercise 4:

a) Determine which states are isoscalar and which are isovector in nuclei with two nucleons outside Z=N=20.

b) Try to find the isoscalar and isovector states in two-hole systems below the core $^{56}_{28}$Ni$_{28}$

c) Is it possible to make such identification if the core is Z=20, N=28?

Exercise 5 (not mandatory):

Derive Eqs. (8.32) & (8.33).

Chapter 9

Nuclear pairing

The possibility of pairing in atomic nuclei was first studied by Bohr, Mottelson and Pines and by Belyaev only one year after the publication of the theory of superconductivity by Bardeen, Cooper and Schrieer (BCS) [3]. Meanwhile, Bogoliubov developed a microscopic theory of superfluidity and superconductivity and explored its consequences for nuclear matter. In 1959, Migdal speculated that the interior of neutron stars might be supefluid.

9.1 Pairing gaps: odd-even binding energy differences

The basic hallmarks of pair condensates are the odd-even staggering in binding energies, the gap in the excitation spectrum of even systems, and the compressed quasiparticle spectrum in odd systems. To examine odd-even staggering, it is convenient to define the even and odd neutron pairing gaps as

$$\Delta^{(3)}_{o,Z}(N) = \frac{1}{2}(E_b(Z,N+1) - 2E_b(Z,N) + E_b(Z,N-1)), \text{ for } N \text{ odd}, \tag{9.1}$$

$$\Delta^{(3)}_{e,Z}(N) = -\frac{1}{2}(E_b(Z,N+1) - 2E_b(Z,N) + E_b(Z,N-1)), \text{ for } N \text{ even}. \tag{9.2}$$

where N and Z are the neutron and proton numbers and E_b is the binding energy of the nucleus. The proton pairing gaps are defined in a similar way. With the above definition, the gaps are positive for normal pairing.

One can also see a systematic trend in the gap values as a function of N, namely the gaps get smaller in heavier nuclei. I will also come back to this behaviour in the theory discussion. Another feature of the odd-N gap systematics is the occurance of dips at particular values of N. In fact the dips occur adjacent to the well-known magic numbers $N = 28, 50, 82$ and 126.

The systematics of the even-N gaps shown in the lower panel is similar with respect to the following: average values, the fluctuations at each N, and the smooth trend downward with increasing N. However, the magic number anomolies are now very striking spikes that occur exactly at the magic numbers. Also, the average values in lighter nuclei appear to be larger for the even-N gaps than for the odd-N. I will also come back to this feature in the theory section.

The corresponding systematics of proton gaps is shown in Fig. 2. The same qualitative features are present here as well, but the magic number effects are less pronounced. I do not know of any explanation of this difference between neutron and proton pairing.

The table below gives some fits to the pairing gap systematics. Shown are the fitted values of the gap parameterizations and the rms errors of the fits, in units of MeV. The simplest model is a constant

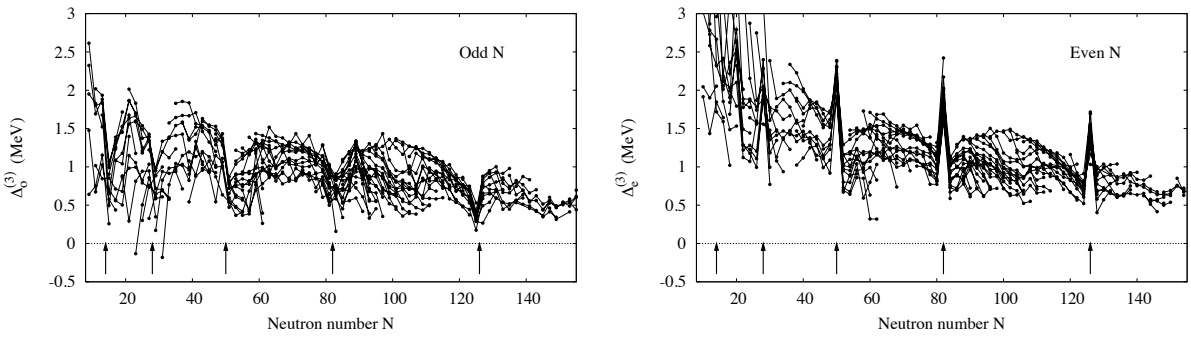

Figure 9.1: Upper panels: odd-N pairing gaps. Lower panels: even-N pairing gaps. Typically, the odd-N nuclei are less bound than the average of their even-N neighbors by about 1 MeV. However, one sees that there can be about a factor of two scatter around the average value at a given N.

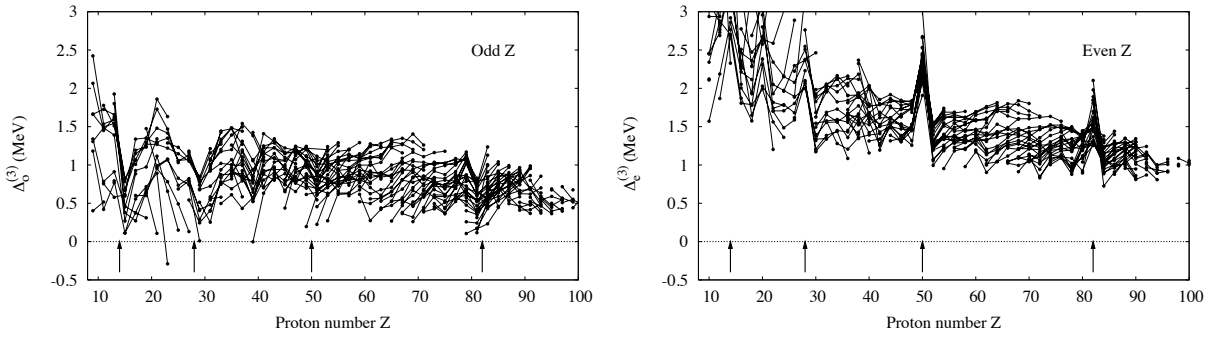

Figure 9.2: Upper panels: odd-Z pairing gaps. Lower panels: even-Z pairing gaps.

gap, $\Delta^{(3)} = C$, shown on the line labeled C. One sees that a typical gap size is 1 MeV, and typical fluctuations about that are smaller by a factor of 3. Beyond that, there are differences between protons and neutrons and between the odd and the even gaps. The even gaps are somewhat larger and have somewhat larger fluctuations, which is to be expected in view of the shell effects exhibited in Fig. 1. The odd proton gap is smaller than the odd neutron gaps which might be expected from the repulsive Coulomb contribution to the pairing interaction. There is also a mean-field contribution of the Coulomb that has opposite signs for even and odd protons. Indeed the even proton gaps are actually larger than their neutron counterparts.

For the next lines in the table, I come back to the broad trend in Fig. 1, a systematic decrease in gaps with increasing mass number. It is conventional to describe this with a fractional power dependence, $\Delta^{(3)} = c/A^{1/2}$. This decreases the rms errors somewhat, but there is no theoretical basis for the fractional power of A. In the last line I show the result of a two-parameter fit to the functional form $\Delta^{(3)} = c_1/A+c_2$. This functional form is more justified by theoretical considerations, as will be discussed in the theory section below.

Basic spectral properties

The other strong signatures of pairing are in excitation spectra. In the simple BCS theory, the lowest excited states in an even system requires breaking two pairs giving an excitation energy

$$E_{ex} \approx 2\Delta_{\rm BCS}. \tag{9.3}$$

On the other hand, in the odd particle number system, the quasiparticle level density diverges at the Fermi energy. This contrasting behavior is very obvious in the nuclear spectrum. As an example, the isotope chain at proton magic number $Z = 50$ (the element Sn) has been a favorite for exhibiting and studying pairing effects. Figure 9.3 shows the low-lying spectra of odd-N members of the chain. One can see that there are several levels within one MeV of the ground state. The spins and parities of the levels (not shown) correspond very well with the single-particle orbitals near the neutron Fermi level. However, the spectrum is very compressed with respect to orbital energies calculated with a shell model potential well. In contrast, the even members of the chain have no excited states at all within the excitation energy range displayed in the Figure.

Let us look now look at the global systematics for excitations in the even-even nuclei. The estimate in Eq. (9.3) is too naive because there can be collective excitations within the gap, as is well-known from early days of BCS theory [**?**]. For example, there are longitudinal sound modes in an uncharged superfluid fermionic liquid. These have a phonon spectrum allowing frequencies within the quasiparticle gap. One might expect that such modes would be absent in finite systems when the size of the system is small compared to the coherence length of the pairing field. In fact the situation for nuclear excitations is much more complicated. However, just for presenting the systematics, we use the right-hand side of Eq. (9.3) to scale the excitation energies, taking the ratio $E_2/2\Delta$, where E_2 is the excitation energy and Δ is the smaller of $\Delta^{(3)}_{eZ}$ and $\Delta^{(3)}_{eN}$.

The scaled excitation energies of the first excited states in even-even are shown in Fig. 9.4. With only a few exceptions these states have angular momentum and parity quantum numbers $J^\pi = 2^+$ and can be considered to be collective quadrupolar excitations of the ground state. All of the ratios are smaller than one, with most in the range 0.1-0.5. The very small excitations in the mass ranges $A = 160 - 180$ and $220 - 250$ correpond to nuclei with static quadrupole deformations.

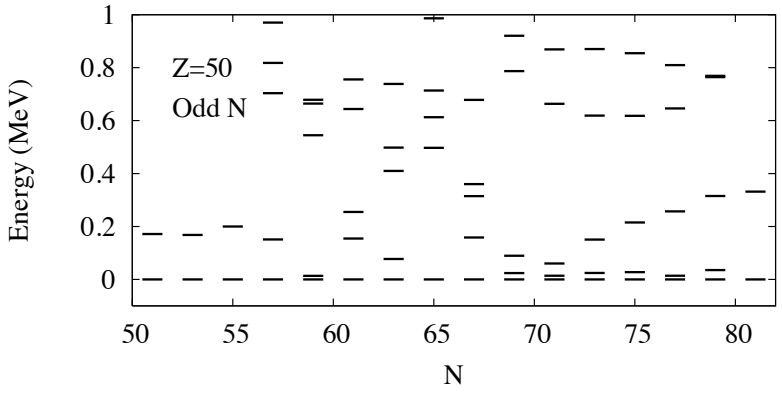

Figure 9.3: Energy levels of odd-N Sn isotopes

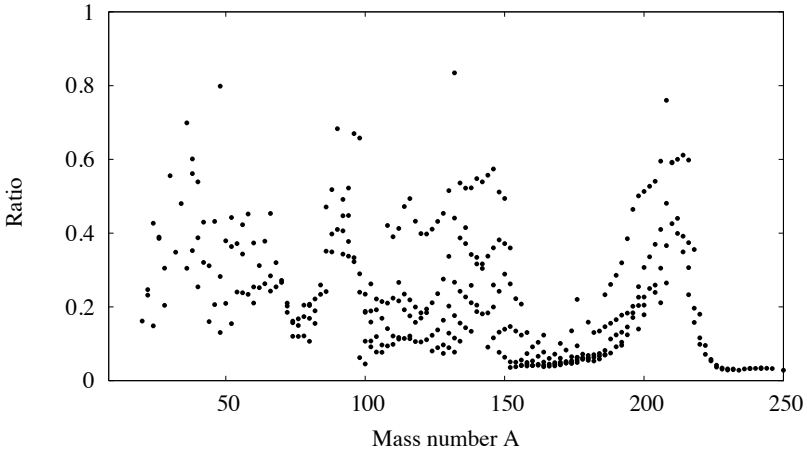

Figure 9.4: Energy gap in the excitation spectrum of even-even nuclei, scaled to $2\Delta^{(3)}$. See text for details.

The physics underlying these excitations is the softness of a typical nucleus with respect to quadrupolar deformations. On a qualitative level, the collectivity is similar to the phonon collectivity in the infinite Fermi gas. A quantitative measure of the collectivity is the sum-rule fraction contained in the excitation, using the energy-weighted sum rule for some density operator. For the phonon case, the sum rule fraction approaches 100% when the frequency of the collective mode is small compared to the gap [**?**]. The collectivity in the nuclear quadrupole excitations is quite different. The sum rule fraction carried by the lowest 2^+ excitation is more or less constant over the entire range of nuclear masses, but it only about 10% of the total (for isoscalar quadrupole transitions.

Turning to odd-A spectrao, some systematics related to the level density are shown in Fig. **??**. The average excitation energy of the first excited state is plotted for each odd mass number A, averaging over even values of Z. For comparison, the solid line is the expected spacing in the Fermi gas formula for the single-particle level density,

$$\frac{dn_s}{dE} = V\frac{mk_F}{2\pi^2} \approx \frac{A}{100} \text{ MeV}. \tag{9.4}$$

The subscript s on N_s indicates that only one spin projection is counted, and k_F is the Fermi momentum. V is the volume of the nucleus, which is (roughly) proportional to the number of nucleons A. One can see from the Figure that a typical spacing is a factor of 10 smaller than that given by the Fermi gas formula. Clearly interaction effects are at work to increase the level density near the ground state.

Mean-field theory has made enormous strides in nuclear physics; the self-consistent mean field theory based on the Hartree-Fock-Bogoliubov approximation and using semi-phenomenological energy functionals is now the tool of choice for the global description of nuclear structure. It is not my intention to review this subject since it is well covered elsewhere in this volume.

Neverless, there are number of aspects of nuclear pairing that can be can rather easily understood using only the more qualitative aspects of pairing theory. Besides the pairing gaps and the effect on level densities, there are important consequences for two-nucleon transfer reactions and on dynamic properties such as radioactive decay modes. This section presents an overview of some of these aspects.

Origin of the pairing interaction

It is no surprise that conditions for pairing are satisfied in nuclei. The nuclear interaction between identical nucleons is strongly attractive in the spin-zero channel, almost to the degree to form a two-neutron bound state. While this explains the origin at a qualitative level, the many-body aspects of the nuclear interaction make it difficult to derive a quantitative theory starting from basic interactions. The progress one has made so far is reviewed in other chapters of this book, so I won't go into detail here. But just for perspective, I mention some of the major issues.

I first recall problems with the mean-field interaction to use at the Hartree-Fock level. Most obviously, the effective interaction between nucleons in the nuclear medium is strongly modified by the Pauli principle. The Pauli principle suppresses correlations between nucleons and that in turn make the effective interaction less attractive. Beyond that, it seems unavoidable to introduce three-body interactions in a self-consistent mean-field theory. These interactions have two origins. The first is the three-nucleon interaction arising from sub-nucleon degrees of freedom. It has been convincingly demonstrated that such interactions are needed to reproduce binding energies of light nuclei and to calculated the bulk properties of nuclear matter. Besides this more fundamental three-body interaction, there may an induced interaction associated with the short-ranged correlations and their suppression in the many-body environment. In the popular parameterization of the effective interaction for use in mean-field theory, the three-body interaction energy has the same order of magitude as the two-body interaction energy. It would thus seem to be a great oversimplication to ignore the three-body effects in the pairing interaction.

The last issue is the role of the induced interaction associated with low-frequency excitations. We have seen that the nucleus is rather soft to surface deformations. the virtual excitation of these modes would contribute to the pairing in exactly the same way that phonon provide an attractive pairing interaction for the electrons in a superconductor. It may well have the same importance as the two-particle interaction. Note that if low-frequency phonons were dominant, the energy scale in Eq. (5) would be greatly reduced.

The dynamic properties of an extended fermionic system depend crucially on the presence of a pairing condensate, changing it from a highly viscous fluid to a superfluid. The effects in nuclei are not quite as dramatic as in extended systems because the pairing coherence length in nuclei exceeds the size of the nucleus. Nevertheless, the presence of a highly deformable surface in nuclei requires that pairing be treated in a dynamical way.

The most clearly documented dynamic influence of pairing is its effect on the moment of inertia of deformed nuclei. Without pairing, the rotational spectrum of a deformed fermionic droplet is believed to follow the spectrum of a rigid rotor,

$$E_J = \frac{\hbar^2}{2\mathcal{I}} J(J+1). \tag{9.5}$$

Here $\hbar J$ is the angular momentum and the moment of inertia $\mathcal{I}$ would be close to the rigid value

$$\mathcal{I} \approx \frac{2}{3} Am\langle r^2 \rangle \approx \frac{2}{5} A^{5/3} m r_0^2. \tag{9.6}$$

If the pairing were strong enough to make the coherence length small compared to the size of the system, the system would be a superfluid having irrotational flow and a corresponding inertial dynamics. What is somewhat surprising is that the weak pairing that is characteristic of nuclei still has a strong effect on the inertia.

9.2 The seniority model

For a system with n identical particles in a single j-shell, the binding energy can be solved analytically in the seniority scheme. The Hamiltonian for such a model can be written as [**?**],

$$H = -G \sum_{m,m'>0} a_m^\dagger a_{-m}^\dagger a_{-m'} a_{m'} = -G S_+ S_- \tag{9.7}$$

where S represents the quasi-spin operator, and $a_m^\dagger$ and a_m are creation and annihilation operators. G is the strength of the pairing interaction. We have

$$S_+ = \sum_m s_+^{(m)} = \sum_m a_m^\dagger a_{-m}^\dagger \tag{9.8}$$

$$S_- = (S_+)^\dagger = \sum_m s_-^{(m)} = \sum_m a_{-m} a_m \tag{9.9}$$

$$S_0 = \sum_m s_0^{(m)} = \frac{1}{2} \sum_m (a_m^\dagger a_m + a_{-m}^\dagger a_{-m} - 1) = \frac{1}{2}(n - \Omega) \tag{9.10}$$

Here, m ($m > 0$) represents each sub-state level, and $a_m^\dagger$ and a_m are creation and annihilation operators. Ω is the maximal number of pairs in the single j-shell ($\Omega = j + \frac{1}{2}$). The eigenvalues S of total quasi-spin are: $S = \frac{1}{2}|N - \Omega|, \cdots, \frac{1}{2}\Omega - 1, \frac{1}{2}\Omega$, and the energy eigenvalues of H are given by:

$$E(S) = -G \left\{ S \cdot (S+1) - \frac{1}{4}(N-\Omega)^2 + \frac{1}{2}(N-\Omega) \right\} \tag{9.11}$$

Or we can introduce *seniority quantum number* s given by $s = \Omega - 2S$, the energy of the state with seniority v can be written as

$$\begin{aligned} E(v) &= -G \frac{n-v}{4}(2j + 3 - n - v) \\ &= \frac{n(n-1)}{4} G - \frac{v(v-1)}{4} G - \frac{1}{2}(n-v)(j+1)G \end{aligned} \tag{9.12}$$

If we assume $v = 0$ for the ground state of even-even system and $v = 1$ for that of the odd system. The expression above can be simplified as,

$$E(v) = \frac{n(n-1)}{4} G - \left[\frac{n}{2}\right] (j+1)G, \tag{9.13}$$

where $[n/2]$ denotes the largest integer not exceeding n/2 and corresponds to the total number of $v = 0$ pairs.

9.3 Basics of pairing correlations

from arXiv:1206.2600

In quantum mechanics of finite many-fermion systems, pairing correlations are best described in terms of number operators $\hat{N}_\mu = a_\mu^+ a_\mu$, where μ represents any suitable set of single-particle (s.p.) quantum numbers. Thus we may have, e.g., $\mu \equiv \boldsymbol{k}\sigma$ for plane waves of spin-$\frac{1}{2}$ particles (electrons); $\mu \equiv \boldsymbol{r}\sigma\tau$ for spin-$\frac{1}{2}$ and isospin-$\frac{1}{2}$ nucleons localized in space at position $\boldsymbol{r}$; and $\mu \equiv n, \ell, j, m$ for fermions moving in a spherical potential well. Since $\hat{N}_\mu^2 = \hat{N}_\mu$, the number operators are projective; hence, one can – at least in principle – devise an experiment that would project any quantum many-fermion state $|\Psi\rangle$ into its component with exactly one fermion occupying state μ. As the rules of quantum mechanics stipulate, any such individual measurement can only give 0 or 1 (these are the eigenvalues of $\hat{N}_\mu$), whereas performing such measurements many times, one could experimentally determine the occupation probabilities $v_\mu^2 = \langle\Psi|\hat{N}_\mu|\Psi\rangle$.

Along such lines, we can devise an experiment that would determine the *simultaneous* presence of two fermions in different orthogonal s.p. states μ and ν. Since the corresponding number operators $\hat{N}_\mu$ and $\hat{N}_\nu$ commute, one can legitimately ask quantum mechanical questions about one-particle occupation probabilities v_μ^2 and v_ν^2, as well as about the two-particle occupation. The latter one reflects the simultaneous presence of two fermions in state $|\Psi\rangle$: $v_{\mu\nu}^2 = \langle\Psi|\hat{N}_\mu\hat{N}_\nu|\Psi\rangle$. In this way, one can experimentally determine the pairing correlation between states μ and ν as the *excess* probability

$$P_{\mu\nu} = v_{\mu\nu}^2 - v_\mu^2 v_\nu^2, \tag{9.14}$$

of finding two fermions simultaneously over that of finding them in independent, or sequential, measurements. Such a definition of pairing is independent of its coherence, collectivity, nature of quasiparticles, symmetry breaking, thermodynamic limit, or many other notions that are often associated with the phenomenon of pairing. In terms of occupations, pairing can be viewed as a measurable property of any quantum many-fermion state.

Obviously, no pairing correlations are present in a quantum state that is an eigenstate of $\hat{N}_\mu$ or $\hat{N}_\nu$, such as the Slater determinant. The beauty of the BCS ansatz is in providing us with a model N-fermion state, in which pairing correlations are explicitly incorporated:

$$|\Phi_N\rangle = \mathcal{N}_N \left(\sum_{\mu>0} s_\mu z_\mu a_{\tilde{\mu}}^+ a_\mu^+ \right)^{N/2} |0\rangle, \tag{9.15}$$

where the summation $\mu > 0$ runs over the representatives of pairs $(\tilde{\mu}, \mu)$ of s.p. states (that is, any one state of the pair is included in the sum, but not both), $z_{\tilde{\mu}} = z_\mu$ are real positive numbers, $s_{\tilde{\mu}} = -s_\mu$ are arbitrary complex phase factors, and $\mathcal{N}_N$ is the overall normalization factor.

It now becomes a matter of technical convenience to employ a particle-number mixed state,

$$|\Phi\rangle = \mathcal{N} \sum_{N=0,2,4,\ldots}^{\infty} \frac{|\Phi_N\rangle}{\mathcal{N}_N (N/2)!} = \mathcal{N} \exp\left(\sum_{\mu>0} s_\mu z_\mu a_{\tilde{\mu}}^+ a_\mu^+ \right) |0\rangle, \tag{9.16}$$

in which the pairing correlations (9.14) are:

$$P_{\mu\nu} = v_\mu^2 u_\nu^2 \delta_{\tilde{\mu}\nu} \quad \text{for} \quad v_\mu^2 = \frac{z_\mu^2}{1+z_\mu^2} \quad \text{and} \quad u_\nu^2 = \frac{1}{1+z_\nu^2}. \tag{9.17}$$

In terms of the s.p. occupations, the state $|\Phi\rangle$ assumes the standard BCS form:

$$|\Phi\rangle = \prod_{\mu>0} \left(u_\mu + s_\mu v_\mu a_{\tilde{\mu}}^+ a_\mu^+ \right) |0\rangle. \tag{9.18}$$

In this many-fermion state, the s.p. states $\tilde{\mu}$ and μ are paired, that is, $|\Phi\rangle$ can be viewed as a pair-condensate. For z_μ=1, the pairing correlation $P_{\tilde{\mu}\mu}$ (9.14) equals 1/4; in fact, in this state, it is twice more likely to find a pair of fermions ($v_{\tilde{\mu}\mu}^2$=1/2) than to find these two fermions independently ($v_{\tilde{\mu}}^2 v_\mu^2$=1/4). For particle-number conserving states (9.15), the occupation numbers can be calculated numerically; qualitatively the results are fairly similar, especially for large numbers of particles.

At this point, we note that the most general pair-condensate state (9.16) has the form of the Thouless state,

$$|\Phi\rangle = \mathcal{N} \exp\left(\tfrac{1}{2}\sum_{\nu\mu} Z^*_{\nu\mu} a^+_\nu a^+_\mu\right)|0\rangle, \tag{9.19}$$

in which pairs $(\tilde{\mu},\mu)$ do not appear explicitly. However, there always exists a unitary transformation U_0 of the antisymmetric matrix Z that brings it to the canonical form $(U_0^+ Z^* U_0^*)_{\nu\mu} = s_\mu z_\mu \delta_{\tilde{\mu}\nu}$ (the Bloch-Messiah-Zumino theorem[**?**, **?**]). Therefore, pairs are present in any arbitrary Thouless state (the so-called canonical pairs), and they can be made explicitly visible by a simple basis transformation.

The canonical pairs exist independently of any symmetry of the Thouless state. In the particular case of a time-reversal-symmetric state, $\hat{T}|\Phi\rangle = |\Phi\rangle$, they can be associated with the time-reversed s.p. states, $\tilde{\mu} \equiv \bar{\mu}$. The ground-states of even-even nuclei can be described in this manner. However, the appearance of pairing phase does not hinge on this particular symmetry – states in rotating nuclei (in which time-reversal symmetry is manifestly broken) can also be paired. In this latter case the canonical states are less useful, because they cannot be directly associated with the eigenstates of the HFB Hamiltonian.

Hartree-Fock-Bogoliubov theory

The simplest route to the HFB theory is to employ the variational principle to a two-body Hamiltonian using Thouless states (9.19) as trial wave functions. The variation of the average energy with respect to the antisymmetric matrix Z results in the HFB equation in the matrix representation, $\mathcal{H}\mathcal{U} = \mathcal{U}\mathcal{E}$, or explicitly,

$$\begin{pmatrix} T+\Gamma & \Delta \\ -\Delta^* & -T^*-\Gamma^* \end{pmatrix}\begin{pmatrix} U & V^* \\ V & U^* \end{pmatrix} = \begin{pmatrix} U & V^* \\ V & U^* \end{pmatrix}\begin{pmatrix} E & 0 \\ 0 & -E \end{pmatrix}, \tag{9.20}$$

where $T_{\mu\nu}$ is the matrix of the one-body kinetic energy, $\Gamma_{\mu\nu} = \sum_{\mu'\nu'} V_{\mu\mu';\nu\nu'}\rho_{\nu'\mu'}$ and $\Delta_{\mu\mu'} = \frac{1}{2}\sum_{\nu\nu'} V_{\mu\mu';\nu\nu'}\kappa_{\nu\nu'}$ are the so-called particle-hole and particle-particle mean fields, respectively, obtained by averaging two-body matrix elements $V_{\mu\mu';\nu\nu'}$ with respect to the density matrix $\rho_{\nu'\mu'} = \langle\Phi|a^+_{\mu'}a_{\nu'}|\Phi\rangle$ and pairing tensor $\kappa_{\nu\nu'} = \langle\Phi|a_{\nu'}a_\nu|\Phi\rangle$, and E is the diagonal matrix of quasiparticle energies[**?**].

The matrices $\mathcal{H}$ and $\mathcal{U}$ are referred to as the HFB Hamiltonian and Bogoliubov transformation, respectively, and columns of $\mathcal{U}$ (eigenstates of $\mathcal{H}$) are vectors of quasiparticle states. The HFB equation (9.20) possesses the quasiparticle-quasihole symmetry. Namely, for each quasiparticle state χ_α (the α-th column of $\mathcal{U}$) and energy E_α there exists a quasihole state ϕ_α of opposite energy $-E_\alpha$,

$$\chi_\alpha = \begin{pmatrix} U_{\mu\alpha} \\ V_{\mu\alpha} \end{pmatrix}, \quad \phi_\alpha = \begin{pmatrix} V^*_{\mu\alpha} \\ U^*_{\mu\alpha} \end{pmatrix}. \tag{9.21}$$

That is, the spectrum of $\mathcal{H}$ is composed of pairs of states with opposite energies. In most cases, the lowest total energy is obtained by using the eigenstates with $E_\alpha > 0$ as quasiparticles χ_α and those with $E_\alpha < 0$ as quasiholes ϕ_α, that is, by occupying the negative-energy eigenstates. States χ_α and ϕ_α can usually be related through a self-consistent discrete symmetry, such as time reversal, signature, or simplex.[**?**, **?**, **?**].

The HFB equation (9.20) is also valid in a more general case, when the total energy is not equal to the average of any many-body Hamiltonian. Within the DFT, it stems from the minimization of the binding energy given by an EDF $\mathcal{E}(\rho,\kappa,\kappa^*)$, subject to the condition of the generalized density matrix being projective, that is, $\mathcal{R}^2 = \mathcal{R}$ for

$$\mathcal{R} = \begin{pmatrix} \rho & \kappa \\ -\kappa^* & 1-\rho^* \end{pmatrix} = \begin{pmatrix} V^*V^T & V^*U^T \\ U^*V^T & U^*U^T \end{pmatrix} = \begin{pmatrix} V^* \\ U^* \end{pmatrix}\begin{pmatrix} V^T & U^T \end{pmatrix} = \sum_\alpha \phi_\alpha\phi^+_\alpha. \tag{9.22}$$

In this case, the mean fields are obtained as functional derivatives of EDF: $\Gamma_{\mu\nu} = \partial\mathcal{E}/\partial\rho_{\nu\mu}$ and $\Delta_{\mu\mu'} = \partial\mathcal{E}/\partial\kappa^*_{\mu\mu'}$. As is the case in DFT, densities (here the density matrix and pairing tensor) become the fundamental degrees of freedom, whereas the state $|\Phi\rangle$ acquires the meaning of an auxiliary entity (the Kohn-Sham state[**?**]). Indeed, for any arbitrary generalized density matrix $\mathcal{R}$ (9.22), one can always find the corresponding state $|\Phi\rangle$. For that, one determines the Bogoliubov transformation $\mathcal{U}$ as the matrix of its eigenvectors, $\mathcal{R}\mathcal{U} = \mathcal{U}\begin{pmatrix} 0 & 0 \\ 0 & 1 \end{pmatrix}$; the Thouless state $|\Phi\rangle$ (9.19) corresponds to $Z = VU^{-1}$. Consequently, the paired state $|\Phi\rangle$ of DFT is not interpreted as a wave function of the system – it only serves as a model for determining one-body densities. Nonetheless, these densities *are* interpreted as those associated with the (unknown) exact eigenstate of the system.

Unrestricted variations of the EDF are not meaningful. Indeed, since Thouless states (9.16) are mixtures of components with different particle numbers, absolute minima will usually correspond to average particle numbers that are unrelated to those one would like to describe. In particular, for self-bound systems governed by attractive two-body forces (nuclei), by adding more and more particles one could infinitely decrease the total energy of the system. Therefore, only constrained variations make sense, that is, one has to minimize not the total energy $\mathcal{E}(\rho,\kappa,\kappa^*)$, but the so-called Routhian, $\mathcal{E}'(\rho,\kappa,\kappa^*) = \mathcal{E}(\rho,\kappa,\kappa^*) + \mathcal{C}(\rho)$, where $\mathcal{C}$ is a suitably chosen penalty functional, ensuring that the minimum appears at prescribed average values of one-body operators. In particular, the average total number of particles can be constrained by $\mathcal{C}(\rho) = -\lambda\langle\Phi|\hat{N}|\Phi\rangle = -\lambda\mathrm{Tr}(\rho)$ (linear constraint) or $\mathcal{C}(\rho) = C_N[\mathrm{Tr}(\rho) - N_0]^2$ (quadratic constraint),[**?**, **?**] where λ becomes the Fermi energy corresponding to N_0 fermions.

For different systems and for different applications, various constraints $\mathcal{C}(\rho)$ can be implemented; for example, in nuclei one can simultaneously constrain numbers of protons and neutrons, as well as multipole moments of matter or charge distributions. When the total energy is a concave function of relevant one-body average values, quadratic constraints are mandatory[**?**, **?**]. The minimization of $\mathcal{E}'(\rho,\kappa,\kappa^*)$ requires solving the HFB equation for the quasiparticle Routhian $\mathcal{H}'$, which, for the simplest case of the constraint on the total particle number, reads $\mathcal{H}' = \mathcal{H} - \lambda\begin{pmatrix} 1 & 0 \\ 0 & -1 \end{pmatrix}$.

9.4 Exact solutions for pairing interactions

Taken from arXiv:1204.2950

The first breakthrough towards a microscopic description of the superconducting phenomenon was due to Cooper[1], who in 1956 showed that a single pair of electrons on top of an inert Fermi sea could be bound by an infinitesimal attractive interaction. The search for a many-body wave function describing a fraction of correlated and overlapping pairs mixed with a Fermi sea was a key goal for the rest of that year. Schrieffer came up with a solution at the beginning of 1957 and the BCS team (Bardeen, Cooper and Schrieffer) started an intensive and fruitful collaboration to explain quantitatively many superconducting properties from the associated BCS wave function. This led to the famous BCS paper [2] which provided a complete microscopic explanation of superconductivity.

The success of the BCS theory quickly spread to other quantum many-body systems, including the atomic nucleus. In the summer of 1957, David Pines visited the Niels Bohr Institute and gave a series of seminars about the yet unpublished BCS theory. Soon thereafter Bohr, Mottelson and Pines published a paper [3] suggesting that the gaps observed in even-even nuclei could be due to superconducting correlations. They noted, however, that these effects should be strongly influenced by the finite size of the nucleus. Since then, and up to the present, number projection and in general symmetry restoration in the BCS and Hartree-Fock-Bogoliubov approximations have been important issues in nuclear structure.

At the beginning of the sixties, while several groups were developing numerical techniques for number-projected BCS calculations [4, 5], Richardson provided an exact solution for the reduced BCS Hamiltonian [6, 7]. In spite of the importance of his exact solution, this work did not have much impact in nuclear physics with just a few exceptions. Later on, his exact solution was rediscovered in the framework of ultrasmall superconducting grains [8] where BCS and number-projected BCS were unable to describe appropriately the crossover from superconductivity to a normal metal as a function of the grain size. Since then, there has been a flurry of work extending the Richardson exact solution to families of exactly-solvable models, now called the Richardson-Gaudin (RG) models [9], and applying these models to different areas of quantum many-body physics including mesoscopic systems, condensed matter, quantum optics, cold atomic gases, quantum dots and nuclear structure [10]. In this paper, we review Richardson's solution, its generalization to the exactly-solvable RG models and discuss the applications of these models in nuclear physics.

The Richardson solution of the reduced BCS hamiltonian

We will focus on a pairing Hamiltonian with constant strength G acting in a space of doubly-degenerate time-reversed states $(k,\bar{k})$,

$$H_P = \sum_k \epsilon_k c_k^\dagger c_k - G\sum_{k,k'} c_k^\dagger c_{\bar{k}}^\dagger c_{\bar{k}'} c_{k'} \ , \tag{9.23}$$

where ϵ_k are the single-particle energies for the doubly-degenerate orbits $k,\bar{k}$.

Cooper considered the addition of a pair of fermions with an attractive pairing interaction on top of an inert Fermi sea (FS) under the influence of this Hamiltonian. He showed that the pair eigenstate is

$$|\Psi_{Cooper}\rangle = \sum_{k>k_F} \frac{1}{2\epsilon_k - E}\ c_k^\dagger c_{\overline{k}}^\dagger\ |FS\rangle\ , \tag{9.24}$$

where E is the energy eigenvalue. Cooper found that for any attractive value of G, the Fermi sea is unstable against the formation of such bound pairs. Therefore, an approach that takes into account a fraction of these correlated pairs mixed with a Fermi sea should be able to describe the superconducting phenomenon.

The BCS approach followed a somewhat different path to the one suggested by Cooper, defining instead a variational wave function as a coherent state of pairs that are averaged over the whole system,

$$|\Psi_{BCS}\rangle = e^{\Gamma^\dagger}\,|0\rangle\ , \tag{9.25}$$

where $\Gamma^\dagger = \sum_k z_k c_k^\dagger c_{\overline{k}}^\dagger$ is the coherent pair. Though errors due to the non-conservation of particle number in (9.25) are negligible when the number of pairs is sufficiently large, they can be important in such finite systems as atomic nuclei [3]. To accommodate these effects, number-projected BCS (PBCS) [4] considers a condensate of pairs of the form

$$|\Psi_{PBCS}\rangle = \left(\Gamma^\dagger\right)^M |0\rangle\ , \tag{9.26}$$

where M is the number of pairs and $\Gamma^\dagger$ has the same form as in BCS.

Richardson [6] proposed an ansatz for the exact solution of the pairing Hamiltonian (9.23) that followed closely Cooper's original idea. For a system with $2M + \nu$ particles, with ν of these particles unpaired, his ansatz involves a state of the form

$$|\Psi\rangle = B_1^\dagger B_2^\dagger \cdots B_M^\dagger\,|\nu\rangle\ , \tag{9.27}$$

where the collective pair operators $B_\alpha^\dagger$ have the form found by Cooper for the one-pair problem,

$$B_\alpha^\dagger = \sum_{k=1}^{L} \frac{1}{2\varepsilon_k - E_\alpha}\ c_k^\dagger c_{\overline{k}}^\dagger\ . \tag{9.28}$$

Here L is the number of single-particle levels and

$$|\nu\rangle \equiv |\nu_1, \nu_2 \cdots, \nu_L\rangle \tag{9.29}$$

is a state of ν unpaired fermions ($\nu = \sum_k \nu_k$, with $\nu_k = 1$ *or* 0) defined by $c_k c_{\overline{k}}\,|\nu\rangle = 0$, and $n_k\,|\nu\rangle = \nu_k\,|\nu\rangle$.

In the one-pair problem, the quantities E_α that enter (9.28) are the eigenvalues of the pairing Hamiltonian, *i.e.*, the *pair energies*. Richardson proposed to use the M pair energies E_α in the many-body wave function of Eqs. (9.27, 9.28) as parameters which are chosen to fulfill the eigenvalue equation $H_P\,|\Psi\rangle = E\,|\Psi\rangle$. He showed that this is the case if the pair energies satisfy a set of M non-linear coupled equations

$$1 - G\sum_{k=1}^{L} \frac{1-\nu_k}{2\varepsilon_k - E_\alpha} - 2G \sum_{\beta(\neq\alpha)=1}^{M} \frac{1}{E_\beta - E_\alpha} = 0\ , \tag{9.30}$$

which are now called the Richardson equations. The second term represents the interaction between particles in a given pair and the third term represents the interaction between pairs. The associated eigenvalues of H are given by

$$\mathcal{E} = \sum_{k=1}^{L} \varepsilon_k \nu_k + \sum_{\alpha=1}^{M} E_\alpha\ , \tag{9.31}$$

namely as a sum of the pair energies.

Each independent solution of the set of Richardson equations defines a set of M pair energies that completely characterizes a particular eigenstate (9.27, 9.28). The complete set of eigenstates of the pairing Hamiltonian can be obtained in this way. The ground state solution is the energetically lowest solution in the $\nu = 0$ or $\nu = 1$ sector, depending on whether the system has an even or an odd number of particles, respectively.

There are a couple of points that should be noted here. First, in contrast to the BCS solution, each Cooper pair $B^\dagger_\alpha$ is distinct. Second, if one of the pair energies E_α is complex, then its complex-conjugate E^*_α is also a solution. From this latter point we see that $|\Psi\rangle$ preserves time-reversal invariance.

On inspection of the Richardson pair (9.28), we see that a pair energy that is close to a particular $2\epsilon_k$, *i.e.* close to the energy of an unperturbed pair, is dominated by this particular configuration and thus defines an uncorrelated pair. In contrast, a pair energy that lies sufficiently far away in the complex plane produces a correlated Cooper pair. This is to be contrasted with the single BCS coherent pair, which has amplitude $z_k = v_k/u_k$ and which mixes correlated and uncorrelated pairs over the *whole* system.

Generalization to the Richardson-Gaudin class of integrable models

In this section, we discuss how to generalize the standard pairing model, which as we have seen is exactly solvable, to a wider variety of exactly-solvable models, the so-called Richardson-Gaudin models[11], all of which are based on the $SU(2)$ algebra. We first introduce the generators of $SU(2)$, using a basis more familiar to nuclear structure,

$$K^0_j = \frac{1}{2}\left(\sum_m a^\dagger_{jm}a_{jm} - \Omega_j\right),\ K^+_j = \sum_m a^\dagger_{jm}a^\dagger_{j\overline{m}},\ K^-_j = (K^+_j)^\dagger. \tag{9.32}$$

Here $a^\dagger_{jm}$ creates a fermion in single-particle state jm, $j\overline{m}$ denotes the time reverse of jm, and $\Omega_j = j + \frac{1}{2}$ is the pair degeneracy of orbit j. These operators fulfill the $SU(2)$ algebra $[K^+_j, K^-_{j'}] = 2\delta_{jj'}K^0_j$, $[K^0_j, K^\pm_{j'}] = \pm\delta_{jj'}K^\pm_j$.

We now consider a general set of L Hermitian and number-conserving operators that can be built up from the generators of $SU(2)$ with linear and quadratic terms,

$$R_i = K^0_i + 2g\sum_{j(\neq i)}\left[\frac{X_{ij}}{2}\left(K^+_iK^-_j + K^-_iK^+_j\right) + Y_{ij}K^0_iK^0_j\right]\ . \tag{9.33}$$

Following Gaudin[12], we then look for the conditions that the matrices X and Y must satisfy in order that the R operators commute with one another. It turns out that there are essentially two families of solutions, referred to as the rational and hyperbolic families, respectively.

i. The rational family

$$X_{ij} = Y_{ij} = \frac{1}{\eta_i - \eta_j} \tag{9.34}$$

ii. The hyberbolic family

$$X_{ij} = 2\frac{\sqrt{\eta_i\eta_j}}{\eta_i - \eta_j}\ ,\ Y_{ij} = \frac{\eta_i + \eta_j}{\eta_i - \eta_j} \tag{9.35}$$

Here the set of L parameters η_i are free real numbers.

The traditional pairing model is an example of the rational family. It can be obtained as a linear combination of the integrals of motion, $H_P = \sum_j \varepsilon_j R_j(\varepsilon_j)$, with $\eta_j = \varepsilon_j$.

The complete set of eigenstates of the rational integrals of motion is given by the Richardson ansatz (9.27, 9.28). This fact led Gaudin [12] to try to relate his integrable models to the BCS Hamiltonian without success. The proof of integrability of the BCS Hamiltonian was found later in ref. [13]. We will not present the general solution of the two integrable families here, referring the reader to refs. [11, 9, 10].

The key point is that any Hamiltonian that can be expressed as a linear combination of the R operators can be treated exactly using this method. In the following sections, we discuss nuclear applications of the standard pairing model and of a new model based on the hyberbolic family.

Applications of the Richardson solution to pairing in nuclear physics

Richardson himself started to explore analytically the exact solution in nuclear structure for few pairs outside a doubly-magic core[14, 15]. He also proposed a numerical method to solve the equations for systems with equidistant levels[16], a model that was subsequently used as a benchmark to test many-body approximations [17]. However, the first application of the Richardson solution to a real nuclear system was reported by Andersson and Krumlinde [18] in 1977. They studied the properties of high-spin states in ^{152}Dy using an oblate deformed oscillator potential and including the effects of pairing

at several different levels of approximation. They compared the results when pairing was treated with the traditional BCS approximation, when it was treated in PBCS approximation (using the saddle point approximation) and when it was treated exactly using the Richardson method.

Following that early work, there were sporadic references to the Richardson method but no realistic studies of atomic nuclei until just a few years ago. In 2007, Dussel *et al.* [19] reported a systematic study of pairing correlations in the even Sm isotopes, from ^{144}Sm through ^{158}Sm, using the self-consistent deformed Hartree Fock+BCS method. The calculations made use of the density-dependent Skyrme force, SLy4, and treated pairing correlations using a pairing force with constant strength G assuming axial symmetry and taking into account 11 major shells.

Using the results at self-consistency to define the HF mean field, pairing effects within *that* mean field were then considered using the alternative number-conserving PBCS approach and the exact Richardson approach. In this way it was possible to directly compare the three approaches to pairing with the same pairing Hamiltonian, a primary focus of the study. It should be noted here that the Hilbert space dimensions associated with the residual neutron pairing Hamiltonian is of the order of 3.9×10^{53} for ^{154}Sm, whereas the exact Richardson approach requires the solution of a coupled set of 46 non-linear equations.

In the one semi-magic nucleus ^{144}Sm that was studied, the principal correlation effects arise when projection is included, taking the system from one that is normal at the level of BCS to one with substantial pairing correlations. Treating pairing exactly provides a further modest increase in pairing correlations of about 0.3 MeV. In non-semi-magic nuclei, the effect on the pairing correlation energy of the exact solution is significantly more pronounced. While there too number projection provides a substantial lowering of the energy, it now misses about 1 MeV of the exact correlation energy that derives from the Richardson solution.

The exact Richardson solution was also used to study the gradual emergence of superconductivity in the Sn isotopes [22]. By making use of an exact mapping between the Richardson equations and a classical electrostatic problem in two dimensions, it was possible to get a physical picture of how superconductivity develops as a function of the pairing strength. In particular, as the pairing strength is increased the pair energies gradually merge into larger structures in the complex plane as pair correlations gradually overcome single-particle effects.

More recently, the Richardson solution has been applied to the treatment of pair correlations involving the continuum. The first work by Hasegawa and Kaneko [23] considered only the effect of resonances in the continuum and as a result obtained complex energies even for the bound states of the system. Subsequent work by Id Betan [24, 25] included the effects of the true continuum. The most recent paper [25] treated nuclear chains that include both bound and unbound systems, *e.g.* the even-A Carbon isotopes up to ^{28}C. When the system is bound, the pair energies that contribute to the ground state occur in complex conjugate pairs, thus preserving the real nature of the ground state energy. Once the system becomes unbound this ceases to be the case. Now the pair energies that contribute to the ground state do not occur in complex conjugate pairs, explaining how a width arises in the energy of an unbound system within the Richardson approach.

The hyperbolic model

The hyperbolic family of models did not find a physical realization until very recently when it was shown that they could model a p-wave pairing Hamiltonian in a 2-dimensional lattice [26], such that it was possible to study with the exact solution an exotic phase diagram having a non-trivial topological phase and a third-order quantum phase transition [27]. Immediately thereafter, it was shown that the hyperbolic family gives rise to a separable pairing Hamiltonian with 2 free parameters that can be adjusted to reproduce the properties of heavy nuclei as described by a Gogny HFB treatment [28]. Both applications are based on a simple linear combination of hyperbolic integrals which give rise to the separable pairing Hamiltonian

$$H = \sum_i \eta_i K_i^0 - G \sum_{i,i'} \sqrt{\eta_i \eta_{i'}} K_i^+ K_{i'}^- . \tag{9.36}$$

If we interpret the parameters η_i as single-particle energies corresponding to a nuclear mean-field potential, the pairing interaction has the unphysical behavior of increasing in strength with energy. In order to reverse this unwanted effect, we define $\eta_i = 2(\varepsilon_i - \alpha)$, where the free parameter α plays the role of an energy cutoff and ε_i is the single-particle energy of the mean-field level i. Making use of the pair

representation of $SU(2)$, the exactly-solvable pairing Hamiltonian (9.36) takes the form

$$H = \sum_i \varepsilon_i \left(c_i^\dagger c_i + c_{\bar{i}}^\dagger c_{\bar{i}} \right) - 2G \sum_{ii'} \sqrt{(\alpha - \varepsilon_i)(\alpha - \varepsilon_{i'})}\; c_i^\dagger c_{\bar{i}}^\dagger c_{\bar{i}'} c_{i'}, \tag{9.37}$$

with eigenvalues $E = 2\alpha M + \sum_i \varepsilon_i \nu_i + \sum_\beta E_\beta$. The pair energies E_β correspond to a solution of the set of non-linear Richardson equations

$$\frac{1}{2} \sum_i \frac{1}{\eta_i - E_\beta} - \sum_{\beta'(\neq\beta)} \frac{1}{E_{\beta'} - E_\beta} = \frac{Q}{E_\beta}\ , \tag{9.38}$$

where $Q = \frac{1}{2G} - \frac{L}{2} + M - 1$. Each particular solution of Eq. (9.38) defines a unique eigenstate.

Due to the separable character of the hyperbolic Hamiltonian, in BCS approximation the gaps $\Delta_i = 2G\sqrt{\alpha - \varepsilon_i} \sum_{i'} \sqrt{\alpha - \varepsilon_{i'}} u_{i'} v_{i'} = \Delta\sqrt{\alpha - \varepsilon_i}$ and the pairing tensor $u_i v_i = \frac{\Delta\sqrt{\alpha-\varepsilon_i}}{2\sqrt{(\varepsilon_i-\mu)^2+(\alpha-\varepsilon_i)\Delta^2}}$ have a very restricted form. In order to test the validity of the exactly solvable Hamiltonian (9.37) we take the single-particle energies ε_i from the HF energies of a Gogny HFB calculation and we fit the parameters α and G to the gaps and pairing tensor in the HF basis. Figure **??** shows the comparison for protons in ^{238}U between the Gogny HFB results in the HF basis and the BCS approximation of the hyperbolic model. From these results we extracted the values $\alpha = 25.25\ MeV$ and $G = 2 \times 10^{-3} MeV$. The valence space determined by the cutoff α corresponds to 148 levels with 46 proton pairs. The size of the Hamiltonian in this space is 4.83×10^{38}, well beyond the limits of exact diagonalization. However, the integrability of the hyperbolic model provides an exact solution by solving a set of 46 non-linear coupled equations. Moreover, the exact solution shows a gain in correlation of more than 2 MeV suggesting the importance of taking into account correlations beyond mean-field.

Up to now, we have restricted our discussion to RG models that are based on the compact rank-1 $SU(2)$ pair algebra. The method of constructing RG models can be extended to the non-compact rank-1 $SU(1,1)$ algebra as well, whereby pairing in bosonic systems[29] is described in complete analogy with the $SU(2)$ case. An early application to the $SO(6)$ to $U(5)$ line of integrability of the Interacting Boson Model (IBM) was reported in ref. [30], with the exact solution being obtained there directly using an infinite dimensional algebraic technique. Further work on the IBM using the integrable $SU(1,1)$ RG model[31] including high-spin bosons (d, g, $\cdots$) revealed a particular feature of the repulsive boson pairing interaction that seems to provide a new mechanism for the enhancement of $s-d$ dominance, giving further support for the validity of the $s-d$ Interacting Boson Model.

The RG models are not constrained to rank-1 algebras. They can be extended to any semi-simple Lie algebra [32]. Richardson himself studied some restricted solutions of the T=1 pairing model [33] and the T=0,1 pairing model [34]. As a general statement, the reduced pairing Hamiltonian is exactly solvable for any multi-component system. The first step in finding an exact solution is to identify the Lie algebra of the commuting pair operators and then to specialize the general solution given in [32]. One has to keep in mind that while the $SU(2)$ RG model has a single set of unknown parameters, the pair energies, larger rank algebras have as many sets of unknown parameters as the rank of the algebra. Therefore, the higher the rank of the algebra, the greater is the complexity of the solution. Several pairing Hamiltonians with relevance to nuclear physics have been studied in the last few years.

i. The rank-2 $SO(5)$ RG model[35] describes T=1 proton-neutron pairing with non-degenerate single particle levels. The exact solution has two sets of spectral parameters, the pair energies and a second set associated with the $SU(2)$ isospin subalgebra. In spite of the greater complexity, it was possible to solve exactly a T=1 pairing Hamiltonian for the nucleus ^{64}Ge using a ^{40}Ca core, with a Hilbert space dimension well beyond the limits of exact diagonalization.

ii. The rank-3 $SO(6)$ RG model [36] describes color pairing, *i. e.* pairing between three-component fermions. The exact Richardson equations have three sets of spectral parameters, of which one correspond the the pair energies and the other two are responsible for the different couplings within the $SU(3)$ color subalgebra. The model has been used to study the phase diagram of polarized three-component fermion atomic gases. However, it could in principle be exploited to describe non-relativistic quark systems.

iii. With increasing complexity, the rank-4 $SO(8)$ RG model [37] describes either T=0,1 proton-neutron pairing or four-component fermion gases. It contains four sets of spectral parameters. The model has been used to study alpha-like structures represented by clusters in the parameter space, and how these clusters dissolve into like-particle pairs with increasing isospin.

iv. The rank-2 non-compact $SO(3,2)$ algebra generalizes the bosonic RG models to systems of interacting proton and neutron bosons[38]. The model describes the IBM2 in the line of integrability between

vibrational and γ-soft nuclei. The exact solution has been employed to study the influence of high-spin f and g bosons in the low-energy spectrum

A key feature of the Richardson-Gaudin integrable models, is that they transform the diagonalization of the hamiltonian matrix, whose dimension grows exponentially with the size of the system, to the solution of a set of M coupled non-linear equations where M is the number of pairs. This makes it possible to treat problems that could otherwise not be treated and in doing so to obtain information that is otherwise inaccessible. For example, we reported an application of the rational RG pairing model to the even-mass Sm isotopes, where the size of the Hilbert space would exceed 10^{53} states, and an application of the hyperbolic RG pairing model to U^{238}, where the size of the Hilbert space would exceed 10^{38} states. In both cases, substantial gains in correlation energy were found when the problem was treated exactly.

The exactly solvable RG Hamiltonians also provide excellent benchmarks for testing approximations beyond HFB in realistic situations both for even-even and odd-mass nuclei. Moreover, a self-consistent HF plus exact pairing approach could in principle be implemented to describe large regions of the table of nuclides. It might be possible to extend such a self-consistent approach to the O(5) RG model, providing in this way a better description of those nuclei with $N \sim Z$ in which T=1 proton-neutron pairing correlations are expected to play a significant role. Unfortunately, the SO(8) T=0,1 RG model cannot accommodate the spin-orbit splitting in the single-particle energies. Nevertheless, this model could play an important role in helping to understand quartet clusterization and quartet condensation in nuclear and cold atom systems. Finally, extension of the RG models to include the effects of the continuum seems to be an especially promising avenue to explore the physics of weakly-bound nuclei.

9.5 Homework problems

Exercise 1: Evaluate the experimental pairing gaps in Ca isotopes based on Eq. (9.1) and compare them with the predictions of the seniority model, Eq. (9.13).

Bibliography

[1] L. N. Cooper, Bound Electron Pairs in a Degenerate Fermi Gas, *Phys. Rev.* **104**, 1189–1190, (1956).

[2] J. Bardeen, L. N. Cooper, and J. R. Schrieffer, Theory of Superconductivity, *Phys. Rev.* **108**, 1175–1204, (1957).

[3] A. Bohr, B. R. Mottelson, and D. Pines, Possible Analogy between the Excitation Spectra of Nuclei and those of the Superconducting Metallic State, *Phys. Rev.* **110**, 936–938, (1958).

[4] A. K. Kerman, R. D. Lawson, and M. H. Macfarlane, Accuracy of the Superconductivity Approximation for Pairing Forces in Nuclei, *Phys. Rev.* **124**, 162–167, (1961).

[5] K. Dietrich, H. J. Mang, and J. H. Pradal, Conservation of Particle Number in the Nuclear Pairing Model, *Phys. Rev.* **135**, 22–34, (1964).

[6] R. W. Richardson, A Restricted Class of Exact Eigenstates of the Pairing-Force Hamiltonian, *Phys. Lett.* **3**, 277–279, (1963).

[7] R. W. Richardson, Exact Eigenstates of Pairing-Force Hamiltonian, *Nucl. Phys.* **52**, 221–238, (1964).

[8] G. Sierra, J. Dukelsky, G. G. Dussel, J. von Delft, and F. Braun, Exact study of the effect of level statistics in ultrasmall superconducting grains, *Phys. Rev. B* **61**, 11890–11893, (2000).

[9] J. Dukelsky, S. Pittel, and G. Sierra, Exactly solvable Richardson-Gaudin models for many-body quantum systems, *Rev. Mod. Phys.* **76**, 643–662 (2004).

[10] G. Ortiz, R. Somma, J. Dukelsky, and S. Rombouts, Exactly-solvable models derived from a generalized Gaudin algebra, *Nucl. Phys. B* **707**, 421–457 (2005).

[11] J. Dukelsky, C. Esebbag, and P. Schuck, Class of Exactly Solvable Pairing Models, *Phys. Rev. Lett* **87**, 066403 1–4 (2001).

[12] M. Gaudin, Diagonalization of a Class of Spin Hamiltonian, *J. Phys. (Paris)* **37**, 1087–1098 (1976).

[13] M. C. Cambiaggio,A. M. F. Rivas, and M. Saraceno, Integrability of the pairing Hamiltonian, *Nuc. Phys. A* **624**, 157–167 (1997).

[14] R. W. Richardson, Application to the Exact Theory of the Pairing Model to some Even Isotopes of Lead, *Phys. Lett.* **5**, 82–84, (1964).

[15] R. W. Richardson and N. Sherman, Pairing Models of ^{206}Pb, ^{204}Pb and ^{202}Pb, *Nuc. Phys.* **52**, 253–268, (1964).

[16] R. W. Richardson, Numerical Study of 8-32 Particle Eigenstates of Pairing Hamiltonian, *Phys. Rev.* **141**, 949–956, (1966).

[17] J. Bang and J. Krumlinde, Model Calculations with Pairing Forces, *Nucl. Phys. A* **141**, 18–32, (1970).

[18] C. G. Andersson and J. Krumlinde, Oblate High-Spin Isomers, *Nucl. Phys. A* **291**, 21–44, (1977).

[19] G. G. Dussel, S. Pittel, J. Dukelsky, P. Sarriguren, Cooper pairs in atomic nuclei, *Phys. Rev. C* **76** 011302 1–5, (2007).

[20] Similar results has been obtained for a 3D homogeneous diluted Fermi gas in the BCS phase. G. Ortiz and J. Dukelsky, BCS-to-BEC crossover from the exact BCS solution, *Phys. Rev. A* **72** 043611 1–5, (2005).

[21] M. Matsuo, Spatial structure of neutron Cooper pair in low density uniform matter, *Phys. Rev. C* **73** 044309 1–16, (2005); and Matsuo's contribution to this Volume.

[22] J. Dukelsky, C. Esebbag, S. Pittel, Electrostatic mapping of nuclear pairing, *Phys. Rev. Lett.* **88** 062501 1–4, (2002).

[23] M. Hasgawa and K. Kaneko, Effects of resonant single-particle states on pairing correlations, *Phys. Rev. C* **67**, 024304 1–4, (2003).

[24] R. Id Betan, Using continuum level density in the pairing Hamiltonian: BCS and exact solutions, *Nucl. Phys. A* **879** 14–24, (2012).

[25] R. Id Betan, Exact eigenvalues of the pairing Hamiltonian using continuum level density, Nucl-th arxiv:1202.3986 (2012).

[26] M. Ibañez, J. Links, G. Sierra, and S-Y Zhao, Exactly solvable pairing model for superconductors with px+ipy-wave symmetry, *Phys. Rev. B* **79** 180501 1–4, (2009).

[27] S. M. A. Rombouts, J. Dukelsky, and G. Ortiz, Quantum phase diagram of the integrable px+ipy fermionic superfluid, *Phys. Rev. B* **82** 224510 1–4, (2010).

[28] J. Dukelsky, S. Lerma H., L. M. Robledo, R. Rodriguez-Guzman, and S. M. A. Rombouts, Exactly solvable Hamiltonian for heavy nuclei, *Phys. Rev. C* **84** 061301 1–4, (2011).

[29] J. Dukelsky and P. Schuck, Condensate Fragmentation in a New Exactly Solvable Model for Confined Bosons, *Phys. Rev. Lett.* **86**, 4207–4210 (2001).

[30] Feng Pan and J.P. Draayer, New algebraic solutions for SO(6) to U(5) transitional nuclei in the Interacting Boson Model, *Nucl. Phys. A* **636**, 156-168 (1998).

[31] J. Dukelsky and S. Pittel, New Mechanism for the Enhancement of sd Dominance in Interacting Boson Models, *Phys. Rev. Lett.* **86**, 4791–4794 (2001).

[32] M. Asorey, F. Falceto, and G. Sierra, ChernSimons theory and BCS superconductivity, *Nucl. Phys. B* **622**, 593–614, (2002).

[33] R. W. Richardson, Eigenstates of the J=0 T=1 Charge-Independent Pairing Hamiltonian, *Phys. Rev.* **144**, 874–883, (1966).

[34] R. W. Richardson, Eigenstates of the L=0 T=1 Charge- and Spin-Independent Pairing Hamiltonian, *Phys. Rev.* **159**, 792–805, (1967).

[35] J. Dukelsky, V. G. Gueorguiev, P. Van Isacker, S. Dimitrova, B. Errea, and S. Lerma H., Exact Solution of the Isovector Neutron-Proton Pairing Hamiltonian, *Phys. Rev. Lett.* **76**, 072503 1–4, (2006).

[36] B. Errea, J. Dukelsky, and G. Ortiz, Breached pairing in trapped three-color atomic Fermi gases, *Phys. Rev. A.* **79**, 051603 1–4, (2009).

[37] S. Lerma H., B. Errea, J. Dukelsky, and W. Satula, Exact Solution of the Spin-Isospin Proton-Neutron Pairing Hamiltonian, *Phys. Rev. Lett.* **79**, 032501 1–4 (2007).

[38] S. Lerma H., B. Errea, J. Dukelsky, S. Pittel,and P. Van Isacker, Exactly solvable models of proton and neutron interacting bosons, *Phys. Rev. C* **74** 024314 1–7, (2011).

Chapter 10

Electromagnetic Transitions

Electric and magnetic multipoles. Transition probability and selection rules. Weisskopf units. Applications to nuclear spectra. The spin of the photon. $0^+ \to 0^+$ transitions. Internal and pair conversion.

In this Chapter we will study nuclear spectroscopic properties that can be extracted from experiments using electromagnetic probes. We will assume that the nucleus is already excited in some initial state and that it decays to a final state in the same nucleus through electromagnetic radiation by emitting a photon. In nuclear electromagnetic decays the radiation, and the photon itself, is called "gamma". Our aim is to analyze the characteristics of that photon. We will present the most important features of the radiation field which are of interest for us without going into the details that can be found in standard books on electromagnetism.

We thus starts by assuming that the electric field $\mathbf{E}$ and the magnetic field $\mathbf{M}$ in free space obey the Maxwell equations, i. e.

$$\mathbf{E} = -\frac{1}{c}\frac{\partial \mathbf{A}}{\partial t} \tag{10.1}$$

$$\mathbf{M} = \nabla \times \mathbf{A} \tag{10.2}$$

where the vector field $\mathbf{A}$ is required to satisfy,

$$(\frac{\partial^2}{\partial x^2} + \frac{\partial^2}{\partial y^2} + \frac{\partial^2}{\partial z^2} - \frac{1}{c^2}\frac{\partial^2}{\partial t^2})\mathbf{A} = 0 \tag{10.3}$$

with the gauge condition

$$\nabla \cdot \mathbf{A} = 0 \tag{10.4}$$

which shows that the electromagnetic fields are perpendicular to the direction of propagation. In quantum mechanics this can be readily seen by noticing that Eq. (10.4) is the same as $\mathbf{p} \cdot \mathbf{A} = 0$.

A solution of Eq. (10.3) is,

$$\mathbf{f_k}(\mathbf{r}) = q_k e^{-i\omega t}\mathbf{A}_k(\mathbf{r}) \tag{10.5}$$

where q_k is a constant, $k = \omega/c$ and,

$$\nabla \times \nabla \times \mathbf{A}_k - k^2\mathbf{A}_k = 0 \tag{10.6}$$

with the condition $\nabla \cdot \mathbf{A}_k = 0$.

We use $\mathbf{j}(\mathbf{r}, \mathbf{t})$ and $\rho(\mathbf{r}, \mathbf{t})$ to denote the current and charge densities (operators) of the nucleus,

$$\nabla \cdot \mathbf{j}(\mathbf{r}, \mathbf{t}) = -\frac{\partial}{\partial t}\rho(\mathbf{r}, \mathbf{t}) = -\frac{\mathbf{i}}{\hbar}[\mathbf{H}, \rho(\mathbf{r}, \mathbf{t})]. \tag{10.7}$$

One may assume

$$\rho(\mathbf{r}) = \sum_{i=1}^{A} e_i \delta(\mathbf{r} - \mathbf{r_i}). \tag{10.8}$$

10.1 The spin of the photon

We have seen in Chapter 1 that in a system with spherical symmetry the angular momentum is a conserved quantity. We proved this by showing that the rotated wave function, which is a solution of the Hamiltonian due to the spherical symmetry, is generated by applying the angular momentum operator to the original wave function. From here we deduced that the angular momentum commutes with the Hamiltonian. In the case of electromagnetism the field $\mathbf{A}$ which, as we showed above, determines the

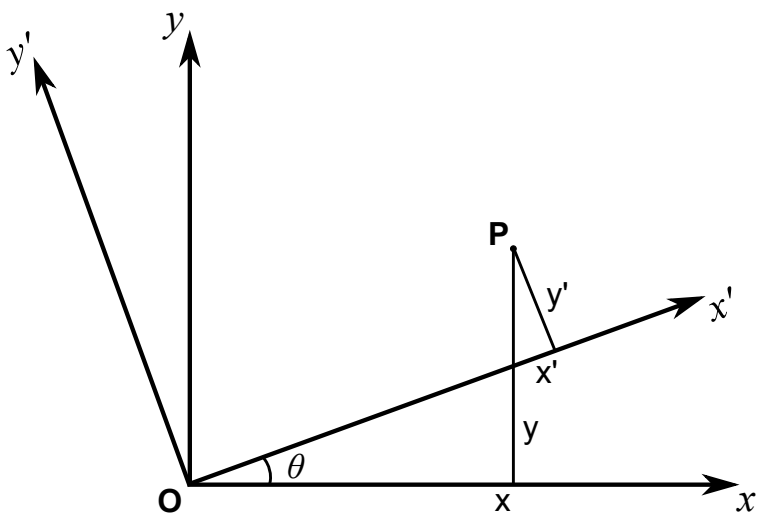

Figure 10.1: Relation between the systems of coordinates related by a rotation θ along the axis $z = z'$.

physical quantities, is a vector and, therefore, its rotation is a bit more complicated than in the scalar case of the wave function.

We will rotate an angle θ along the z-axis. In the original system the coordinates of a point P are $P = (x, y, z)$ while in the rotated system we will use the notation $P = (x', y', z')$. As can be seen from Fig. 10.1, the relation between the two coordinates is,

$$\begin{array}{rcl} x' & = & \cos\theta x + \sin\theta y \\ y' & = & -\sin\theta x + \cos\theta y \\ z' & = & z \end{array} \tag{10.9}$$

In the same fashion the components of the vector $\mathbf{A}$ transform as

$$\begin{array}{rcl} A'_x(x', y', z') & = & \cos\theta A_x(\cos\theta x + \sin\theta y, -\sin\theta x + \cos\theta y, z) \\ & + & \sin\theta A_y(\cos\theta x + \sin\theta y, -\sin\theta x + \cos\theta y, z) \\ A'_y(x', y', z') & = & -\sin\theta A_x(\cos\theta x + \sin\theta y, -\sin\theta x + \cos\theta y, z) \\ & + & \cos\theta A_y(\cos\theta x + \sin\theta y, -\sin\theta x + \cos\theta y, z) \\ A'_z(x', y', z') & = & A_z(\cos\theta x + \sin\theta y, -\sin\theta x + \cos\theta y, z) \end{array} \tag{10.10}$$

performing an infinitesimal rotation it is $\cos\theta \approx 1$, $\sin\theta \approx \theta$ and one gets,

$$A_x(\cos\theta x + \sin\theta y, -\sin\theta x + \cos\theta y, z) \approx A_x(x, y, z) - i\theta L_z A_x \tag{10.11}$$

where the definition of the angular momentum operator, i. e. $L_z = i(y\frac{\partial}{\partial x} - x\frac{\partial}{\partial y})$ was used. Therefore up to order θ it is

$$A'_x(x', y', z') = A_x(x, y, z) - i\theta(L_z A_x + A_y(x, y, z)) \tag{10.12}$$

repeating the same for the components A'_y and A'_z one gets, that

$$\mathbf{A}' = \mathbf{A} - i\theta(L_z + S_z)\mathbf{A} \tag{10.13}$$

where

$$S_z \begin{pmatrix} A_x \\ A_y \\ A_z \end{pmatrix} = \begin{pmatrix} -iA_y \\ iA_x \\ 0 \end{pmatrix} \tag{10.14}$$

It is left as an exercise to show that the eigenvalues of S_z are $-1, 0$ and $+1$. In the same fashion one can define S_x and S_y by rotating along the axis x and y, respectively.

We thus see that the generator of rotations for a vector field is $\mathbf{J} = \mathbf{L} + \mathbf{S}$, where S is the intrinsic spin of the vector field with eigenvector $S = 1$. This implies that the photon carries a spin $S = 1$.

10.2 Electric and magnetic multipoles

The functions (10.5) form a complete set of vectors. Any electromagnetic field can be expressed as a series within this representation. Each one of the components (10.5) corresponds to a quantized photon with energy $E = \hbar\omega$. They are determined by Eq. (10.6), which has two independent solutions. One of them is given by

$$\mathbf{A}^E_{\lambda\mu}(k\mathbf{r}) = \frac{-i}{k}\nabla \times (\mathbf{r} \times \nabla)(j_\lambda(kr)Y_{\lambda\mu}(\theta\phi)) \tag{10.15}$$

where $j_\lambda(kr)$ is a Bessel function and $Y_{\lambda\mu}(\theta\phi)$ is the spherical harmonics eigenfunctions of the angular momentum operator. This solution is called "electric" component of the electromagnetic field. The other solution is,

$$\mathbf{A}^M_{\lambda\mu}(k\mathbf{r}) = (\mathbf{r} \times \nabla)(j_\lambda(kr)Y_{\lambda\mu}(\theta\phi)) \tag{10.16}$$

which is called the "magnetic" component. In both cases the photon carries angular momentum λ with z-projection μ. Therefore they are multipole components, with multipolarity λ, of the electromagnetic field. However, for the case $\lambda = 0$ there is no angular dependence ($Y_{00}(\theta\phi) = 1/\sqrt{4\pi}$) and since for any angle independent function $\phi(r)$ it is $\nabla\phi(r) \propto \mathbf{r}$, the electromagnetic field vanishes ($\mathbf{r} \times \mathbf{r}$=0). In other words, there is no monopole photon in the electromagnetic field.

We have

$$\nabla \times (\mathbf{r} \times \nabla) = -\nabla\frac{\partial}{\partial r}r + \mathbf{r}\nabla^2, \tag{10.17}$$

and

$$\nabla \cdot (\mathbf{r} \times \nabla) = -\nabla \cdot (\nabla \times \mathbf{r}) = -(\nabla \times \nabla) \cdot \mathbf{r} = 0. \tag{10.18}$$

For the parity we have $\pi_\mathcal{O} = (-1)^\lambda$ for Y^λ, $\pi_\mathcal{O} = -1$ for the vectors $\boldsymbol{r}$, $\boldsymbol{\nabla}$ and $\boldsymbol{p}$, and $\pi_\mathcal{O} = +1$ for pseudo vectors $\boldsymbol{l} = \boldsymbol{r} \times \boldsymbol{p}$ and $\boldsymbol{\sigma}$. We have

$$\hat{\pi}L\hat{\pi}^{-1} = \hat{\pi}\mathbf{r} \times (-i\hbar\nabla)\hat{\pi}^{-1} = L, \tag{10.19}$$

$$\hat{\pi}\nabla\hat{\pi}^{-1} = -\nabla, \tag{10.20}$$

and

$$\hat{\pi}\nabla \times \hat{\pi}^{-1} = \hat{\pi}\frac{1}{i\hbar}\hat{S} \cdot \nabla\hat{\pi}^{-1} = -\nabla\times, \tag{10.21}$$

where $\hat{S}$ is the spin operator mentioned above. The presence of the ∇ operator introduce an minus sign under the pairty transformation. Thus the parity of the electromagnetic field is

$$\begin{aligned} &-(-1)^\lambda \quad \text{for electric multipole} \\ &+(-1)^\lambda \quad \text{for magnetic multipole} \end{aligned} \tag{10.22}$$

The two multipoles can be distinguished by the parity and are related to each other. We have

$$\mathbf{A}^E_{\lambda\mu}(k\mathbf{r}) = \frac{1}{k}\nabla \times \mathbf{A}^M_{\lambda\mu}(k\mathbf{r}). \tag{10.23}$$

Integrating over the current density one obtains the electric component as,

$$\mathcal{O}(E\lambda\mu) = \frac{-i(2\lambda+1)!!}{ck^{\lambda+1}(\lambda+1)}\int \mathbf{j}_E(r) \cdot \nabla \times (\mathbf{r} \times \nabla)\big(\mathrm{j}_\lambda(\mathrm{kr})\mathrm{Y}_{\lambda\mu}(\theta\phi)\big)\mathrm{d}\mathbf{r} \tag{10.24}$$

and the magnetic component becomes,

$$\mathcal{O}(M\lambda\mu) = \frac{-(2\lambda+1)!!}{ck^{\lambda}(\lambda+1)}\int \mathbf{j}_M(r) \cdot (\mathbf{r} \times \nabla)\big(\mathrm{j}_\lambda(\mathrm{kr})\mathrm{Y}_{\lambda\mu}(\theta\phi)\big)\mathrm{d}\mathbf{r}, \tag{10.25}$$

where the double factorial is defined as

$$(2\lambda+1)!! = (2\lambda+1)(2\lambda+1-2)(2\lambda+1-3)...3 \cdot 1. \tag{10.26}$$

The electric and magnetic current densities are defined as

$$\mathbf{j}_E(r) = \frac{1}{2}\sum_i e_i[\delta(\mathbf{r}-\mathbf{r}_i)]\frac{\mathbf{p_i}}{M} + \frac{\mathbf{p_i}}{M}\delta(\mathbf{r}-\mathbf{r}_i)], \tag{10.27}$$

and

$$\mathbf{j}_M(r) = \frac{e\hbar}{2M}\sum_i \mu_i \nabla \times \sigma_i[\delta(\mathbf{r}-\mathbf{r}_i)]. \tag{10.28}$$

In nuclear electromagnetic processes it is convenient to take into account the range of the quantities involved. Thus nuclear photo transitions occur at large wavelengths of the photons as compared to the nuclear radius $R = 1.2A^{1/3}fm$. Therefore kR is small (remember that the photon energy is $E = h\nu = hc/\lambda = k\hbar c$ and in nuclear transitions it is $E \approx 1MeV$). One can expand the Bessel function as,

$$j_\lambda(kr) = \frac{(kr)^\lambda}{(2\lambda+1)!!}(1 - \frac{(kr)^2}{2(2\lambda+3)} + ...). \tag{10.29}$$

We can take the first order of this expansion only in the long wave approximation. The electric multipole can be rewritten as

$$\begin{aligned}\mathbf{A}^E_{\lambda\mu}(k\mathbf{r}) &= \frac{i}{k}\left[\nabla\frac{\partial}{\partial r}r(j_\lambda(kr)Y_{\lambda\mu}(\theta\phi)) - \mathbf{r}\nabla^2(j_\lambda(kr)Y_{\lambda\mu}(\theta\phi))\right] \\ &= \frac{i}{k}\left[\nabla\frac{\partial}{\partial r}r(j_\lambda(kr)Y_{\lambda\mu}(\theta\phi)) + k^2\mathbf{r}(j_\lambda(kr)Y_{\lambda\mu}(\theta\phi))\right].\end{aligned} \tag{10.30}$$

The later term can be neglected in the long wave approximation. The multipole components of the field acquire the simple forms,

$$\begin{aligned}\mathcal{O}(E\lambda\mu) &= \int \frac{-1}{\hbar kc}[H,\rho(\mathbf{r})]\mathrm{r}^\lambda \mathrm{Y}_{\lambda\mu}(\theta\phi)\mathrm{d}\mathbf{r} \\ &= \int \rho(\mathbf{r})\mathrm{r}^\lambda \mathrm{Y}_{\lambda\mu}(\theta\phi)\mathrm{d}\mathbf{r}.\end{aligned} \tag{10.31}$$

and

$$\mathcal{O}(M\lambda\mu) = \frac{-1}{c(\lambda+1)}\int \mathbf{j}_M(r)\cdot(\mathbf{r}\times\nabla)\mathrm{r}^\lambda \mathrm{Y}_{\lambda\mu}(\theta\phi)\mathrm{d}\mathbf{r}. \tag{10.32}$$

Selection rules are the results of conservation laws. They express certain symmetry conditions that hold for the system under consideration. For instance, the invariance of a nuclear system as a whole under spatial rotations leads to the conservation of the total angular momentum. When a nucleus emits (absorbs) a photon, the initial (final) total nuclear angular momentum should be equal to the sum of the final (initial) total nuclear angular momentum and the angular momentum carried by the radiation. The selection rules are given by the triangle condition for the angular momenta $\Delta(J_i, J_f, \lambda)$. The electromagnetic interaction conserves parity which depends on the spatial inversion properites of the current densities. The operators for $E\lambda$ and $M\lambda$ can be classified according to their transformation under parity change:

$$P\mathcal{O}P^{-1} = \pi_\mathcal{O}\mathcal{O} \tag{10.33}$$

For a given matrix element we have:

$$\langle\Psi_f|\mathcal{O}|\Psi_i\rangle = \langle\Psi_f|P^{-1}P\mathcal{O}P^{-1}P|\Psi_i\rangle = \pi_i\pi_f\pi_\mathcal{O}\langle\Psi_f|\mathcal{O}|\Psi_i\rangle \tag{10.34}$$

The matrix element will vanish unless $\pi_i\pi_f\pi_\mathcal{O} = +1$. Thus the transitions are divided into two classes, the ones which do not change parity change $\pi_i\pi_f = +1$ which go by the operators with $\pi_\mathcal{O} = +1$:

$$\pi_i\pi_f = +1 \quad \text{for M1, E2, M3, E4...} \tag{10.35}$$

and the ones which do change parity change $\pi_i\pi_f = -1$ which go by the operators with $\pi_\mathcal{O} = -1$:

$$\pi_i\pi_f = -1 \quad \text{for E1, M2, E3, M4...} \tag{10.36}$$

The lowest allowed multipolarity in the decay rate dominates over the next higher one (when more than one is allowed) by several orders of magnitude. The most common types of transitions are electric dipole (E1), magnetic dipole (M1), and electric quadrupole (E2).

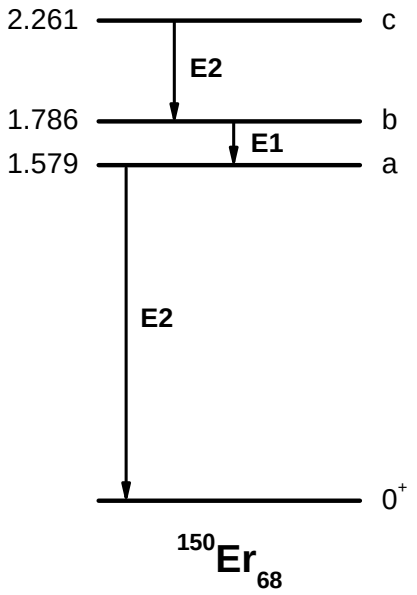

Figure 10.2: The first four levels in the nucleus ^{150}Er with the measured gamma ray transitions. The task is to determine the spins and parities of the levels a, b and c.

10.3 Applications to nuclear spectra

The property that the electromagnetic transitions are strongly dependent upon the angular momentum λ carried by the emitted photon is used to determine the angular momenta of the states involved in the decaying process. From an experimental point of view the first thing that has to be done is to assess the value of λ. This is done by measuring the angular distribution of the emitted radiation, which is determined by the harmonic function $Y_{lm}(\theta\phi)$. One measures also the polarization of the radiation and thus whether the transition is of electric or magnetic character. The energy of the photon, that is of the transition that emits the photon, is just hc/λ. The transition rate per second is obtained by measuring the time that elapses between successive emitted photons, and from this one evaluates the corresponding B-value and the half life, which is $\tau_{1/2} = \ln 2 \; /T(\sigma, \lambda)$.

Once the multipolarities and energies of the possible transitions are known one assigns the angular momenta of the states associated with those transitions following the probabilities given in Eq. (10.41). This procedure can best be clarified by means of an example. We thus show in Fig. (10.2) the first four states of the nucleus ^{150}Er (Z=68) with the corresponding gamma transitions. The ground state is 0^+, as it should be for an even-even nucleus. Since the state labeled a decays to the ground state emitting an E2 photon, the spin J_a and parity π_a of this state should be $J_a^{\pi_a} = 2^+$. The state a is connected to the state b by an E1 transition, which implies that the parity of this state is minus. The angular momentum should be $1 \leq J_b \leq 3$. But it cannot be $J_b = 1^-$ because then it would decay to the ground state, and not to the state a, by an E1 transition (since the large energy of E_b=1.786 MeV contributes with E_b^3 to the transition rate. see Eq. (10.41)). Therefore the state b could be 2^- or 3^-. But in the B-factor, Eq. (10.40) the matrix element is larger for states with aligned angular momenta, which implies that the most likely assignment is $J_b^{\pi_b} = 3^-$. For the same reason it is $J_c^{\pi_c} = 5^-$.

In gamma transitions the emission of a λ=0 photon does not exist, as shown above by analyzing the expression of the monopole component of the electromagnetic field. That was a mathematical proof. But there is also a physical reason why such a photon does not exist, and that is that the intrinsic spin of the photon is one.

10.4 Operators and transition rates

The interaction of the electromagnetic field with the nucleons can be expressed in terms of a sum of electric and magnetic multipole operators with tensor rank λ

$$\mathcal{O} = \sum_{\lambda,\mu} [\mathcal{O}(E\lambda)_\mu + \mathcal{O}(M\lambda)_\mu] \tag{10.37}$$

The transition rate (transition probability) for a specific set of states and a given operator is given by:

$$T_{i,f,\lambda} = \left(\frac{8\pi(\lambda+1)}{\lambda[(2\lambda+1)!!]^2} \right) \frac{k^{2\lambda+1}}{\hbar} B(i \to f) \tag{10.38}$$

where k is the wave-number for the electromagnetic transition of energy E_γ given by:

$$k = \frac{E_\gamma}{\hbar c} = \frac{E_\gamma}{197.33\text{MeV fm}} \tag{10.39}$$

The last factor in Eq. (25.2) is referred to as a "reduced transition probability" B defined by:

$$B(i \to f) = \sum_{\mu M_f} |\langle J_f M_f | \mathcal{O}(\sigma\lambda\mu) | J_i M_i \rangle|^2 = \frac{\left|\langle J_f || \mathcal{O}(\lambda) || J_i \rangle\right|^2}{2J_i + 1} \tag{10.40}$$

This, which is also called "$B(\sigma\lambda)$ value", is a very important quantity because it contains all the nuclear structure information. In particular, only are allowed transitions which satisfy the conservation laws implicit in the matrix element $\langle J_f M_f | \mathcal{O}(\sigma\lambda\mu) | J_i M_i \rangle$. Thus, the $B(\sigma\lambda)$ value vanishes (and the corresponding electromagnetic transition is forbidden) unless the parity condition $\pi_i \pi_f = \pm(-1)^\lambda$ is fulfilled, where π_i (π_f) is the parity of the initial (final) state and the plus (minus) sign corresponds to electric (magnetic) transitions. It should also fulfilled the angular momentum conservation law which, as usual, is expressed by the triangular relation $|J_i - J_f| \leq \lambda \leq J_i + J_f$.

The $B(\sigma\lambda)$-value also provides information on the structure of the initial and final states of the decaying nucleus. Thus if, for instance, $B(E1)$ is very large, as it is for transitions to the ground state from what are called "dipolar giant resonances", then it indicates that the initial state of the nucleus is built upon some uncommon mechanism induced by the nuclear dynamics.

It should be noticed that the unit of $B(E\lambda)$ is $[B(E\lambda)] = e^2 fm^{2\lambda}$ while it is $[B(M\lambda)] = (\mu/c)^2 fm^{2\lambda-2}$, where $\mu = eh/2m_p$ is the nuclear magneton, and m_p is the proton mass. Using these units the transition rate per second becomes, for the most common values of the transfer angular momentum λ,

$$\begin{aligned} T(E1) &= 1.59 \times 10^{15} E^3 B(E1) \\ T(E2) &= 1.22 \times 10^{9} E^5 B(E2) \\ T(E3) &= 5.67 \times 10^{2} E^7 B(E3) \\ T(E4) &= 1.69 \times 10^{-4} E^9 B(E4) \end{aligned} \tag{10.41}$$

$$\begin{aligned} T(M1) &= 1.76 \times 10^{13} E^3 B(M1) \\ T(M2) &= 1.35 \times 10^{7} E^5 B(M2) \\ T(M3) &= 6.28 \times 10^{0} E^7 B(M3) \\ T(M4) &= 1.87 \times 10^{-6} E^9 B(M4) \end{aligned} \tag{10.42}$$

where the energies are in units of MeV.

The lifetime of the transition is given as $1/T_{i,f,\lambda}$ and the partial half-life is defined as

$$t^{if}_{1/2} = \frac{\ln 2}{T_{i,f,\lambda}}. \tag{10.43}$$

The total half-life of a given (initial) state is given as

$$\frac{1}{t_{1/2}} = \sum_f \frac{1}{t^{if}_{1/2}}. \tag{10.44}$$

With our definition of the reduced matrix element,

$$\left|\langle J_f||\mathcal{O}(\lambda)||J_i\rangle\right|^2 = \left|\langle J_i||\mathcal{O}(\lambda)||J_f\rangle\right|^2 \tag{10.45}$$

B depends upon the direction of the transition by the factor of $(2J_i+1)$. For electromagnetic transitions J_i is that for the higher-energy initial state. But in Coulomb excitation the initial usually taken as the ground state, and one can use the notation $B(\uparrow)$ for this situation.

Electric transition operators

The electric transition operators are given by:

$$\mathcal{O}(E\lambda) = r^\lambda Y^\lambda_\mu(\hat{r}) e_{t_z} e \tag{10.46}$$

were $Y^\lambda_\mu$are the spherical harmonics. The e_{t_z} are the electric charges for the proton and neutron in units of e. For the free-nucleon charge we would take $e_p = 1$ and $e_n = 0$, for the proton and neutron, respectively. Although the bare operator acts upon the protons, we will keep the general expression in terms of e_{t_z} in order to incorporate the "effective charges" for the proton and neutron, which represent the center-of-mass corrections and the average effects of the renormalization from wave function admixtures outside the model space.

The most probable types of transitions are E1 and E2 (and M1 below). The E1 transition operator is given with $\lambda = 1$ as

$$\mathcal{O}(E1) = rY^{(1)}_\mu(\hat{r}) e_{t_z} e = \sqrt{\frac{3}{4\pi}} \boldsymbol{r} e_{t_z} e \tag{10.47}$$

The E2 transition operator is given with $\lambda = 2$:

$$\mathcal{O}(E2) = r^2 Y^{(2)}_\mu(\hat{r}) e_{t_z} e \tag{10.48}$$

Magnetic transition operators

The magnetic transition operators are given by:

$$\begin{aligned}\mathcal{O}(M\lambda) =& \left[\boldsymbol{l}\frac{2g^l_{t_z}}{\lambda+1} + \boldsymbol{s}g^s_{t_z}\right] \boldsymbol{\nabla}\left[r^\lambda Y^\lambda_\mu(\hat{r})\right]\mu_N \\ =& \sqrt{\lambda(2\lambda+1)}\left[\left[Y^{\lambda-1}\otimes\boldsymbol{l}\right]^\lambda_\mu \frac{2g^l_{t_z}}{\lambda+1} + \left[Y^{\lambda-1}\otimes\boldsymbol{s}\right]^\lambda_\mu g^s_{t_z}\right] r^{\lambda-1}\mu_N.\end{aligned} \tag{10.49}$$

The M1 transition operator is given as

$$\mathcal{O}(M1) = \sqrt{\frac{3}{4\pi}}\left[\boldsymbol{l}g^l_{t_z} + \boldsymbol{s}g^s_{t_z}\right]\mu_N \tag{10.50}$$

One-body transition operator in the coupled form

As mentioned before, a one-body operator can be written as

$$\mathcal{O}^\lambda_\mu = \sum_{\alpha\beta}\langle\alpha|\mathcal{O}^\lambda_\mu|\beta\rangle a^\dagger_\alpha a_\beta, \tag{10.51}$$

where the Greek letters denote the single-particle states $|nljm\rangle$. We use j to denote the state $|nlj\rangle$. One has,

$$\begin{aligned}\mathcal{O}^\lambda_\mu &= \sum_{j_\alpha j_\beta}\sum_{m_\alpha m_\beta}\langle\alpha|\mathcal{O}^\lambda_\mu|\beta\rangle a^\dagger_\alpha a_\beta \\ &= \sum_{j_\alpha j_\beta}\langle j_\alpha||\mathcal{O}^\lambda_\mu||j_\beta\rangle \sum_{m_\alpha m_\beta}(-1)^{j_\alpha - m_\alpha}\begin{pmatrix} j_\alpha & \lambda & j_\beta \\ -m_\alpha & \mu & m_\beta\end{pmatrix} a^\dagger_\alpha a_\beta \\ &= \sum_{j_\alpha j_\beta}\langle j_\alpha||\mathcal{O}^\lambda_\mu||j_\beta\rangle \frac{[a^\dagger_\alpha\otimes\tilde{a}_\beta]^\lambda_\mu}{\sqrt{2\lambda+1}},\end{aligned} \tag{10.52}$$

where $\tilde{a}_{jm} = (-1)^{j+m} a_{j,-m}$. For the one-body transition density we have

$$\langle j_f m_f | [a^\dagger_\alpha \otimes \tilde{a}_\beta]^\lambda_\mu | j_i m_i \rangle = \delta_{\alpha f}\delta_{\beta i}(-1)^{j_i - m_i} < j_f m_f j_i - m_i | \lambda\mu > . \tag{10.53}$$

The reduced single-particle matrix element for $E\lambda$ operator is given by:

$$\begin{aligned}\langle j_a || \mathcal{O}(E\lambda) || j_b \rangle =& (-1)^{j_a+1/2} \frac{1+(-1)^{l_a+\lambda+l_b}}{2} \sqrt{\frac{(2j_a+1)(2\lambda+1)(2j_b+1)}{4\pi}} \\ & \times \begin{pmatrix} j_a & \lambda & j_b \\ 1/2 & 0 & -1/2 \end{pmatrix} \langle j_a | r^\lambda | j_b \rangle e_{t_z} e\end{aligned} \tag{10.54}$$

The reduced single-particle matrix element for the spin part of the magnetic operator is:

$$\begin{aligned}\langle j_a || \mathcal{O}(M\lambda, s) || j_b \rangle =& \sqrt{\lambda(2\lambda+1)} \langle j_a || \left[Y^{\lambda-1} \otimes \boldsymbol{s} \right]^\lambda || j_b \rangle \langle j_a | r^{\lambda_1} | j_b \rangle g^s_{t_z} \mu_N \\ =& \sqrt{\lambda(2\lambda+1)} \sqrt{(2j_a+1)(2j_a+1)(2\lambda+1)} \begin{Bmatrix} l_a & 1/2 & j_a \\ l_b & 1/2 & j_b \\ \lambda-1 & 1 & \lambda \end{Bmatrix} \\ & \times \langle l_a || Y^{\lambda-1} || l_b \rangle \langle s || \boldsymbol{s} || s \rangle \langle j_a | r^{\lambda-1} | j_b \rangle g^s_{t_z} \mu_N\end{aligned} \tag{10.55}$$

where

$$\langle s || \boldsymbol{s} || s \rangle = \sqrt{3/2} \tag{10.56}$$

The reduced single-particle matrix element for the orbital part of the magnetic operator is:

$$\begin{aligned}\langle j_a || \mathcal{O}(M\lambda, l) || j_b \rangle =& \frac{\sqrt{\lambda(2\lambda+1)}}{\lambda+1} \langle j_a || \left[Y^{\lambda-1} \otimes \boldsymbol{l} \right]^\lambda || j_b \rangle \langle j_a | r^{\lambda-1} | j_b \rangle g^l_{t_z} \mu_N \\ =& \frac{\sqrt{\lambda(2\lambda+1)}}{\lambda+1} (-1)^{l_a+1/2+j_b+\lambda} \sqrt{(2j_a+1)(2j_a+1)} \\ & \times \begin{Bmatrix} l_a & l_b & \lambda \\ j_b & j_a & 1/2 \end{Bmatrix} \langle l_a || \left[Y^{\lambda-1} \otimes \boldsymbol{l} \right]^\lambda || l_b \rangle \langle j_a | r^{\lambda-1} | j_b \rangle g^l_{t_z} \mu_N\end{aligned} \tag{10.57}$$

where

$$\begin{aligned}\langle l_a || \left[Y^{\lambda-1} \otimes \boldsymbol{l} \right]^\lambda || l_b \rangle =& (-1)^{\lambda+l_a+l_b} \sqrt{(2\lambda+1) l_b (l_b+1)(2l_b+1)} \\ & \times \begin{Bmatrix} \lambda-1 & 1 & \lambda \\ l_b & l_a & l_b \end{Bmatrix} \langle l_a || Y^{\lambda-1} || l_b \rangle\end{aligned} \tag{10.58}$$

with

$$\langle l_a || Y^{\lambda-1} || l_b \rangle = (-1)^{l_a} \sqrt{\frac{(2l_a+1)(2l_b+1)(2\lambda-1)}{4\pi}} \begin{pmatrix} l_a & \lambda-1 & l_b \\ 0 & 0 & 0 \end{pmatrix} \tag{10.59}$$

For the M1 operator the radial matrix element is:

$$\langle j_a | r^0 | j_b \rangle = \delta_{n_a, n_b} \tag{10.60}$$

and the reduced single-particle matrix element simplify to:

$$\begin{aligned}\langle j_a || \mathcal{O}(M1, s) || j_b \rangle =& \sqrt{\frac{3}{4\pi}} \langle j_a || \boldsymbol{s} || j_b \rangle \delta_{n_a, n_b} g^s_{t_z} \mu_N \\ =& \sqrt{\frac{3}{4\pi}} (-1)^{l_a+j_a+3/2} \sqrt{(2j_a+1)(2j_b+1)} \\ & \times \begin{Bmatrix} 1/2 & 1/2 & 1 \\ j_b & j_a & l_a \end{Bmatrix} \langle s || \boldsymbol{s} || s \rangle \delta_{l_a, l_b} \delta_{n_a, n_b} g^s_{t_z} \mu_N\end{aligned} \tag{10.61}$$

and

$$\begin{aligned}\langle j_a || \mathcal{O}(M1, l) || j_b \rangle =& \sqrt{\frac{3}{4\pi}} \langle j_a || \boldsymbol{l} || j_b \rangle \delta_{n_a, n_b} g^l_{t_z} \mu_N \\ =& \sqrt{\frac{3}{4\pi}} (-1)^{l_a+j_b+3/2} \sqrt{(2j_a+1)(2j_b+1)} \\ & \times \begin{Bmatrix} l_a & l_b & 1 \\ j_b & j_a & 1/2 \end{Bmatrix} \langle l_a || \boldsymbol{l} || l_b \rangle \delta_{n_a, n_b} g^l_{t_z} \mu_N\end{aligned} \tag{10.62}$$

where

$$\langle l_a||\boldsymbol{l}||l_b\rangle = \delta_{l_a,l_b}\sqrt{l_a(l_a+1)(2l_a+1)} \tag{10.63}$$

Thus the M1 operator can connect only a very limited set of orbits, namely those which have the same n and l values.

We also have

$$\langle j_a||\boldsymbol{j}||j_b\rangle = \delta_{a,b}\sqrt{j_a(j_a+1)(2j_a+1)}, \tag{10.64}$$

and

$$\langle s||\boldsymbol{s}||s\rangle = \sqrt{s(s+1)(2s+1)}. \tag{10.65}$$

Moments in terms of electromagnetic operators

There are two type of electromagnetic moments: the electric moments associated with the static distribution of charge and the magnetic moments associated with the magnetic currents. The parity conservation requires λ=even for the static moments and λ=odd for the magnetic moments. The electromagnetic moment for λ=0 simply counts the number of particles with charge e_k.

A compilation of experimental magnetic and quadrupole moments

http://www.nndc.bnl.gov/publications/preprints/nuclear-moments.pdf

The operator for electromagnetic moment can be expressed in terms of the electromagnetic transition operators. By the parity selection rule, the moments are nonzero only for M1, E2, M3., E4,.... The most common are:

$$\begin{aligned}\mu =& \sqrt{\frac{4\pi}{3}}\langle J, M=J|\mathcal{O}(M1)|J, M=J\rangle \\ =& \sqrt{\frac{4\pi}{3}}\begin{pmatrix} J & 1 & J \\ -J & 0 & J\end{pmatrix}\langle J||\mathcal{O}(M1)||J\rangle\end{aligned} \tag{10.66}$$

and

$$\begin{aligned}Q =& \sqrt{\frac{16\pi}{5}}\langle J, M=J|\mathcal{O}(E2)|J, M=J\rangle \\ =& \sqrt{\frac{16\pi}{5}}\begin{pmatrix} J & 2 & J \\ -J & 0 & J\end{pmatrix}\langle J||\mathcal{O}(E2)||J\rangle\end{aligned} \tag{10.67}$$

10.5 Nuclear matrix elements

The matrix element of a one-body operator can be written as

$$\langle J_f M_f|\mathcal{O}(\lambda\mu)|J_i M_i\rangle = \sum_{\alpha\beta}\langle\alpha|\mathcal{O}(\lambda\mu)|\beta\rangle\langle J_f M_f|c^\dagger_\alpha c_\beta|J_i M_i\rangle \tag{10.68}$$

Electromagnetic transitions and moments (and beta decays) depend upon the reduced nuclear matrix elements $\langle f||\mathcal{O}(\lambda)||i\rangle$. These can be expressed as a sum over reduced one-body transition densities times single-particle matrix elements:

$$\langle f||\mathcal{O}(\lambda)||i\rangle = \sum_{j_\alpha j_\beta}\mathcal{T}(j_\alpha j_\beta\lambda)\langle j_\alpha||\mathcal{O}(\lambda)||j_\beta\rangle \tag{10.69}$$

where the reduced one-body transition density is given by

$$\mathcal{T}(j_\alpha j_\beta\lambda) = \frac{\langle f||\left[\alpha^\dagger_{j_\alpha}\otimes\tilde{\alpha}_{j_\beta}\right]^\lambda||i\rangle}{\sqrt{2\lambda+1}} \tag{10.70}$$

The labels i and f are a short-hand notation for the initial and final state quantum numbers. Thus the problem is divided into two parts, one involving the nuclear structure dependent reduced one-body transition density, and the other involving the reduced single-particle matrix elements.

For a closed shell plus one particle the only term contributing to the sum comes from the transition between two specific particle states as

$$\langle j_f||\left[\alpha^\dagger_{j_\alpha}\otimes\tilde{\alpha}_{j_\beta}\right]^\lambda||j_i\rangle=\delta_{\alpha f}\delta_{\beta i}\sqrt{2\lambda+1}, \tag{10.71}$$

and

$$\langle J_f=j_f||\mathcal{O}(\lambda)||J_i=j_i\rangle=\langle j_f||\mathcal{O}(\lambda)||j_i\rangle. \tag{10.72}$$

The reduced transition probability for this cases is:

$$B(\lambda)=\frac{\left|\langle j_f||\mathcal{O}(\lambda)||j_i\rangle\right|^2}{2j_i+1} \tag{10.73}$$

Single-j configurations

For a closed shell plus n particles in an orbital j the matrix elements reduce to:

$$\langle j^n,\alpha_f,J_f||\mathcal{O}(\lambda)||j^n,\alpha_i,J_i\rangle=\mathcal{T}(j\lambda)\langle j||\mathcal{O}(\lambda)||j\rangle \tag{10.74}$$

$$\begin{aligned}\mathcal{T}(j\lambda)=&n\sqrt{(2J_f+1)(2J_i+1)}\sum_{\alpha J}(-1)^{J_f+\lambda+J+j}\\&\times\left\{\begin{array}{ccc}J_i&J_f&\lambda\\j&j&J\end{array}\right\}[j^{n-1}(\alpha J)jJ_f|\}j^n\alpha_fJ_f][j^{n-1}(\alpha J)jJ_i|\}j^n\alpha_iJ_i],\end{aligned} \tag{10.75}$$

where the square brackets denote the one-particle coecients of fractional parentage (cfp's).

For $n=2$, the cfp's are unity and the sum only contains $J=j$ in which case we have

$$\mathcal{T}(j\lambda)=(-1)^{J_f+\lambda+1}n\sqrt{(2J_f+1)(2J_i+1)}\left\{\begin{array}{ccc}J_i&J_f&\lambda\\j&j&j\end{array}\right\} \tag{10.76}$$

The reduced transition rate becomes:

$$\begin{aligned}B(\lambda)=&n^2(2J_f+1)\left\{\begin{array}{ccc}J_i&j_f&\lambda\\j&j&j\end{array}\right\}^2\left|\langle j||\mathcal{O}(\lambda)||j\rangle\right|^2\\=&n^2(2J_f+1)(2j+1)\left\{\begin{array}{ccc}J_i&j_f&\lambda\\j&j&j\end{array}\right\}^2\frac{\left|\langle j||\mathcal{O}(\lambda)||j\rangle\right|^2}{2j+1}.\end{aligned} \tag{10.77}$$

$0^+\to0^+$ transitions. Internal and pair conversion

The physical reason why there is no electromagnetic decay with the photon carrying angular momentum $\lambda=0$ is that the spin of the photon is unity. In general this implies that the decay proceeds through other angular momenta. For instance if both the initial and final states have angular momenta J, then it should be, since $\lambda=0$ is not allowed, $1\leq\lambda\leq2J$. However, if $J=0$ then the electromagnetic decay is not possible. In this case there are two different mechanism which can induce the decay.

Assuming that the decay proceeds from an excited state 0^+_2 to a lower state 0^+_1, one of the mechanisms of decay is called "internal conversion". In this the nucleus transfers energy from the state 0^+_2 and decays to the state 0^+_1. This energy is absorbed by the electrons that surrounds the nucleus. The most affected of those electrons are the ones which are closer to the nucleus, that is the ones that move in $l=0$ orbits, and of these the closest to the nucleus are the ones with lowest energy, i. e. the ones called "K electrons". The internal electron thus affected converts the energy transferred from the nucleus (therefore the name "internal conversion") into kinetic energy and escapes the atom as a free electron. The nucleus performs the transition $0^+_2\to0^+_1$.

The second mechanism by which the nucleus performs that transition requires that the energy between the states 0^+_2 and 0^+_1 is larger than twice the electron mass $m_e=0.511$ MeV, i. e. larger than 1.022 MeV. If this happens then there is enough energy to create an electron-positron pair. Any energy in excess of $2m_e$ is transformed in kinetic energy which is shared by the electron-positron pair. Therefore this form of decay is called "pair conversion".

10.6 Weisskopf units

One sees that the decay rates (10.41) are very much dependent upon the multipolarity of the emitted photon, decreasing as λ increases. This property is only determined by the electromagnetic field since the nuclear dynamics is contained in the B-values. As mentioned above, this quantity depends upon the structure of the nucleus. A rough estimation for the most simple case, that is the one corresponding to the decay from a single-particle state j_i to a final one j_f, is obtained by using Eqs. (10.31) and (10.32). For this one assumes first that the radial wave functions are constant inside the nuclear radius and vanish outside it. Second the angular part of the matrix element is evaluated assuming that the transition occurs from the state $J_i = \lambda + 1/2$ to the state $j_f = 1/2$. And third in the magnetic case (10.32) appears the quantity $F = \lambda^2(g_s - 2(\lambda+1)^{-1}g_l)^2$, where g_l and g_s are the g-factors of Chapter 2. This quantity is assumed to have the value F=10. With these approximations the B-values become,

$$B_W(E\lambda) = \frac{1.2^{2\lambda}}{4\pi}(\frac{3}{\lambda+3})^2 A^{2\lambda/3} e^2 fm^{2\lambda}, \tag{10.78}$$

and

$$B_W(M\lambda) = \frac{10}{\pi} 1.2^{2\lambda-2}(\frac{3}{\lambda+3})^2 A^{(2\lambda-2)/3} \frac{e\hbar}{2Mc} fm^{2\lambda-2}. \tag{10.79}$$

For instance we have

$$B_W(M1) = 1.790\frac{e\hbar}{2Mc}. \tag{10.80}$$

These values allow one to estimate whether the transition probabilities are strongly dependent upon λ even when the influence of the nuclear structure contained in the B-values are taken into account. For this we evaluate the ratio $R = B_W(\sigma,\lambda)/B_W(\sigma,\lambda+1)$, which turns out to be independent of σ, i. e. it is the same for electric or magnetic components.

$$R = \frac{B_W(\sigma,\lambda)}{B_W(\sigma,\lambda+1)} = \frac{1}{1.44A^{2/3}}(\frac{\lambda+4}{\lambda+3})^2 \tag{10.81}$$

which for a light nucleus with $A = 20$ is $R \approx 0.1((\lambda+3)/(\lambda+4))^2$ while for $A = 200$ $R \approx 0.02((\lambda+3)/(\lambda+4))^2$. These numbers do not affect the conclusion that the transition probabilities (10.41) are strongly dependent upon λ. Therefore a nucleus in an initial state with a given angular momentum J_i will decay most probably by emitting a photon carrying the minimum angular momentum λ allowed by the selection rules.

The importance of the Weisskopf units, Eqs. (10.78) and (10.79), is that they allow one to estimate the strength of the B-values. In a transition where only one state takes part, then the B-value should be ≈ 1 Weisskopf unit. This will be the case of a particle moving outside a double magic core. But, as we saw in the last Chapter, a nuclear excited state can consist of many configurations, and therefore many single-particle states can contribute to the B-value. If these contributions occur all with the same phase then the B-value will become very large in Weisskopf units. Since in this case the single-particle states add collectively to the B-value and, therefore, to the transition probability, the decaying state is called "collective state". A typical collective state is the giant dipole resonance mentioned above, for which the B(E1)-value for the decay to the ground state can be greater than 100 Weisskopf units.

In some cases the reduced transition probability B(Eλ) is expressed in the unit of e$^\lambda$barn$^\lambda$. We have 1barn=100fm^2 and e$^\lambda$barn$^\lambda$=10$^{2\lambda}$e$^\lambda$fm$^{2\lambda}$. For instance we have

$$B_W(E1) = 6.446 * 10^{-4} A^{2/3} e * barn = 6.446 * 10^{-2} A^{2/3} e * fm, \tag{10.82}$$

and

$$B_W(E2) = 5.940 * 10^{-6} A^{4/3} e^2 barn^2 = 5.940 * 10^{-2} A^{4/3} e^2 fm^2. \tag{10.83}$$

10.7 Deuteron Structure

The deuteron is the only bound state of 2 nucleons, with isospin $T = 0$, spin-parity $J^\pi = 1^+$, and binding energy $E_B = 2.225$MeV. For two spin 1/2 nucleons, only total spins $S = 0, 1$ are allowed. Then the orbital angular momentum is restricted to $J - 1 < l < J + 1$, i.e., $l = 0, 1$ or 2. Since the parity is $\pi = (-)^l = +$, only $l = 0$ and $l = 2$ are allowed; this also implies that we have $S = 1$.

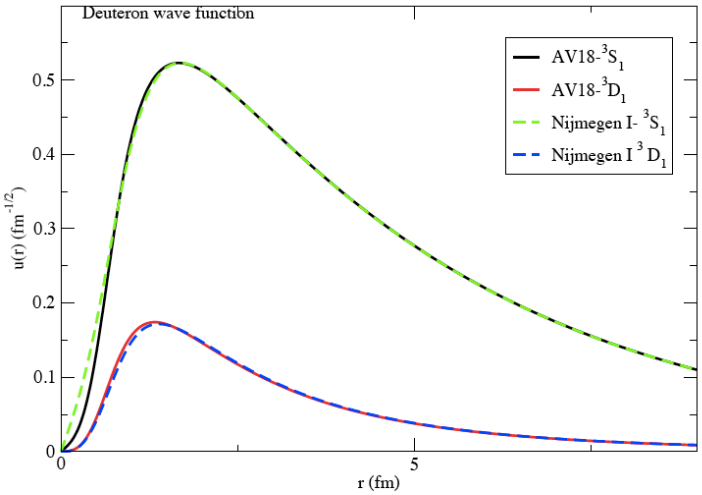

Figure 10.3: Radial wave functions $R_0(r)$ and $R_2(r)$ calculated from realistic NN interactions.

If the Hamiltonian is

$$H = -\frac{\hbar^2}{M}\frac{1}{r}\frac{\mathrm{d}^2}{\mathrm{d}r^2}r + \frac{\hbar^2}{M}\frac{L^2}{r^2} + V_C(r) + V_T(r)S_{12} \tag{10.84}$$

using the following relation,

$$S_{12}\mathcal{Y}^M_{001} = \sqrt{8}\mathcal{Y}^M_{211}; \quad S_{12}\mathcal{Y}^M_{211} = \sqrt{8}\mathcal{Y}^M_{011} - 2\mathcal{Y}^M_{211}; \quad L^2\mathcal{Y}^M_{011} = 0; \quad \boldsymbol{L}^2\mathcal{Y}^M_{211} = 6\mathcal{Y}^M_{211} \tag{10.85}$$

we find the radial equations

$$\begin{aligned}\left[\frac{\hbar^2}{M}\frac{\mathrm{d}^2}{\mathrm{d}r^2} + E - V_c(r)\right]u_S &= \sqrt{8}V_T(r)u_D \\ \left[\frac{\hbar^2}{M}\left(\frac{\mathrm{d}^2}{\mathrm{d}r^2} - \frac{6}{r^2}\right) + E + 2V_T(r) - V_c(r)\right]u_D &= \sqrt{8}V_T(r)u_S\end{aligned} \tag{10.86}$$

These equations can be solved numerically.

Other important information on the structure of the deuteron comes from the values of the magnetic moment μ and quadrupole moment Q:

$$\mu = 0.8574\mu_N; \quad Q = 0.2857e\ \mathrm{fm}^2 \tag{10.87}$$

Since $Q \neq 0$, the deuteron cannot be pure $l = 0$. But generally $l = 0$ is energetically favored for a central potential. Therefore, we write the deuteron wave function as a linear combination of S- and D- waves

$$\begin{aligned}\psi(\boldsymbol{r}) &= a\psi_{^3S_1}(\boldsymbol{r}) + b\psi_{^3D_1}(\boldsymbol{r}) \\ &= aR_0(r)\mathcal{Y}^1_{011} + bR_2(r)\mathcal{Y}^1_{211}\end{aligned} \tag{10.88}$$

where a and b are constants with $\sqrt{a^2+b^2} = 1$. R_0 and R_2 are the radial wave functions.

$$\mathcal{Y}^1_{011} = Y_{00}\chi_{00} \tag{10.89}$$

$$\begin{aligned}\mathcal{Y}^1_{211} &= \sum_M \langle 1(1-M)2M|11\rangle Y_{2M}\chi_{1,1-M} \\ &= \sqrt{\frac{1}{10}}Y_{20}\chi_{1,1} - \sqrt{\frac{3}{10}}Y_{21}\chi_{1,0} + \sqrt{\frac{3}{5}}Y_{22}\chi_{1,-1}\end{aligned} \tag{10.90}$$

Magnetic Moment

As mentioned before, the free-nucleon values for the g-factors are $g^l_p = 1$, $g^l_n = 0$, $g^s_p = 5.586$ and $g^s_n = -3.826$. The magnetic moment operator can be rewritten as

$$\mu = \mu_N \sum_i (g_s s_{zi} + g_l l_{zi}) \tag{10.91}$$

where $g_s = 4.706\tau_i + 0.88$, where the first term is isovector, and the second term is isoscalar. $g_l = (\tau_i + 1)/2$. Since the deuteron is an isoscalar particle with $T = 0$, only the isoscalar magnetic moment operator contributes to μ. Then, the above equation becomes,

$$\begin{aligned}\mu &= \mu_N \sum_i (0.88 s_{zi} + \frac{1}{2} l_{zi}) \\ &= \mu_N \sum_{i=1}^{2} \left[0.88 \langle s_i^z \rangle_{M=1} + \frac{1}{2} \langle l_i^z \rangle_{M=1} \right] \\ &= \mu_N \left[0.88 \langle S^z \rangle + \frac{1}{2} \langle L^z \rangle \right]\end{aligned}$$

The matrix element of S_z is calculated to be

$$\begin{aligned}\langle \mathcal{Y}^1_{011} | S_z | \mathcal{Y}^1_{011} \rangle &= 1 \\ \langle \mathcal{Y}^1_{211} | S_z | \mathcal{Y}^1_{011} \rangle &= 0 \\ \langle \mathcal{Y}^1_{211} | S_z | \mathcal{Y}^1_{211} \rangle &= \sum_{M_S} \left| \langle 2(1 - M_S) 1 M_S | 11 \rangle \right|^2 = -1/2 \end{aligned} \tag{10.92}$$

Thus, for pure $l = 0$ or $l = 2$ states we would have the values $\mu = 0.88\mu_N$, $0.31\mu_N$. More generally we obtain the relation

$$\mu = \left[a^2 (0.88) + b^2 (0.31) \right] \mu_0 = (0.88 - 0.57 b^2) \mu_0 \tag{10.93}$$

Therefore, the experimental value $\mu_D = 0.857\mu_N$ implies that $b^2 = 0.04$. However, in more sophisticated treatments one finds that it is quantitatively important to explicitly include the effects of meson exchanges on the magnetic moment. For example, the virtual photon can couple to the pion in flight between the nucleons and convert it to a ρ meson. (These effects are clearly observed in elastic electron deuteron scattering at higher momentum transfers, as discussed below.) Including the effects of these "meson-exchange" currents on the deuteron's magnetic moment yields values of $b^2 = 0.05 \sim 0.07$.

Quadrupole Moment

The quadrupole moment of the deuteron is calculated to be

$$\begin{aligned}Q =& \sqrt{\frac{16\pi}{5}} \int \psi^*_{J=M=1}(\boldsymbol{r}) \left[\sum_{i=1}^{2} e_{t_z} r_i^2 Y_{20}(\hat{r}_i) \right] \psi_{J=M=1}(\boldsymbol{r}) \mathrm{d}^3\boldsymbol{r} \\ =& e \sqrt{\frac{16\pi}{5}} \int \psi^*_{J=M=1}(\boldsymbol{r}) \frac{r^2}{4} Y_{20}(\hat{r}) \psi_{J=M=1}(\boldsymbol{r}) \mathrm{d}^3\boldsymbol{r},\end{aligned} \tag{10.94}$$

where we have used the fact that for each nucleon the distance from the center of mass is only half the distance between them, $r_i = r/2$. Inserting the wave function introduced above, we get

$$\begin{aligned}Q =& e \sqrt{\frac{\pi}{5}} \Bigg\{ |a^2| \int r^2 R_0(r)^2 \mathrm{d}r \int Y^*_{00} Y_{20} Y_{00} \mathrm{d}\Omega + 2Re(ab^*) \int r^2 R_0(r) R_2(r) \mathrm{d}r \\ &\times \sum_M \langle 1(1-M) 2M | 11 \rangle \int Y^*_{00} Y_{20} Y_{2M} \mathrm{d}\Omega \\ &+ |b|^2 \int r^2 R_2^2(r) \mathrm{d}r \times \sum_M \left| \langle 1(1-M) 2M | 11 \rangle \right|^2 \int Y^*_{2M} Y_{20} Y_{2M} \mathrm{d}\Omega \Bigg\}.\end{aligned} \tag{10.95}$$

After evaluating the angular integrals and putting in the CG coefficients, one finds

$$Q = e \left\{ \frac{\sqrt{2}}{10} Re(ab^*) \int dr r^2 R_0(r) R_2(r) - \frac{|b|^2}{20} \int dr r^2 R_2(r)^2 \right\} \tag{10.96}$$

For our purposes, we will use our knowledge that $b = 0.2 \ll 1$ from the magnetic moment analysis and keep only the first term. This will give us an approximate expression that we can set equal to the experimental value $Q_{exp} = 0.286e$ fm^2 to obtain the result

$$Q \simeq e \frac{0.2\sqrt{2}}{10} \int r^4 R_0 R_2 \mathrm{d}r = 0.286e \text{ fm}^2 \tag{10.97}$$

Solving for the unknown radial integral yields

$$\int r^4 R_0 R_2 \mathrm{d}r \simeq 10.1\mathrm{fm}^2 \tag{10.98}$$

for the radial integral. This value seems quite reasonable given that the mean squared charge radius of the deuteron is 4.0 fm^2. [Note: $\langle r_{ch}^2 = \frac{1}{4}\int R_0^2 r^4 \mathrm{d}r\rangle$]

The dominant S-D interference term in the quadrupole moment has $M_S = 1$. So the spins of both the two nucleons are predominantly aligned parallel to $\hat{z}$. Let's simply take $\boldsymbol{\sigma}_1 = \boldsymbol{\sigma}_2 = +\hat{z}$, and then $\boldsymbol{\sigma}_1 \cdot \boldsymbol{\sigma}_2 = +1$. Then we need to consider the relative orientation of $\hat{r}$, and we will focus (see Fig. 10.7.2 on two extreme cases: (a)$\hat{r}||\hat{z}$ and (b)$\hat{r}\perp\hat{z}$.

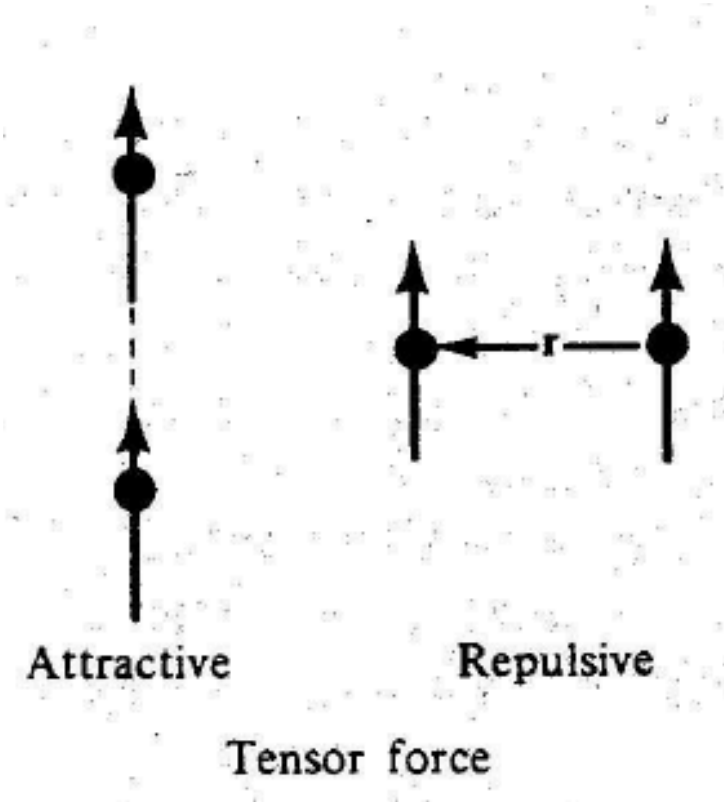

Figure 10.4: Schematic picture of the relative orientation of $\hat{z}$ and $\hat{r}$.

In case (a)$\boldsymbol{\sigma}_1 \cdot \hat{r} = \boldsymbol{\sigma}_2 \cdot \hat{r} = 1$, so we have $S_{12} = +2$ for this geometrical arrangement. This is a prolate configuration so we expect $Q > 0$ for case (a). In case (b) we have $\boldsymbol{\sigma}_1 \cdot \hat{r} = \boldsymbol{\sigma}_2 \cdot \hat{r} = 0$ so $S_{12} = -1$ and the oblate shape relative to the $\hat{z}$ axis would imply $Q < 0$.

Since experimentally $Q > 0$, case (a) must be energetically favored which corresponds to $V_T(r) < 0$. This then gives an attractive force when the configuration is such that $S_{12} > 0$ (case (a)) and a repulsive force when $S_{12} < 0$(case (b)).

One may also read

http://www.nature.com/nature/journal/v144/n3645/abs/144476a0.html

10.8 Homework problems

Exercise 1:

a) Show that the electric component $\mathbf{A}^{E}_{\lambda\mu}(\mathbf{r})$ of the electromagnetic field carries parity $(-1)^{\lambda+1}$ and that for the magnetic component $\mathbf{A}^{M}_{\lambda\mu}(\mathbf{r})$ the parity is $(-1)^{\lambda}$.

b) Which are the parity and triangular conditions that the $B(\sigma\lambda)$-value should fulfilled?

Exercise 2:

The first excited state of the nucleus $^{116}\mathrm{Sn}_{50}$ lies at 1.294 MeV and decays to the ground state by emitting an E2 photon with a half life $\tau_{1/2} = 0.374$ ps (1 ps $=10^{-12}$ sec).

a) Determines the corresponding B(E2)-value in units of e^2fm^4.

b) As a) but in Weisskopf units.

Exercise 3:

a) As Exercise 2 but for the level $^{210}\mathrm{Pb}_{82}(2^+_1)$ lying at 800 keV. It decays by an E2 transition to the ground state with a half live of 17 ps.

b) What conclusion you draw from the differences of the B(E2) values in Weisskopf units for the states $^{116}\mathrm{Sn}(2^+_1)$ and $^{210}\mathrm{Pb}(2^+_1)$?

Exercise 4:

The spectrum of $^{90}\mathrm{Zr}_{40}$ consists of the 0^+ ground state and the excited states 0^+_2 (at 1.761 MeV), 2^+_1 (2.186 MeV), 5^-_1 (2.319 MeV), 4^-_1 (2.739 MeV), 4^+_1 (3.077 MeV), 6^+_1 (3.448 MeV) and 8^+_1 (3.589 MeV).

Determine the most likely decay pattern of the excited states.

Exercise 5:

Show that the photon has intrinsic spin S=1?

Bibliography

[1] P. J. Brussaard and P. W. M. Glaudemans, Shell-model applications in nuclear spectroscopy, North-Holland Pub. Co. (Amsterdam ; New York; Oxford), 1977

[2] B. Alex Brown, Lecture Notes in Nuclear Structure Physics, 2005

Chapter 11

Beta and alpha readioactive decays

Beta decay. Q-values in β^-, β^+ and electron capture decays. Theory of beta decay. Fermi and Gamow-Teller operators. The logaritm of ft. Alpha decay. Thomas expression for the width.

We have seen in the previous Chapter that a nucleus in an excited state can decay to a lower lying state in the same nucleus by emitting a gamma ray. There are other paths which the nucleons in an unstable nucleus can take to eventually reach a more stable configuration. These paths are called "channels". Some of these channels may require that particles other than photons are emitted. In this Chapter we will first study channels in which electrons are emitted. These are called beta decay channels. In the second part we will study channels where alpha particles, i. e. $^4He_2$ nuclei, are emitted. These are called alpha decay channels.

The names of these three forms of radiation, i. e. "alpha", "beta" and "gamma", have an historical origin. The alpha and beta modes of radioactive decay were the first to be discovered. Already in 1896 Becquerel found that charged particles were emitted by uranium, and soon afterwards Marie and Pierre Curie confirmed these observations. In 1899 Rutherford discovered that the radiation could be divided in two separated strings according to the penetration power they had. He called this two forms of radiation "alpha" and "beta". Alpha radiation could penetrate only thin foils of aluminium while beta rays could go through many millimeters of the same material. Only in 1900 the third form of radiation was found, which had even more penetration power than beta rays, and these were called "gamma" rays. It was soon found that the alpha ray was actually an alpha particle, that the beta ray was an e^- electron and that the gamma ray was a photon.

In all these decays the outgoing particle should travel with a kinetic energy which is just the diference between the energies of the initial and final states. However, in 1911 Lise Meitner and Otto Hahn found that the electron emitted in beta decay had a continuum spectrum, thus seemingly violating the energy conservation law. It took a long time before the explanation of this phenomenom was found. It was Pauli who in 1930 proposed that a particle that interacts very weakly with matter (and therefore undetected up to that time) was also emitted together with the electron. This hypothetical particle was called neutrino. The total energy in the beta decay process was thus shared between the electron and the neutrino. Since then the neutrino was measured experimentally and was found to play a crucial role in many branches of physics, particularly in beta decay processes. These are the processes which we will now analyze.

11.1 Introduction to beta decay

The lighest nucleus that decays by beta emission is the free neutron, which undergoes the spontaneous process

$$n \to p + e^- + \bar{\nu} \tag{11.1}$$

with a half life of about 10.3 minutes. In this equation n (p) is a neutron (proton), e^- is an electron and $\bar{\nu}$ is an antineutrino. Antiparticles have the same mass and spin as the corresponding particles, but opposite charge and spin projection. Thus the antiparticle of the electron (e^-) is the positron (e^+). The neutron is heavier than the proton, which explains why it is unstable.

The neutrino ν is a chargeless particle which interacts very weakly with other particles. Therefore the interaction responsible for beta decay is called "weak interaction". One can assess its intensity by comparing the dimensionless strengths of the forces known in Nature. Thus, for the nuclear interaction this strength is approximately 10, for the electromagnetic field it is 1/137, for the weak interaction 10^{-23} and for the gravitational field 10^{-45}.

There are experimental evidences showing that the neutrino has a very small mass, probably less than 1 eV. However, for the purpose of this Course we will assume that the neutrino is massles and, therefore, that it moves at the speed of light at a certain frequency ν and energy $h\nu$.

In all decay processes the total charge is conserved. Therefore the decay of the neutron to a proton requires that an electron e^- is also emitted. This is why the name β^- is used for this decay.

The electron e^- and the antineutrino $\bar{\nu}$ which are emitted are called "leptons". Even the number of leptons is conserved in all decay processes. The application of this law requires that one has to give a value to the lepton number. For convention the electron and the neutrino have lepton number 1, while the positron e^+ and the antineutrino $\bar{\nu}$ have lepton number -1. With this convention in the decay (11.1) the lepton number is zero before as well as after the decay.

The electron and the antineutrino appear always together in beta decay. This pair of leptons form what is called the electronic leptons or the first "lepton generation". There are three lepton generations. Besides the electron and its neutrino, also called electron neutrino and denoted by ν_e, there is the muonic leptons, comprising a particle called muon (μ) and its muon neutrino (ν_μ) and the tauonic leptons, comprising a particle called tau (τ) and the corresponding tau neutrino (ν_τ). However, we will only deal with the first lepton generation. That is our leptons will only be the electron, the electron neutrino and their antiparticles.

Q-values in β^-, β^+ and electron capture decays

The decay energy associated to the process (11.1), which is called "the Q-value", is given by

$$Q_{\beta^-} = m_n c^2 - m_p c^2 - m_e c^2 \tag{11.2}$$

Since $m_n c^2$=939.566 MeV, $m_p c^2$=938.272 MeV and $m_e c^2$=0.511 MeV, the Q-value is Q_{β^-}=0.783 MeV. This is the kinetic energy shared by the three particles in the exit channel of Eq. (11.1).

For the β^+ decay, i. e.

$$p \to n + e^+ + \nu \tag{11.3}$$

it is a positron and a neutrino that are emitted. Since the masses of the antiparticles are the same as the ones of the corresponding particles one has, $Q_{\beta^+} = m_p c^2 - m_n c^2 - m_e c^2$=-1.805 MeV, which implies that this decay, with negative kinetic energies for the outgoing particles, is forbidden. Or, in other words, for the process (11.3) to take place it is necessary that energy is provided from the outside.

Another form of decay is electron capture (EC) by a proton in the process,

$$p + e^- \to n + \nu \tag{11.4}$$

for which the Q-value is $Q_{EC} = m_p c^2 + m_e c^2 - m_n c^2 -$=-0.783 MeV, which is also a forbidden transition.

All these transitions can also occur within the nucleus, where the Q-value of the decay from a particular nucleon is modified by the energies provided by the other nucleons. Thus, if the decay occurs from a nucleus (Z,N), where the nucleon number is A=N+Z, the nuclear beta minus decay becomes

$$(Z, N) \to (Z + 1, N - 1) + e^- + \bar{\nu} \tag{11.5}$$

with the Q-value given by $Q_{\beta^-} = M(Z, N) - M(Z + 1, N - 1) - m_e c^2$, where M is the atomic mass (in units of energy) given by the sum of the masses of the neutrons, protons and electrons, minus the corresponding binding energies, i. e.

$$M(Z, N) = N m_n c^2 + Z m_p c^2 + Z m_e c^2 - B_{el}(Z, N) - B(Z, N) \tag{11.6}$$

where $B_{el}(Z, N)$ is the binding enery of the electrons in the atom and $B(Z, N)$ is the nuclear binding energy. We have assumed that the atom is not ionized and therefore the number of electrons is the same as the number Z of protons.

The value of Q_{β^-} can now be positive or negative, depending upon the structure of the nuclei involved in the decay.

For the nuclear β^+ decay it is,

$$(Z, N) \to (Z - 1, N + 1) + e^+ + \nu \tag{11.7}$$

and $Q_{\beta^+} = M(Z, N) - M(Z - 1, N + 1) - m_e c^2$, which can also be positive or negative according to the structure of the nuclei.

Finally, the nuclear electron capture occurs when one of the electrons orbiting around the nucleus is absorved by a proton in the nucleus. The proton is transformed into a neutron and an electrino is emitted following the process (11.4), i. e.

$$(Z, N) + e^- \to (Z - 1, N + 1) + \nu \tag{11.8}$$

with $Q_{EC} = M(Z, N) + m_e c^2 - M(Z - 1, N + 1)$

Beta decay rates and the ft value

A formalism was developed during the 1960's and early 1970's, called electroweak theory, which describes in an unified fashion the electromagnetic and the weak interactions. The description of decay processes within this formalism requires a knowledge of field theory which is outside the scope of this Course. However, at the energies that we will be concerned a simpler form of a field theory can explain well the properties which are relevant for our purpose. This is actually the first field theory ever applied outside electromagnetism. It was performed by Fermi, as we show below.

The creation of the neutrino in beta decay implies that the force that induces the transition from the initial to the final state is weak since, as mentioned above, the neutrino interacts very weakly with matter.

Neither the electron nor the neutrino exist in the nucleus, therefore they must be formed at the moment of their emission, just as a photon is created at the moment of its emission in electromagnetic decay. From this simple argument Fermi developed a theory of beta decay by following the same steps as in electromagnetic decay. We will follow Fermi's argument, which is very simple and forms the ground on which all field theories are based.

We will assume, for simplicity, that the Coulomb force does not affect the escaping electron, which would be true only is the electron energy is large. This approximation will be lifted later. With this assumption the lepton-lepton and lepton-nucleon interaction is weak and therefore one can consider that the leptons move freely inside the nucleus. One can thus consider that the lepton wave functions inside the nucleus are plane waves of the form $\Psi_e(\mathbf{r}) = N_e e^{i\mathbf{j_e}\cdot\mathbf{r}}$ for the electron and for the neutrino $\Psi_\nu(\mathbf{r}) = N_\nu e^{i\mathbf{j}_\nu\cdot\mathbf{r}}$, where $\mathbf{k}$ is the wave number, $k = 2\pi/\lambda$, and N is a normalization constant.

The emission probability will depend upon the expectation value for the leptons to be inside the nucleus. With $\mathbf{r}$ within the nucleus this expectation value is $|\Psi_e(\mathbf{r})|^2|\Psi_\nu(\mathbf{r})|^2 = |N_e|^2|N_\nu|^2$. This describes the lepton sector of the decay. For the nucleon sector, Fermi compared with electromagnetic transitions and concluded that another factor that has to appear in the beta emission probability is the matrix element of some operator between the initial and final nuclear states, in the same fashion as the matrix element of the multipole operator $\mathcal{M}$ determines the transition probability per second, called T in Eq. (10) of the previous Chapter. We will assume that it is a neutron that decays and that this neutron belongs to a nucleus in a state $|\alpha(N)\rangle$, as the nucleus called (Z, N) in Eq. (11.5). The nucleus in the final state, that is $(Z+1, N-1)$, will be assumed to be in the state $|\beta(P)\rangle$. The nuclear matrix element should thus have the form

$$\mathcal{M} = \int \Psi^*_{\beta(P)}(\mathbf{r})\mathcal{O}\Psi_{\alpha(N)}(\mathbf{r})d\mathbf{r} \tag{11.9}$$

where $\mathcal{O}$ is some operator that one has to introduce to explain the experimental data.

The transition probability per unit of time is given by the "golden rule" of quantum mechnics, i. e. it is the square of the transition matrix element times the density of states, which in our case is,

$$T = \frac{2\pi}{\hbar}|N_e N_\nu \mathcal{M}|^2 \frac{d\mathcal{N}}{dE} \tag{11.10}$$

We will assume that the system is contained in a box of volume V and, therefore, $N_e = N_\nu = 1/\sqrt{V}$. $d\mathcal{N}/dE$ is the density of final states. A change in E implies a change in the energy of the electron, which determines any change in the energy of the neutrino. This is because the transition energy $E_t = E_e + E_\nu$ is a constant, i. e. $dE_t = 0$, and one has $dE = dE_e = -dE_\nu$. One can then write the density of states as $d\mathcal{N}/dE = d\mathcal{N}/dE_e$.

To calculate $d\mathcal{N}/dE_e$ we start by evaluating the number of states with momenta between p and $p+dp$. One of the Exercises corresponding to this Chapter is to evaluate that number for the plane wave confined within the box and for the particle i (i is electron or neutrino). It is

$$d\mathcal{N}_i = \frac{p_i^2 dp_i V}{2\pi^2\hbar^3} \tag{11.11}$$

and the total number of states is

$$d\mathcal{N} = d\mathcal{N}_e d\mathcal{N}_\nu = \frac{p_e^2 dp_e V}{2\pi^2\hbar^3}\frac{p_\nu^2 dp_\nu V}{2\pi^2\hbar^3} \tag{11.12}$$

For the neutrino (massless) one has $dE_\nu = cdp_\nu$. The transition probability has to be a positive number, therefore we replace $dE_\nu = |dE_e| = cdp_\nu$. The maximum value of the electron energy E_e corresponds

to $E_\nu = 0$. Therefore the transition energy is $E_t = E_e^{max}$ and $E_\nu = cp_\nu = E_e^{max} - E_e$. The neutrino is a relativistic particle and even the electron is emitted at high speed. Therefore one has to use the relativistic expression for the energy E, which for a particle with mass m carrying a linear momentum p is $E^2 = m^2c^4 + c^2p^2$. Therefore it is $p_e^2p_\nu^2 = (E_e^2/c2 - m_ec^2)(E_e^{max} - E_e)^2/c^2$ and

$$\frac{d\mathcal{N}}{dE_e dp_e} = \frac{V^2}{4\pi^4\hbar^6c^3}(E_e^2/c^2 - m_ec^2)(E_e^{max} - E_e)^2 \tag{11.13}$$

which gives an excellent representation of the shape of the beta decay spectrum that Fermi wanted to explain, supporting his theory as well as the neutrino assumption.

The transition probability (11.10) for the electron in a range of momentum dp_e becomes,

$$Tdp_e = \frac{|\mathcal{M}|^2}{2\pi^3\hbar^7c^3}(E_e^{max} - E_e)^2p_e^2dp_e \tag{11.14}$$

notice that the volumen V has been cancelled out in this expression, which implies that its exact value is irrelevant, as it should be. Calling $P_e = p_e^{max}$ one has $E_e^{max} = \sqrt{m_e^2c^4 + c^2P_e^2}$. Replacing this in Eq. (11.14) one obtains,

$$Tdp_e = \frac{|\mathcal{M}|^2}{2\pi^3\hbar^7c^3}\big(\sqrt{m_e^2c^4 + c^2P_e^2} - \sqrt{m_e^2c^4 + c^2p_e^2}\,\big)^2p_e^2dp_e \tag{11.15}$$

The total transition probability T_{total} per unit time is obtained by integrating this equation over the linear momentum p_e. The mean life $\tau = 1/T_{total}$ is obtained from,

$$\frac{1}{\tau} = \frac{|\mathcal{M}|^2}{2\pi^3\hbar^7c^3}\int_0^{P_e}\big(\sqrt{m_e^2c^4 + c^2P_e^2} - \sqrt{m_e^2c^4 + c^2p_e^2}\,\big)^2p_e^2dp_e \tag{11.16}$$

To obtain this equation we assumed that the electron was not affected by the Coulomb interaction and also that the decaying neutron existed in the nucleus as a free particle. None of these two assumptions is valid in general. The inclusion of the Coulomb interaction is a relatively easy task, but to assess the extend to which the nucleon is free can be a rather challenging task. The outcome of this calculation is that in Eq. (11.16) a Fermi factor $F(Z_f, p_e)$ has to be added. The half life $\tau_{1/2} = \ln 2\ \tau$ thus becomes,

$$\tau_{1/2} = \big\{\frac{|\mathcal{M}|^2}{2\ln 2\pi^3\hbar^7c^3}\int_0^{P_e}F(Z_f,p_e)\big(\sqrt{m_e^2c^4 + c^2P_e^2} - \sqrt{m_e^2c^4 + c^2p_e^2}\,\big)^2p_e^2dp_e\big\}^{-1} \tag{11.17}$$

One sees that the transition energy $E_t = E_e^{max}$, or its corresponding momentum P_e. appears only in the factor

$$f(P_e)m_e^5c^7 = \int_0^{P_e}F(Z_f,p_e)\big(\sqrt{m_e^2c^4 + c^2P_e^2} - \sqrt{m_e^2c^4 + c^2p_e^2}\,\big)^2p_e^2dp_e \tag{11.18}$$

and the quantity

$$f\tau_{1/2} = \frac{2\ln 2\pi^3\hbar^7}{|\mathcal{M}|^2m_e^5c^4} \tag{11.19}$$

is a constant independent of the energy. This is called ft factor. One determines experimentally this quantity by evaluating the function $f(P_e)$ numerically and using the experimental half life. We will see below that the ft factor provides a fair measure of the beta decay transition probability.

We have

$$\frac{2\pi^3\hbar^7}{m_e^5c^4} = 1.8844 \times 10^{-94}\text{erg}^2\text{cm}^6\text{s}. \tag{11.20}$$

We have analyzed β^- decay only, but the formalism is the same for β^+ decay. In the case of electron capture the nucleus traps an electron of the atomic electronic cloud. For this to happen there should be a large overlap between the electron and the nuclear wave functions. The most internal electronic orbit corresponds to K-electrons, i. e. electrons moving in the lowest atomic orbit. The electron thus absorved undergoes the beta-like decay process shown in Eq. (11.4). However there is an important difference since the K-electron is absorved at the energy of the K-shell. Instead, as we have seen above, in beta decay the electron is emitted into the continuum with any energy, and the corresponding transition probability has to take into account the density of continuum states. Therefore, in electron capture the statistical factor (11.18), which is an outcome of the density of states, does not appear.

Another difference between electron capture and beta decay is that in electron capture the K-electron moves in a $l = 0$ state, and cannot be considered a plane wave. It is not difficult to include the proper electron wave function in the transition matrix element, but we will not go into more details of this process since conceptually it is similar to beta decay.

11.2 Fermi Theory of allowed beta decays

One has still to evaluate the matrix element $\mathcal{M}$, and to do that one has first to choose the operator $\mathcal{O}$ in Eq. (11.9). This is a crucial point for the Fermi theory as well as for all field theories developed afterwards. There are some restrictions which confine the choice one can make of $\mathcal{O}$. The most important of these restrictions is that the system is relativistic and, therefore, the physics should be the same for observes moving at different (but constant) relative speeds while keeping the light velocity c constant. Or, more precisely, the system should be invariant under Lorentz transformations. The types of beta decay can be classified by the angular momenta carried away by the electron and neutrino. The most important are those for $\Delta l = 0$ which are referred to as "allowed" beta decay. There are two type of allowed beta decay – Fermi (F) and Gamow- Teller (GT).

Fermi took first the simplest form, which is just $\mathcal{O} = 1$, resulting in what is known as the Fermi matrix element, i. e.

$$\mathcal{M}_F = \langle|\mathcal{O}|\rangle = g_V \int \Psi^*_{\beta(P)}(\mathbf{r})\Psi_{\alpha(N)}(\mathbf{r})d\mathbf{r} \tag{11.21}$$

where g_V is the strength of the coupling that gives rise to the emission, as the fine structure constant $\alpha = e^2/(\hbar c) \approx 1/137$ is the strength of the electromagnetic interaction.

For the second form Fermi made an analogy with electromagnetism, where the simplest multipole operator $\mathcal{M}(E\lambda\mu)$ corresponds to $\lambda = 1$ (remember that a $\lambda = 0$ photon does not exist). In this dipolar case one finds that the matrix element is $< l'm'|Y(E1\mu)|lm > \propto < l'm'|\rho|lm >$, where $\rho = (x - iy, \sqrt{2}z, x + iy)/\sqrt{2}$, i. e. it acquires a vector form. In beta decay the equivalent operator should be, according to Fermi, the spin operator σ. This is related to the relativistic character of beta decay because σ is an operator that appears naturally when writing the relativistic invariant version of the Schrödinger equation (the Dirac equation). This second form, which is called Gamow-Teller, becomes,

$$\mathcal{M}_{\mathbf{GT}} = g_A \int \Psi^*_{\beta(P)}(\mathbf{r})\sigma\Psi_{\alpha(N)}(\mathbf{r})d\mathbf{r} \tag{11.22}$$

where g_A is the strength of the Gamow-Teller interaction.

The Pauli matrices $\sigma = (\sigma_x, \sigma_y, \sigma_z)$ only affect the spin degrees of freedom. Therefore σ does not change the parity of the states involved in the transition. It does not change the orbital angular momentum either, and $l_\alpha = l_\beta$. But the vector σ carries one unit of angular momentum. This implies that $0^+ \to 0^+$ transitions are forbidden and that the total final spin j_β is constraint by the triangular relation $|j_\alpha - 1| \leq j_\beta \leq j_\alpha + 1$.

The radial functions are also very similar to each other in this case, since they only differ by the spin coupling (assuming n_α=n_β). Yet the matrix element (11.22) is smaller than the corresponding Fermi matrix element because the recoupling of angular momenta induce a factor which is less than unity.

Comparisson with experiment has provided for the coupling constants the values $g_V \sim 1.36 \times 10^{-3} e^2\hbar^2/(m_p^2c^2)$, where m_p is the proton mass, and $g_A/g_V = -1.275$. We have (to be checked)

$$g_V = (1.41271 \pm 0.00032) \cdot 10^{-49}\text{erg} \cdot \text{cm}^3, \tag{11.23}$$

and

$$g_A = (1.781 \pm 0.011) \cdot 10^{-49}\text{erg} \cdot \text{cm}^3. \tag{11.24}$$

At the quark level it is $g_V = -g_A$.

logaritm of ft

One sees from Eq. (11.19) that the bigger the matrix element $\mathcal{M}$ the smaller is the ft-value. That implies that small values of ft corresponds to faster transition rates and shorter half lives. In the two cases analyzed here, the Fermi transition is more likely than the Gamow-Teller one. Other choices of the operator O may change parity and involve large differences in the transfer angular momenta. This induces large differences between the corresponding radial functions and, as a result, the ft values can change by many orders of magnitude. Due to this one defines the logaritm of ft. As seen in Table 11.1 the $logft$ indeed varies very much for various transitions. Besides the Fermi and Gamow-Teller, there are other transitions with names which were introduced as more complex transitions were found.

This vast variations in the $logft$ values makes beta decay a powerful tool to determine the spin and parities of nuclear states, as seen in the Exercises.

Table 11.1: Values of $log_{10}ft$ and the corresponding restrictions upon the angular momentum transfer ΔJ and parity change $\Delta\pi$.

$log_{10}ft$	ΔJ	l_β	$\Delta\pi$	Decay type
2.9 - 3.7	0	0	no	Supperallowed (Fermi)
3.8 - 6	0,1	0	no	Allowed Gamow-Teller & Fermi
6 - 10	0,1,2	0,1	yes	First forbidden
10 - 13	1,2,3	1,2	no	Second forbidden
17-19	2,3,4	2,3	yes	Third forbidden

Fermi decay

As we have seen before, the single-particle wave function contains a radial part and a spin-orbit part. The radial part is determined by the principal quantum number n, the orbital angular momentum l and the total spin j. The parity of the state is $(-1)^l$. In our case it is $\Psi_{\alpha(N)}(\mathbf{r}) = R_{n_\alpha l_\alpha j_\alpha}(r)\left[Y_{l_\alpha}(\hat{r})\chi_{1/2}\right]_{j_\alpha m_\alpha}$ and the same for $\Psi^*_{\beta(P)}(\mathbf{r})$. Integrating over the angles the matrix element becomes

$$\mathcal{M} = g_V \delta_{l_\alpha l_\beta}\delta_{j_\alpha j_\beta}\int R^*_{n_\beta l_\beta j_\beta(P)}(r)R_{n_\alpha l_\alpha j_\alpha(N)}(r)r^2dr \tag{11.25}$$

which shows that in the Fermi transition there is no change of parity or angular momentum. The residual nucleus has the same spin and parity as the decaying nucleus.

The integral in Eq. (11.25) is very close to unity if n_α=n_β since, except the Coulomb interaction, the proton and neutron feel the same correlations. If isospin is conserved, and neglecting the influence of the Coulomb field upon $R_{n_\beta l_\beta j_\beta(P)}(r)$, the neutron and proton radial wave functions are the same and

$$\mathcal{M} = g_V \delta_{n_\alpha n_\beta}\delta_{l_\alpha l_\beta}\delta_{j_\alpha j_\beta} \tag{11.26}$$

In this case the initial and final nuclear states are isobaric analogous, that is they differ only by their isospin projections.

The operator associated with Fermi decay is proportional to the isospin raising and lowering operator. As such it can only connect isobaric analogue states and it provides an exacting test of isospin conservation in the nucleus. The operator for Fermi beta decay in terms of sums over the nucleons is

$$\mathcal{O}(F_\pm) = \sum_k t_{k\pm} \tag{11.27}$$

The matrix element is

$$B(F) = \left|\langle f|T_\pm|i\rangle\right|^2 \tag{11.28}$$

where

$$T_\pm = \sum_k t_\pm \tag{11.29}$$

is the total isospin raising and lowering operator for total isospin constructed out of the basic nucleon isospin raising and lowering operators

$$t_-|n\rangle = |p\rangle, \quad t_-|p\rangle = 0 \tag{11.30}$$

and

$$t_+|p\rangle = |n\rangle, \quad t_+|n\rangle = 0 \tag{11.31}$$

The matrix elements obey the triangle conditions $J_f = J_i(\Delta J = 0)$. The Fermi operator has $\pi_\mathcal{O} = +1$, and thus the initial and final nuclear states must have $\pi_i\pi_f = +1$ for the matrix element to be nonzero under the parity transform.

When isospin is conserved the Fermi matrix element must obey the isospin triangle condition $T_f - T_i(\Delta T = 0)$, and the Fermi operator can only connect isobaric analogue states. For β_- decay

$$T_-|\omega_i, J_i, M_i, T_i, T_{zi}\rangle = \sqrt{T_i(T_i+1) - T_{zi}(T_{zi}-1)}|\omega_i, J_i, M_i, T_i, T_{zi}-1\rangle \tag{11.32}$$

and

$$\begin{aligned} B(F_-) =& \left|\langle\omega_f, J_f, M_f, T_f, T_{zi}-1|T_-|\omega_i, J_i, M_i, T_i, T_{zi}\rangle\right|^2 \\ =& \left[T_i(T_i+1) - T_{zi}(T_{zi}-1)\right]\delta_{\omega_i,\omega_f}\delta_{J_i,J_f}\delta_{M_i,M_f}\delta_{T_i,T_f} \end{aligned} \tag{11.33}$$

For β_+ we have

$$\begin{aligned} B(F_+) =& \big|\langle \omega_f, J_f, M_f, T_f, T_{zi}+1|T_+|\omega_i, J_i, M_i, T_i, T_{zi}\rangle\big|^2 \\ =& \big[T_i(T_i+1) - T_{zi}(T_{zi}+1)\big]\delta_{\omega_i,\omega_f}\delta_{J_i,J_f}\delta_{M_i,M_f}\delta_{T_i,T_f} \end{aligned} \tag{11.34}$$

For neutron-rich nuclei ($N_i > Z_i$) we have $T_i = T_{zi}$ and thus

$$B(F_-)(N_i > Z_i) = 2T_{zi} = (N_i - Z_i)\delta_{\omega_i,\omega_f}\delta_{J_i,J_f}\delta_{M_i,M_f}\delta_{T_i,T_f} \tag{11.35}$$

and

$$B(F_+)(N_i > Z_i) = 0 \tag{11.36}$$

For proton-rich nuclei ($Z_i > N_i$) we have $T_i = -T_{zi}$ and thus

$$B(F_+)(Z_i > N_i) = -2T_{zi} = (Z_i - N_i)\delta_{\omega_i,\omega_f}\delta_{J_i,J_f}\delta_{M_i,M_f}\delta_{T_i,T_f} \tag{11.37}$$

and

$$B(F_-)(Z_i > N_i) = 0 \tag{11.38}$$

Gamow-Teller decay

The operator associated with Gamow-Teller decay also contains the nucleon spin operator. Since the total spin S is not a good quantum number, Gamow-Teller beta decay goes in general to many final states and provides a sensitive test of shell-model configuration mixing in the nucleus. The operator for Gamow-Teller beta decay in terms of sums over the nucleons is

$$\mathcal{O}(GT_\pm) = \sum_k \sigma_k t_{k\pm} \tag{11.39}$$

The reduced matrix elements is

$$B_{i,f}(GT_\pm) = \frac{\big|\langle f||\mathcal{O}(GT_\pm)||i\rangle\big|^2}{2J_i+1} = \frac{M^2_{i,f}(GT_\pm)}{2J_i+1} \tag{11.40}$$

The matrix elements are reduced in orbital space and the $2Ji+1$ factor comes from the average over initial M_i states. The magnitude of reduced matrix element $M(GT)$ does not depend on the direction of the transition, i.e.,

$$M_{i,f}(GT_\pm) = \langle f||\mathcal{O}(GT_\pm)||i\rangle \tag{11.41}$$

The matrix elements obey the triangle $\Delta(J_i, j_i, \Delta J = 1)$. The Gamow-Teller operator has $\pi_\mathcal{O} = +1$, and thus the initial and final nuclear states must have $\pi_i\pi_f = +1$ for the matrix element to be nonzero under the parity transform. When isospin is conserved the Gamow-Teller matrix elements obey the isospin triangle condition $\Delta(T_f, T_i, \Delta T = 1)$.

In second-quantized form the GT_- operator has the form

$$\mathcal{O}(GT_-) = \sum_{\alpha\beta}\langle\alpha|\sigma t_-|\beta\rangle a^\dagger_{\alpha,p}a_{\beta,n} \tag{11.42}$$

where $a_{\beta,n}$ destroys a neutron in state β and $a^\dagger_{\alpha,p}$ creates a proton in state α. The J-coupled form is

$$\mathcal{O}(GT_-) = \sum_{j_a,j_b}\langle j_a, p||\sigma t_-||j_b, n\rangle\frac{\big[a^\dagger_{\alpha,p}\otimes\tilde{a}_{\beta,n}\big]^\lambda}{\sqrt{2\lambda+1}} \tag{11.43}$$

where $\lambda = 1$ for the GT operator. The reduced transition probability for the transition from an initial state i to a final state f is given by

$$B(GT_-) = \sum_{j_a,j_b}\langle j_a, p||\sigma t_-||j_b, n\rangle\frac{\langle f||\big[a^\dagger_{\alpha,p}\otimes\tilde{a}_{\beta,n}\big]^\lambda||i\rangle}{\sqrt{2\lambda+1}} \tag{11.44}$$

The analogous equations for GT_+ are

$$\mathcal{O}(GT_+) = \sum_{\alpha\beta}\langle\alpha|\sigma t_+|\beta\rangle a^\dagger_{\alpha,n}a_{\beta,p} \tag{11.45}$$

Table 11.2: Gamow-Teller reduced single-particle matrix elements $\frac{2\langle j_a||\boldsymbol{s}||j_b\rangle}{\sqrt{3}}$.

a/b	$s_{1/2}$	$p_{3/2}$	$p_{1/2}$	$d_{5/2}$	$d_{3/2}$	$f_{7/2}$	$f_{5/2}$
$s_{1/2}$	$\sqrt{2}$						
$p_{3/2}$		$2\sqrt{5}/3$	-4/3				
$p_{1/2}$		4/3	$-\sqrt{2}/3$				
$d_{5/2}$				$\sqrt{14/5}$	$-4/\sqrt{5}$		
$d_{3/2}$				$4/\sqrt{5}$	$-2/\sqrt{5}$		
$f_{7/2}$						$2\sqrt{6/7}$	$-4\sqrt{2/7}$
$f_{5/2}$						$4\sqrt{2/7}$	$-\sqrt{10/7}$

where $a_{\beta,p}$ destroys a proton in state β and $a^\dagger_{\alpha,n}$ creates a neutron in state α. The J-coupled form is

$$\mathcal{O}(GT_+) = \sum_{j_a,j_b} \langle j_a, n||\sigma t_+||j_b, p\rangle \frac{\left[a^\dagger_{\alpha,n} \otimes \tilde{a}_{\beta,p}\right]^\lambda}{\sqrt{2\lambda+1}} \tag{11.46}$$

and the reduced transition probability is

$$B(GT_+) = \sum_{j_a,j_b} \langle j_a, n||\sigma t_+||j_b, p\rangle \frac{\langle f||\left[a^\dagger_{\alpha,n} \otimes \tilde{a}_{\beta,p}\right]^\lambda||i\rangle}{\sqrt{2\lambda+1}}. \tag{11.47}$$

The reduced single-particle matrix elements are given by

$$\langle j_a, p||\sigma t_-||j_b, n\rangle = \langle j_a, n||\sigma t_+||j_b, p\rangle = 2\langle j_a||\boldsymbol{s}||j_b\rangle \tag{11.48}$$

where the matrix elements of $\boldsymbol{s}$ are given by

$$\langle j_a||\boldsymbol{s}||j_b\rangle = (-1)^{l_a+j_a+3/2}\sqrt{(2j_a+1)(2j_b+1)} \begin{Bmatrix} 1/2 & 1/2 & 1 \\ j_b & j_a & l_a \end{Bmatrix} \langle s||\boldsymbol{s}||s\rangle \delta_{l_a,l_b}\delta_{n_a,n_b} \tag{11.49}$$

with

$$\langle s||\boldsymbol{s}||s\rangle = \sqrt{3/2}. \tag{11.50}$$

The orbits which are connect by the GT operator are very selective since the matrix elements of $\boldsymbol{s}$ has the selection rules δ_{l_a,l_b} and δ_{n_a,n_b}.

We have

$$\langle j_a||\boldsymbol{s}||j_b\rangle = (-1)^{j_a+j_b+1}\langle j_b||\boldsymbol{s}||j_a\rangle = (-1)^{\delta_{ab}+1}\langle j_b||\boldsymbol{s}||j_a\rangle. \tag{11.51}$$

In practice, we have $\langle j_>||\boldsymbol{s}||j_b\rangle > 0$ and $\langle j_<||\boldsymbol{s}||j_b\rangle < 0$ where $j_{>(<)} = l + 1/2(|l-1/2|)$. This is because the $6j$ symbols in above equation take positive values for $j_a = j_b$ and negative values for $j_a \neq j_b$.

Effective operators for the Gamow-Teller decay

There are several reasons why the "free-nucleon" calculations may differ from experiment. In reality the nuclear wave functions are more complicated than the theoretical model we use in that they may incorporate nucleon degrees of freedom beyond the shell space. In addition, non-nucleonic degrees of freedom involving the delta isobars and mesons in the nucleus may also be important. The calculation of the corrections corresponding to these processes have been the subject of many theoretical investigations.

Since the factor g_A^2 appears in front of $B(GT)$ one might parameterize the effective matrix in terms of an effective g_A value, as we are doing in electromagnetic transition studies. In nuclei we have $g_A \sim 1$.

11.3 Sum rules

Sum rules for Fermi and Gamow-Teller matrix elements can be obtained. The sum rule for Fermi is obtained from the sum

$$\sum_f \left[B_{i,f}(F_-) - B_{i,f}(F_+)\right] = \sum_f \left[\left|\langle f|T_-|i\rangle\right|^2 - \left|\langle f|T_+|i\rangle\right|^2\right] \tag{11.52}$$

The final states f in the T_- matrix element go with the $Z_f = Z_i + 1$ nucleus and those in the T_+ matrix element to with the $Z_f = Z_i - 1$ nucleus. One can explicitly sum over the final states to obtain

$$\sum_f \left[\langle i|T_+|f\rangle\langle f|T_-|i\rangle - \langle i|T_-|f\rangle\langle f|T_+|i\rangle\right] = \langle i|T_+T_- - T_-T_+|i\rangle = \langle i|2T_z|i\rangle = N_i - Z_i \tag{11.53}$$

The sum rule for Gamow-Teller is obtained as follows.

$$\begin{aligned}
&\sum_{f,\mu} \left|\langle f|\sum_k \sigma_{k,\mu} t_{k-}|i\rangle\right|^2 - \sum_{f,\mu} \left|\langle f|\sum_k \sigma_{k,\mu} t_{k+}|i\rangle\right|^2 \\
=&\sum_{f,\mu} \langle i|\sum_k \sigma_{k,\mu} t_{k+}|f\rangle\langle f|\sum_{k'} \sigma_{k',\mu} t_{k'-}|i\rangle - \sum_{f,\mu} \langle i|\sum_k \sigma_{k,\mu} t_{k-}|f\rangle\langle f|\sum_{k'} \sigma_{k',\mu} t_{k'+}|i\rangle \\
=&\sum_\mu \left[\langle i|\left(\sum_k \sigma_{k,\mu} t_{k+}\right)\left(\sum_{k'} \sigma_{k',\mu} t_{k'-}\right) - \left(\sum_k \sigma_{k,\mu} t_{k-}\right)\left(\sum_{k'} \sigma_{k',\mu} t_{k'+}\right)|i\rangle\right] \\
=&\sum_\mu \langle i|\sum_k \sigma_{k,\mu}^2 [t_{k+}t_{k-} - t_{k-}t_{k+}]|i\rangle = 3\langle i|\sum_k [t_{k+}t_{k-} - t_{k-}t_{k+}]|i\rangle \\
=&3\langle i|T_+T_- - T_-T_+|i\rangle = 3\langle i|2T_z|i\rangle = 3(N_i - Z_i)
\end{aligned} \tag{11.54}$$

We have used the fact that $\sigma_x^2 = \sigma_y^2 = \sigma_z^2 = 1$ When $k \neq k'$ the operators commute and cancel. These sum rules hold for each M_i value and thus also hold for $B(F)$ and $B(GT)$ when we take an average over the M_i values. Thus

$$\sum_f \left[B_{i,f}(F_-) - B_{i,f}(F_+)\right] = N_i - Z_i \tag{11.55}$$

and

$$\sum_f \left[B_{i,f}(GT_-) - B_{i,f}(GT_+)\right] = 3(N_i - Z_i) \tag{11.56}$$

The sum-rule for the Fermi matrix elements applies even when isospin is not conserved. For and $N > Z$ we usually have $T_i = T_{zi}$ which means that $B(F_+) = 0$ and we can obtain $B(F_-) = Ni - Zi$ for the transition to the isobaric analogue state. For $N = Z(T_{zi} = 0)$ and $T_i = 0$ we have $B(F_+) = B(F_-) = 0$, and for $T_i = 1$ we have $B(F_+) = B(F_-) = 2$. Fermi transitions which would be zero if isospin is conserved are called isospin-forbidden Fermi transitions.

When $N > Z$ there are some situations where one has $B(GT_+) = 0$, and we have $B(GT_-) = 3(Ni - Zi)$. In particular for the β_- decay of the neutron we have $B(F_-) = 1$ and $B(GT_-) = 3$.

11.4 ^{14}C-dating beta decay

The radioisotope ^{14}C is the basis for radiocarbon dating in which it is assumed that living organisms have a $^{14}\mathrm{C}/^{12}\mathrm{C}$ ratio which is the same as that in the atmosphere and that this atmospheric ratio has been constant in the past. The interaction between the organism and the atmosphere stops at death, and the ^{14}C that remains in the organism decays. By measuring the $^{14}\mathrm{C}/^{12}\mathrm{C}$ ratio directly (using Accelerator Mass Spectrometry) or the rate of decay of ^{14}C (using radiometric methods), the time since death can be estimated. Clearly there is another assumption underlying this process, namely that the decay of ^{14}C is exactly exponential for all time. The half-life for ^{14}C was initially found to be $5,568 \pm 30$ yr (the Libby half-life) but was later changed to $5,730 \pm 40$ yr (the Cambridge half life).

The anomalously long β decay half-life of ^{14}C has been of continuous theoretical interest since the appearance of the nuclear shell model [3, 4, 5, 6]. The decay involves the $J^\pi = 0^+$ ground state of ^{14}C and the $J^\pi = 1^+$ ground state of ^{14}N and satisfies the selection rule for typical allowed Gamow-Teller (GT) transitions. However, the extracted transition amplitude from experimental half-life is thousands of times smaller than that of allowed transitions. The inhibition should be attributed to the accidental cancellation of certain components of the wave functions of the involved states that contribute to the transition. It was recognized long ago that the tensor part of the nuclear force play an essential role in inducing the cancellation [7, 8].

In the original paper of Jancovici and Talmi's [7], an unreasonably large tensor force was introduced to induce the cancellation. Later studies show that this problem can be rectified by redefining the radial dependence of the tensor component (for reviews, see Ref. [4]). One may expect that the shape

and strength of the tensor force were confined in realistic nucleon-nucleon (NN) potentials which are determined by fitting NN scattering observables. However, the studies of Zamick and collaborators [5, 9, 10] showed that the cancellation cannot be reproduced by calculations with realistic Hamiltonians [11] derived from microscopic NN potentials like the Hamada-Johnston potential or the Bonn potential. This failure was also seen in very recent calculations of Refs. [6, 12, 13, 14] with modern one-boson-exchange and chiral potentials. It was suggested that the problem may indicate that the tensor component of the in-medium NN interaction is much weaker than that of the bare potential [5, 9, 10]. Holt *et al.* claimed that the problem of realistic calculations in reproducing the long β decay half-life of the ^{14}C can be solved by taking into account the Brown-Rho scaling in-medium modification [6] or three-nucleon corrections [12] of the NN interaction. No-core shell model calculations by Maris *et al.* [14] also show that the cancellation can be reproduced by introducing a three-nucleon force of chiral perturbation theory.

The wave functions of the ^{14}C ($J^\pi = 0^+$, $T = 1$) and ^{14}N ($J^\pi = 1^+$, $T = 0$) ground states, denoted by $|\psi_i\rangle$ and $|\psi_f\rangle$, respectively, can be well described as two holes occupying the $0p_{1/2}$ and $0p_{3/2}$ single-particle orbits by assuming ^{16}O as the inert core [7, 8]. (Recent large space calculations of Ref. [14] also suggested that the cancellation mostly occurs in the p shell.) In the jj coupling scheme, the wave functions can be written as [9]

$$\begin{aligned} |\psi_i\rangle &= \kappa|0p_{1/2}^{-2}\rangle + \eta|0p_{3/2}^{-2}\rangle, \\ |\psi_f\rangle &= a|0p_{1/2}^{-2}\rangle + b|0p_{3/2}^{-1}0p_{1/2}^{-1}\rangle + c|0p_{3/2}^{-2}\rangle, \end{aligned} \tag{11.57}$$

where the κ and η and a, b and c denote the corresponding wave function amplitudes. The GT transition matrix element is determined by

$$M(\mathrm{GT}) = \langle\psi_f||\sigma\tau||\psi_i\rangle = \sqrt{\frac{2}{3}}\left[\kappa(a+2b) + \eta(\sqrt{2}b - \sqrt{5}c)\right]. \tag{11.58}$$

In many cases the wave functions of ^{14}C and ^{14}N were calculated in the LS coupling scheme [7]. The transformation between wave functions in LS and jj coupling schemes is known in analytic forms in terms of $6j$ and $9j$ symbols. To facilitate the comparison between wave functions in different coupling schemes available on the market, the explicit expressions for the transformation are listed below as

$$\begin{pmatrix} |^1S_0\rangle \\ |^3P_0\rangle \end{pmatrix} = \frac{1}{\sqrt{3}} \begin{pmatrix} 1 & \sqrt{2} \\ \sqrt{2} & -1 \end{pmatrix} \begin{pmatrix} |0p_{1/2}^{-2}\rangle \\ |0p_{3/2}^{-2}\rangle \end{pmatrix}, \tag{11.59}$$

and

$$\begin{pmatrix} |^3S_1\rangle \\ |^1P_1\rangle \\ |^3D_1\rangle \end{pmatrix} = \frac{1}{\sqrt{3}} \begin{pmatrix} -1 & -4 & \sqrt{10} \\ \sqrt{6} & \sqrt{6} & \sqrt{15} \\ \sqrt{20} & -\sqrt{5} & -\sqrt{2} \end{pmatrix} \begin{pmatrix} |0p_{1/2}^{-2}\rangle \\ |0p_{3/2}^{-1}0p_{1/2}^{-1}\rangle \\ |0p_{3/2}^{-2}\rangle \end{pmatrix}. \tag{11.60}$$

In evaluating above wave function amplitudes and the transition amplitude $M(\mathrm{GT})$, one may start from empirical as well as realistic shell-model interactions. It has been established that realistic interactions derived from bare NN potentials are in general close to empirical ones which are obtained by fitting experimental data [15, 16, 17, 18]. This can also be seen from Table 11.3 where the diagonal matrix elements of some well-defined empirical p-shell interactions [19, 20, 21, 22] and those of the realistic interactions are listed for comparison.

The realistic interactions in Table 11.3 are derived from the underlying NN potentials for which we take the state-of-the-art Bonn potential (CD-Bonn) of Ref. [23] and the chiral potential (N^{3}LO) of Ref. [24]. The have to be renormalized to include contributions from excluded configurations and to avoid the hard core of the bare NN potential. In this work the short-range repulsion is taken into account with the momentum-space renormalization group decimation method (V_{low-k}) [25] and the G-matrix approach [15]. In the V_{low-k} method, high momentum contributions are integrated out with the introduction of a cutoff in momentum space for which we take $\Lambda = 2$ fm^{-1}. The G-matrix is calculated by using the double-partitioned approach with the standard starting energies of $\omega = -5$, -20, -50, -90 and -140 MeV [15] and the HO parameter of $\hbar\omega_0 = 45A^{-1/3} - 25A^{-2/3} \approx 14.37$ MeV. The detailed description of the renormalized G-matrix calculation can be found in Ref. [15] with a public code available. Core polarization effects upto the second order in perturbation theory are taken into account through the folded-diagram method. The projection operator appearing in the calculation is defined with the HO orbital boundaries (see Fig. 31 of Ref. [15] as an illustration) of n_1=1, n_2=3 and n_3=36. It means we take ^{4}He as the closed core, $0p_{3/2}$ and $0p_{1/2}$ as the valence single-particle orbits and we take into account

Table 11.3: Comparison between diagonal matrix elements $\langle ij|V|ij\rangle^{JT}$ (in MeV) of empirical and realistic interactions. The realistic interactions are calculated from the CD-Bonn and N^{3}LO potentials with the G-matrix (G) and V_{low-k} (K) renormalization approaches. Only the few terms that related to the description of the dating β decay are listed for simplicity.

	$J=0,T=1$		$J=1,T=0$		
Interaction	$0p^2_{3/2}$	$0p^2_{1/2}$	$0p^2_{3/2}$	$0p_{3/2}0p_{1/2}$	$0p^2_{1/2}$
Empirical					
CK [19]	-3.19	-0.26	-3.58	-6.22	-4.15
VWG [20]	-3.68	-0.15	-2.62	-6.55	-3.95
WBT [21]	-3.85	-1.22	-4.16	-6.86	-3.45
WBP [21]	-3.91	-1.15	-3.86	-6.94	-3.45
Realistic					
CD-Bonn(K)	-4.26	-0.77	-3.30	-8.26	-3.56
N^{3}LO(K)	-4.06	-0.66	-3.23	-8.18	-3.65
CD-Bonn(G)	-4.09	-0.74	-3.24	-8.20	-3.69
N^{3}LO(G)	-3.86	-0.60	-3.86	-8.10	-3.74

the influence from higher-lying HO orbitals with quantum number $N = 2n + l \leq 7$. The calculation is done in the isospin space. The charge independence breaking effect of the NN potential is neglected for simplicity.

The empirical interactions of Refs. [19, 20, 21] are constructed in the particle-particle channel by assuming ^{4}He as the inert core and the single-particle energies as free parameters. In above cases it was assumed that the interactions are are same in the hole-hole channel. The energy splitting between $0p^{-1}_{1/2}$ and $0p^{-1}_{3/2}$ orbits in ^{15}C and ^{15}N is calculated to be $\varepsilon = \varepsilon(0p^{-1}_{3/2}) - \varepsilon(0p^{-1}_{1/2}) = 6.3$ MeV [19], 7.3 MeV [20] and 6.5 MeV [21]. The calculations are very close to the experimental result, i.e, $\varepsilon = 6.3$ MeV.

The ground state of ^{14}C is dominated by the configuration of $|0p^{-2}_{1/2}\rangle$ due to the large spin-orbit splitting between orbits $0p^{-1}_{1/2}$ and $0p^{-1}_{3/2}$. This is supported by calculations with both empirical and realistic interactions, as seen from Table 11.4. As a result, the coefficient κ of Eq. (1) is significantly larger than η (κ and η have the same sign and $\kappa = 1$ and $\eta = 0$ in the single-particle limit). The mixing of the two corresponding configurations is induced by the non-diagonal matrix element $\langle 0p^2_{3/2}|V|0p^2_{1/2}\rangle^{J=0,T=1}$ for which realistic and empirical interactions give a similar strength. Comparison between the non-diagonal matrix elements is done in Table 11.5.

Table 11.4: Comparison between different wave functions calculated with empirical and realistic interactions. All calculations are done with the code [26] except those of Jancovici and Talmi's and of the chiral potential which are taken from Ref. [7] and Ref. [13], respectively.

Interaction	η	κ	c	b	a
Empirical					
CK [19]	0.38	0.92	-0.027	-0.31	0.95
VWG [20]	0.36	0.93	-0.063	-0.27	0.96
WBT [21]	0.31	0.95	0.033	-0.43	0.90
WBP [21]	0.30	0.95	0.014	-0.41	0.91
JT [7]	0.09	0.99	0.20	-0.41	0.89
Zamick [9]	0.22	0.98	0.014	-0.40	0.92
VF [27]	0.25	0.97	0.12	-0.36	0.97
Realistic					
CD-Bonn(K)	0.40	0.92	0.20	-0.77	0.61
N^3LO(K)	0.39	0.92	0.15	-0.71	0.69
CD-Bonn(G)	0.39	0.92	0.14	-0.70	0.70
N^3LO(G)	0.38	0.93	0.11	-0.65	0.75
Chiral [13]	0.40	0.92	0.14	-0.68	0.72

Table 11.5: Same as Table 11.3 but for the non-diagonal matrix elements $\langle ij|V|kl\rangle^{JT}$ (in MeV) of empirical and realistic interactions.

$ijkl^{JT}$	CK [19]	VWG [20]	WBT [21]	WBP [21]	CD-Bonn(K)	N^{3}LO(K)	CD-Bonn(G)	N^{3}LO(G)
1133^{01}	-4.86	-4.99	-3.84	-3.70	-4.92	-4.77	-4.77	-4.58
1113^{10}	1.69	1.71	1.81	1.70	1.82	1.99	1.96	2.09

Table 11.6: The central (C), spin-orbit (SO) and tensor (T) components of the matrix elements $\langle ij|V|kl\rangle^{JT}$ of empirical and realistic interactions.

	VWG			WBT			CD-Bonn(K)			N^{3}LO(G)		
$ijkl$	C	SO	T	C	SO	T	C	SO	T	C	SO	T
$J^\pi = 0^+, T = 1$												
1111	-1.66	0.58	0.92	-1.33	054	-0.42	-2.14	0.37	1.00	-2.02	0.38	1.04
3333	-4.43	0.29	0.46	-3.96	0.33	-0.21	-4.93	0.19	0.50	-4.56	0.17	0.52
1133	-3.93	-0.41	-0.65	-3.72	-0.42	0.29	-3.94	-0.27	-0.71	-3.58	-0.26	-0.73
$J^\pi = 1^+, T = 0$												
1111	-4.27	0.41	-0.098	-4.49	1.11	-0.075	-4.64	-0.10	1.17	-4.65	-0.15	1.15
1113	1.08	-0.21	0.83	0.43	-0.0019	1.38	1.17	0.26	0.39	1.29	0.30	0.50
1313	-5.85	0.10	-0.80	-5.85	0.35	-1.36	-7.70	0.13	-0.69	-7.46	0.15	-0.78
1133	2.72	-0.13	-0.46	1.55	-0.046	-0.82	3.80	0.07	-0.99	3.76	0.18	-1.03
1333	3.72	0.065	-0.016	2.41	0.045	-0.012	5.73	0.01	0.19	5.49	0.02	0.18
3333	-2.96	0.041	0.30	-4.11	-0.58	0.53	-3.49	-0.32	0.51	-3.34	-0.36	0.54

Similarly, one may safely expect that $|0p_{1/2}^{-2}\rangle$ should be the dominated configuration in the ground state wave function of ^{14}N since the other two configurations lie at much higher energies. This expectation is supported by all calculations with empirical interactions listed in Table 11.4. Since the amplitude κ is much larger than η, the suppression of the Gamow-Teller transition strength [Eq. (2)] should be largely due to the cancellation between a and $2b$ (a and b have different signs). That is, the term $|0p_{3/2}^{-1}0p_{1/2}^{-1}\rangle$ should most likely be the second largest component in the ground state wave function of ^{14}N. Most of our calculations with different interactions predict small values for the absolute value of the wave function amplitude of configuration $|0p_{3/2}^{-2}\rangle$. In this case we should have $a \sim -(2\kappa + \sqrt{2}\eta)b$ in reproducing the cancellation.

It can be seen from Table 11.4 that the problem of the realistic calculation in reproducing the cancellation is related to the fact that the predicted amplitude a (b) is significantly smaller (larger) than expected. The ratio between the amplitudes a and b are sensitive to the strengths of diagonal matrix elements $\langle 0p_{1/2}^2|V|0p_{1/2}^2\rangle^{J=1,T=0}$ and $\langle 0p_{3/2}0p_{1/2}|V|0p_{3/2}0p_{1/2}\rangle^{J=1,T=0}$ and the non-diagonal matrix element $\langle 0p_{3/2}\ 0p_{1/2}\ |V|\ 0p_{1/2}^2\rangle^{\ J=1,T=0}$. If we neglect the contribution from the configuration $|0p_{3/2}^2\rangle$ and restrict the calculation to dimension two, the mixing between above two components would be solely dominated by the perturbation term

$$\frac{\langle 0p_{3/2}0p_{1/2}|V|0p_{1/2}^2\rangle}{\varepsilon + \langle 0p_{3/2}0p_{1/2}|V|0p_{3/2}0p_{1/2}\rangle - \langle 0p_{1/2}^2|V|0p_{1/2}^2\rangle}. \tag{11.61}$$

By comparing the interaction matrix elements listed in Tables 11.3 & 11.5, it can be seen that the problem of realistic interaction is that the strength for diagonal matrix element $\langle 0p_{3/2}0p_{1/2}\ |V|0p_{3/2}0p_{1/2}\rangle^{J=1,T=0}$ it predicted is much larger than empirical ones.

It may still be of interest to figure out the way how the tensor force induces the cancellation in the jj coupling scheme (The impossibility of inducing cancellation with effective interactions without tensor force was first shown by Inglis [3]). Although the different components are mixed in usual construction of empirical interactions, it is possible to separate the central, spin-orbit (vector) and tensor force components of the effective interaction through the spin-tensor decomposition procedure [28]. As examples in Table 11.6 is listed the different components of realistic interactions and the empirical interactions of Refs. [20, 21]. The decompositions of various Cohen-Kurath interactions can be found in Ref. [29] and will not be presented here for simplicity. It can be seen from the figure that for the diagonal matrix element of concern, $\langle 0p_{3/2}0p_{1/2}\ |V|0p_{3/2}0p_{1/2}\rangle^{J=1,T=0}$, empirical and realistic interactions predict similar strength for the spin-orbit and tensor component. Large difference is only seen in the central channel. But as pointed out in Ref. [28], there is no trivial relation between the spin-tensor decomposition of the effective interaction and different components of the underlying NN potential. Especially, the tensor force of the NN potential may contribute significantly to the overall effective interaction when renormalization and core-polarization effects are taken into account [11].

In Table 11.7 is listed the wave functions calculated with the tensor force component removed from the effective interactions. In this case it is seen that the ground state wave function of ^{14}N is overwhelmingly dominated by the configuration of $|0p_{1/2}^{-2}\rangle$. This is because the non-diagonal matrix element $\langle 0p_{3/2}0p_{1/2}|V|0p_{1/2}^2\rangle^{J=1,T=0}$, which is crucial in inducing the configuration mixing, contain important contribution from the tensor force.

11.5 Alpha decay

In this form of decay the nucleus emits a ^{4}He$_2$ nucleus, i. e. an alpha particle. This is a traditional decay process which, as already mentioned above, was discovered even before beta and gamma decay. The physical mechanism which induces this form of decay has been found to be also responsible for other similar processes, like cluster and proton decay. We will study all these processes together, since formally there is no diference among them. However, we will concentrate in the alpha particle first because that was the historical sequence.

Alpha decay is the emission of an alpha particle from an unstable state in the decaying nucleus, i. e.

$$A \to B + \alpha \tag{11.62}$$

where A is called "mother mucleus", B "daughter mucleus" and α is the outgoing alpha particle.

Table 11.7: Wave functions of ^{14}C and ^{14}N calculated with the central force and central and spin-orbit force components of empirical and realistic effective interactions.

Interaction	η	κ	c	b	a
Central force only					
CK [19]	0.33	0.94	-0.15	-0.085	0.99
VWG [20]	0.29	0.96	-0.14	-0.086	0.99
WBT [21]	0.30	0.95	-0.11	-0.033	0.99
CD-Bonn(K)	0.33	0.94	-0.30	0.14	0.94
N^{3}LO(K)	0.32	0.95	-0.20	-0.017	0.98
CD-Bonn(G)	0.32	0.95	-0.27	0.0080	0.96
N^{3}LO(G)	0.30	0.95	-0.25	0.037	0.97
Central plus spin-orbit					
CK [19]	0.34	0.94	-0.15	-0.085	0.99
VWG [20]	0.32	0.95	-0.15	-0.053	0.99
WBT [21]	0.33	0.94	-0.12	-0.030	0.99
CD-Bonn(K)	0.35	0.94	-0.27	0.04	0.96
N^{3}LO(K)	0.34	0.94	-0.18	-0.11	0.98
CD-Bonn(G)	0.34	0.94	-0.25	-0.0071	0.97
N^{3}LO(G)	0.32	0.95	-0.23	-0.054	0.97

The theoretical study of this process was performed by Gamow in 1928, that is at the beginning of quantum mechanics. Gamow's explanation of the decay was the first application of the probabilistic interpretation of quantum mechanics.

Gamow assumed that the alpha particle exists on the surface of the mother nucleus at an excitation energy which is above the continuum threshold. From here it escapes the nucleus with a kinetic energy which, at large distances, takes the value E. This cannot happen in classical mechanics, since at that energy the kinetic energy of the particle would be imaginary while penetrating the barrier, that is the region denoted by a dashed line in Fig. (11.1). But Gamow realized that in quantum mechanics the centrifugal and Coulob barriers would trap the alpha particle inside the nucleus during a time before decaying. He evaluated the probability of the particle penetrating the barrier seen in Fig. 11.1 and could thus explain the relation between the decay half life and the kinetic energy of the escaping alpha particle. This was a tremendous success not only for Gamow himself but also, and specially, for quantum mechanics as a subject, since due to its apparent contradictions quantum mechanics was questioned by outstanding physicists at that time.

To evaluate the alpha decay half life we will consider the motion of the outgoing alpha particle. Inside the nucleus the two neutrons and two protons which eventually will form the alpha particle move under the influence of the interactions of the other nucleons. A proper microscopic calculation should be able to describe this motion and also the mechanism that clusters those neutrons and protons in the nuclear surface to become the alpha particle. We will not go into that mechanism, but rather assume that the alpha particle is already formed just inside the nuclear surface. The $^4He_2$ nucleus thus formed will be considered a spinless point particle located at a distance $\mathbf{r}$ from the center of the mother nucleus. We will denote the corresponding wave function by $\Psi^{(int)}_{lm}(\mathbf{r})$, where l is the alpha particle orbital angular momentum and m its z-projection. The label "(int)" indicates that this is the solution of the Schrödinger equation *inside* the nucleus. Since the intrinsic spin of the alpha particle is zero l is also the total angular momentum. When the alpha particle leaves the nucleus the only interaction it feels is the Coulomb force from the daugther nucleus. The solution of the corresponding Schrödinger equation, which also includes the centrifugal term, is known analytically. It has the form

$$\Psi^{(out)}_{lm}(\mathbf{r}) = N_l \frac{G_l(r) + iF_l(r)}{r} Y_{lm}(\hat{r}) \tag{11.63}$$

Where F_l (G_l) is a real function called the "regular" ("irregular") Coulomb function and $Y_{lm}(\hat{r})$ is the spherical harmonics. Since we assume spherical symmetry the angular momentum projection m does not influence the physics of the problem. We include it in the wave functions, e. g. in Eq. (11.63), for mathematical completeness.

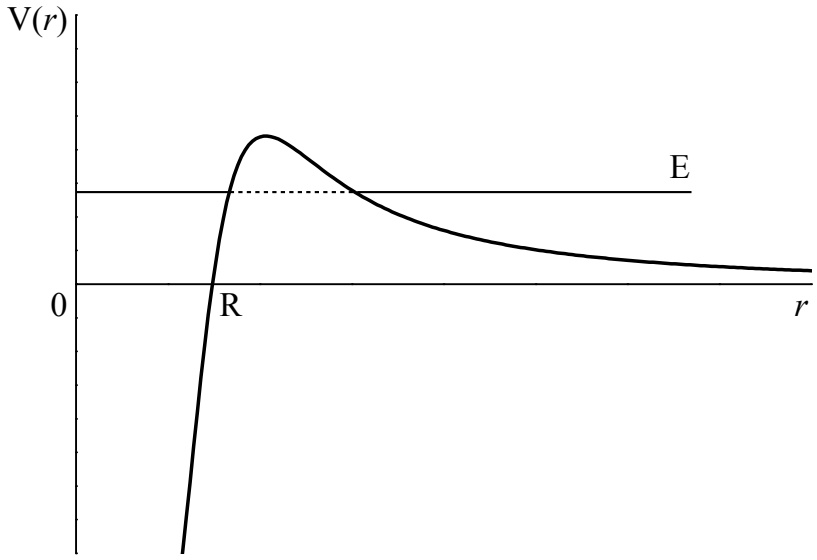

Figure 11.1: Unstable state at energy E from where the alpha particle is emitted. The penetrability is determined by the width of the barrier at the energy of the state, indicated by a dashed line.

At very large distances, where the Coulomb and centrifugal forces vanish, it is

$$G_l(r) + iF_l(r) \underset{r\to\infty}{\longrightarrow} e^{ikr} \tag{11.64}$$

where k is the wave number related to the kinetic energy E of the alpha particle by

$$E = \frac{\hbar^2 k^2}{2\mu} \tag{11.65}$$

μ is the alpha particle reduced mass. We can now evaluate the alpha decay rate, that is the probability rate per second that the alpha particle is emitted. For this we first notice that the measurement of the decaying alpha particle is performed at very large distance in comparisson to the nuclear size, since the nuclear size is of the order of 10^{-11} cm while the distance where the detector of the alpha particle is located is of the order of 10^2 cm. At that distance the alpha particle moves following a radial trajectory, i. e. its velocity is $\mathbf{v} = v\mathbf{r}/r$, where $v = \hbar k/\mu$. The number of alpha particles going through a volume $dV = dSdr$, where dS is a surface perpendicular to $\mathbf{v}$, is, at large distance, $d\mathcal{N}_l = |\Psi_{lm}^{(out)}(\mathbf{r})|^2 dV = |N_l e^{ikr} Y_{lm}(\hat{r})|^2 dV/r^2$. In spherical coordinates it is $dS = r^2 sin\theta d\theta d\phi$. Therefore the number of particles per unit time going through the surface dS is

$$\frac{d\mathcal{N}_l}{dt} = |N_l|^2 |Y_{lm}(\theta\phi)|^2 sin\theta d\theta d\phi \frac{dr}{dt} \tag{11.66}$$

Integrating over the angles one gets $\int |Y_{lm}|^2(\theta\phi) sin\theta d\theta d\phi$=1 and since $dr/dt = v$ the mean life τ, which is defined by $1/\tau = d\mathcal{N}_l/dt$, is

$$\frac{1}{\tau} = |N_l|^2 v \tag{11.67}$$

The width Γ_l of the resonance is related to the mean life by the energy-time relation $\Gamma_l \tau = \hbar$.

The constant N_l is obtained by matching the internal and external wave functions just outside at the surface of the nucleus, where the nuclear interaction is negligible and only the Coulomb and centrifugal forces are active. Calling that radius R one gets,

$$N_l = \frac{R\Psi_l^{(int)}(R)}{G_l(R) + iF_l(R)} \tag{11.68}$$

Thomas expression for the width

Collecting all factors together we finally get for the width the expression,

$$\Gamma_l = \frac{\hbar^2 k}{\mu} \frac{R^2 |\Psi_l^{(int)}(R)|^2}{F_l^2 + G_l^2} \tag{11.69}$$

The penetrability through the Coulomb and centrifugal barriers is

$$P_l(R) = \frac{kR}{F_l^2 + G_l^2} \tag{11.70}$$

In terms of the penetrability the width acquires the form,

$$\Gamma_l = \frac{\hbar^2 kR |\Psi_l^{(int)}(R)|^2}{\mu} P_l(R) \tag{11.71}$$

The penetrability is an exponential function of the energy and is the determinant factor in the value of the width. If the energy increases, then the penetrability also increases, as can be seen in Fig. (11.1). Therefore the probability that the particle is emitted increases strongly with increasing energy. That is, the half life decreases and the width increases.

The centrifugal barrier increases with the angular momentum. This implies that an alpha unstable nucleus will decay to a state that corresponds to the largest transition energy and the minimun angular momentum transfer.

The Gamow expression for the width contains the penetrability P_l but for the other factors in Eq. (11.71) he used a phenomenological form and instead of those factors he included a free parameter, which could be interpreted as a hitting frequency of the alpha particle on the walls of the nucleus. The expression (11.71) was obtained much later.

In principle one can evaluate the alpha decay width microscopically by using the shell model. One thus determines the probability that the alpha particle is formed on the nuclear surface and also whether the four nucleons that constitute the alpha particle are indeed clustered in a point. One then matches this function with the external function (11.63), as we did above. The width should not depend upon the matching point R. This is an important point, since if $\Gamma_l(R)$ depends on R then that is a sign that the calculation is defective.

In the late 1970's and early 1980's other radioactive decays were discovered, where instead of alpha particles heavier nuclei were emitted. These processes are called "cluster decay". Also proton decay was discovered, in which the emitted particle is a proton. All these cases can be evaluated in the same fashion as we did above. The only difference is that the internal wave function $\Psi_{lm}^{(int)}(\mathbf{r})$ should correspond to the case under study. This is rather straightforward to do for the proton case, but for heavy clusters it is a formidable task which was barely attempted so far.

11.6 Homework problems

Exercise 1:

a) Read the literature and describe briefly the reason why the neutrino was introduced as an elementary particle and which law requires that in the neutron beta decay an antineutrino is emitted?

c) Explain why the beta decay $p \rightarrow n + e^+ + \bar{\nu}$ and the electron capture $p + e^- \rightarrow n + \bar{\nu}$ are not possible.

d) Why the beta decay ${}^{147}_{68}Er \rightarrow e^- + \bar{\nu} + {}^{147}_{69}Tm$ is possible but ${}^{147}_{68}Er \rightarrow e^- + \bar{\nu} + {}^{147}_{63}Eu$ is not?.

Exercise 2:

a) Determine in the decay scheme shown in Fig. 11.2 whether it is β^+ or β^- the decay from the state 3^+ and from the state 3^-.

b) Determine the most likely spins and parities of the states in the nucleus $(N-1, Z+1)$ and the electromagnetic transitions among the levels in that Figure.

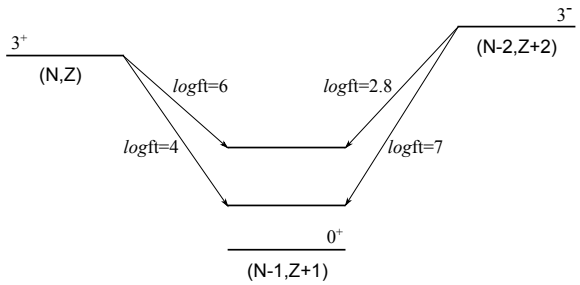

Figure 11.2: Beta decays of the odd-odd nuclei (N, Z) and $(N-2, Z+2)$.

c) Assign the most likely spins and parities, and the corresponding electromagnetic transition in the nucleus $(N-1, Z+1)$ of Fig. 11.3

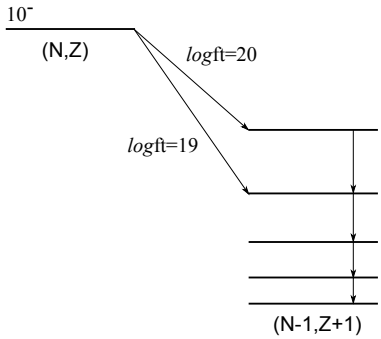

Figure 11.3: Beta decay of the odd-odd nucleus (N, Z).

Exercise 3:

Determine the order of importance regarding the transition probabilities among the alpha decay transitions shown in Fig. 11.4.

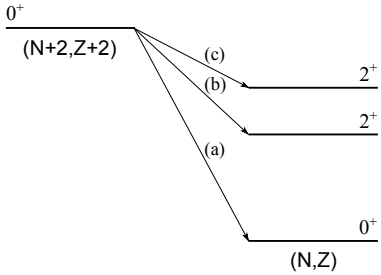

Figure 11.4: Alpha decay scheme of the even-even nucleus $(N+2, Z+2)$.

Exercise 4:

a)Give the coupling constants of beta decay (G_V and G_A) and compare them with those of EM, Strong interaction and gravitation. Is the weak interaction weaker than gravitation?

b) How does an experimental nuclear physicist proceed to determine the log ft value in a beta decay transition?

Exercise 5:

Calculate the Fermi and Gamow-Teller partial decay half-lives of the neutron. How long is the total half-life?

Bibliography

[1] Colloquium: The neutron lifetime Fred E. Wietfeldt and Geoffrey L. Greene Rev. Mod. Phys. 83, 1173 (2011).

[2] J. Liu et al. (UCNA Collaboration) Phys. Rev. Lett. 105, 181803 (2010). Determination of the Axial-Vector Weak Coupling Constant with Ultracold Neutrons

[3] D.R. Inglis, Rev. Mod. Phys. **25** 390 (1953).

[4] I. Talmi, *Fifty Years of the Shell Model– The Quest for the Effective Interaction*, Adv. Nucl. Phys. **27** 1 (2003).

[5] M.S. Fayache, L. Zamick, and H. Müther, Phys. Rev. C **60** 067305 (1999).

[6] J.W. Holt, G.E. Brown, T.T.S. Kuo, J.D. Holt, and R. Machleidt, Phys. Rev. Lett. **100** 062501 (2008).

[7] B. Jancovici and I. Talmi, Phys. Rev. **95** 289 (1954).

[8] H. J. Rose, O. Häusser, and E. K. Warburton, Rev. Mod. Phys. **40** 591 (1968).

[9] L. Zamick, Phys. Lett. **21** 194 (1966).

[10] D.C. Zheng and L. Zamick, Ann. Phys. (N.Y.) **206** 106 (1991).

[11] T.T.S. Kuo, G.E. Brown, Phys. Lett. **18** 54 (1965).

[12] J.W. Holt, N. Kaiser and W. Weise, Phys. Rev. C **79** 054331 (2009).

[13] J.W. Holt, N. Kaiser and W. Weise, arXiv: 1011.6623.

[14] P. Maris, J.P. Vary, P. Navratil, W.E. Ormand, H. Nam, and D.J. Dean, Phys. Rev. Lett. **106** 202502 (2011).

[15] M. Hjorth-Jensen, T.T.S. Kuo, and E. Osnes, Phys. Rep. **261** 125 (1995).

[16] A. Poves and A.P. Zuker, Phys. Rep. **70** 235 (1981).

[17] B. A. Brown and W. A. Richter Phys. Rev. C **74** 034315 (2006).

[18] M. Honma, T. Otsuka, T. Mizusaki, and M. Hjorth-Jensen, Phys. Rev. C **80** 064323 (2009).

[19] S. Cohen and D. Kurath, Nucl. Phys. **101** 1 (1967).

[20] A. G. M. van Hees, A. A. Wolters, P. W. M. Glaudemans, Nucl. Phys. **476** 61 (1988).

[21] E.K. Warburton and B.A. Brown, Phys. Rev. C **46** 923 (1992).

[22] W. T. Chou, E. K. Warburton, and B. A. Brown, Phys. Rev. C **47** 163 (1993).

[23] R. Machleidt, Phys. Rev. C **63** 024001 (2001).

[24] D.R. Entem and R. Machleidt, Phys. Rev. C **68** 041001(R) (2003).

[25] S.K. Bogner, T.T.S. Kuo, and A. Schwenk, Phys. Rep. **386** 1 (2003).

[26] C. Qi and F.R. Xu, Chin. Phys. C **32** (S2) 112 (2008).

[27] W. Visscher and R. Ferrell, Phys. Rev. **107** 781 (1957).

[28] M.W. Kirson, Phys. Lett. **B47** 110 (1973).

[29] K. Yoro, Nucl. Phys. **A333** 67 (1980).

Chapter 12

Nuclear energy and Nucleosynthesis

Fission. Energy production. Chain reactions. Fusion. Nucleosynthesis in stars. Hydrogen burning: the pp chain and CNO cycle. Helium burning. The burning of heavy elements. The end of the star.

The subject of this Chapter is vast and it is beyond the scope of this course to go into details of the calculations that will be presented here. Our aim is to give the main concepts leading to the explanation of the dynamic fission and fusion processes and the appearence of the observed matter in the Universe.

12.1 Fission

We have seen at the end of last Chapter that one of the channels taken by unstable nuclei in their way to stable configurations is alpha decay. In this case, as well as in all radioactive cluster decays, the nucleons that eventually constitute the emitted particle get clustered before emission. The formation of the cluster and its penetration through the Coulomb and centrifugal barriers takes a certain time which in average is the decay half life. The emitted particle escapes the daughter nucleus with an energy which is the Q-value of the process. It corresponds to the relative kinetic energy between the daughter nucleus and the particle. Since we will use this concept extensively in this Chapter, it is worthwhile to describe it shortly once again.

In the radioactive decay process

$$M \rightarrow D + C \tag{12.1}$$

where M is the mother nucleus, D the daughter and C the emitted cluster, energy conservation implies that the Q-value is

$$Q = B(D) + B(C) - B(M) \tag{12.2}$$

If the Q-value is positive then the decay occurs spontaneously. But there is another very similar process in which the mother nucleus breaks up spontaneously into two or more pieces, each piece consisting of a lighter nucleus. This is called fission.

Fission occurs spontaneously only in heavy nuclei. This is because the binding energy per nucleon increases up to the isotope Fe (Z=26) and for heavier isotopes it decreases steadily. Therefore light isotopes cannot fission, since the smaller binding energies of the outgoing particles with respect to the mother binding energy makes that the Q-value becomes negative.

Heavy isotopes usually decay by emitting alpha particles. This is because the binding energy of the alpha particle is large, and the nucleus decay by alpha emission before the fission process starts. Therefore it is not spontaneous fission which makes this process so important in nuclear physics. Rather it is induced fission which has become a very important tool in nuclear physics research and applications. The most common and useful induced fission is by bombarding a heavy isotope with neutrons at very small energy (that is moving slowly). In this condition the neutron will be absorbed by the target and the mother nucleus thus formed becomes unstable triggering the fission process described above. The neutron should carry an energy of about 0.025 eV only. These low energy neutrons are called "thermal neutrons".

This process is used in experimental nuclear physics to reach isotopes which are otherwise very difficult to detect. An example is the measurement of the spectrum of ^{141}Ba (Barium 141). This nucleus is produced in the reaction

$$^{235}U + n \rightarrow ^{236}U \underset{fission}{\longrightarrow} ^{141}Ba + ^{92}Kr + 3n \tag{12.3}$$

in which also are produced Krypton 92 and three neutrons, with the release of huge amounts of energy. With the help of magnetic fields the nucleus ^{141}Ba is directed to the measurement chamber.

The energy released in this reaction is used in energy production applications, as we will see below.

Energy production

The big fragments that result of the partition of the nucleus are isotopes with a definite proton value Z. But the number N of neutrons may differ by a few units. Therefore in the fission of a nucleus there is not an exact number of neutrons which are emitted, In particular the neutrons emitted in the reaction (12.3) are three in average. The energies of these neutrons are of the order of 1 MeV and, therefore, are many orders of magnitude larger than what is needed for any of them to start a new fission reaction. This is what happened in the first attempt, in the 1930's, to extract energy from the fission process. It was Fermi who realized that if one mixes the fissioning nuclei with a material that scatters the neutrons absorbing their energy, then one may get thermal neutrons which would start the fissioning process again. This material is called "moderator".

As it is shown in the Exercises, the energy output of the fission reaction is huge, of about 200 MeV. This energy is released as kinetic energy of the outgoing particles. The machines that transform this energy to forms which are of practical use (i. e. to thermal or electrical energy) are called "nuclear reactors". In thermal power plants it is the fuel that provides heat. In the same fashion, in nuclear reactors the fuel is the fissioning material. The nuclear fuel is usually contained in rods ("fuel rods") which are immersed in watter pools. The particles that are emitted in the fissioning process are absorbed by the water, thus transforming the kinetic energy into thermal energy. At the same time, this water acts also as moderator for the neutrons, contributing to the number of thermal neutrons that induce fission.

Chain reactions

The most common uranium isotope found in nature is ^{238}U and, therefore, one has to purify this isotope to get the quantity of ^{235}U needed to start the fissioning reaction (12.3). This is called uranium enrichmente. Only about 3 % of ^{235}U is contained in the fuel rods.

The process of fissioning through a thermal neutron hitting a fissionable material, thus generating new thermal neutrons which start the reaction again is called "chain reaction". The number of neutrons available in the chain reaction is a result of the equilibrium between the production of neutrons in the fission process and the losses due to absorption by other materials in the fuel rods or neutrons which leave the reactor without been scattered. When the number of neutrons which are available at the start of the reaction is the same from one generation to the next the chain reaction is self sustained and the reactor working condition is called "critical". If the production of neutrons increases from one fission event to the next, i. e. as the reaction chain proceeds, the power level also increases, and the reactor is said to be in a "supercritical" condition. Finally if the production of neutrons is low, and decreases from one generation to the next, the reactor is in a "subcritical" condition. To get a reactor to be critical, as all energy production reactors are, one has to use proper moderators, although also the amount of fissionable material and the configuration of the reactor is important.

Finally, and unfortunately, supercritical devices constitute the basis of nuclear weapon production.

Besides ^{235}U, two other fissionable heavy nuclei used in nuclear reactors are ^{239}Pu and ^{233}U. The process followed by these isotopes in the fission chain is the same as described above.

Theory of nuclear fission

Nuclear matter is incompressible and therefore models to explain fission treats nuclei as continuous fluids. The most successful is the liquid drop model, in which the nucleus is represented as a fluid drop, for instance a drop of water. According to this model the nucleus in an unstable state vibrates and changes form from spherical to a peanut-like, or like a number 8, shape. The Coulomb repulsion between the two lobes in the 8-shape separates them, arriving to two well differentiated spheres which finally depart from each other, thus fissioning the mother nucleus. Usually this process occurs so fast that it is not possible to measure any half-life. But in some cases the tunneling processes required to go from the spherical to the fissioning shape may take a long time. Therefore fission and decay can be viewed as similar mechanisms of decay. In fact the discovery of cluster decay mentioned at the end of last chapter, was predicted by analyzing the decay process within a fission theory.

http://www.nature.com/nature/journal/v409/n6822/pdf/409785a0.pdf

```
BARRIER code: Calculation of fission barriers
http://www.sciencedirect.com/science/article/pii/S001046559900199X
http://cpc.cs.qub.ac.uk/
```

12.2 Stability of superheavy elements

It has long been a fundamental question as to what are the maximum charge and mass that a nucleus may attain. According to classical physics, elements with $Z \geq 104$ should not exist due to the large Coulomb repulsive force. In the region of transuranium elements, the nuclei soon become unstable with increasing atomic number. They decay very fast through α emissions and spontaneous fissions. The occurrence of superheavy elements with $Z \geq 104$ is entirely due to quantal shell effects. Theoretically, predictions have been made that there should be an island of stability of superheavy nuclei around $N = 162$ or 184 and $Z = 108$, 114, 120, or 126.

Recently, signicant progress has been made experimentally in the synthesis of the heaviest elements. http://physics.aps.org/articles/v3/31

12.3 Fusion

Another form of nuclear energy is provided by fusion processes which are just the opposite to fission reactions. In fusion two light nuclei fuse together to form a heavier nucleus, releasing also huge amount of energy. From the energy production point of view the most promising fusion reaction is

$$^3H +^2 H \rightarrow^4 He + n \tag{12.4}$$

where tritium and deuteron, two isotopes of Hydrogen, fuse to form ^4He. These isotopes are found abundantly in Nature, since water (H_2O) consists mostly of Hydrogen and Helium is a noble gas which do not produce any contamination. Therefore if the fusion reaction would be technologically feasible, one part of the energy problem that affects society would disappear. although the large number of neutrons emitted in fusion reactions may still give rise to undesirable effects. But such a technology has not been developed yet, although huge and expensive efforts are been pursued in various places around the World (http://www.iter.org/).

Since the nuclear force is strongly attractive one may think that it should be relatively easy to fuse two nuclei. However, to achieve fusion one has to penetrate the Coulomb barrier induced by the protons in the nuclei, which requires very large energies and very high temperatures. This is the main difficult in the developing of fusion reactors.

Yet, fusion reactions are very common, since it is through these reactions that stars are powered and the elements that exist in Nature are created, as we will now study.

Heavy-ion fusion

When the incident energy is not so large and the system is not so light, the reaction process is predominantly governed by quantum tunneling over the Coulomb barrier created by the strong cancellation between the repulsive Coulomb force and the attractive nuclear interaction. Extensive experimental as well as theoretical studies have revealed that fusion reactions at energies near and below the Coulomb barrier are strongly influenced by couplings of the relative motion of the colliding nuclei to several nuclear intrinsic motions. Heavy-ion sub-barrier fusion reactions thus provide a good opportunity to address the general problem on quantum tunneling in the presence of couplings, which has been a popular subject in the past decade in many branches of physics and chemistry.

Theoretically the standard way to address the effects of the coupling between the relative motion and the intrinsic degrees of freedom on fusion is to numerically solve the coupled-channel equations, including all the relevant channels.

```
http://omnis.if.ufrj.br/~carlos/artigos/liqdrop1.pdf
http://iopscience.iop.org/0029-5515/47/8/001/pdf/0029-5515_47_8_001.pdf
Nucl. Fusion 47 (2007) 721727

A program for coupled-channel calculations with all order couplings
for heavy-ion fusion reactions
http://www.sciencedirect.com/science/article/pii/S001046559900243X
```

12.4 Nucleosynthesis in stars

Stars are formed through the presence of free protons in space which clump together under the influence of the gravitational field. Free neutrons do not exist in space since, as we discussed in the previous Chapter, they decay into protons.

In the center of the stars thus formed the protons are concentrated in a high temperature and high density environment. In this environment the protons interact with each other to produce heavier isotopes in a process that goes on until the protons are depleted.

The reactions that induce the creation of isotopes heavier than protons follow a rather complicated pattern. First occurs a series of proton-proton reactions (called the pp chain), and then protons collide with the heavier particles that are created through the pp chain, particularly Carbon, Nitrogen and Oxygen (called the CNO cycle).

Hydrogen burning: the pp chain and CNO cycle

Our Sun belongs to the category of stars where the pp reaction chain takes place. The energy released in these reactions is the solar energy which in our planet is responsible for everything which is alive.

As we have already mentioned, there are no free neutrons available after the formation of stars. The question is then how the pp reactions could produce heavier elements without neutrons available to yield deuterons. It was Bethe who realized in 1938 that nucleosynthesis in stars begins with the beta-decay reaction

$$p + p \longrightarrow d + e^{+} + \nu \tag{12.5}$$

The energy released in this reaction is Q=1.44 MeV. To obtain this energy one can not use Eq. (12.2), since now the number of neutrons and protons in the entrance channel (two protons and no neutrons) is not the same as in the exit channel (deuteron, i. e. one neutron and one proton). One has to use the atomic binding energies instead of the nuclear ones. As function of the mass excess the Q-value corresponding to the reaction

$$a + A \longrightarrow b + B \tag{12.6}$$

acquires the form.

$$Q = (\Delta M_a + \Delta M_A - \Delta M_b - \Delta M_B)c^2 \tag{12.7}$$

The mass excesses and other related quantities are tabulated in a number of papers. In Internet these values can be found in the same site as the nuclear binding energies.

The 1.44 MeV released by each pair of protons in the process (12.5) induces in the center of the star huge temperatures. If one considers the star as an energy emitting black body, which is a quiet reasonable approximation, then one would expect the energy and temperature to be related by $E = kT$, where $k = 8.62 \times 10^{-11} MeV/T$ is the Boltzmann constant and T is degree-Kelvin. Therefore the temperature would be $T = 1.7 \times 10^{10} K$. But one has also to consider the reaction probability in the stellar environment and the corresponding thermal distribution. This calculation is beyond the scope of the present course. We will only give the final result which corresponds to the state of equilibrium at the center of the star. This occurs at a temperature of about $T = 1.6 \times 10^{7} K$.

To estimate the production of deuterons in the process (12.5) one has to evaluate the corresponding cross section, which turns out to be very small because it is determined by the weak forces in that process. One can say that it is because the weak interaction determines the first step of the stellar nucleosynthesis that the sun is still shining today. If instead of the weak force it was the strong force that started the solar nucleosynthesis, the corresponding cross section would be many orders of magnitude larger and the burning of protons would occur very fast. As a result the Sun would have died just in the beginning of the Earth creation. On the contrary, at the present rate of hydrogen consumption, the sun will leave about 5 billion years more, when it will become a red giant. We will come back to this subject.

Another reaction that could produce a deuteron, instead of (12.5), is

$$p + e^{-} + p \longrightarrow d + \nu. \tag{12.8}$$

It was found that the cross section corresponding to this reaction, which is called PEP, is even smaller than the reaction (12.5) by 4 orders of magnitude and, therefore, does not play a significant role in the production of deuterons.

Deuterons in stars are then produced through the reaction (12.5). With deuterons thus formed the next question is how these deuterons react with other particles to continue the burning process leading to heavier elements. Of all the possible reactions having the deuteron as a target the most likely to occur is $d(p,\gamma)^3He$. This is because in the environment of the star at this stage of nucleosynthesis the number of protons is overwhelmingly larger than the number of any other particle. This reaction has the lowest Coulomb barrier of all fusion reactions in the pp chain (except the weak $p+p \to d$)

Rather involved calculations showed that the burning of ^{3}He is done through a chain of reactions as follows,

- *Chain I* (86% of the burning)

$p(p,e^+\nu)d \to d(p,\gamma)^3He \to^3 He(^3He,2p)^4He$

- *Chain II* (14% of the burning)

$p(p,e^+\nu)d \to d(p,\gamma)^3He \to^3 He(\alpha,\gamma)^7Be \to^7 Be(e^-,\bar{\nu})^7Li \to^7 Li(p,\alpha)^4He$

- *Chain III* (0.02% of the burning)

$p(p,e^+\nu)d \to d(p,\gamma)^3He \to^3 He(\alpha,\gamma)^7Be \to^7 Be(p,\gamma)^8B \to^8 B(e^+,\gamma)^8Be^*$
$\to^8 Be^*(\alpha)\alpha$

One sees that at the end of these reactions only alpha particles, i. e. Helium, is left.

CNO cycle

Besides the pp chain there is another path through which Hydrogen is burned. One of the most abundant of the heavy elements present in the star is ^{12}C. Protons react with ^{12}C inducing a cycle as follows
$^{12}C(p,\gamma)^{13}N \to^{13} N(e^+,\nu)^{13}C \to^{13} C(p,\gamma)^{14}N \to^{14} N(p,\gamma)^{15}O \to^{15} O(e^+,\nu)^{15}N \to^{15} N(p,\alpha)^{12}C$

The net result of this cycle, called the CN cycle, is that four protons are converted into Helium (Q=26.73 MeV). These four protons, which are consumed at the end of the cycle, are the ones involved in the reactions $^{12}C(p,\gamma)^{13}N$, $^{13}C(p,\gamma)^{14}N$, $^{14}N(p,\gamma)^{15}O$ and $^{15}N(p,\alpha)^{12}C$. The Helium (α particle) is created at the end of the cycle. Besides there are two positrons and two neutrinos created in this cycle.

The extraordinary feature of the CN cycle is that ^{12}C is only used as a catalyst. That is, it is not consumed at all, it starts the cycle and at the end it appears again to start a new cycle. Therefore, although its abundance is very small (about 3×10^{-6}) it contributes significantly to the production of alpha particles and also to the burning of protons.

Attach to the CN cycle appears another one starting in ^{16}O as follows,
$^{16}O(p,\gamma)^{17}F \to^{17} F(e^+,\nu)^{17}O \to^{17} O(p,\alpha)^{14}N \to^{14} N(p,\gamma)^{15}O \to^{15} O(e^+,\gamma)^{15}N \to^{15} N(p,\gamma)^{16}O$

Once again the cycle is completed without any consumption of ^{16}O, which is restored at the end of the cycle at it happened above with ^{12}C. As in that case, four protons are burned to produce an alpha particle, two neutrinos and two positrons. Noticed that ^{16}O is produced through ^{15}N, which was created in the CN cycle. But since no element is burned here the two cycles go in parallel without interruption. The combination of these two cycles is called the CNO cycle.

The hydrogen burning of the pp chain and the CNO cycle continues until the hydrogen fuel is nearly consumed. As a result the outgoing pressure of the radiation diminishes and the ashes, i. e. helium, are pressed towards the center of the star. The remaining hydrogen, being much lighter than helium, forms a layer above the helium ground. Under the gravitational force, the helium core contracts itself and, at the same time, becomes hotter. This induces an increasing rate of pp reactions in the outer layer of hydrogen (instead of in the center of the star, as have happened so far) which vastly raises the luminosity of the star by a factor of 1,000 to 10,000 times. The very hot hydrogen gas on the surface of the star expands also by very large factors and, at the same time, the outer regions of the layer becomes cooler. This causes the spectrum of the light emitted from the star to shift towards the red, thus given rise to the stars called red giants.

The first step after the burning of hydrogen is the burning of helium. This we will study in the next Section.

Helium burning

When a star reaches the stage of a red giant its core consists mainly of helium. But it is very difficult to proceed farther from helium in the path of heavier isotopes because the N=5 nuclei are not stable. The most likely channel is

$$\alpha + \alpha \to {}^8\text{Be}. \tag{12.9}$$

The ground state of ^{8}Be is unbound with respect to α decay with a Q_α value of 91.84keV and a decay width of 5.57eV. But from here no reasonable reaction was found to proceed forward. Yet, after helium

it is oxygen, carbon and nitrogen the most abundant elements in the Universe. The only way out of this difficult was to assume that there was a resonance at about 7.7 MeV in ^{12}C such that the reaction proceeds through the resonance by means of the reaction

$$\alpha + {}^{8}\mathrm{Be} \rightarrow {}^{12}\mathrm{C}^{*} \tag{12.10}$$

where $^{12}C^*$ is the resonant state. This process is referred to as triple-α reaction. This mechanism was proposed by Hoyle in 1953. Hoyle used the fact that ^{12}C is abundant in the universe as evidence for the existence of the ^{12}C resonance. Since no experimental evidence of such resonance existed, Hoyle's idea induced some experimental efforts in that direction. One of the greatest success of nucleosynthesis occurred in 1957 when it was experimentally found that a resonance with the exact properties needed for the production of carbon indeed existed. The existence of such resonant states, greatly increases the nuclear reaction rate.

Helium burning continues via the $^{12}\mathrm{C}(\alpha,\gamma)^{16}\mathrm{O}$ reaction. There is no resonance near or above the α-particle threshold in ^{16}O and thus this process must proceed via broadresonance tails and direct mechanisms.

Summarizing what we have described so far, i. e. the creation of isotopes up to oxygen, we have started with the burning of protons in the production of helium through the pp chain. This process went on until hydrogen was near exhaustion and the pp chain was terminated. Due to its higher weight, the helium left as ashes built a core upon which rested a layer of hydrogen. The helium core then contracted under the influence of gravitation and high temperatures were reached. This ignited the hydrogen in the layer, which expanded forming an enormous halo of a warm gas that irradiated light in the red region of the spectrum. A red giant star was thus formed. The core of a red giant star consists of helium, which under additional gravitational contraction reacts to form ^{8}Be and through it ^{12}C. The path leading to this nucleus is very involved. It was predicted before it was corroborated experimentally in one of the most resonant success of rather simple nuclear physics arguments. The carbon thus created, still immerse in a see of alpha particles, reacts to create oxygen and small quantities of other nearby isotopes. This process of helium burning proceeds up to the point when helium itself is not enough to induce additional reactions and the helium burning process is terminated. The core consists now mainly of carbon and oxygen. Above this heavy core there are two layers, the lowest consists of helium and the upper one, forming the surface of the star, is hydrogen. As in previous stages of nucleosynthesis, gravitation contracts the core farther and carbon, oxygen and, in successive steps, heavier elements start to react. This we will analyze below.

The burning of heavy elements

The burning of heavy elements depends strongly upon the capacity of the gravitational force. If the star is massive enough the core will contract and the temperature and density will increase until the residues of the helium burning, i. e. carbon and oxygen ashes, starts to ignite. Since the Coulomb barrier is lower for carbon, this will be the first to react, resulting in the formation of neon, sodium and magnesium. The corresponding carbon burning reactions are

$^{12}_{6}C_6 + {}^{12}_{6}C_6 \rightarrow {}^{20}_{10}Ne_{10} + {}^{4}_{2}He_2$
$^{12}_{6}C_6 + {}^{12}_{6}C_6 \rightarrow {}^{23}_{11}Na_{12} + {}^{1}_{1}H_0$
$^{12}_{6}C_6 + {}^{12}_{6}C_6 \rightarrow {}^{23}_{12}Mg_{11} + n$

The path followed by this carbon burning process depends upon the mass of the star. We will come back to this point. In what follows we will assume that the mass is high enough for nucleosynthesis to proceed farther. This continues in the same fashion as before. Thus, the production of the heavy elements neon, sodium and magnesium in the reactions above is terminated when the fuel, i. e. carbon, is nearly consumed, The heavy nuclei become now the core of the star. Carbon floats above this core forming the deepest layer in the surface of the star. Gravitation induces the core to contract until a temperature and density is reached such that high energy photons are produced. These photons interact with neon inducing the reactions

$^{20}_{10}Ne_{10} + \gamma \rightarrow +{}^{16}_{8}O_8 + \alpha$
$^{20}_{10}Ne_{10} + \alpha \rightarrow {}^{24}_{12}Mg_{12} + \gamma$

After neon is consumed the core consists of magnesium and oxygen. Again this core contracts and the oxygen burning process starts. A series of reactions takes place the result of which is that silicon is produced. Even more complex is the mechanism induced by silicon burning. Hundreds of reactions take place and high energy neutrinos are abundantly produced. Since these neutrinos escape the star

carrying with them an appreciable amount of energy, the energy output of silicon burning is not very large. Instead, the energy produced in the burning process is spent in producing a very rapid conversion of the core to iron and nickel. These are the most tightly bound nuclei that exist in Nature and, as a result, they cannot participate in any reaction leading to even tighter elements, thereby releasing energy, as it happened so far. Without this outflow of radiation to stabilize the inner pressure of gravitation, the core collapses. In its way to its end the star undergoes a rapid succession of reactions in what is called the "r-process".

The end of the star

The evolution of the star depends upon its capacity to burn different isotopes in its interior. The energy that induces this burning is provided by the gravitational force, which compress the star and heats its core. Since the gravitational force is determined by the mass of the star, it is this quantity that governs the evolution of the star. Thus, a star with a mass of less than about 0.5 $M_\odot$, where $M_\odot$ is the solar mass, will be able to burn protons, but the fuel will not be enough to start the burning of helium. Due to the low gravitation a layer of hydrogen floats on the surface of the star, where it becomes cooler and its emitted light turns to the red part of the spectrum. These stars are called red dwarfs. They can live very long time, since the burning of hydrogen proceeds very slowly. But eventually the hydrogen fuel will be consumed and the star will contract under the effect of gravitation to become an small and very compact object. The big pressure inside this stage of the star makes that the electrons present in the star are packed together up to the limit of what the Pauli principle allows. Farther pressure will be resisted and the collapse of the star will be prevented. This process is called "electron degeneracy pressure".

After shrinking to the limit allowed by electron degeneracy the outer hydrogen layer in the red dwarf disappears and the light emitted by the small and compact object which is left turns to white. The star becomes a white dwarf. The white dwarf will also live a very long time, emitting the thermal radiation left after hydrogen burning. When this source of energy is also depleted, the star will become a black dwarf. However, this process will take much more time than the age of the Universe, and therefore no black dwarfs, or effects induced by their presence, have been observed so far.

But the white dwarf may finish in a much more dramatic fashion if another star lying nearby provides mass. Usually this companion star is surrounded by a disk of gaseous matter which is absorbed by the white dwarf. When the mass of the white dwarf reaches the value of 1.4 $M_\odot$ (this is called the Chandrasekhar limit) the electron degeneracy pressure is overcome and the star collapses under gravitation. An enormous explosion occurs and the mass of the star is irradiated. The radiation energy thus emitted may be at least as high as the radiation emitted by the whole galaxy where the star belongs (depending on the size of the galaxy). This brilliant object is called supernova. Actually, and as we will see below, there other ways of producing supernovas. The one induced by white dwarfs by accretion of matter from a companion star is called supernova Ia. These supernovas are excellent candles in astronomy since one knows exactly the energy emitted by the supernova and, equally important, the spectrum of the light emitted has a very characteristic shape and composition which makes it possible to recognize it.

Stars with masses in the range (0.5-6)$M_\odot$ become red giants following the process that we have described above. Given the mass of our Sun, it will finish as a red giant.

Stars with masses in the range 6 to 20 $M_\odot$ follow the same pattern of evolution as red giants but to a larger extend and, therefore, they become red supergiants. The interplay among all the quantities that influence the evolution of these stars is very complicated and it may take different paths towards the end. They may evolve as red giants do, finishing as white dwarfs. But they may also keep a heavy core that induces a gravitational force large enough to overcome the electron degeneracy pressure. Without this pressure the star contracts without opposition and eventually, in a period that last about one day only (in this period occurs the r-process!) finishes as a supernova called type II.

Stars with masses up to $120M_\odot$ generates so much heat in their interior that the resulting radiation pressure may blow up the whole stellar envelope. After this the star evolves into a red supergiant and finally either a supernova or even a black hole. A black hole is an object from where, due to gravitation, light cannot escape. It does not need to be an extremely dense object, as can be seen by calculating its density (General Relativity and Classical Mechanics provide the same result for this number and, therefore, its calculation is left as an Exercise). It is very difficult to predict which star would finish as a black hole, since the mechanism of supernova collapse itself is not well understood.

Stars cannot be more massive than $120M_\odot$ because this is the limit where the external pressure of the radiation equilibrates the internal pressure of gravity (this is called "Eddington limit"). Over this limit

the heat generated in the center of the star produces an external pressure which overruns gravitation. The star thus disappears before even it is formed.

When stars collapse a process of electron capture may take place. These electrons convert the protons into neutrons, thus forming a neutral object. The Coulomb forces that keeps nucleons apart disappears and the star becomes a very small and dense neutral object called neutron star. The neutron stars do not collapse to become black holes because the neutrons feel the Pauli effect in a similar way as electrons do in the electron degeneracy pressure. But they become extremely dense and small objects, with radii of a few kilometers. As they shrink, these objects rotates more and more rapidly due to conservation of angular momentum, reaching an angular velocity of several hundred revolutions per second. Under such extremely rapid rotations the intrinsic magnetic moment of the star induces a very strong magnetic field that is detected in Earth as a pulse of radiation, which gave to these stars the name of "pulsars". When pulsars were first observed in 1967 it was thought that they were radio signals emitted by an advanced extraterrestrial civilization. The researchers that found this object called it LGM-1, which means Little Green Man number 1.

The dynamics of neutron stars are determined by the physical properties of neutrons in dense nuclear matter. This is a subject which is at the front of nuclear physics studies at present.

http://www.int.washington.edu/PHYS554/2011/2011.html

AlterBBN: A program for calculating the BBN abundances of the elements
in alternative cosmologies
http://www.sciencedirect.com/science/article/pii/S0010465512001233

The r-process of stellar nucleosynthesis:
Astrophysics and nuclear physics
achievements and mysteries
http://arxiv.org/pdf/0705.4512.pdf

http://arxiv.org/pdf/1202.6577.pdf

Big Bang Nucleosynthesis
http://arxiv.org/abs/astro-ph/0406663

Bibliography

[1] Rep. Prog. Phys. 74 (2011) 096901. Nuclear astrophysics: the unnished quest for the origin of the elements, Jordi Jose, and Christian Iliadis.

Chapter 13

Constants and units

Natural units are physical units of measurement based only on universal constants. For example the elementary charge e is a natural unit of electric charge, or the speed of light c is a natural unit of speed. In nuclear physics, the most useful units are $\hbar$, c, fm, MeV.

Table 13.1: The values in SI units of some non-SI units based on the 2010 CODATA adjustment of the values of the constants.

Quantity	Symbol	Numerical value	Unit	Relative std. uncert. u_r
electron volt: (e/C) J	eV	$1.602\,176\,565(35) \times 10^{-19}$	J	2.2×10^{-8}
atomic mass unit: $\frac{1}{12}m(^{12}\mathrm{C})$	u	$1.660\,538\,921(73) \times 10^{-27}$	kg	4.4×10^{-8}
		Natural units (n.u.)		
n.u. of velocity	c, c_0	299 792 458	m s^{-1}	exact
n.u. of action: $h/2\pi$	$\hbar$	$1.054\,571\,726(47) \times 10^{-34}$	J s	4.4×10^{-8}
		$6.582\,119\,28(15) \times 10^{-16}$	eV s	2.2×10^{-8}
	$\hbar c$	197.326 9718(44)	MeV fm	2.2×10^{-8}
n.u. of mass	m_e	$9.109\,382\,91(40) \times 10^{-31}$	kg	4.4×10^{-8}
n.u. of energy	$m_e c^2$	$8.187\,105\,06(36) \times 10^{-14}$	J	4.4×10^{-8}
		0.510 998 928(11)	MeV	2.2×10^{-8}
n.u. of momentum	$m_e c$	$2.730\,924\,29(12) \times 10^{-22}$	kg m s^{-1}	4.4×10^{-8}
		0.510 998 928(11)	MeV/c	2.2×10^{-8}
n.u. of length: $\hbar/m_e c$		$386.159\,268\,00(25) \times 10^{-15}$	m	6.5×10^{-10}
n.u. of time	$\hbar/m_e c^2$	$1.288\,088\,668\,33(83) \times 10^{-21}$	s	6.5×10^{-10}
		Atomic units (a.u.)		
a.u. of charge	e	$1.602\,176\,565(35) \times 10^{-19}$	C	2.2×10^{-8}
a.u. of mass	m_e	$9.109\,382\,91(40) \times 10^{-31}$	kg	4.4×10^{-8}
a.u. of action: $h/2\pi$	$\hbar$	$1.054\,571\,726(47) \times 10^{-34}$	J s	4.4×10^{-8}
a.u. of Bohr radius $\alpha/4\pi R_\infty$	a_0	$0.529\,177\,210\,92(17) \times 10^{-10}$	m	3.2×10^{-10}
a.u. of Hartree energy $e^2/4\pi\epsilon_0 a_0 = \alpha^2 m_e c^2$	E_h	$4.359\,744\,34(19) \times 10^{-18}$	J	4.4×10^{-8}
a.u. of time	$\hbar/E_h$	$2.418\,884\,326\,502(12) \times 10^{-17}$	s	5.0×10^{-12}
a.u. of force	E_h/a_0	$8.238\,722\,78(36) \times 10^{-8}$	N	4.4×10^{-8}
a.u. of velocity: αc	$a_0 E_h/\hbar$	$2.187\,691\,263\,79(71) \times 10^{6}$	m s^{-1}	3.2×10^{-10}
a.u. of momentum	$\hbar/a_0$	$1.992\,851\,740(88) \times 10^{-24}$	kg m s^{-1}	4.4×10^{-8}
a.u. of current	$eE_h/\hbar$	$6.623\,617\,95(15) \times 10^{-3}$	A	2.2×10^{-8}
a.u. of charge density	e/a_0^3	$1.081\,202\,338(24) \times 10^{12}$	C m^{-3}	2.2×10^{-8}
a.u. of electric potential	E_h/e	27.211 385 05(60)	V	2.2×10^{-8}
a.u. of electric field	E_h/ea_0	$5.142\,206\,52(11) \times 10^{11}$	V m^{-1}	2.2×10^{-8}
a.u. of el dipole mom	ea_0	$8.478\,353\,26(19) \times 10^{-30}$	C m	2.2×10^{-8}
a.u. of el quadrupole mom	ea_0^2	$4.486\,551\,331(99) \times 10^{-40}$	C m^2	2.2×10^{-8}

The Bohr radius approximately equals to the most probable distance between the proton and electron in a hydrogen atom in its ground state.

$$a_0 = \frac{4\pi\varepsilon_0\hbar^2}{m_e e^2} = \frac{\hbar}{m_e c\alpha} = \frac{\alpha}{4\pi R_\infty}, \tag{13.1}$$

where ε_0 is the permittivity of free space. The Rydberg constant is defined as $R_\infty = \alpha^2 m_e c/2h$. A muonic hydrogen atom consists of a negative muon and a proton. Since $m_\mu/m_e \approx 207$, the Bohr radius of the muon is about 200 times smaller than the electron Bohr radius.

Table 13.2: The values of some energy equivalents derived from the relations $E = mc^2 = hc/\lambda = h\nu = kT$; 1 eV = (e/C) J, 1 u = $m_\mathrm{u} = \frac{1}{12}m(^{12}\mathrm{C}) = 10^{-3}$ kg mol$^{-1}/N_\mathrm{A}$.

	Relevant unit			
	J	kg	m^{-1}	Hz
1 J	$(1\ \mathrm{J}) =$ 1 J	$(1\ \mathrm{J})/c^2 =$ $1.112\,650\,056\ldots \times 10^{-17}$ kg	$(1\ \mathrm{J})/hc =$ $5.034\,117\,01(22) \times 10^{24}$ m^{-1}	$(1\ \mathrm{J})/h =$ $1.509\,190\,311(67) \times 10^{33}$ Hz
1 kg	$(1\ \mathrm{kg})c^2 =$ $8.987\,551\,787\ldots \times 10^{16}$ J	$(1\ \mathrm{kg}) =$ 1 kg	$(1\ \mathrm{kg})c/h =$ $4.524\,438\,73(20) \times 10^{41}$ m^{-1}	$(1\ \mathrm{kg})c^2/h =$ $1.356\,392\,608(60) \times 10^{50}$ Hz
1 m^{-1}	$(1\ \mathrm{m}^{-1})hc =$ $1.986\,445\,684(88) \times 10^{-25}$ J	$(1\ \mathrm{m}^{-1})h/c =$ $2.210\,218\,902(98) \times 10^{-42}$ kg	$(1\ \mathrm{m}^{-1}) =$ 1 m^{-1}	$(1\ \mathrm{m}^{-1})c =$ 299 792 458 Hz
1 Hz	$(1\ \mathrm{Hz})h =$ $6.626\,069\,57(29) \times 10^{-34}$ J	$(1\ \mathrm{Hz})h/c^2 =$ $7.372\,496\,68(33) \times 10^{-51}$ kg	$(1\ \mathrm{Hz})/c =$ $3.335\,640\,951\ldots \times 10^{-9}$ m^{-1}	$(1\ \mathrm{Hz}) =$ 1 Hz
1 K	$(1\ \mathrm{K})k =$ $1.380\,6488(13) \times 10^{-23}$ J	$(1\ \mathrm{K})k/c^2 =$ $1.536\,1790(14) \times 10^{-40}$ kg	$(1\ \mathrm{K})k/hc =$ 69.503 476(63) m^{-1}	$(1\ \mathrm{K})k/h =$ $2.083\,6618(19) \times 10^{10}$ Hz
1 eV	$(1\ \mathrm{eV}) =$ $1.602\,176\,565(35) \times 10^{-19}$ J	$(1\ \mathrm{eV})/c^2 =$ $1.782\,661\,845(39) \times 10^{-36}$ kg	$(1\ \mathrm{eV})/hc =$ $8.065\,544\,29(18) \times 10^{5}$ m^{-1}	$(1\ \mathrm{eV})/h =$ $2.417\,989\,348(53) \times 10^{14}$ Hz
1 u	$(1\ \mathrm{u})c^2 =$ $1.492\,417\,954(66) \times 10^{-10}$ J	$(1\ \mathrm{u}) =$ $1.660\,538\,921(73) \times 10^{-27}$ kg	$(1\ \mathrm{u})c/h =$ $7.513\,006\,6042(53) \times 10^{14}$ m^{-1}	$(1\ \mathrm{u})c^2/h =$ $2.252\,342\,7168(16) \times 10^{23}$ Hz
1 E_h	$(1\ E_\mathrm{h}) =$ $4.359\,744\,34(19) \times 10^{-18}$ J	$(1\ E_\mathrm{h})/c^2 =$ $4.850\,869\,79(21) \times 10^{-35}$ kg	$(1\ E_\mathrm{h})/hc =$ $2.194\,746\,313\,708(11) \times 10^{7}$ m^{-1}	$(1\ E_\mathrm{h})/h =$ $6.579\,683\,920\,729(33) \times 10^{15}$ Hz

Table 13.3: The values of some energy equivalents derived from the relations $E = mc^2 = hc/\lambda = h\nu = kT$; 1 eV = (e/C) J, 1 u = $m_\mathrm{u} = \frac{1}{12}m(^{12}\mathrm{C}) = 10^{-3}$ kg mol$^{-1}/N_\mathrm{A}$.

	Relevant unit			
	K	eV	u	E_h
1 J	$(1\ \mathrm{J})/k =$ $7.242\,9716(66) \times 10^{22}$ K	$(1\ \mathrm{J}) =$ $6.241\,509\,34(14) \times 10^{18}$ eV	$(1\ \mathrm{J})/c^2 =$ $6.700\,535\,85(30) \times 10^{9}$ u	$(1\ \mathrm{J}) =$ $2.293\,712\,48(10) \times 10^{17}\ E_\mathrm{h}$
1 kg	$(1\ \mathrm{kg})c^2/k =$ $6.509\,6582(59) \times 10^{39}$ K	$(1\ \mathrm{kg})c^2 =$ $5.609\,588\,85(12) \times 10^{35}$ eV	$(1\ \mathrm{kg}) =$ $6.022\,141\,29(27) \times 10^{26}$ u	$(1\ \mathrm{kg})c^2 =$ $2.061\,485\,968(91) \times 10^{34}\ E_\mathrm{h}$
1 m^{-1}	$(1\ \mathrm{m}^{-1})hc/k =$ $1.438\,7770(13) \times 10^{-2}$ K	$(1\ \mathrm{m}^{-1})hc =$ $1.239\,841\,930(27) \times 10^{-6}$ eV	$(1\ \mathrm{m}^{-1})h/c =$ $1.331\,025\,051\,20(94) \times 10^{-15}$ u	$(1\ \mathrm{m}^{-1})hc =$ $4.556\,335\,252\,755(23) \times 10^{-8}\ E_\mathrm{h}$
1 Hz	$(1\ \mathrm{Hz})h/k =$ $4.799\,2434(44) \times 10^{-11}$ K	$(1\ \mathrm{Hz})h =$ $4.135\,667\,516(91) \times 10^{-15}$ eV	$(1\ \mathrm{Hz})h/c^2 =$ $4.439\,821\,6689(31) \times 10^{-24}$ u	$(1\ \mathrm{Hz})h =$ $1.519\,829\,846\,0045(76) \times 10^{-16}\ E_\mathrm{h}$
1 K	$(1\ \mathrm{K}) =$ 1 K	$(1\ \mathrm{K})k =$ $8.617\,3324(78) \times 10^{-5}$ eV	$(1\ \mathrm{K})k/c^2 =$ $9.251\,0868(84) \times 10^{-14}$ u	$(1\ \mathrm{K})k =$ $3.166\,8114(29) \times 10^{-6}\ E_\mathrm{h}$
1 eV	$(1\ \mathrm{eV})/k =$ $1.160\,4519(11) \times 10^{4}$ K	$(1\ \mathrm{eV}) =$ 1 eV	$(1\ \mathrm{eV})/c^2 =$ $1.073\,544\,150(24) \times 10^{-9}$ u	$(1\ \mathrm{eV}) =$ $3.674\,932\,379(81) \times 10^{-2}\ E_\mathrm{h}$
1 u	$(1\ \mathrm{u})c^2/k =$ $1.080\,954\,08(98) \times 10^{13}$ K	$(1\ \mathrm{u})c^2 =$ $931.494\,061(21) \times 10^{6}$ eV	$(1\ \mathrm{u}) =$ 1 u	$(1\ \mathrm{u})c^2 =$ $3.423\,177\,6845(24) \times 10^{7}\ E_\mathrm{h}$
1 E_h	$(1\ E_\mathrm{h})/k =$ $3.157\,7504(29) \times 10^{5}$ K	$(1\ E_\mathrm{h}) =$ 27.211 385 05(60) eV	$(1\ E_\mathrm{h})/c^2 =$ $2.921\,262\,3246(21) \times 10^{-8}$ u	$(1\ E_\mathrm{h}) =$ 1 E_h

Table 13.4: Some exact and measured quantities.

Quantity	Symbol	Value
speed of light in vacuum	c, c_0	299 792 458 m s^{-1}
magnetic constant	μ_0	$4\pi 10^{-7}$ N A^{-2} = 12.566 370 614 $\times 10^{-7}$ N A^{-2}
electric constant	ϵ_0	$(\mu_0 c^2)^{-1}$ = 8.854 187 817... $\times 10^{-12}$ F m^{-1}
Newtonian constant	G	6.673 84(80) $\times 10^{-11}$ m^3 kg^{-1} s^{-2}
of gravitation	$G/\hbar c$	6.708 37(80) $\times 10^{-39}$ $(GeV/c^2)^{-2}$
Planck constant	h	6.626 069 57(29) $\times 10^{-34}$ J s
		4.135 667 516(91) $\times 10^{-15}$ eV s
$h/2\pi$	$\hbar$	1.054 571 726(47) $\times 10^{-34}$ J s
		6.582 119 28(15) $\times 10^{-16}$ eV s
	$\hbar c$	197.326 9718(44) MeV fm
Planck mass $(\hbar c/G)^{1/2}$	m_P	2.176 51(13) $\times 10^{-8}$ kg
energy equivalent	$m_P c^2$	1.220 932(73) $\times 10^{19}$ GeV
Planck temperature $(\hbar c^5/G)^{1/2}/k$	T_P	1.416 833(85) $\times 10^{32}$ K
Planck length $\hbar/m_P c = (\hbar G/c^3)^{1/2}$	l_P	1.616 199(97) $\times 10^{-35}$ m
Planck time $l_P/c = (\hbar G/c^5)^{1/2}$	t_P	5.391 06(32) $\times 10^{-44}$ s
elementary charge	e	1.602 176 565(35) $\times 10^{-19}$ C
	e/h	2.417 989 348(53) $\times 10^{14}$ A J^{-1}
Bohr magneton $e\hbar/2m_e$	μ_B	927.400 968(20) $\times 10^{-26}$ J T^{-1}
		5.788 381 8066(38) $\times 10^{-5}$ eV T^{-1}
	μ_B/h	13.996 245 55(31) $\times 10^{9}$ Hz T^{-1}
	μ_B/hc	46.686 4498(10) m^{-1} T^{-1}
	μ_B/k	0.671 713 88(61) K T^{-1}
nuclear magneton $e\hbar/2m_p$	μ_N	5.050 783 53(11) $\times 10^{-27}$ J T^{-1}
		3.152 451 2605(22) $\times 10^{-8}$ eV T^{-1}
	μ_N/h	7.622 593 57(17) MHz T^{-1}
	μ_N/hc	2.542 623 527(56) $\times 10^{-2}$ m^{-1} T^{-1}
	μ_N/k	3.658 2682(33) $\times 10^{-4}$ K T^{-1}
molar mass of ^{12}C	$M(^{12}C)$	12 $\times 10^{-3}$ kg mol^{-1}
molar mass constant	M_u	10^{-3} kg mol^{-1}
relative atomic mass of ^{12}C	$A_r(^{12}C)$	12
electron relative atomic mass	A_r(e)	0.000 548 579 9111(12)
neutron relative atomic mass		1.008 664 915 74(56)
^{1}H relative atomic mass		1.007 825 032 07(10)
^{2}H relative atomic mass		2.014 101 777 85(36)
^{4}He relative atomic mass		4.002 603 254 153(63)
electron mass	m_e	9.109 382 91(40) $\times 10^{-31}$ kg
		5.485 799 0946(22) $\times 10^{-4}$ u
energy equivalent	$m_e c^2$	8.187 105 06(36) $\times 10^{-14}$ J
		0.510 998 928(11) MeV
electron-muon mass ratio	m_e/m_μ	4.836 331 66(12) $\times 10^{-3}$
electron-tau mass ratio	m_e/m_τ	2.875 92(26) $\times 10^{-4}$
electron-proton mass ratio	m_e/m_p	5.446 170 2178(22) $\times 10^{-4}$
electron-neutron mass ratio	m_e/m_n	5.438 673 4461(32) $\times 10^{-4}$
proton mass	m_p	1.672 621 777(74) $\times 10^{-27}$ kg
		1.007 276 466 812(90) u
energy equivalent	$m_p c^2$	1.503 277 484(66) $\times 10^{-10}$ J
		938.272 046(21) MeV
proton-electron mass ratio	m_p/m_e	1836.152 672 45(75)
proton-neutron mass ratio	m_p/m_n	0.998 623 478 26(45)
neutron mass	m_n	1.674 927 351(74) $\times 10^{-27}$ kg
		1.008 664 916 00(43) u
energy equivalent	$m_n c^2$	1.505 349 631(66) $\times 10^{-10}$ J
		939.565 379(21) MeV
alpha particle mass	m_α	6.644 656 75(29) $\times 10^{-27}$ kg

Table 13.4: *(Continued).*

Quantity	Symbol	Value
		4.001 506 179 125(62) u
energy equivalent	$m_\alpha c^2$	$5.971\,919\,67(26) \times 10^{-10}$ J
		3727.379 240(82) MeV
fine-structure constant $e^2/4\pi\epsilon_0\hbar c$	α	$7.297\,352\,5698(24) \times 10^{-3}$
inverse fine-structure constant	α^{-1}	137.035 999 074(44)
Bohr radius $\alpha/4\pi R_\infty = 4\pi\epsilon_0\hbar^2/m_e e^2$	a_0	$0.529\,177\,210\,92(17) \times 10^{-10}$ m
electron magnetic moment	μ_e	$-928.476\,430(21) \times 10^{-26}$ J T^{-1}
to Bohr magneton ratio	μ_e/μ_B	$-1.001\,159\,652\,180\,76(27)$
to nuclear magneton ratio	μ_e/μ_N	$-1838.281\,970\,90(75)$
proton rms charge radius	r_p	$0.8775(51) \times 10^{-15}$ m
deuteron rms charge radius	r_d	$2.1424(21) \times 10^{-15}$ m
proton magnetic moment	μ_p	$1.410\,606\,743(33) \times 10^{-26}$ J T^{-1}
to Bohr magneton ratio	μ_p/μ_B	$1.521\,032\,210(12) \times 10^{-3}$
to nuclear magneton ratio	μ_p/μ_N	2.792 847 356(23)
proton g-factor $2\mu_p/\mu_N$	g_p	5.585 694 713(46)
p-n magnetic moment ratio	μ_p/μ_n	$-1.459\,898\,06(34)$
neutron g-factor $2\mu_n/\mu_N$	g_n	$-3.826\,085\,45(90)$
triton g-factor $2\mu_t/\mu_N$	g_t	5.957 924 896(76)

The mass of the tau lepton m_τ, the Fermi coupling constant G_F and the mass ratio of the $W^\pm$ and Z^0 bosons obtained from the most recent report of the Particle Data Group are

$$m_\tau c^2 = 1776.82(16) \text{ MeV} \tag{13.2}$$

$$\frac{G_F}{(\hbar c)^3} = 1.166\,364(5) \times 10^{-5} \text{ GeV}^{-2} \tag{13.3}$$

$$\frac{m_W}{m_Z} = 0.8819(12) \tag{13.4}$$

http://physics.nist.gov/cuu/Constants/index.html
http://arxiv.org/abs/1203.5425
http://pdg.web.cern.ch/pdg/